Investigating the roles of candidate gap genes from the neuroblast timer series during axial patterning in the beetle *Tribolium*

Olivia Rose Annecy Tidswell

Trinity College

University of Cambridge

Submitted August 2020

This dissertation is submitted for the degree of Doctor of Philosophy

DECLARATION

This dissertation is the result of my own work and includes nothing which is the outcome of work done in collaboration except where indicated in the text.

None of this work has been submitted or is being concurrently submitted for a degree or diploma or other qualification at the University of Cambridge or any other University or similar institution.

It does not exceed the prescribed word limit for the Biology Degree Committee (60,000 words).

Investigating the roles of candidate gap genes from the neuroblast timer series during axial patterning in the beetle *Tribolium*

Olivia Rose Annecy Tidswell

SUMMARY

The gap genes encode transcription factors that play a central role in the process of segment patterning in *Drosophila*. Specifically, they interact to form the well-characterised 'gap gene network', which directs the formation of segment boundaries (through regulation of pair-rule genes), and the subsequent diversification of segments (through regulation of Hox genes). Although homologues of the gap genes play important roles in segment patterning in many insects, there is as yet no clear understanding of the network as a whole outside of *Drosophila*. In particular, the existence of a 'gap gene gap' (a region of the axis that expresses no gap genes) in embryos of the beetle *Tribolium castaneum* may indicate the existence of additional, as yet unidentified gap genes in this species.

In this work, I investigate the hypothesis that the neuroblast timer genes *nubbin* (*nub*) and *castor* (*cas*) may act as components of the gap gene network in *Tribolium*. I first utilise Hybridisation Chain Reaction *in situ* hybridisation to produce a comprehensive description of the dynamics of gap gene expression in *Tribolium*, concluding that, although the non-canonical gap genes *Tc-mille-pattes* and *Tc-shavenbaby* are expressed in the gap gene gap, their role may be distinct from that of the canonical gap genes, and that there are likely to be other, unknown gap genes expressed alongside them. I show that the four genes of the neuroblast timer series (*hunchback*, *Krüppel*, *nub* and *cas*) are expressed sequentially in the segment addition zone, with the result that *nub* and *cas* are expressed in the gap gene gap. Knocking down the expression of *nub,* but not *cas,* using RNAi results in weak homeotic transformations of the first abdominal segment towards a thoracic fate. Finally, I show that this phenotype is dramatically increased in severity and penetrance when *Tc-nub* is knocked down in addition to the trunk gap genes *Tc-gt* and/or *Tc-kni.* In triple knockdowns, all abdominal segments are transformed into thoracic segments due to a posterior expansion of the thoracic gap gene *Tc-Kr* and subsequent loss of expression of the abdominal Hox genes *Tc-abdominal A* and *Tc-Ultrabithorax.* These data indicate that *Tc-nub*, *Tc-gt* and *Tc-kni* act redundantly to repress the expression of *Tc-Kr* in the abdomen, and that both *Tc-nub* and *Tc-kni* should therefore be considered as components of the gap gene network in *Tribolium*.

My work strengthens the hypothesis that the gap gene network may have ancient evolutionary ties to the neuroblast timer network, and promotes a more 'modular' view of the gap gene network. I hope that this will inform future studies that aim to unravel the developmental role of the gap genes in sequentially segmenting arthropods, and the evolutionary origins of the gap gene network.

ACKNOWLEDGEMENTS

I am extremely grateful to my supervisor, Michael, for lending his keen mind to my project, and for his kindness when the sailing was not so smooth. I will dearly miss our discussions about garden wildlife, and hope that he can forgive me for delaying his retirement.

I would also like to extend my heartfelt thanks to Erik Clark (who got me hooked on the project) and Matt Benton (who acted as my local beetle expert and listened to all of my wild ideas with a straight face). I feel exceedingly lucky to have both of them as mentors and friends.

I am grateful for the generosity of Andrew Peel and Rahul Sharma, who dedicated so much of their time and energy into helping me to get established with *Tribolium*.

My PhD experience would have been much poorer without the friendship of numerous people in the department (including, but not limited to, Toby Andrews, Margherita Battistara, Emília Santos, Aleksandra Marconi and Joel Elkin) and in Trinity College (a special shout out to the wonderful Kiwis Mark Burrell, Max Wilkinson, Laura and Reece Oosterbeek and Natalie Jones).

Thank you also to the Wellcome Trust, the Cambridge Trust and the Cambridge Philosophical Society for supporting me during my studies.

Thanks and love to all of my family, for instilling in me a passion for science and for encouraging me to chase my dreams.

And finally, to my partner, Rory – you have been my rock and my sunshine every step of the way. Thank you for making my world a little brighter.

LIST OF ABBREVIATIONS

A1-10 – abdominal segments 1-10
AEL – after egg lay
abdA – abdominal A
AbdB – abdominal B
Antp - Antennapedia
AP – anterior-posterior
cad - caudal
cas - castor
eve – even-skipped
grh - grainyhead
gt - giant
hb - hunchback
HCR – Hybridisation Chain Reaction
hkb - huckebein
ISH – *in situ* hybridisation
kni - knirps
Kr - Krüppel
lb = labial segment
md = mandibular segment
mlpt – mille-pattes
mx = maxillary segment
nub - nubbin
PS = parasegment
SAZ – segment addition zone
svb - shavenbaby
T1-3 - thoracic segments 1-3
TF – transcription factor
Tl10 – Toll-10
tll - tailless
Ubx - Ultrabithorax
Wg – Wingless

A note on terminology

Throughout this text, gene names are italicised (*e.g., nub*), while protein names are capitalised in plain text (*e.g.,* Nub). The prefixes Dm- and Tc- refer to genes or proteins specifically from *Drosophila melanogaster* or *Tribolium castaneum,* respectively.

TABLE OF CONTENTS

1. GENERAL INTRODUCTION

The evolutionary success of the phylum Arthropoda, which includes centipedes, millipedes, spiders, crustaceans and insects, among others, is often attributed to their characteristically modular, or segmented, body plan. Segmented body plans provide a great deal of evolutionary flexibility, as individual segments can be added, deleted or modified without disrupting functions carried out by others. Arthropods have made great use of this flexibility, with different groups adapting their body plans to invade nearly every habitat on earth. Understanding how this segmented body plan is generated during early development, and how it is modified in different lineages to produce diverse larval and adult morphologies, is a major area of focus for the field of evolutionary and developmental biology (Clark et al., 2019; Peel et al., 2005).

This thesis is specifically focused on the evolution and function of the gap genes: a network of genes that encode DNA-binding transcription factors (TFs) involved in segment patterning in many arthropods. In particular, I am interested in similarities between the gap gene network and a network of genes involved in regulating cell fate in the insect nervous system (known as the neuroblast timer series), and what this might tell us about the origins of the gap gene network.

Most of what is known about gap genes comes from studies in the ubiquitous arthropod model, *Drosophila melanogaster*. However, development in *Drosophila* is derived in several ways compared to other arthropods, including in the way that segments are patterned (Clark et al., 2019; Peel et al., 2005). Recent research on segmentation in arthropods has therefore turned to more representative species, notably the beetle *Tribolium castaneum*, as a point of comparison (Clark et al., 2019). This thesis attempts to further develop our understanding of the evolution and functions of the gap gene network, using *Tribolium* as a model system.

1.1. The gap gene network and segmentation in *Drosophila*

An introduction to the gap genes of *Drosophila*

The gap gene network of the fruit fly, *Drosophila melanogaster* (referred to throughout this thesis as simply *Drosophila*), is one of the best studied gene networks in any organism. The existence of gap genes was first inferred from mutagenesis screens carried out in 1978-1980 (Nüsslein-Volhard and Wieschaus, 1980). In these experiments, thousands of larval cuticles from laboratory-generated mutant *Drosophila* lines were examined for patterning defects, and assigned into different phenotypic classes (Wieschaus and Nüsslein-Volhard, 2016). Gap mutants were so named because they were lacking one or two regions of contiguous segments along the anterior-posterior (AP) axis (*i.e.,* a 'gap' had been introduced) (Wieschaus and Nüsslein-Volhard, 2016). The genes responsible for these gap phenotypes were later identified and correspondingly called gap genes. Segment deletions in the trunk (comprising the gnathal, thoracic and abdominal segments) arise from mutations in the so-called 'trunk gap genes': *hunchback* (*hb*), *Krüppel* (*Kr*), *giant* (*gt*) and *knirps* (*kni*) (Nüsslein-Volhard and Wieschaus, 1980; Nüsslein-Volhard et al., 1984; Wieschaus et al., 1984). In contrast, segment deletions in the head or tail regions arise from mutations in the 'terminal gap genes', *tailless* (*tll*) and *huckebein* (*hkb*) (Jürgens et al., 1984; Weigel et al., 1990). These genes are encoded on different chromosomes across the fly genome (Table 1.1), and are not closely related in evolutionary terms. However, it was later found that the TFs encoded by these genes interact to form a single network, and that they regulate many of the same target genes, during segment patterning in *Drosophila* (reviewed in Jaeger, 2011).

Table 1.1. Gap gene locations and transcription factor (TF) families. Adapted from Jaeger (2011).

Region patterned	Gene name	Chromosome	TF family
Trunk	*hunchback (hb)*	3R	Zinc-finger (C2H2-type)
	Krüppel (Kr)	2R	Zinc-finger (C2H2-type)
	knirps (kni)	3L	Zinc-finger (nuclear hormone receptor)
	giant (gt)	X	Basic leucine-zipper
Terminal	*tailless (tll)*	3R	Zinc-finger (nuclear hormone receptor)
	huckebein (hkb)	3R	Zinc-finger (C2H2-type)

The gap gene network is part of the *Drosophila* segmentation cascade

The gap genes are one of four major gene classes that have been found to regulate the process of segment formation during *Drosophila* embryogenesis, the other three being the maternal co-ordinate genes, the pair-rule genes, and the segment polarity genes. These four gene classes are expressed and regulate each other in a hierarchical manner to form the segment boundaries in the embryonic ectoderm (Figure 1.1) (reviewed in Akam, 1987; Ingham, 1988; Nasiadka et al., 2002). At each level of this so-called 'segmentation cascade', the subdivision of the embryo by segment patterning genes becomes more precise.

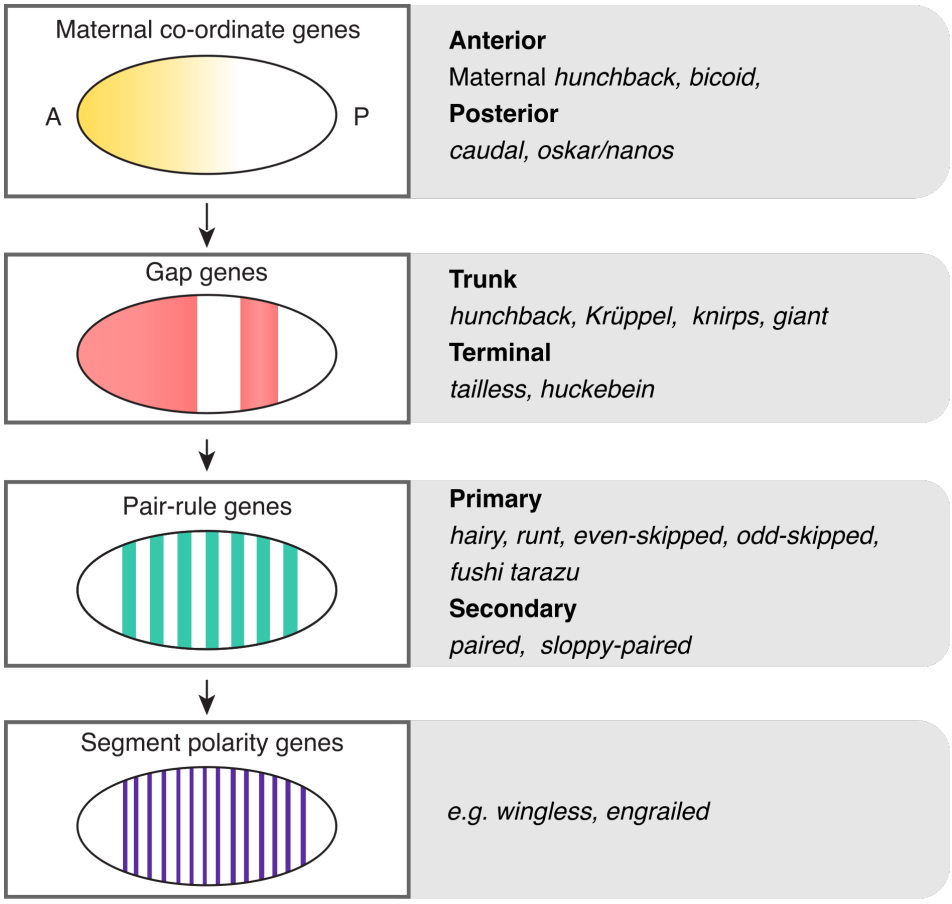

Figure 1.1. Genes of the segmentation cascade of *Drosophila*. A hierarchy of transcription factors interacts to divide the anterior-posterior axis of the embryo into increasingly precise units during early development. Examples of the genes comprising each level of the segmentation cascade are provided on the right.

The maternal co-ordinate genes, as their name suggests, are transcribed maternally and their mRNA provided to the oocyte while it is still in the ovary. Following fertilisation, interactions between maternally deposited mRNAs and the proteins they encode result in the formation of anterior-to-posterior gradients of Bicoid (Bcd) and Hunchback (Hb) proteins, and a posterior-to-anterior gradient of Caudal (Cad) protein (reviewed in Nasiadka et al., 2002). These three long-range gradients are largely responsible for establishing the initial expression of gap genes in broad domains along the trunk of the embryo (reviewed in Jaeger, 2011). In contrast, terminal gap genes are regulated primarily through localised Torso MAP-kinase signaling at the embryonic poles (reviewed in Furriols and Casanova, 2003; Jaeger, 2011).

Gap gene expression domains are subsequently sharpened by gap-gap cross regulation (Figure 1.2) (reviewed in Jaeger, 2011). Gap proteins with non-overlapping expression domains (Hb/Kni and Kr/Gt) exhibit strong mutual repression (Figure 1.2A). Overlapping gap genes exhibit weaker, asymmetrical repression. Specifically, more anteriorly-expressed gap genes tend to be weakly repressed by overlapping posterior gap genes, but not *vice versa* (Figure 1.2B). This asymmetric repression, in tandem with strong repression of trunk gap genes by the posterior terminal gap genes (Figure 1.2C), results in a gradual posterior-to-anterior shift in the entire gap expression pattern (Jaeger et al., 2004).

Following the gap genes, the next set of genes expressed in the segmentation cascade are the pair-rule genes. The pair-rule genes are activated by numerous broadly expressed genes, including the maternal co-ordinate genes; however, their restriction into spatially periodic patterns depends on repression by gap genes (reviewed in Nasiadka et al., 2002). Most pair-rule genes are expressed transiently in a seven stripe pattern along the length of the embryo (Figure 1.1. and Nasiadka et al., 2002). These stripes are established via stripe-specific enhancer sequences, each of which responds to a unique combination of maternal co-ordinate and gap proteins (Schroeder et al., 2011). The striped patterns of different pair-rule genes are out of register with each other, so that together their overlapping expression patterns cover the entirety of the trunk. The posterior-to-anterior shift in the gap gene expression pattern drives a similar shift in the pair-rule gene pattern (Surkova et al., 2008) which is essential for normal segment patterning (Clark, 2017).

Finally, pair-rule proteins regulate the spatial expression of the segment polarity genes, which are each expressed in 14-15 stripes along the length of the embryo (reviewed in Nasiadka et al., 2002). The segment polarity genes do not define the boundaries of morphological segments, but rather of patterning units known as ‘parasegments’ (Martinez-Arias and Lawrence, 1985). Parasegments are the same size as segments, but shifted anteriorly so as to

be out of register with the final, exterior segmental pattern. The discrepancy is believed to reflect a similar offset in the organisation of metameric elements of the nervous system (which are patterned early in development, and have parasegmental boundaries) and of the exoskeleton (which are formed later, and have segmental boundaries) (Deutsch, 2004).

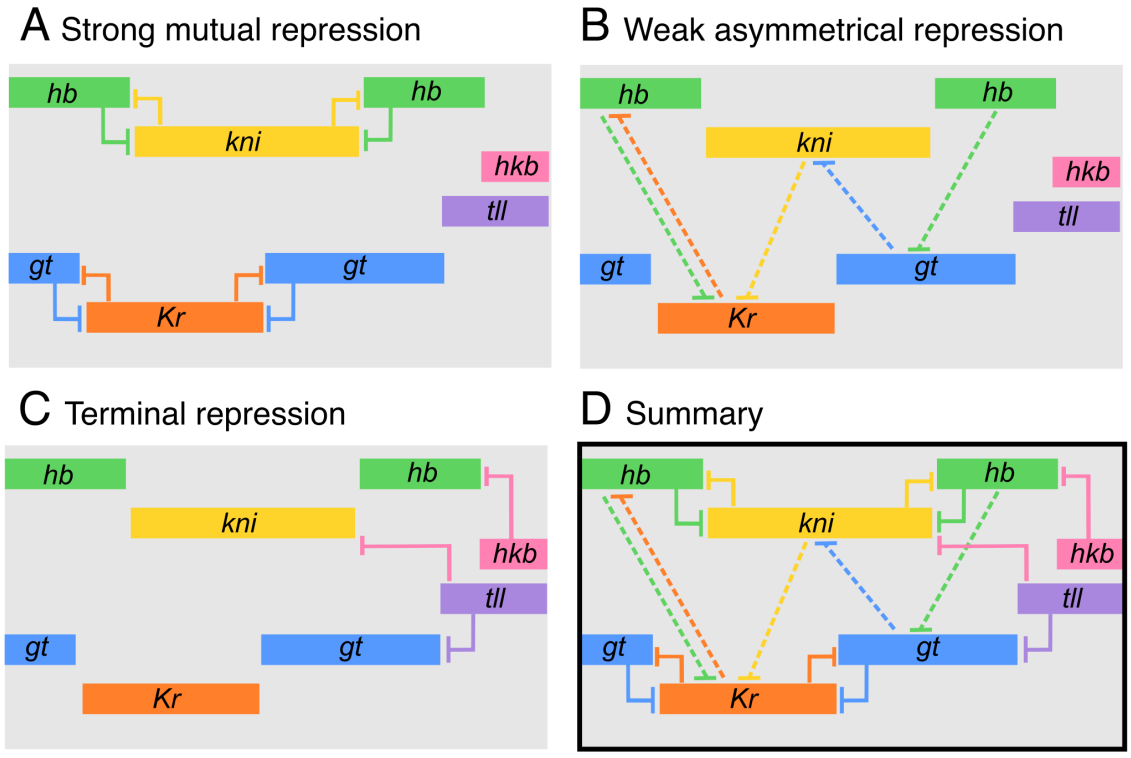

Figure 1.2. Gap-gap cross-regulatory interactions in *Drosophila*. A-D show abstractions of the trunk and tail region of the *Drosophila* embryo, with anterior to the left and posterior to the right. Coloured bars indicate the approximate extent of expression of each gap gene along the length of the AP axis of the embryo. Strong mutual repression between gap proteins with non-overlapping domains establishes the basic staggered pattern of gap gene expression (A). Weaker, asymmetrical repression between overlapping gap genes refines boundaries and leads to a posterior-to-anterior shift in the entire gap gene pattern over time (B). The terminal gap genes prevent the expression of trunk gap genes in the posterior of the embryo (C). A summary of these interactions is shown in D.

Segment diversification in *Drosophila*

In addition to their role in the segmentation cascade, gap genes also play a key role in the diversification of segments towards different morphologies and functions (termed 'segment identity'). Segment identity in *Drosophila* is driven by the Hox genes (Figure 1.3). Hox genes encode transcription factors that act as regulators of axial identity across the Bilateria (reviewed by many, including Akam, 1998a; Akam, 1998b; Duboule, 2007; Hughes and Kaufman, 2002; Krumlauf, 1994; Maeda and Karch, 2006; Mallo and Alonso, 2013). I present here only the aspects of their regulation that are relevant for the purposes of this thesis.

Gap proteins are major regulators of the Hox genes. While the expression of Hox genes in *Drosophila* is activated globally, expression is restricted to specific domains largely by repression via gap proteins (reviewed in Nasiadka et al., 2002). For example, the gap proteins Hb and Kr are required to restrict expression of the Hox genes *Ultrabithorax* (*Ubx*) and *abdominal A (abdA)*, respectively, to the posterior of the embryo, and to establish their anterior boundaries (Casares and Sánchez-Herrero, 1995; White and Lehmann, 1986). The gap gene-mediated regulation of Hox gene expression is controlled by specific regulatory elements associated with each Hox gene (reviewed in Maeda and Karch, 2006). The role of gap genes in Hox regulation is clearly demonstrated in the case of weaker gap gene mutant alleles, where parasegments in the affected region are not deleted but instead take on an altered identity (also known as homeosis) (Lehmann and Nüsslein-Volhard, 1987).

Like the gap genes, cross-regulation between Hox genes is also important for establishing the correct expression domains. Trunk Hox genes display a feature known as 'posterior prevalence', wherein more posterior Hox genes are able to repress the expression of more anterior Hox genes (Duboule and Morata, 1994). Although gap genes are required to establish proper Hox gene expression domains, these domains are subsequently maintained by Polycomb and Trithorax proteins, which are able to remodel chromatin to create cellular 'memory' of Hox gene expression state (reviewed in Nasiadka et al., 2002).

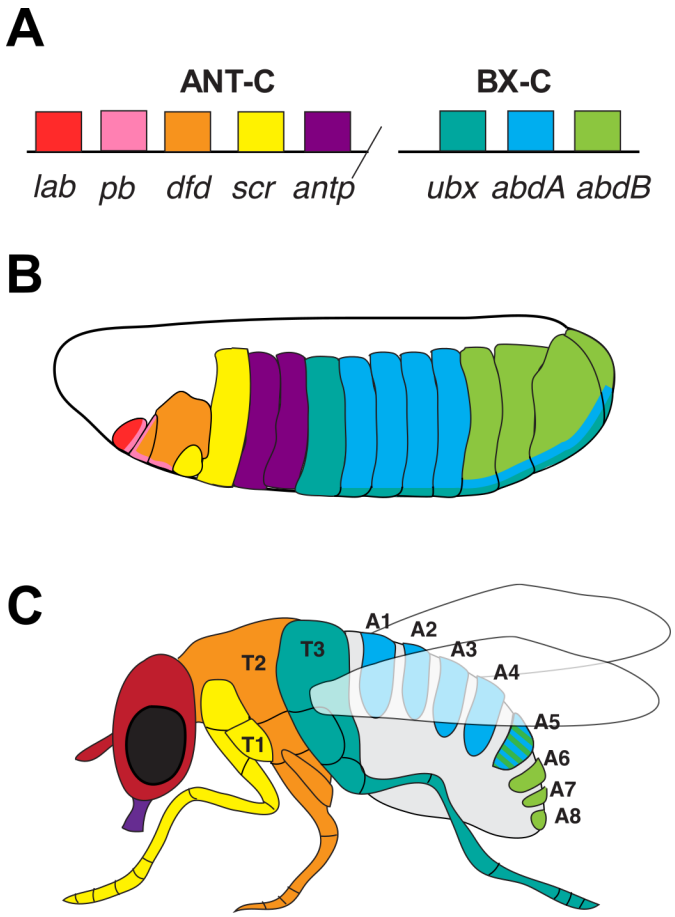

Figure 1.3. Hox genes are master regulators of segment identity in *Drosophila*. **A|** The Hox genes are encoded in two clusters in *Drosophila*, the Antennapedia Complex (ANT-C) and the Bithorax complex (BX-C). Ancestrally, these two clusters were joined into a single cluster (the Homeotic Cluster, or HOM-C). **B|** The Hox genes are expressed along the AP axis in the same order in which they are encoded in the genome, a phenomenon known as spatial collinearity. Note that many segments express more than one Hox gene. **C|** Segments expressing different Hox genes (or combinations of Hox genes) will develop towards different fates in the adult fly. Adapted from Gilbert (2013).

1.2. Segment patterning in *Drosophila* is derived compared to the majority of arthropods

Most of what we know about gap gene function and regulation comes from studies in *Drosophila*. However, *Drosophila* is far from a representative model of arthropod development with respect to segmentation (Peel et al., 2005). During early development, arthropod embryos typically form a blastoderm (a monolayer of nuclei or cells surrounding the yolk). The blastoderm will go on to form both the embryo proper (the "germ rudiment"), and extraembryonic membranes. Most arthropod embryos have an extensive extraembryonic membrane that covers the yolk surface (Jacobs et al., 2013). This single membrane has been elaborated in insects to form the serosa (which envelops the whole egg contents and protects against desiccation and infection, among other roles) and the amnion (which envelops the embryo itself) (reviewed in Jacobs et al., 2013; Panfilio, 2008). In most arthropods, a large proportion of the blastoderm must therefore be allocated to forming extraembryonic membranes, with only a small portion allocated to forming the germ rudiment (Davis and Patel, 2002). In embryos with a small germ rudiment, only a few anterior segments are patterned early in development, and the majority of the AP axis is generated after cellularisation through elongation (Clark et al., 2019). Elongation is driven by a combination of cell division and cell intercalation in a mass of unspecified cells at the posterior end of the embryo, known as the segment addition zone (SAZ) (reviewed in Clark et al., 2019). The majority of the segments are therefore patterned sequentially, from anterior to posterior, as tissue is gradually added to the developing germband; a mode of segmentation known as 'sequential segmentation' (Figure 1.4A) (Clark et al., 2019).

Drosophila, and several other insect lineages, have increased the size of the germ rudiment at the expense of tissue allocated to extraembryonic membranes (*e.g.*, in *Drosophila*, the serosa and amnion have been reduced to the amnioserosa) (Grimaldi and Engel, 2005). In these species, there is sufficient space to pattern all, or nearly all, of the segments of the embryo onto the germ rudiment early in development, prior to elongation and even cellularisation. Extensive maternal provisioning establishes a pre-pattern so that subsequent segment patterning can occur rapidly, and simultaneously, across the length of the AP axis through the activity of the segmentation cascade (Davis and Patel, 2002). This mode of segmentation is known as 'simultaneous segmentation' (Figure 1.4B).

Most arthropods display some combination of simultaneous and sequential segmentation, with the number of segments patterned by each method varying between species (Clark et al., 2019). However, sequential segmentation is proposed to be the ancestral mode

within the arthropods (Davis and Patel, 2002). Only a few lineages form the majority of their segments by simultaneous segmentation, and these are largely limited to the Holometabola (insects with complete metamorphosis) (Figure 1.5). Despite this, our understanding of how segment patterning occurs in sequentially-segmenting arthropod species lags significantly behind our understanding in the simultaneously-segmenting *Drosophila*. Segmenting animals outside of the Arthropoda, such as the annelids and vertebrates, also display a sequential mode of segmentation, although this has been proposed to be largely convergently evolved (Clark et al., 2019).

It is important to note that arthropod embryos possessing a relatively small germ rudiment and undergoing sequential segmentation have historically been referred to as being 'short germ', whereas those possessing a relatively large germ rudiment and undergoing simultaneous segmentation, have been termed 'long germ', respectively (Davis and Patel, 2002). However, germ size does not always correlate perfectly with the mode of segmentation an arthropod employs, and so I will follow recent convention of eschewing these terms in favour of more specific reference to the processes of sequential and/or simultaneous segmentation themselves (Clark et al., 2019).

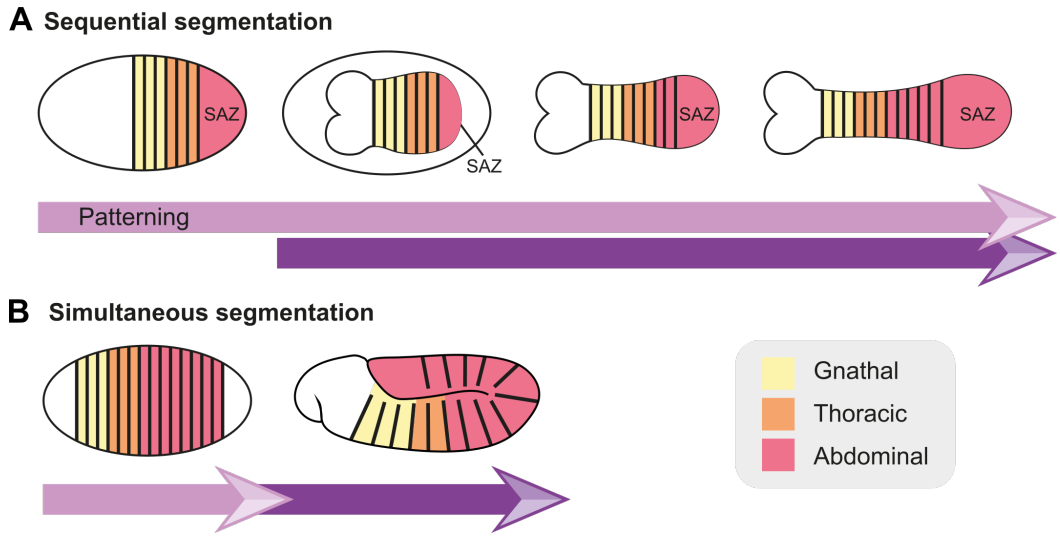

Figure 1.4. Arthropods pattern their segments simultaneously or sequentially. A| Sequentially segmenting arthropods form the majority of their segments sequentially, from a posterior segment addition zone (SAZ) as the embryo condenses and elongates. The schematic here shows a red flour beetle (*Tribolium castaneum*) embryo as an example. **B|** *Drosophila* forms its trunk segments simultaneously, by subdivision of the embryo prior to any major embryonic morphogenesis. Based on a figure by T. Andrews.

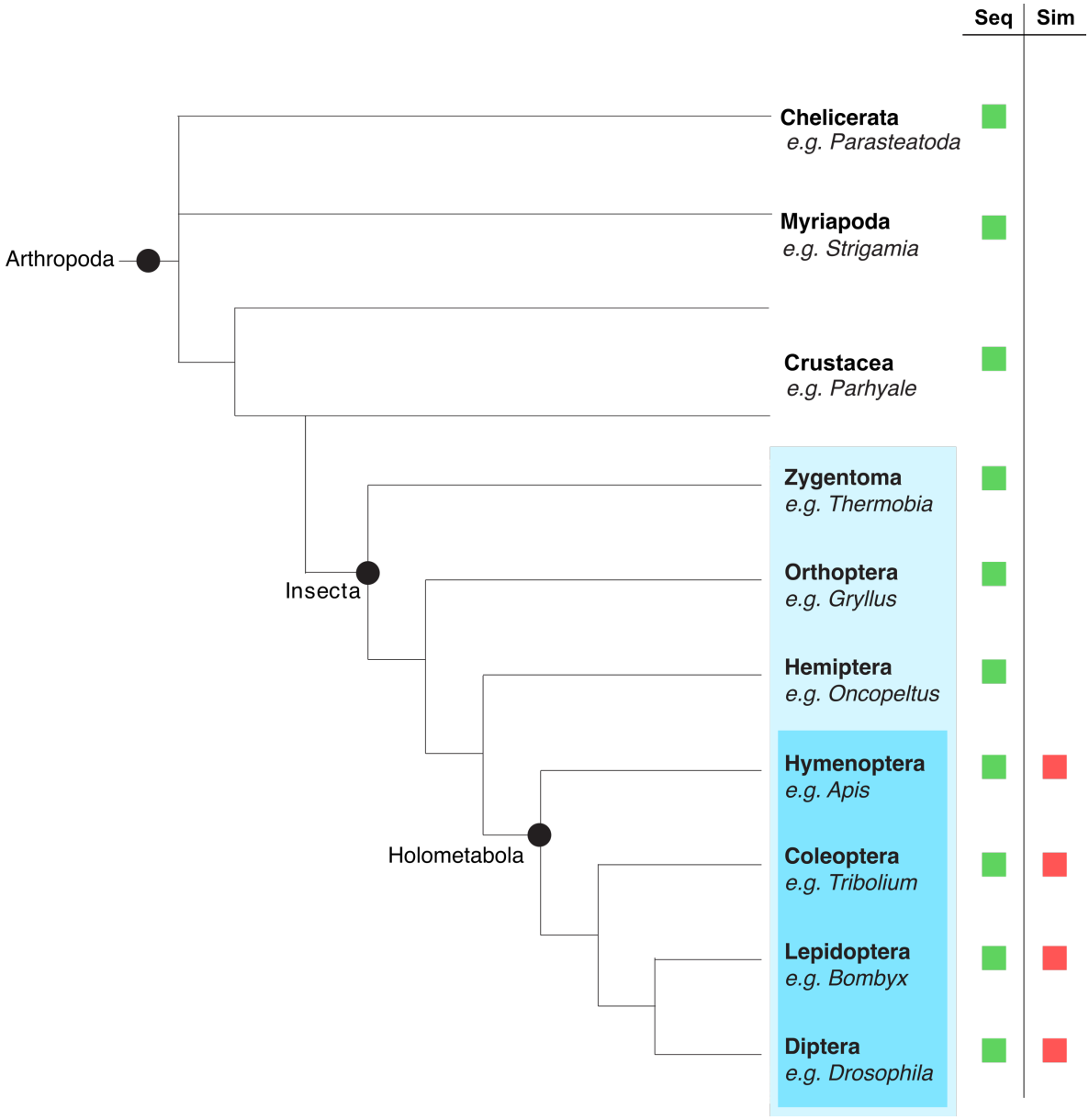

Figure 1.5. A phylogeny of the arthropod phylum demonstrating that sequential segmentation (Seq) is the most common and likely ancestral mode of segmentation among arthropods. Species that form all or most of their segments by simultaneous segmentation (Sim) are found only in holometabolous insect lineages, where it has most likely evolved independently several times (Clark et al., 2019). Phylogeny is based on Rehm et al. (2014).

1.3. The molecular mechanisms of sequential segment patterning

The generation of spatially periodic pair-rule gene expression in simultaneously-segmenting insects like *Drosophila* is largely under the control of non-periodic spatial cues from the gap genes (reviewed in Nasiadka et al., 2002). In contrast, sequential segmentation relies on inherently periodic oscillations in expression of the pair-rule gene network to generate stripes (Clark et al., 2019). These oscillations are driven by interactions between the pair-rule genes themselves (reviewed in Clark et al., 2019). As is the case in vertebrates (Liao and Oates, 2017), these oscillations in pair-rule gene expression are co-ordinated between cells, most likely via intercellular Notch signaling (Clark et al., 2019), which has been shown to be required for segmentation in some non-insect arthropods (Eriksson et al., 2013; Stollewerk et al., 2003) and at least one sequentially-segmenting insect species (Pueyo et al., 2008).

Pair-rule gene oscillations are limited to the SAZ, where they are activated by posterior factors (the most likely candidates are the TF *caudal* (*cad*) or the signaling factor *Wg*) (reviewed in Clark et al., 2019). Each oscillation begins in the posterior SAZ, where these signals are strongest, and subsequently spreads anteriorly, creating the appearance of a travelling wave (Brena and Akam, 2013; El-Sherif et al., 2012; Sarrazin et al., 2012). At the anterior of the SAZ, these waves slow and are stabilised to form spatially periodic stripes. In at least some species, the stabilisation of pair-rule gene expression in the anterior SAZ is driven by the TF Odd-paired (Opa), which is expressed in the anterior SAZ and acts as a cofactor for pair-rule proteins, changing their regulatory interactions (reviewed in Clark et al., 2019). Following the formation of stable pair-rule gene expression stripes, regulation of segment polarity genes follows much as described in *Drosophila* (reviewed in Clark et al., 2019). This method of segment patterning, in which waves of gene expression are stabilised after crossing a ‘wavefront’ of gene expression, is similar to the ‘clock and wavefront’ model that describes somite segmentation in vertebrates (Clark et al., 2019; Cooke and Zeeman, 1976).

Remnants of this oscillatory segment patterning system are still present in *Drosophila* – pair-rule stripes are initially dynamic, shifting anteriorly across the blastoderm, and only become stabilised after *opa* is switched on across the tissue (Clark, 2017; Clark and Peel, 2018). Indeed, recent studies are highlighting that segmentation in *Drosophila* has more in common with sequential segmentation than once thought (Clark, 2017; Clark and Peel, 2018; Clark et al., 2019; Verd et al., 2018). However, the evolution of gap gene-responsive stripe specific elements is thought to be an adaptation associated with simultaneous segmentation (Clark et

al., 2019; Peel et al., 2005). This raises the question of what the role of gap genes might be in sequentially-segmenting arthropods.

1.4. Evolution of gap gene expression and function in arthropods

Homologues of all four trunk gap genes (*hb*, *Kr*, *gt* and *kni*) are widely conserved across the arthropods (Peel et al., 2005). Of the four, *kni* is the most recently derived, resulting from a Drosophilid-specific gene duplication of an ancestral *knirps*-family gene (Naggan Perl et al., 2013) which I will also refer to as *kni*. The duplicate in *Drosophila* is known as *knirps-related* (*knrl*), and plays redundant roles with *kni* outside of segmentation (Rothe et al., 1992). The ancestral *kni* gene has been duplicated independently in a few other arthropod lineages, but is otherwise usually present as a single copy (Naggan Perl et al., 2013).

Gap gene homologues do not appear to be utilised in the process of segment patterning outside of arthropods (for example, see Iwasa et al., 2000; John and Ward, 2011; Kerner et al., 2006; Pinnell et al., 2006), suggesting that they were only co-opted to this role within the Arthropoda. Exactly when this co-option occurred is still a matter of some debate, as research on gap gene expression and function in non-insect arthropods is limited (Jaeger, 2011) (Figure 1.6). None of the trunk gap genes are expressed in the SAZ during axial patterning of the centipede *Strigamia* (Chipman and Stollewerk, 2006). However, a homologue of *hb* is expressed in the anterior ectoderm of both the spider *Achaearanea tepiadariorum* and the millipede *Glomeris marginata* during segment addition (Janssen et al., 2011; Schwager et al., 2009). In the former, genetic knockdown results in a canonical gap phenotype (*i.e.* deletion of several consecutive segments), although no obvious effect on Hox gene expression is detected (Schwager et al., 2009). *Kr* is also expressed in a stripe in the ectoderm of *Achaearanea* during segment patterning, but its function is yet to be tested (McGregor et al., 2008). Only the homologue for *hb* has been examined in crustaceans, and it does not appear to be expressed in the SAZ during axial patterning (Kontarakis et al., 2006).

There is considerably more data available on gap gene expression and function within the insect clade (Figure 1.6) (reviewed in Jaeger, 2011). Homologues of all four trunk gap genes are expressed in "gap-like" domains in various insect lineages, including in the sequentially-segmenting species *Tribolium* and *Oncopeltus* (reviewed in Jaeger, 2011) (Figure 1.5). In these two species, the gap genes are expressed sequentially in the SAZ, forming travelling waves that eventually stabilise to cover specific regions of the AP axis (Ben-David and Chipman, 2010; Zhu et al., 2017). The order of expression of gap gene domains along the

length of the axis is very similar to that observed in *Drosophila*, but the pattern appears to be shifted anteriorly, so that domains expressed in the posterior abdomen in *Drosophila* are shifted towards the anterior abdomen (reviewed in Jaeger, 2011). The sequential expression of the gap genes within the SAZ appears to be driven by regulatory interactions between the gap genes themselves (Boos et al., 2018). The remnants of a similar network drive damped oscillation of gap gene expression within cells in *Drosophila*, contributing to the anterior shifts of gap gene domains across the AP axis in this species (Verd et al., 2018 and section 1.1.2). This evidence suggests that these dynamics are an ancestral feature of the gap gene network, at least within the insect clade. However, not all of the interactions between gap genes are conserved between species. Studies of gap gene interaction in the sequentially-segmenting species *Tribolium* and *Oncopeltus* have revealed differences in the nature of interactions between different gap proteins and genes compared to *Drosophila*, and to each other (Ben-David and Chipman, 2010; Bucher and Klingler, 2004; Marques-Souza et al., 2008).

As in *Drosophila*, the homologues of *hb*, *Kr* and *gt* appear to play a dual role in regulating segment formation and segment identity in other insect species. Knockdown or mutation of any one of these three genes leads to misexpression of Hox genes and homeosis in all of the insect species in which they have been functionally tested (Figure 1.6). Such genetic disruptions also typically result in either a canonical "gap" phenotype (*i.e.,* the deletion of several contiguous segments within the domain of expression of a gap gene), or to a distinct phenotype in which segmentation terminates within or shortly after the gap gene's domain of expression ('truncation') (Figure 1.6). These data indicate that in some cases, gap genes are required to regulate the formation specific pair-rule stripes, while in others they are required instead to maintain the activity of the pair-rule oscillator, either directly or through regulation of the environment in the SAZ (Bucher and Klingler, 2004; Cerny et al., 2005). Interestingly, gap gene knockdown has, on at least one occasion, been found to lead to the formation of supernumerary segments (Nakao, 2016). If gap genes are able to regulate when segmentation begins and ends, then they may act as a 'timer' to determine the duration of segmentation and therefore the number of segments formed during sequential segmentation (Bucher and Klingler, 2004; Cerny et al., 2005; Clark et al., 2019).

Although homologues of the ancestral *kni* gene (which was duplicated to give rise to the paralogues *Dm-kni* and *Dm-knrl* in *Drosophila*) are often expressed in the right time and place to regulate trunk segment patterning in other insect species, their role in this process is usually minimal (or non-existent) compared to *Dm-kni* (Ben-David and Chipman, 2010; Cerny et al., 2005; Peel et al., 2013). This suggests that members of the *kni* family may only have

become a central component of the gap gene network in *Drosophila*, with the origin of *Dm-kni* (though a role in head patterning may be more conserved).

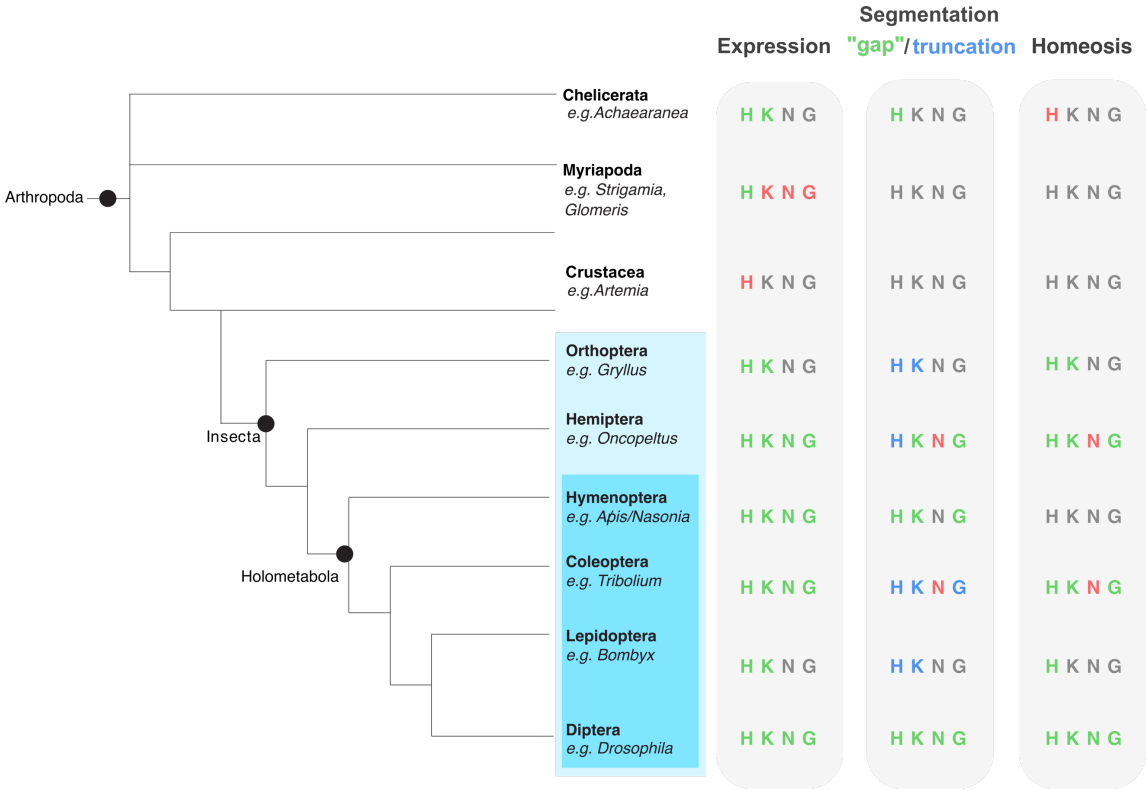

Figure 1.6. The evolution of gap gene expression and function within the arthropod phylum. Each of the lineages shown on the phylogeny are represented by one or two model species for which data on gap gene expression and/or function exists. Columns indicate whether particular gap genes (*hb* = H; *Kr* =K; *kni* = N; *gt* = G) are (green/blue) or are not (red) expressed in a "gap-like"domain (Expression column), and whether their knockdown results in defects in segment formation (Segmentation column) or segment identity (Homeosis column). Grey gene labels indicate a lack of relevant data for this species. In the Segmentation column, letters may be green, indicating a canonical gap phenotype, or blue, indicating a truncation phenotype (see text for more details). Figure is adapted from Jaeger (2011), using the following references for each species: *Achaearanea* (McGregor et al., 2008; Schwager et al., 2009); *Strigamia* (Chipman and Stollewerk, 2006); *Artemia* (Kontarakis et al., 2006); *Gryllus* (Mito et al., 2005; Mito et al., 2006)*; Oncopeltus* (Ben-David and Chipman, 2010; Liu and Kaufman, 2004a; Liu and Kaufman, 2004b; Liu and Patel, 2010)*; Apis* (Wilson et al., 2010) and *Nasonia* (Lynch et al., 2006; Olesnicky, 2006; Pultz, 2005); *Tribolium* (Bucher and Klingler, 2004; Cerny et al., 2005; Cerny et al., 2008; Marques-Souza et al., 2008; Peel et al., 2013) *Bombyx* (Nakao, 2015; Nakao, 2016); *Drosophila* (Jaeger, 2011).

1.5. The "gap gene gap" and new candidate gap genes

In *Drosophila*, the expression domains of the four trunk gap genes are sufficient to cover the entire length of the trunk. In contrast, in the sequentially-segmenting insect *Tribolium*, the expression domains of these four genes covers only the anterior part of the axis (Cerny et al., 2008). A large region of the abdomen is therefore patterned in the absence of apparent gap gene expression, creating what has been described as a "gap gene gap". The existence of this gap suggests that there may be additional gap genes, outside of the homologues of *Drosophila* gap genes, active in non-Drosophilid insects. In support of this theory, subsequent research has identified two gap gene candidates – *mille-pattes* (*mlpt*) and *shavenbaby* (*svb*). *mlpt*, also known as *tarsal-less* or *polished-rice*, does not encode a TF, but instead several short peptides (Galindo et al., 2007). These peptides are able to interact with a TF known as *shavenbaby* (*svb*) and trigger its transformation from a transcriptional repressor to a transcriptional activator (Kondo et al., 2010). Both of these genes are expressed in domains spanning contiguous segments during segment patterning in a range of different insect species (Ray et al., 2019). Furthermore, in some (but not all) of these species, knockdown of either *mlpt* or *svb* results in homeotic transformations and segmentation truncations (Jiménez-Guri et al., 2018; Ray et al., 2019; Savard et al., 2006; Tobias-Santos et al., 2019) in addition to misexpression of other gap genes (Savard et al., 2006). These two genes therefore appear to share many of the key features of the canonical gap genes, and *mlpt*, at least, has been incorporated into models of the gap gene network in *Tribolium* (Boos et al., 2018; Zhu et al., 2017).

1.6. The neuroblast timer genes *nubbin* and *castor* are promising candidate gap genes

Another potential source of gap gene candidates to "fill the gap" in the series are the genes of the neuroblast timer network. 'Neuroblasts' are stem cells that give rise to the majority of the central and peripheral nervous system in insects during embryogenesis and later development. In *Drosophila*, each neuroblast gives rise to a number of different kinds of daughter cells in a stereotyped order (reviewed in Brody and Odenwald, 2005). To co-ordinate this process, the neuroblast sequentially expresses four TFs known as neuroblast timer genes – *hb*, *Kr*, *nubbin* (*nub*) and *castor* (*cas*) - that regulate the sequential assignment of fates to neuroblast progeny (Figure 1.7A) (reviewed in Brody and Odenwald, 2005). The same series is expressed during neuroblast development in *Tribolium* (Biffar and Stollewerk, 2014), indicating that this is likely a conserved feature of at least the higher Holometabola. Two of

these genes, *hb* and *Kr*, act as gap genes during segmentation in *Drosophila* and other arthropods, as discussed previously. However, *nub* and *cas* are also expressed in the ectoderm during segment patterning in *Drosophila*, in broad, gap-like domains (Cockerill et al., 1993; Fisher et al.; Isshiki et al., 2001; Mellerick et al., 1992). In fact, the *nub* gene appears to be regulated by other gap genes, and *nub* mutants even display disruptions in abdominal segment patterning (Cockerill et al., 1993; Ma et al., 1998). Despite this, *nub* has traditionally been considered a "gap-like" gene in *Drosophila*, sitting one tier below the 'real' gap genes, as it is apparently unable to influence the expression of other gap genes (Cockerill et al., 1993; Jaeger, 2011) or Hox genes (Hrycaj et al., 2008). In contrast, in the sequentially-segmenting insect *Oncopeltus*, *nub* seems to be required for abdominal Hox expression, but not segment patterning (Hrycaj et al., 2008). *nub* is therefore theoretically capable of regulating both segment patterning and segment identity, as the canonical *Drosophila* gap genes do. In contrast, *cas* is a slightly less promising gap gene candidate, as mutants show no obvious axial phenotype in *Drosophila* (Mellerick et al., 1992); however, data on *cas* expression and function from outside of *Drosophila* is sorely lacking.

Interestingly, the spatial sequence of expression of the four neuroblast timer genes along the *Drosophila* axis is identical to the temporal order in which they are expressed in neuroblasts (Isshiki et al., 2001) (Figure 1.7B). This similarity has led to the intriguing proposal that the two networks may share an evolutionary history, being co-opted for use from one context to another (Isshiki et al., 2001; Peel et al., 2005). Certain elements of the neuroblast timer series are extremely ancient; for example, the Hb homologue Ikaros and Cas homologue Casz1 are required for the generation of early- and late-born neuronal daughter cells, respectively, in mice (Alsiö et al., 2013; Elliott et al., 2008; Mattar and Cayouette, 2015; Mattar et al., 2015). In addition, *hb* and *Kr* are known to be expressed in the neural progenitors of non-insect arthropods, even in species where they are not expressed in a gap-like pattern (Chipman and Stollewerk, 2006; Kontarakis et al., 2006). This suggests that the neural role of these genes likely predates a role in segment patterning.

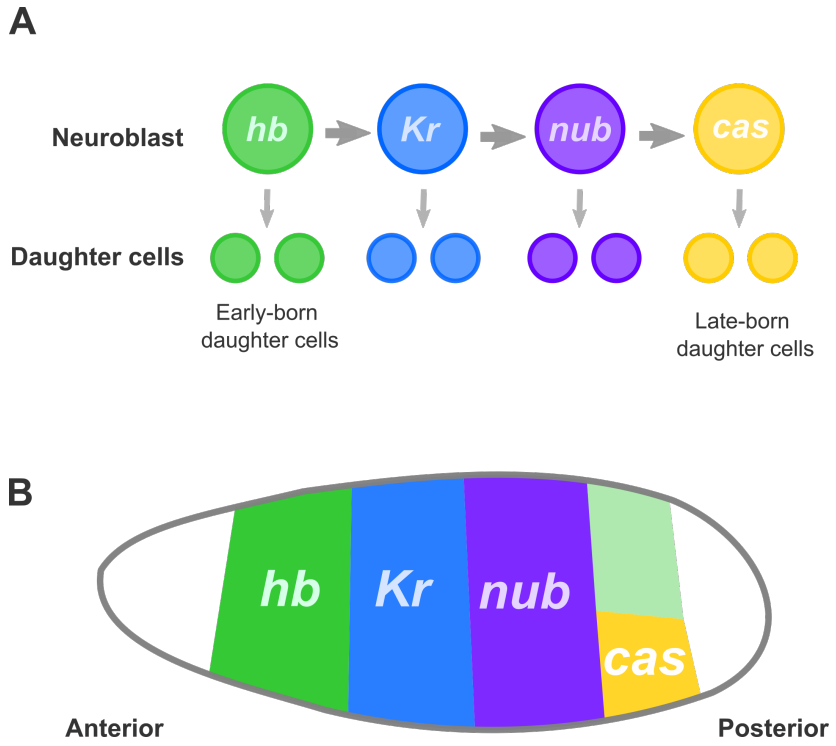

Figure 1.7. The genes of the neuroblast timer series (*hb*, *Kr*, *nub* and *cas*) are expressed sequentially in neuroblasts to drive the sequential assignment of daughter cell fates (A). They are also expressed in the same spatial order in broad domains along the length of the AP axis in *Drosophila* embryos (B). Note that there is also an additional posterior domain of *Dm-hb* expression, represented here in light green, which overlaps with *Dm-cas* expression.

1.7. The definition of a gap gene

The prospect of identifying additional gap genes begs the question of how, exactly, this class of genes can be defined outside of *Drosophila*. As discussed in section 1.1, gap genes were initially defined simply by their characteristic 'gap' phenotype, in which several contiguous segments of the embryo are deleted. However, this definition excludes genes that are now considered to be gap genes – for example, *gt*, which does not produce canonical gap phenotypes when mutated on its own due to redundancy with other gap genes (Capovilla et al., 1992) – as well as including genes that are now not considered to be gap genes – for example, *unpaired* and *hopscotch* (Akam, 1987). This is because the title of 'gap gene' was repurposed to refer specifically to the subset of genes that interact as part of a discrete network, occupying a distinct level of the segmentation hierarchy (the "gap gene network"). As it turns out, the similar phenotypes generated from mutants of these genes also reflect similar underlying molecular properties – all of the *Drosophila* gap genes are able to interact directly with pair-rule and Hox gene cis-regulatory elements to regulate gene expression (reviewed in Jaeger, 2011). The title of gap gene in *Drosophila* therefore describes a discrete group of genes that can be linked both by network and by molecular function. The shared mutant phenotype is simply an unreliable proxy for more meaningful similarities.

Homologues of *Drosophila* gap genes appear to play broadly analogous roles during segment patterning, and to interact as part of a network, in other insects. It is therefore reasonable to theorise that there may be networks of genes equivalent to the "gap gene network", with similar overarching functions, in other insects. It is possible that the roles of individual genes in the network will differ and vary between each other and between species, even if the emergent function of the network remains conserved. For the purposes of this work, I will be defining a gap gene as **any gene that interacts with homologues of at least some *Drosophila* gap genes, in a discrete network that regulates segment formation and/or segment identity**. In practise, given how little is known about the molecular interactions between gap genes and their targets outside of *Drosophila*, I will be using expression patterns and phenotypes as proxies for gap gene identification – specifically, if the expression of a gene overlaps with the expression of a known gap gene (so that direct interaction is theoretically possible), and its knockdown results in misexpression of other gap genes **and** disruptions in segment formation or diversification, then I will consider it to be a strong candidate for a gap gene.

1.8. *Tribolium castaneum* as a model for studying the evolution of the gap gene network

Much of the research on the gap gene network in sequentially-segmenting insects has been conducted using the red flour beetle, *Tribolium castaneum* (Boos et al., 2018; Bucher and Klingler, 2004; Cerny et al., 2005; Cerny et al., 2008; Marques-Souza et al., 2008; Peel et al., 2013; Rudolf et al., 2019; Savard et al., 2006; Zhu et al., 2017). *Tribolium* has long been a popular model organism for studies of population ecology, population genetics and quantitative genetics, largely due its ease of culture and its status as a globally distributed pest species of flour and grain products (Brown et al., 2009; Denell, 2008). Over the last four decades it has also become second only to *Drosophila* as a model for studying the evolution of development (reviewed in Brown et al., 2009; Denell, 2008; Schröder et al., 2008). As a beetle, *Tribolium* is, like *Drosophila*, a member of the Holometabola; however, it differs from *Drosophila* in many aspects of development, often displaying features more representative of arthropod development in general. These include a non-involuted head, the presence of external legs in the larva, and, most relevant to this work, a sequential mode of segmentation (Brown et al., 2009).

Current models of sequential segmentation in insects have largely been built on data gleaned from studies on *Tribolium* (Choe et al., 2006; Clark and Peel, 2018; El-Sherif et al., 2012; Sarrazin et al., 2012). Like most insects, *Tribolium* patterns its most anterior segments in the blastoderm, prior to gastrulation – specifically, the three gnathal segments and the first two thoracic segments (Brown et al., 1997; Patel et al., 1994). Despite being patterned at the blastoderm stage, these segments are still patterned sequentially via a pair-rule oscillator mechanism (El-Sherif et al., 2012; El-Sherif et al., 2014), in contrast to *Oncopeltus* where segmentation is more obviously biphasic (segmentation is almost simultaneous in the anterior, and sequential in the posterior) (Liu, 2005). The third thoracic and ten abdominal segments are then patterned sequentially from the SAZ during germband extension (Brown et al., 1994). The final two abdominal segments are fused in the larva to produce the telson, which bears the terminal structures known as urogomphi (dorsally) and pygopodia (ventrally) (Bucher and Klingler, 2004). Elongation appears to rely on both cell rearrangement (Nakamoto et al., 2015; Sarrazin et al., 2012), and localised, temporally restricted cell division in the SAZ (Cepeda et al., 2017).

There is one particular element of segment patterning in *Tribolium* that appears to be less representative of arthropods in general. Neither the Notch ligand *Delta* nor Notch signaling target *hairy* appear necessary for segmentation in *Tribolium* (Aranda, 2006; Aranda et al.,

2008). Other sequentially segmenting insects (for example, *Gryllus*) are also able to form segments in the absence of Notch signaling (Kainz et al., 2011)), but this does differ from the inferred ancestral state for insects (Pueyo et al., 2008) and arthropods as a whole (Eriksson et al., 2013; Stollewerk et al., 2003).

The gap gene network in *Tribolium*

Recent papers (for example Boos et al., 2018; Zhu et al., 2017) consider four trunk gap genes as the canonical set in *Tribolium*: *Tc-hb* (Marques-Souza et al., 2008; Schröder et al., 2000), *Tc-Kr* (Cerny et al., 2005), *Tc-gt* (Bucher and Klingler, 2004) and *Tc-mlpt* (Savard et al., 2006). *Tc-kni* is expressed during segment addition, but has been largely excluded from consideration as a gap gene due to its weak phenotype in the trunk (specifically, there is partial fusion of several segments in the posterior abdomen, well outside of the abdominal domain of *Tc-kni* expression) (Cerny et al., 2008; Peel et al., 2013). Although it is likely that the gap gene function of *Tc-mlpt* relies on interaction with *Tc-svb* (Ray et al., 2019), the latter gene has not yet been officially added to the list of gap genes in *Tribolium*. Knockdown of any one of *Tc-hb*, *Tc-Kr*, *Tc-gt*, *Tc-mlpt* or *Tc-svb* results in both homeotic transformations and early termination of segmentation (Bucher and Klingler, 2004; Cerny et al., 2005; Marques-Souza et al., 2008; Ray et al., 2019; Savard et al., 2006), as is often observed for gap genes in other sequentially-segmenting insects.

As is typical for gap genes in other sequentially-segmenting insects, the gap genes in *Tribolium* are activated sequentially in the SAZ, with each retracting from the posterior as the next gap gene becomes expressed (Boos et al., 2018; Zhu et al., 2017). RNAi experiments have shown that knocking down gap genes that are expressed early in the series can prevent the expression of later gap genes (Zhu et al., 2017), and that ectopic expression of an early gap gene by heat shock leads to ordered expression of the next genes in the series (Boos et al., 2018). These experiments suggest that, within the context of the SAZ, the interactions between gap genes are necessary and sufficient for their ordered expression and subsequently for correct spatial patterning across the germband. The most current published model of the gap gene network in *Tribolium* is shown in Figure 1.8.

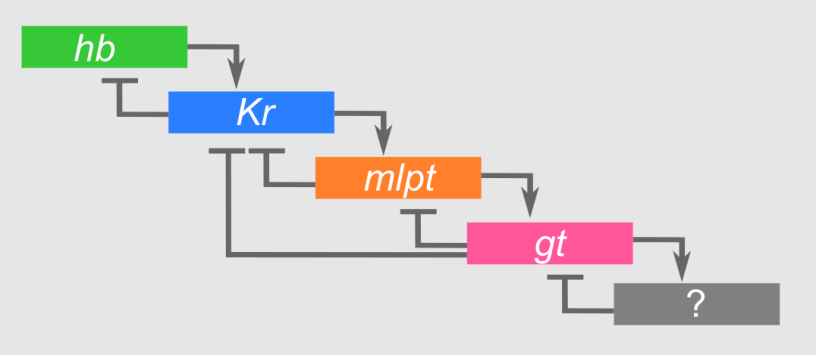

Figure 1.8. A current model of gap gene interactions in *Tribolium*. The relative positions of the coloured bars indicate, in broad terms, the distribution of expression domains along the length of the trunk (with anterior to the left). Based on the expression patterns of these four genes, there are likely additional, as yet unidentified gap genes that are expressed subsequently to *Tc-gt*, as represented by the question mark. Adapted from Zhu et al. (2017).

Although the expression pattern of each of these genes has been described individually, we still lack an understanding of exactly how their expression domains relate to one another, and whether there is a "gap gene gap" in the abdomen when *Tc-mlpt* and *Tc-svb* are taken into account. In addition, preliminary data suggests that both *Tc-nub* and *Tc-cas* are expressed in the SAZ during segment patterning in *Tribolium* (E. Raymond & A. Peel, unpublished; Biffar and Stollewerk, 2014). This raises the possibility that one or both genes act as components of the gap gene network in *Tribolium*, in which case current models of the gap gene network are incomplete.

Given the breadth of the existing literature on gap gene expression and function, and the tractability of *Tribolium* as a model system, this species is a prime candidate as a model for developing a deeper understanding of how the gap gene network functions during sequential segmentation and how it has evolved within the insect clade.

1.9. Aims of this thesis

In this thesis, I aimed to use *Tribolium* as a model to study the evolution and function of the gap gene network, with a focus on similarities to the neuroblast timer series. Specifically, I had three main aims:

1. To describe in more detail the expression patterns and dynamics of the canonical gap genes, and the 'unofficial' gap gene *svb*, in *Tribolium* (Chapter 3).
2. To examine the expression patterns and dynamics of the neuroblast timer genes during segment patterning in *Tribolium* (Chapter 4).
3. To test whether *nub* and *cas* play an active role in axial patterning in *Tribolium* (Chapters 4 and 5).

In accomplishing these aims, I hoped to gain a better understanding of the dynamics of the gap gene series as a whole, and to identify any remaining 'gaps' in the gap gene series; to investigate whether *nub* and *cas* might help to fill these gaps, if they exist; and also to investigate how the genes of the neuroblast timer series relate to the gap gene network in *Tribolium*.

2. MATERIALS AND METHODS

2.1. *Tribolium* husbandry

Tribolium castaneum (San Bernadino strain) were obtained from Andrew Peel, University of Leeds. Beetles were reared at 30 ºC in plastic boxes (with mesh windows in the lid to allow for air flow), on a coarse flour made by mixing 1 kg organic wholemeal flour (Doves Farm Organic Wholemeal Flour), ~50g of yeast (Sainsbury's Fast Action Dried Yeast Sachets) and 5 g of the antifungal agent Fumagillin-B (Medivet). Wholemeal flour was sieved using an 800 µm steel sieve (Retsch test sieve 200 mm x 50 mm) before mixing to remove large particles. Incubators were maintained between 40-60 % RH (relative humidity) where possible. For egg collection, beetles were removed from the coarse flour mix using an 800 µm steel sieve (Retsch test sieve 200 mm x 50 mm) and moved onto organic white flour (Doves Farm Organic Strong White Bread Flour). Eggs could then be separated from the white flour using a 300 µm steel sieve (Retsch test sieve 200 mm x 50 mm). More details on *Tribolium* husbandry can be found in The Beetle Book (Bucher, 2009).

2.2. Embryo dechorionation and fixation

Collected eggs were transferred into small mesh baskets (with a mesh aperture of 250 µm) and were rinsed several times in ddH_2O to remove all traces of flour. Their chorions were then removed by washing twice in bleach (Fisher Scientific, #10527752), diluted with ddH_2O to a final concentration of 2.5 % (v/v) hypochlorite, for 30-45 seconds. Eggs were rinsed in ddH_2O again and transferred using a paintbrush into glass vials containing 6 mL heptane and 3 mL of PBT (phosphate buffered saline + 0.01 % (v/v) Tween-20) containing 4 % (v/v) formaldehyde. Vials were rocked on a nutator for 30 minutes to allow for fixation to occur. The lower phase of the fixative (PBT + formaldehyde) was removed, and 8 mL of ice-cold methanol added. Eggs were devitellinised by first shaking the vials and then by repeatedly forcing the eggs through a 19G BD Microlance surgical needle (Medisave, #ND500) using a syringe (removing devitellinised embryos from the bottom of the vial using a glass pipette between attempts). Devitellinised eggs were then rinsed several times in 100 % methanol and stored at -20 °C.

2.3. Ovary dissection and fixation

Shannon Taylor (University of Otago, New Zealand) assisted with the ovary dissections from adult *Tribolium*. Ovaries were removed from sedated females in PBS using Dumont number 5 Dumostar Biologie forceps (Fine Scientific Tools, #11295-10). Dissected ovaries were transferred directly into Eppendorf tubes containing 4 % formaldehyde in PBT on ice. An equal volume of heptane was added, and the tubes then rocked on a nutator for 20 minutes to allow for fixation. The ovaries were then rinsed several times in PBT and then washed into 100% methanol for storage at -20 ºC.

2.4. Hybridisation Chain Reaction (HCR) *in situ* hybridisation (ISH)

Version 3 HCR probes (Table 1) and fluorescently-labelled hairpins were ordered from Molecular Instruments (https://www.molecularinstruments.com) using NCBI or BeetleBase mRNA sequences as references. For each gene, 20 pairs of short probes were ordered, as per recommendations by Molecular Instruments. All required buffers were made according to the instructions provided by Molecular Instruments, with the one exception that the percentage of dextran sulfate in the probe hybridisation and amplification buffers was reduced from 10 % (v/v) to 5 % (v/v) to reduce viscosity and improve retention of embryos during washes.

Fixed embryos or ovaries were prepared for HCR by removing methanol and replacing it with 1 mL of PBT containing 4 % formaldehyde. Tubes were rocked on the nutator for 30 minutes to allow for additional fixing and rehydration to occur. The HCR was then carried out as per the Molecular Instruments protocol for whole-mount fruit fly embryos (Version 3.0) (https://files.molecularinstruments.com/MI-Protocol-HCRv3-FruitFly-Rev5.pdf), with the exception that the amount of hybridisation, wash and amplification buffers used for each tube of embryos was halved (to 100 µL) and the volume of probes and hairpins adjusted to give the same final concentration (4 nM/mL). Additionally, 1 ng/µL DAPI was added to the first 30 minute wash on the final day so that nuclear staining could be carried out in parallel. After washing, embryos or ovaries were transferred first into 25 % (v/v)glycerol and then into 50 % (v/v) glycerol before being stored at 4 ºC for mounting.

Table 1. HCR probes ordered from Molecular Instruments and the reference sequences that were provided as templates.

Organism	Gene	Initiator(s)	Reference sequence
Tribolium castaneum	*Tc-Wingless*	B1, B3, B4, B5	NM_001114350.1
	Tc-Toll10	B2, B5	TC004901
	Tc-even-skipped	B2	NM_001039449.1
	Tc-caudal	B1	XM_008193508.2
	Tc-single-minded	B1, B3, B4	XM_008200873.2
	Tc-engrailed	B5	NM_001039422.2
	Tc-distalless		AF317551.1
	Tc-twist	B3	TC014598
	Tc-hunchback	B2, B4	NM_001044628.1
	Tc-Krüppel	B1, B5	NM_001039438.2
	Tc-mille-pattes	B5	NM_001134483.1
	Tc-shavenbaby	B3	XM_008193917.2
	Tc-giant	B3	NM_001039442.1
	Tc-knirps	B4	NM_001128495.1
	Tc-tailless	B3	NM_001039413.1
	Tc-nubbin	B4, B5	XM_015979462.1
	Tc-castor	B1	XM_015980923.1
	Tc-grainyhead	B5	XM_015978959.1
	Tc-labial	B3	NM_001114290.1
	Tc-proboscipedia	B2	NM_001114335.1
	Tc-deformed	B1	NM_001039421.1
	Tc-Sex combs reduced	B4	NM_001039434.1
	Tc-Antennapedia	B5	NM_001039416.1
	Tc-Ultrabithorax	B1	XM_008203013.2
	Tc-abdominal A	B2	NM_001039429.1
	Tc-Abdominal B	B3	NM_001039430.1
Drosophila melanogaster	*Dm-Wingless*	B1, B4	NM_078778.5
	Dm-odd-skipped	B1	NM_164546.2
	Dm-nubbin	B5	NM_001103683.2
	Dm-abdominal A	B3	NM_001260216.2

2.5. Mounting and imaging of embryos and adult tissue after HCR ISH

Embryos, ovaries or gut tissue suspended in 50 % (v/v) glycerol were transferred into watch glasses for examination under a dissecting microscope. From there, blastoderm-stage embryos were transferred to glass-bottomed petri dishes (Cellvis, #D35-14-1.5-N) using a cut-off plastic pipette tip. Excess glycerol was then removed, and ProLong™ Gold Antifade Mountant (ThermoFisher Scientific) added to cover the embryos. Germband embryos had to be dissected away from the yolk under a dissecting microscope using tungsten needles. Sharpened tungsten needles were produced using tungsten wire (Fisher Scientific, 0.375mm, #11390548) and a sodium nitrite stick (McCrone UK). The tungsten wire was repeatedly heated in a Bunsen flame and then run against the sodium nitrite stick to generate a fine tip, as demonstrated here: https://www.youtube.com/watch?v=WvepYAwiKU8 ("Hooke College: Making and Repairing Tungsten Needles. Accessed July 20th, 2020). Germband embryos were then transferred to a glass microscope slide and the remaining yolk gently removed using a paintbrush hair and an eyelash hair mounted in 240B Pin Vises (Starrett, #51137). Yolk-free embryos were transferred into ProLong™ Gold Antifade Mountant on a fresh slide and covered with a coverslip. Ovaries and gut tissue were flat mounted on glass slides in ProLong™ Gold Antifade Mountant under a coverslip. All slides and dishes using for mounting were left at room temperature in the dark to set for 1-2 days prior to imaging and subsequently stored at 4 ºC. Mounted embryos or adult tissues were imaged on an Olympus FV3000 confocal microscope at the Department of Zoology Imaging Facility (University of Cambridge). Image stacks of 10-50 focal planes (z-step size of 0.5-3 µm) were taken using 20x/0.75NA dry, 30x/0.95NA silicone oil or 60x/1.4NA silicone oil immersion objectives.

2.6. RNA extraction and cDNA synthesis

Total RNA was extracted from 0-48 hour old embryos using TRIZol reagent (ThermoFisher Scientific, #15596026) as per the manufacturer's instructions, with the exception that a butanol wash was carried out following RNA precipitation (but prior to the 75% ethanol wash) to further clean the RNA. RNA quality was examined on a 1 % (w/v) agarose gel, using the sharpness and relative intensity of the 28S and 18S rRNA bands as a proxy for overall RNA quality. cDNA synthesis was carried out using the Superscript First-Strand Synthesis System for RT-PCR kit (Invitrogen, #18080-051), according to the manufacturer's instructions. Oligo(dT) primers were used.

2.7. *Tribolium* gene cloning

Although HCR ISH probes could be ordered directly from Molecular Instruments, any genes to be targeted by dsRNA had to be manually cloned. Clones for many of the genes that I planned to target using RNAi were provided by Andrew Peel and Rahul Sharma (University of Leeds), but I cloned *Tc-mille-pattes* (*Tc-mlpt*) and *Tc-shavenbaby* (*Tc-svb*) myself (Table 2). (Additional genes cloned but not eventually used for experiments in the thesis are listed in Appendix 1). Both genes have previously been cloned (Ray et al., 2019; Savard et al., 2006). Predicted mRNA sequences for *Tc-mlpt* (AM269505.1) and *Tc-svb* (XM_008193917.2) were used to design the primers indicated in Table 2 with the aid of the primer design web-interface Primer-Blast (NCBI). Fragments of the *Tc-mlpt* and *Tc-svb* mRNA sequences (477bp and 566bp, respectively) were amplified from embryonic cDNA (0-48 hour old embryos) by PCR using the Phusion® High-Fidelity PCR Kit (New England BioLabs). PCR products were purified using the QIAquick PCR Purification Kit (Qiagen) and ligated into the vector pGEM®-T Easy using the pGEM®-T Easy System (Promega, #A1360) according to manufacturer's instructions (using 50 µg/mL carbenicillin as a selection agent). The ligation mixture was transformed into NEB® 5-alpha Competent *E.coli* (Subcloning Efficiency) (New England BioLabs) according to manufacturer's instructions. Blue-white selection and subsequent PCR colony screening using M13F and M13R primers was used to identify colonies with the correct size insert. Positive colonies were grown up in 5 mL of liquid culture with 50 µg/mL carbenicillin at 37 ºC on a shaker (~225rpm) overnight, and plasmid extracted from the liquid cultures using the QIAprep Spin Miniprep Kit (Qiagen) according to manufacturer's instructions. Sanger sequencing of inserts was carried out by Source Bioscience to confirm identity and sequence fidelity.

Table 2. Source of cloned genes and the primers used to clone them. All genes were cloned into the pGEM®-T Easy vector. AP = Andrew Peel (University of Leeds), GB = Gregor Bucher (University of Göttingen), RS = Rahul Sharma (University of Leeds).

Gene	Source	Primers (5'-3')
GFP	AP	F: ATGGGTAGTAAAGGAGAAGAACTTT
		R: GGGATTACACATGGCATGGA
Tc-hunchback	AP	F: TGGCAATTCGGCGTTTCCCAGA
		R: TGCAAGTGAACGGGTTGTGGAA
Tc-Krüppel	AP	F: GCTGGACTCTCAGGAGAAGA
		R: CTTTCCACCTTGAAACCGATAAAG
Tc-mille-pattes	Cloned myself	F: GCGAGTCGTGCCAAGTTATG
		R: ACTGAGTGTCATTCTTAAGGAACTT
Tc-shavenbaby	Cloned myself	F: CTTACAGTTCACCGCCACCT
		R: CCAACTGCAACAGCAACCTG
Tc-giant	RS	F: AATACAGCCCCGTCTCTAATAGC
		R: CTGTAGCTTCTCCAGCTCCTTC
Tc-knirps	AP (originally GB)	Not recorded – fragment sequence available on request
Tc-nubbin 5' fragment	AP	F: CGTCAGCACGGCAAAGAA C
		R: CCTCCTCCTCGGAGCTAC
Tc-nubbin 3' fragment	AP	F: CGCCCACAACAACTTCAA C
		R: GGGTATGTCAGTCTAATGTTTGTAGA
Tc-castor	AP	F: CCACATCAAAGACGAGCAACT
		R: CCACACTTCAATGACCCGATT

2.8. Double-stranded RNA synthesis

Double-stranded RNA (dsRNA) was prepared as per The Beetle Book (Bucher, 2009), except that dsRNA was purified using a phenol-chloroform extraction and precipitated with isopropanol (instead of lithium chloride). dsRNA was resuspended in 20 µL nuclease-free water and a 1:20 dilution used to examine RNA quality by running on an agarose gel (checking for a sharp, clear band of approximately the right size), and to examine concentration and quality on a Nanodrop™ spectrophotometer. Aliquots of stock dsRNA were stored at -80 ºC or at -20 ºC while in use. *Tc-odd-skipped* dsRNA was provided by Andrew Peel.

2.9. Parental RNAi in *Tribolium*

Injection of dsRNA or water into adult females was carried out as described by Posnien et al. (2009). Specifically, injections were performed through the dorsal abdomen, under the elytra. Needles for microinjection were prepared on a needle puller (Sutter Instrument Co. Model P-87) using borosilicate glass capillaries with an outer diameter of 1 mm, an inner diameter of 0.58 mm and an internal filament (Warner Instruments, model number G100F-4). Before use, the tips were broken using forceps to produce an opening approximately 50 μM in diameter, and then bevelled at an angle of 30 ° using a microgrinder (Narishige, EG-4) to produce a smooth, angled opening. Needles were backloaded using Microloader™ tips (Eppendorf, #5242956003). Pressure for microinjection was supplied by nitrogen gas and regulated with a Pico-injector system (Medical Systems Corporation, model number PLI-100). dsRNA diluted in nuclease free water was injected at a concentration of 0.5-4 μg/μL. dsRNA was centrifuged for 2 minutes at 13,000 RPM before injection to pull particulates out of solution and reduce the risk of blockage.

Post-injection, female beetles were left to recover at 30 ºC for a few hours in petri dishes containing a small section of tissue paper (to aid in drying any efflux from the wound site). They were then moved onto coarse flour mix (described in section 2.1) in a plastic box with a mesh window and left to recover overnight at 30 ºC. Male beetles were added in the next day. Eggs were then collected by shifting beetles onto white flour as described in section 2.1. Eggs were collected regularly (every 1-2 days) for 3-4 weeks after injection and used for cuticle preparations (as described below in section 2.10) or fixed for HCR ISH (as described in section 2.4).

2.10. Cuticle preparation after pRNAi

0-24 hour old eggs were collected and left to develop in petri dishes at 30 ºC for up to 10 days (hatching normally occurs after 3-4 days (Bucher, 2009)). As larvae hatched, they were removed and processed for cuticle preparation. Larvae were first rinsed in 2.5 % (v/v) bleach to remove flour particles. They were then rinsed several times in water and transferred using a paintbrush to a clean glass slide. Larvae were then covered with a droplet of 1:1 Hoyer's medium (Dahmann, 2008):lactic acid and a coverslip, and heated at 60 ºC until cleared. Image stacks of 10-50 focal planes (z-step size of 1-5 μm) were taken using the 10x/0.4NA or 20x/0.75NA dry objectives on the Olympus FV3000 in the Department of Zoology (University of Cambridge).

2.11. Embryonic RNAi in *Tribolium*

My embryonic RNAi procedure for *Tribolium* is a modified version of the protocols published by Posnien et al. (2009) and Berghammer et al. (2009), adapted by myself and Matt Benton (University of Cambridge). 0-1 hour old eggs were collected and aged for an additional hour at 30 ºC to ensure that all eggs would be at least one hour old. They were then transferred into small mesh baskets (with a mesh aperture of 250 μm) and rinsed several times in ddH_2O. Chorions were removed by washing twice in bleach, diluted with ddH_2O to a final concentration of ~0.6% (v/v) hypochlorite, for 30-45 seconds. Eggs were rinsed again and then transferred using a cut-off glass pipette tip to a glass slide for sorting under a dissecting microscope. Apparently viable eggs were transferred onto 25 mm x 40 mm coverslips and arranged into two lines along the long axis, with the anterior end of the egg facing outwards. Traditionally *Tribolium* embryos are injected 'dry', as they are able to tolerate some degree of desiccation (Berghammer et al., 2009; Posnien et al., 2009). However, we encountered issues with survival using this approach, and opted instead to cover embryos in a halocarbon oil mix, made up of 50% Halocarbon oil 700 (Sigma Aldrich, #H8898-100ML) and 50% Halocarbon 27 (Sigma Aldrich, #H8773-100ML).

Needles were prepared and loaded, and dsRNA prepared, as described in section 2.9, save that the needles were not broken using forceps, and instead were bevelled at an angle of 30 ° to give as small a tip diameter as possible. For double or triple knockdown, dsRNAs were combined before injection. Pressure for microinjection was supplied by nitrogen gas and regulated with a Pico-injector system (Medical Systems Corporation, model number PLI-100).

Injection and balance pressure were initially set to 40 and 1 psi, respectively, and adjusted on a case-by-case basis. Needles were inserted into the anterior pole of the egg (the presumptive serosa) to reduce the risk of damage to the embryo proper (Posnien et al., 2009). A footswitch was used to determine injection duration, rather than the internal clock. The size of the efflux of cytoplasm from the egg was used as a measure for consistency in injection volume.

To prevent spreading of the halocarbon oil post-injection (which we found to reduce survival, presumably through exerting pressure on the egg surface), the coverslips used for injection were prepared with 'feet' attached at either end. These feet were made of sections of #1 coverslip cut with a Fisherbrand™ Diamond Tip Pencil (Fisher Scientific). Sections of coverslip were attached to each other and to the base coverslip using UV curable resin (Sigma Aldrich, #900164-250G) set under a UV LED nail dryer lamp. Each 'foot' was approximately 450 μm thick. Turning the coverslip onto the oxygen-permeable membrane of a Lumox tissue culture dish (Sarstedt, #94.6077.305) limits the spread of the halocarbon oil mix while still permitting the embryos to breathe. The feet on the coverslip create space to prevent pressure on the embryos as they develop. Lumox dishes with coverslips on top were placed into plastic containers containing damp tissue paper (to maintain humidity) and placed into a 30 ºC incubator to develop. Embryos were then processed for either cuticle preparation (section 2.12) or HCR ISH (section 2.13).

2.12. Cuticle preparation after eRNAi

Eggs were left to develop for approximately 7 days, to allow time for development of cuticle in eggs which might be developmentally delayed. The coverslip was then carefully removed from the Lumox dish membrane using forceps and placed egg-side up onto a glass slide. Cuticles were dissected out of the chorion using sharpened tungsten needles (described in section 2.4) if necessary. Cuticles were then transferred into watch glasses and submerged in heptane and then ethanol for one hour each, to help disperse the oil on their surfaces. Cuticles were moved from ethanol to a clean slide using a cut-off pipette tip and the ethanol allowed to evaporate. A droplet of 1:1 Hoyer's medium:lactic acid was added and the cuticles subsequently baked and imaged as per section 2.10.

2.13. Preparation of eRNAi embryos for HCR ISH

Eggs were left to develop for the desired amount of time on Lumox dishes at 30 ºC. The coverslip was then carefully removed from the Lumox dish and turned onto a glass slide. Embryos were injected with a PBT + 10 % (v/v) formaldehyde solution using the microinjection protocol described in section 2.11 and left to fix at room temperature for one hour. Without this 'pre-fix', embryos are liable to burst as they are transferred from the slide into fixative. After an hour, embryos were transferred using a paintbrush into eppendorf tubes containing 500 µL of heptane and 500 µL of PBT + 4 % (v/v) formaldehyde. These tubes were rocked on a nutator for one hour to allow for further fixing. The bottom phase of solution (4 % formaldehyde) was then removed, and 500 µL of ice-cold methanol added. The chorion and vitelline membrane were then removed either by passing embryos vigorously through a needle, as described in section 2.2, or by manual dissection. I opted for the latter, as in my hands it resulted in a better yield of intact embryos. I left embryos overnight in fresh 100 % methanol (to improve tissue stiffness) before dissecting in PBT using sharpened tungsten needles. Dissected embryos were then kept in 100 % methanol at -20 ºC until required for HCR ISH.

2.14. *Drosophila* husbandry and HCR

Drosophila were reared and embryos collected at 25 ºC according to standard protocols (Dahmann, 2008). Two mutant lines (both *pdm1/pdm2* null mutants) were used in my research; Df(2L)GR4/CyO (Bloomington #8857) and w^{1118};Df(2L)ED769/SM6a (Kyoto #150100). Wild-type flies were Oregon-R. HCR ISH was carried out as per section 2.4. After HCR ISH, embryos were flat mounted in ProLong™ Gold Antifade Mountant and imaged on the Olympus FV3000 as per section 2.5.

2.15. Image processing and figure assembly

Images and Z stacks were stitched using the Olympus FV3000 software. Additional image processing was carried out in Fiji (Schindelin et al., 2012). To account for an alignment issue between dichroic mirrors on the Olympus FV3000 in our department, channel alignment was corrected using a Fiji plugin created by Matt Wayland (https://github.com/WaylandM/dichroic-mirror-offsets). Fiji was used to adjust image brightness and contrast, and to rotate, crop and reslice images where necessary. The Spectral

Unmixing plugin, made by Joachim Walter (https://imagej.nih.gov/ij/plugins/spectral-unmixing.html), was used to remove bleedthrough from selected channels in images or Z stacks where necessary. Figures were assembled in the open source vector graphics editor Inkscape (https://inkscape.org).

3. EXPRESSION DYNAMICS OF CANONICAL GAP GENES IN *TRIBOLIUM*

3.1. INTRODUCTION

3.1.1. Limitations of existing gap gene expression data for *Tribolium*

The expression patterns of six trunk gap and gap-like genes – *Tc-hb*, *Tc-Kr*, *Tc-mlpt*, *Tc-gt*, *Tc-kni* and *Tc-svb* – have been examined in *Tribolium* (Bucher and Klingler, 2004; Cerny et al., 2005; Cerny et al., 2008; Marques-Souza et al., 2008; Peel et al., 2013; Ray et al., 2019; Savard et al., 2006). However, these analyses have invariably been carried out using colorimetric *in situ* hybridisation (ISH), which presents several limitations for describing gene expression thoroughly.

Firstly, when genes are expressed in overlapping domains, the chromogenic products utilised in colorimetric ISH can be hard to distinguish, making expression boundaries difficult to pinpoint. This is obviously a drawback when considering the densely overlapping domains of gap genes. A second, related issue is the ease of multiplexing, or visualisation of multiple gene products in a single embryo. In colorimetric ISH, chromogens are typically applied one after the other in sequential enzymatic reactions. This increases the time required for visualising increasing numbers of gene products in a single ISH, but more importantly, finding multiple reactions that are both compatible and produce distinctive chromogenic products can represent a significant hurdle. Together, these considerations have meant that analysis of gap gene expression in *Tribolium* has typically been in single or double ISHs, making it difficult to piece together the relative expression of all of the genes in the series.

Tribolium presents an additional problem for colorimetric ISH approaches compared to *Drosophila*, due to its more convoluted morphogenesis. During gastrulation, the *Tribolium* embryo becomes a complicated multi-layered structure, with a flattened epithelial tube (consisting most dorsally of cells destined to become the amnion, and laterally and ventrally of the ectoderm proper) sitting atop the mass of mesoderm. Many segmentation genes are expressed in rings around the entire epithelial tube, and additionally in the underlying mesoderm. Delays in patterning between the different tissue layers, and a slight dorsal bias in the position of the posterior patterning centre of the embryo, mean that the expression domains

for segmentation genes may appear to be 'out of sync' when viewed from above (for example, see the supplementary material of Benton et al. (2016) regarding *Toll* gene expression). Such discrepancies can obscure the boundaries of gene expression domains unless embryos are viewed in physical or optical sections. The former is laborious, and the latter is impossible unless alternative detection methods, such as fluorophores, are used. Fluorescent ISH (FISH) can be used in *Tribolium* (Sprecher, 2020 and personal experience), but still presents issues for multiplexing, as standard methods still rely on sequential enzymatic reactions for addition of fluorescent tags to gene products.

3.1.2. Hybridisation chain reaction as a method for multiplexed *in situ* hybridisation

Within the last five years, a widely adopted technique known as Hybridisation Chain Reaction (HCR) *in situ* hybridisation (Choi et al., 2018) has circumvented many of the difficulties of multiplexed visualisation of gene expression. In this technique, each gene product is targeted by a set of short nucleic acid probe pairs, usually between 10-20 per gene. Each of these probe pairs consists of two short ssDNA sequences (25bp long), both tagged with complementary halves of an 'initiator' sequence. If either member of the probe pair binds at an off-target site, the partial initiator sequence remains inert and the reaction stalls. However, when each member of a probe pair binds correctly to adjacent sites, the partial initiator sequences are also are brought into close contact. The complete initiator sequence can then trigger the unfolding and polymerisation of fluorescently-tagged DNA hairpins that are added subsequently, leading to amplification of fluorescent signal along the length of a gene product of interest. The most significant benefit of this technique is that probes for different gene products can be tagged with different initiators and detected by hairpins tagged with different fluorophores. The specificity of these interactions means that targeting and detection of multiple genes can be done in parallel rather than sequentially. Currently, up to five gene products can be detected in a single sample using the commercially provided initiators and hairpin sets.

One of my first aims during my PhD was therefore to use this new potential for easy multiplexed analysis of gene expression to create a thorough description of gap gene expression in *Tribolium*. In particular, I wanted to produce a centralised description of the current gap and candidate gap genes against a standardised marker gene (discussed further in section 3.1.3); and also to use multiplexed expression data to confirm or refute the existence of a 'gap gene gap'.

3.1.3. *Toll* genes as putative spatial and staging markers

In arthropods, segment polarity genes such as *Wingless* (*Wg*) or *engrailed* (*en*) are commonly used to track the progress of segmentation and, by extension, the stage of embryonic development (e.g. Auman et al., 2017; Nakamoto et al., 2015). They may also be used as spatial markers for describing gene expression patterns (e.g. Savard et al., 2006; Serano et al., 2016). However, they become expressed only as parasegment boundaries are set, and therefore provide little spatial information within the pre-segmental SAZ. To account for this, many researchers use a combination of segment polarity genes and pair-rule genes (such as *even-* or *odd-skipped*, abbreviated *eve* and *odd*) for staging or spatial information (e.g. Cerny et al., 2005; Kainz et al., 2011). Pair-rule genes are typically expressed in dynamic stripes in the SAZ (reviewed in Clark et al., 2019), marking the early stages of parasegment boundary formation and allowing temporal differentiation of embryos with the same number of mature parasegments. Unfortunately, the expression of these genes typically fades outside of the SAZ (e.g. Auman and Chipman, 2018; Green and Akam, 2013), and so the two markers must be used together if comprehensive spatial mapping and/or precise staging are needed. This represents an inconvenience for protocols where the number of genes that can be detected is limited.

The *Toll* genes provide a potential alternative to a segment polarity/pair-rule gene marker system. *Toll* genes encode transmembrane receptors that play a range of roles in development and immunity in both invertebrates and vertebrates (reviewed in Leulier and Lemaitre, 2008). In *Drosophila*, a subset of the *Toll* genes are expressed in stripes along the anterior-posterior axis of the embryo as readouts of the pair-rule gene network (Graham et al., 2019), where they act to promote cell intercalation and therefore convergent extension (Paré et al., 2014). This role seems to be conserved broadly across the arthropods (Benton et al., 2016).

Tribolium has 9 *Toll* genes (Zou et al., 2007), two of which (*Tc-Toll7* [*Tc-Tl7]* and *Tc-Toll10* [*Tc-Tl10*]) are expressed in stripes along the AP axis during segment formation (Benton et al., 2016). Starting at the blastoderm stage, 'primary' stripes with double segmental periodicity arise dynamically in the SAZ in a similar manner to pair-rule genes (Benton et al., 2016). 'Secondary' segmental stripes later arise in the maturing segments of the germband, and both are maintained throughout the course of segment addition (Benton et al., 2016). The expression patterns of *Tc-Tl7* and *Tc-Tl10* have been broadly examined alongside the segment polarity gene *Tc-Wg* and the pair-rule gene *Tc-eve* (Benton et al., 2016). Of the two, *Tc-Tl10* provides a more promising spatial marker, as its primary stripes appear to neatly abut the

boundaries of odd-numbered parasegments (unlike *Tc-Tl7*, which overlaps even-numbered parasegment boundaries) (Benton et al., 2016). Because it is expressed in both the SAZ and the segmented germband, *Tc-Tl10* has the potential to be an excellent, stand-alone spatial and staging marker.

3.1.4. Specific aims

To begin my research, I aimed to produce a dataset of multiplexed and finely staged gap gene expression in *Tribolium* embryos, covering the entire period of segment addition (approximately 8-22 hours AEL at 30 °C), using HCR ISH. I utilised two markers – *Tc-Wingless (Tc-Wg)* and *Tc-Tl10* – as a staging and spatial mapping system, described in section 3.2.1 (note that due to unforeseen complexities in *Tc-Tl10* expression, this section is rather dense, and it might be useful to simply skim it on first reading in order to focus on the following description of gap gene dynamics) . In section 3.2.2, I present a full staged series of expression for each of the previously described trunk gap genes in *Tribolium* (*Tc-hb*, *Tc-Kr*, *Tc-gt*, *Tc-kni* and *Tc-mlpt*), as well as the candidate gap gene *Tc-svb*. I describe their expression dynamics relative to my spatial and staging markers. Finally, in section 3.2.3, I present multiplexed expression data for the gap and candidate gap genes. From this data, I evaluate the likelihood of previously predicted interactions and infer additional possible interactions.

3.2. RESULTS

3.2.1. Development of a temporal and spatial mapping system

Validation of *Tc-Tl10* as a spatial and staging marker

I first examined the expression of *Tc-Tl10* against *Tc-Wg* and *Tc-eve* in staged embryo collections using HCR to confirm that its relationships to parasegmental boundaries are consistent across the course of segment maturation and between different parasegments. *Tc-cad* expression was also included in these HCRs as a marker for the posterior SAZ. Information about the relative phasing of *Tc-Tl10* stripes in each embryo was abstracted into a graphical format as shown in Figure 3.1. The process of *Tc-Tl10* stripe maturation is described in more detail in the text that follows.

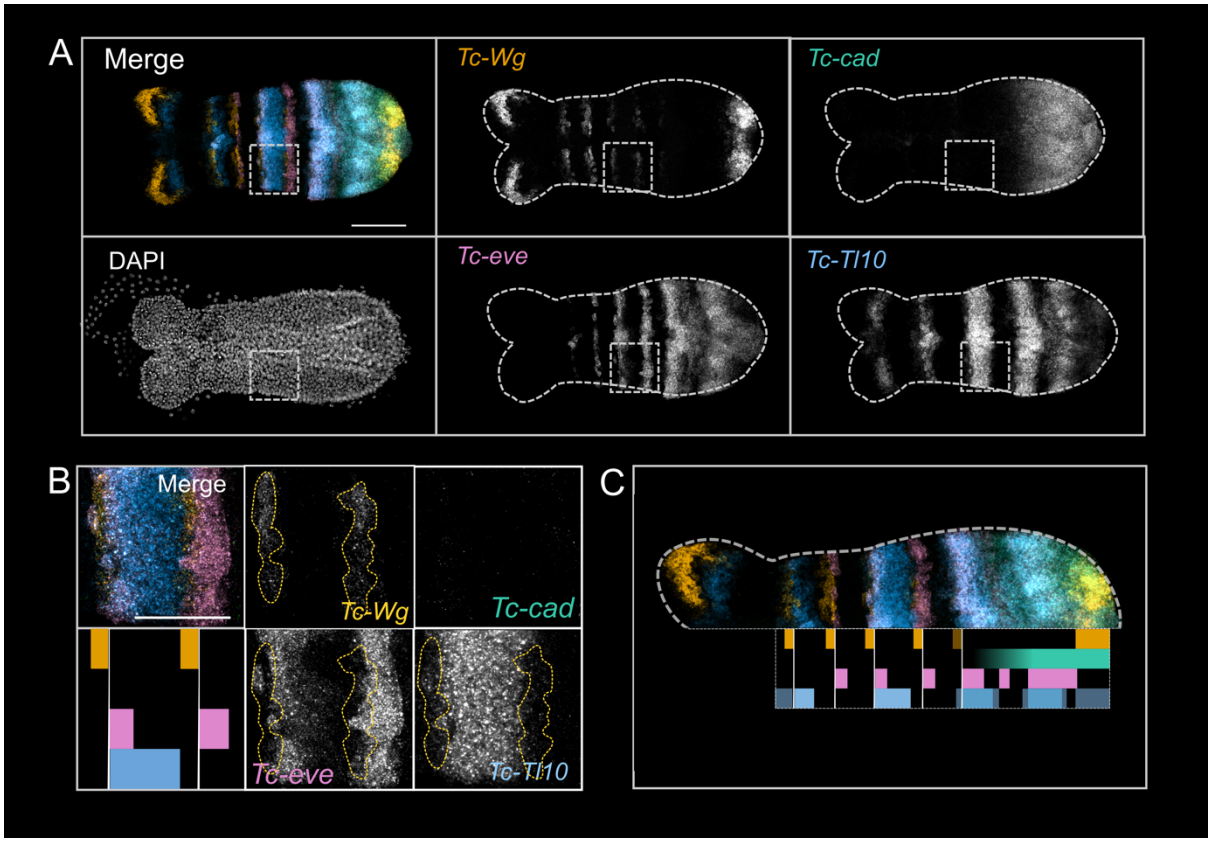

Figure 3.1. Translating HCR data on *Tc-Tl10* stripe phasing into a graphical abstract of gene expression. All images are maximum projections of Z-stacks, spanning only the optical sections that contain ectoderm. **A|** Expression of the segment polarity gene *Tc-Wingless* (*Tc-Wg*), the posterior SAZ marker *Tc-caudal* (*Tc-cad*), the pair-rule gene *Tc-even-skipped* (*Tc-eve*), my candidate marker gene *Tc-Toll10* (*Tc-Tl10*) and the nuclear marker DAPI, detected using HCR ISH in a single embryo. Scale bar is 100 µM. **B|** A close up showing expression of a single *Tc-Tl10* stripe in the ectoderm and a graphical representation of gene expression in this region. Scale bar = 50 µM. **C|** The same embryo from A aligned against a graphical representation of gene expression in the ectoderm along the entire segmented trunk and SAZ.

Emergence and maturation of primary *Tc-Tl10* stripes

I have found that all of the primary *Tc-Tl10* stripes mature following an almost identical pattern, described in detail here.

As previously reported, the primary stripes of *Tc-Tl10* share many aspects of their expression with the primary stripes of the pair-rule gene *Tc-eve*, including dynamic expression in the SAZ (Benton et al., 2016). Each primary *Tc-Tl10* stripe emerges as a broad domain in the posterior SAZ shortly after the appearance of, and overlapping with, a new *Tc-eve* domain (Figure 3.2, A1-A3). The two genes share an anterior boundary at this stage, and both extend to overlap with the posterior *Tc-Wg* domain (Figure 3.2, A1-A5). The anterior and posterior boundaries of both genes subsequently begin to shift towards the anterior of the embryo (Figure 3.2, B1-C5). Cell-tracking suggests that, for *Tc-eve* at least, these shifts cannot be explained by cell movements, and that they are instead best explained by intracellular changes in gene expression (Sarrazin et al., 2012). This conclusion is supported by my observations of *Tc-Tl10* expression. As each *Tc-Tl10* stripe shifts anteriorly, it displays a leading edge of expression where transcripts are localised to the nuclei in distinct punctae (Figure 3.2, B2 and C2). This pattern is suggestive of newly initiated transcription localised to the leading edge of the stripe, something that has so far not been detected using less sensitive ISH methods (Benton et al., 2016). Each primary *Tc-Tl10* stripe also displays a weaker trailing edge while it is shifting (Figure 3.2, B2 and C2). Transcripts are more diffuse in this region, with fewer bright punctae; possibly the result of transcription turning off at the trailing edge of the stripe.

The spatial relationship between the primary stripes of *Tc-Tl10* and other segment patterning genes in *Tribolium* is largely consistent with that proposed by Benton et al. (2016). The anterior border of each primary *Tc-Tl10* stripe (excluding the leading edge) aligns with that of the overlapping *Tc-eve* stripe throughout the SAZ, and abuts the posterior of an odd-numbered *Tc-Wg* stripe in the segmented germband (Figure 3.2). This means that the position of this boundary relative to other segment patterning genes is consistent throughout segment maturation. Specifically, it marks the region of the pattern that will form the posterior boundary of an odd-numbered parasegment.

By contrast, the posterior boundary of each primary *Tc-Tl10* stripe does not maintain a consistent position relative to other segment patterning genes. The posterior boundary of each primary *Tc-Tl10* stripe retracts to a greater extent than that of its overlapping *Tc-eve* stripe (Figure 3.2, C2-C3). The posterior boundary of the trailing edge eventually abuts the anterior boundary of a secondary *Tc-eve* stripe (Figure 3.2 C2-C3 and D2-D3). In the segmented

germband, the trailing edge overlaps with an even-numbered *Tc-Wg* stripe (Figure 3.2, D2, D4-D5). As parasegments mature, however, this trailing edge is lost, and the posterior boundary of the primary stripe begins to gradually retract anteriorly until the *Tc-Tl10* stripe is only a few cells wide, similar to a *Tc-Wg* stripe (Figure 3.2, E2 and E4-E5). From the location and width of these stripes, we can surmise that they likely overlap with stripes of the segment polarity gene *Tc-en*, which mark the anterior part of each parasegment (equivalent to the posterior compartment of each segment) (Brown et al., 1994). The posterior boundary of each primary *Tc-Tl10* stripe therefore marks different elements of the segment pattern in different parts of the embryo. In the SAZ, the posterior of the trailing edge aligns with the anterior boundary of secondary *Tc-eve* stripes, which prefigures the posterior boundary of odd-numbered parasegments (Figure 3.3, B5, C5). By contrast, in mature segments, after retraction, the primary stripe likely overlaps neatly with *Tc-en* stripes in odd-numbered parasegments, so that the posterior boundary of the stripe marks the compartment boundary of an odd-numbered parasegment (Figure 3.2, D5, E5).

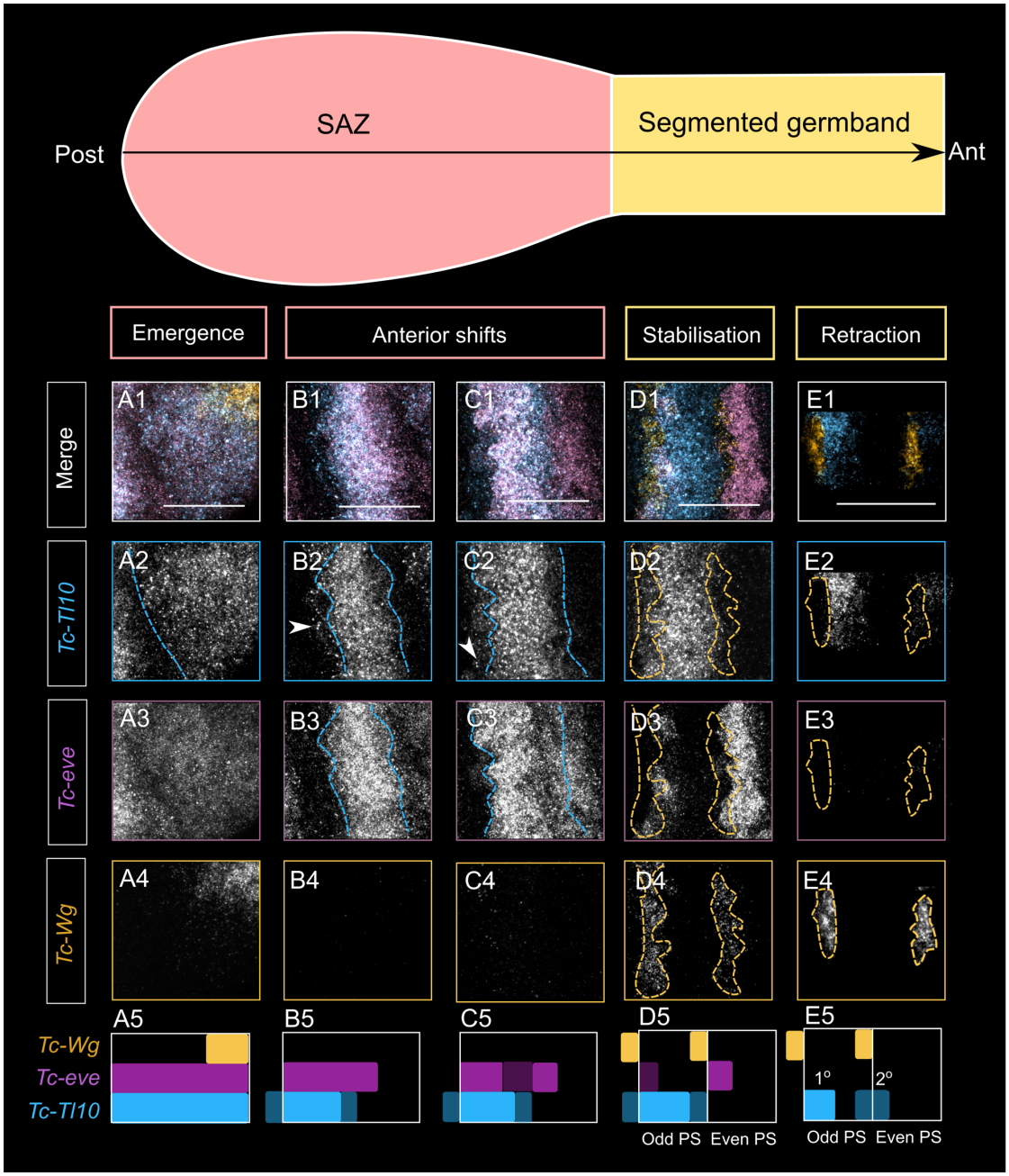

Figure 3.2. Expression of primary *Tc-Tl10* stripes relative to *Tc-eve* and *Tc-Wg* at different points along the anterior-posterior axis of the embryo, illustrating the process of stripe maturation. Stripes emerge in the posterior SAZ (A1-A5), shift anteriorly across the SAZ (B1-C5), and then stabilise and retract in the segmented germband (D1-E5). Dotted lines are used to compare boundaries within a single column. Arrowheads in B2 and C2 point to nuclear foci of transcription in the leading edge of the *Tc-Tl10* stripe. The bottom row shows a graphical abstraction of gene expression in each column, illustrating how this relates to parasegment boundary formation in the segmented germband. In E5, 1° = mature primary *Tc-Tl10* stripe, 2° = emerging secondary *Tc-Tl10* stripe. Scale bar = 50 µM.

Emergence and maturation of secondary *Tc-Tl10* stripes

The majority of secondary *Tc-Tl10* stripes also mature in a stereotyped manner, save for the first secondary *Tc-Tl10* stripe (described below). They are not expressed in the SAZ, instead emerging *de novo* in mature segments in the segmented germband (Benton et al., 2016). They are first expressed as relatively diffuse domains centred on odd-numbered *Tc-Wg* stripes (Figure 3.3, A1-A3). As they mature, expression fades in the region overlapping the *Tc-Wg* stripe (Figure 3.3, B1-B3). Mature secondary stripes are a similar width to the mature primary *Tc-Tl10* stripes (about 3 cell widths), and I presume that they, too, overlap with *Tc-en* stripes. Emerging stripes therefore overlap the posterior-most region of each odd-numbered parasegment, while mature stripes overlap with the anterior part of each even-numbered parasegment. This positional shift between emerging and mature secondary stripes was not detected by Benton and colleagues (2016), possibly because the sensitivity of my ISH method is higher.

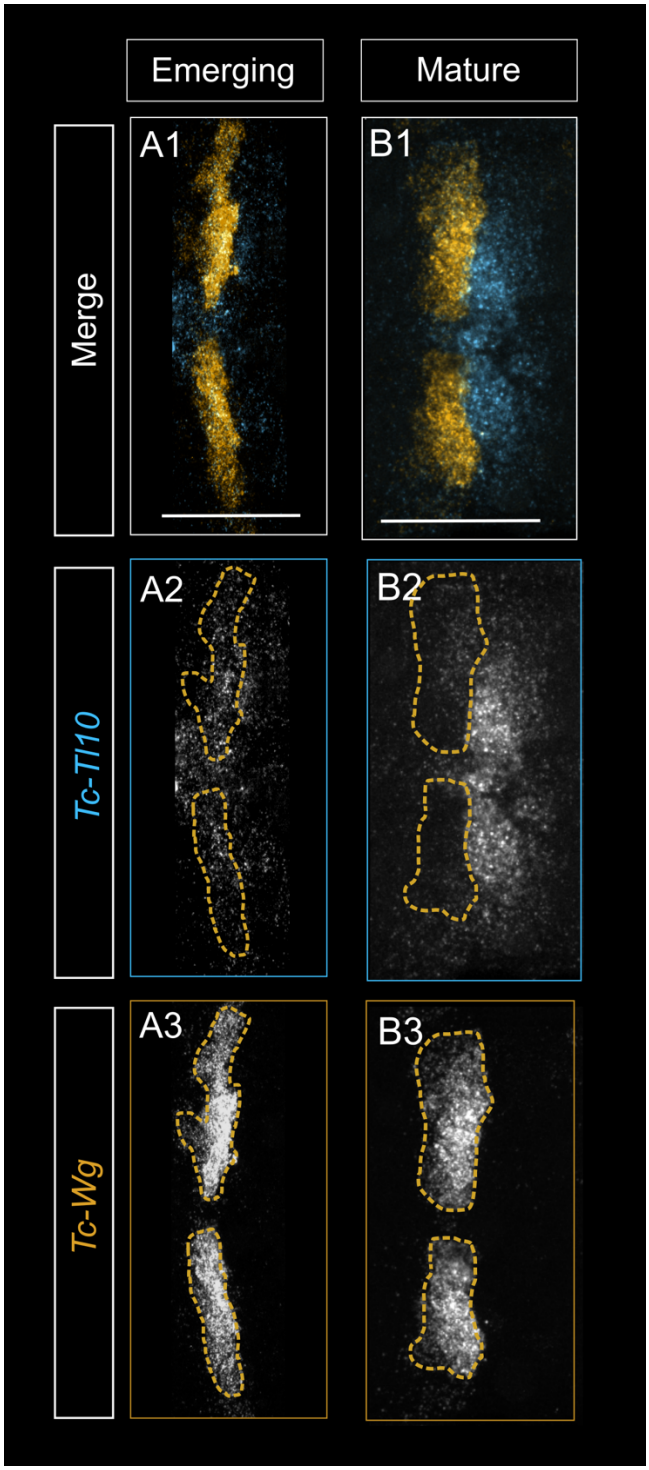

Figure 3.3. Emergence (A) and maturation (B) of secondary *Tc-Tl10* stripes relative to *Tc-Wg*. Dotted lines are used to highlight the same boundaries in a single column. Scale bar = 50 µM.

Emergence and maturation of the first secondary *Tc-Tl10* stripe

In contrast to most secondary stripes of *Tc-Tl10*, which emerge *de novo*, the first secondary *Tc-Tl10* stripe emerges through splitting of the first primary stripe. Following maturation, the first primary *Tc-Tl10* stripe abuts the posterior of the first *Tc-Wg* stripe in the trunk (Figure 3.4, A1-A3). However, it then begins to expand anteriorly, eventually encompassing this *Tc-Wg* stripe (Figure 3.4, B1-B3). Over time, the centre of this domain becomes cleared, leaving a ring of *Tc-Tl10* expression (Figure 3.4, C1-D3). The posterior of this ring sits just behind the first trunk *Tc-Wg* stripe, equivalent to the location of the first primary stripe, and the anterior of the ring sits just behind the newly-emerging intercalary *Tc-Wg* stripe. I refer to the anterior of this ring as a secondary stripe, as it occupies a similar position to other mature secondary stripes, but it is expressed in a head segment rather than a trunk segment and will therefore not be relevant for most of my work on the trunk gap genes.

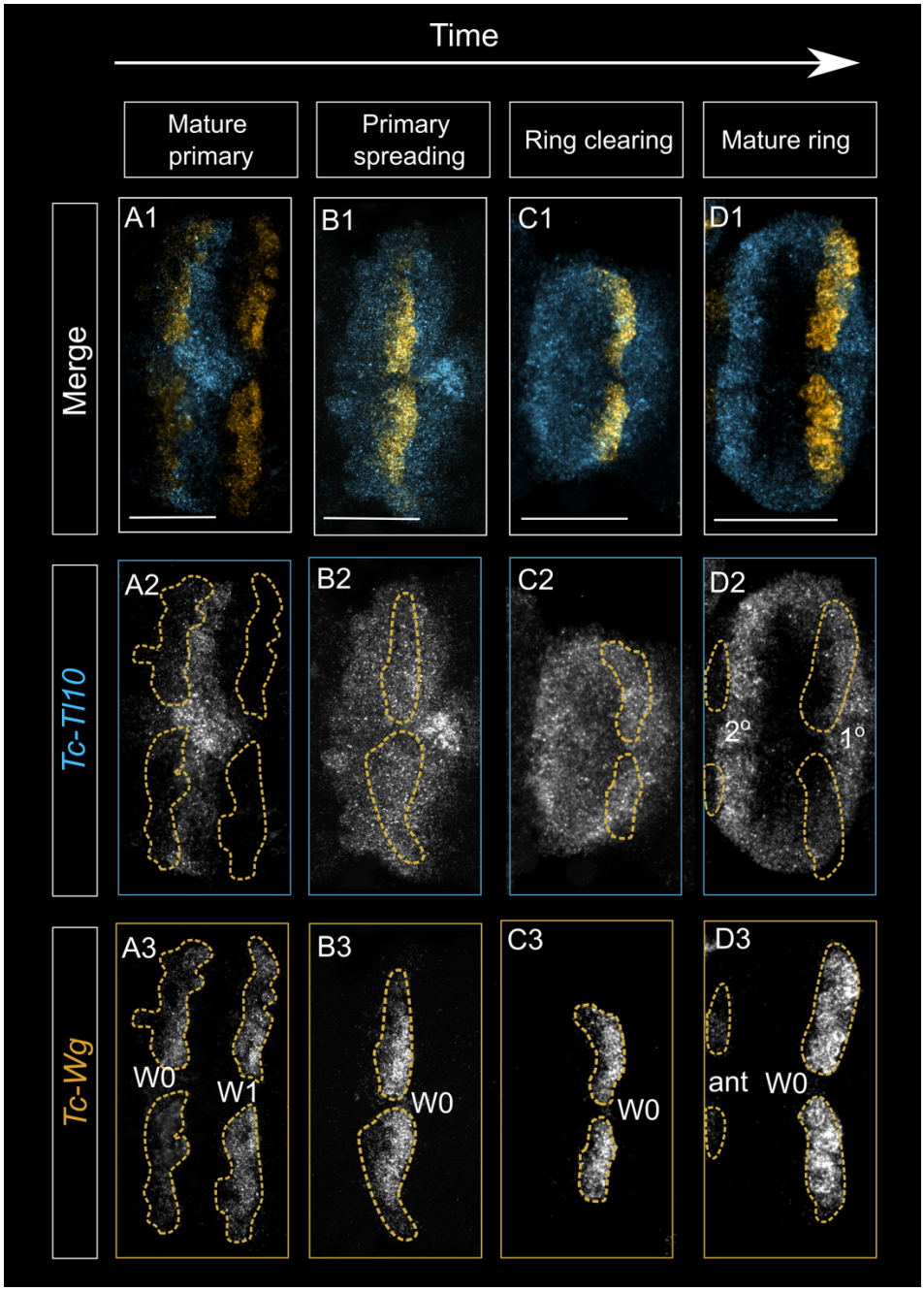

Figure 3.4. Development of the first secondary *Tc-Tl10* stripe over time. The mature primary stripe initially abuts the posterior of the *Tc-Wg* stripe at the posterior of parasegment 0 (W0) (A). This stripe spreads anteriorly to form a broad domain encompassing W0 (B). The centre of this *Tc-Tl10* domain is subsequently cleared to form a ring, with the anterior of the ring (the new secondary stripe, 2° in D2) sitting just behind the intercalary *Tc-Wg* stripe (ant), and the posterior of the ring (the mature primary stripe, 1° in D2) sitting behind W0 (C and D). Dotted lines are used to highlight the same boundaries in a single column. Scale bar = 50 µM.

A spatial mapping system using *Tc-Tl10*

I have shown that the spatial relationships between *Tc-Tl10* stripes and the segment patterning genes *Tc-eve* and *Tc-Wg* are consistent between different stripes, and vary in a predictable way along the length of the axis. *Tc-Tl10* can therefore, in theory, be used as a stand-alone marker for mapping the expression of genes against the segment pattern in both the SAZ and the segmented germband.

When considering *Tc-Tl10* as a spatial marker, it is important to keep in mind that 'spatial' here refers to space **relative to the segment pattern**. *Tc-Tl10* and segment patterning genes are expressed dynamically in the SAZ, so a gene that is not expressed dynamically here will appear to be shifting relative to *Tc-Tl10* stripes. Likewise, a gene that undergoes similar anterior shifts in expression will appear to be stationary relative to *Tc-Tl10* stripes. In the segmented germband, by contrast, shifts relative to stable, mature *Tc-Tl10* stripes represent shifts relative to both the segment pattern and the tissue.

I have developed a numbering system to refer to specific stripes of *Tc-Wg* and *Tc-Tl10* expression in the embryo, described in more detail below and represented graphically in Figure 3.5A. Figure 3.5B summarises how stripes of each gene relate to the segmental pattern over the course of segment maturation, and Figure 3.5C shows how stripe numbering relates to parasegment numbering in a fully elongated embryo (*i.e.* where all stripes are stabilised and mature).

***Tc-Wg* stripe numbering:** *Tc-Wg* stripe numbering is directly linked to parasegment identity. The first trunk *Tc-Wg* stripe, which is expressed at the posterior of parasegment 0, will be referred to as W0. The next *Tc-Wg* stripe will be labelled as Wg1 and so on until Wg15, marking the posterior of the 15th parasegment. There are additionally three *Tc-Wg* stripes anterior of W0 (the head, antennal and intercalary stripes) and a *Tc-Wg* domain in the posterior of the SAZ. These domains will be referred to by name where necessary.

***Tc-Tl10* stripe numbering:** My numbering system for *Tc-Tl10* stripes draws on existing conventions for *eve*, as the two genes overlap extensively, and this will facilitate comparison with work using *eve* as a spatial marker. The primary stripes will therefore be numbered 1-8 (To1, To2 and so on). Secondary *eve* stripes arise from splitting, and so the two resulting stripes are usually referred to as the number of the original primary stripe plus a letter to distinguish them (*e.g. eve* stripes 2a and 2b). However, the majority of secondary *Tc-Tl10*

stripes arise *de novo*, and I decided that it would be more appropriate to give them unique numbers that represent their relative position to primary *Tc-Tl10* stripes. Therefore, the secondary *Tc-Tl10* stripe that forms between To1 and To2 will be referred to as To1.5; the stripe that forms between To2 and To3 will be To2.5; and so on, until To8.5. Although it forms by splitting, the first secondary stripe will be numbered as To0.5 for consistency. There is also a *Tc-Tl10* domain in the head (the head stripe) that will be referred to by name if necessary. Note that this means that the parasegment in which any specific *Tc-Tl10* stripe is expressed can be calculated by multiplying the stripe number by 2 and subtracting 1 (for example, stripe To3.5 is expressed at the anterior of parasegment 6).

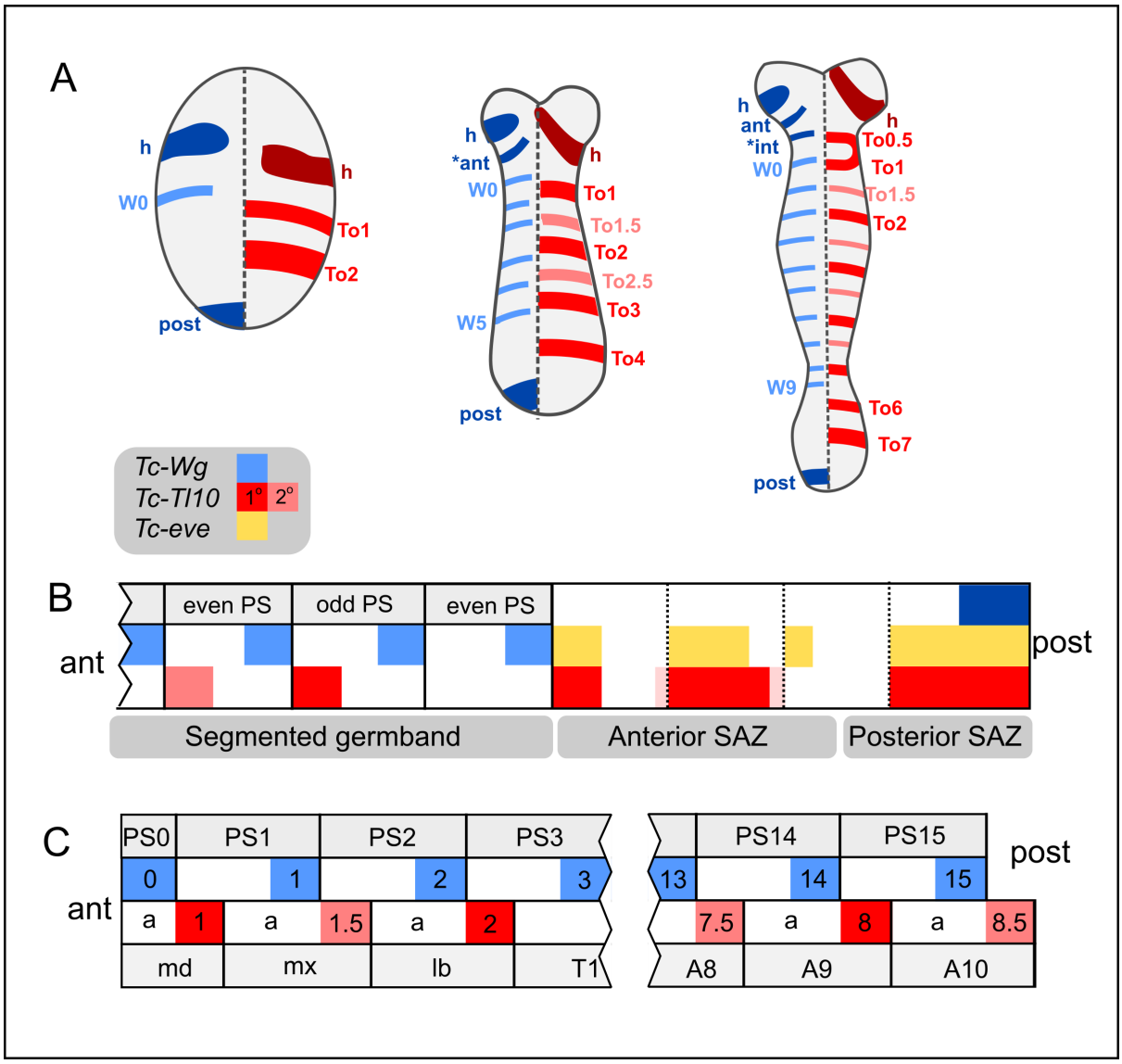

Figure 3.5. A graphic representation of my stripe numbering system for *Tc-Wg* (light blue for stripes in the trunk, and dark blue for stripes or domains outside of the trunk) and *Tc-Tl10* (red and pink for primary and secondary stripes, respectively). A) shows specific stripes *in situ*, to indicate how they arise over time and to highlight the head and posterior domains that are not numbered. B) summarises how stripes of *Tc-Wg*, *Tc-eve* (yellow) and *Tc-Tl10* relate to parasegment boundaries and each other throughout segment maturation (using a simplified representation of the posterior of the segmented germband and the SAZ). C) provides a brief overview of how stripe number relates to parasegment number (using a simplified representation of the anterior and posterior segments of a fully elongated embryo). h = head domain, post = posterior domain, ant = antennal stripe, int = intercalary stripe, PS = parasegment.

Tc-Tl10 is not a precise marker for embryonic stage

In addition to using *Tc-Tl10* as a spatial marker, I wanted to test its utility as a proxy for the progression of segmentation and therefore as an embryonic staging marker. My main concern was whether the development of primary and secondary stripes together would provide a similar level of temporal precision for staging as a standard staging marker such as *Tc-Wg*. To determine this, I examined *Tc-Tl10* expression in embryos spanning the course of segment addition (from 8-22h AEL), against a marker of parasegment boundary formation, *Tc-Wg*.

Primary *Tc-Tl10* stripes are added sequentially, from anterior to posterior, beginning at the start of segment addition (~8h AEL) and ending at its completion (~22h AEL) (Figure 3.6). The majority of secondary stripes begin to emerge later, from around 12-14h AEL (the first secondary stripe is a little delayed, appearing about 14-16h AEL) (Figure 3.6). The second and third secondary stripes emerge almost simultaneously, and the more posterior stripes then emerge sequentially from anterior to posterior as parasegments mature (Figure 3.6). Unfortunately, although primary and secondary *Tc-Tl10* stripes do emerge gradually over the course of segment addition, the rate of their formation is not consistent with the rate of *Tc-Wg* stripe formation (Figure 3.7). This means that an embryo with different numbers of parasegments may display the same number of *Tc-Tl10* stripes (Figure 3.6 and Figure 3.7). *Tc-Tl10* is therefore a less precise marker for the progress of segmentation than *Tc-Wg*.

Tc-Tl10 can reliably be used to distinguish between embryos that differ in their number of parasegments by at least two (Figure 3.7), a similar level of precision as that provided by a pair-rule gene such as *Tc-eve*. This level of precision may be suitable for some lines of research, and so *Tc-Tl10* may still has use as a stand-alone marker. However, for my work, I decided that this would not be sufficient.

Figure 3.6 (overleaf). The relationship between *Tc-Wg* stripe number, *Tc-Tl10* stripe number and time after egg lay (AEL) at 30 °C. *Tc-Wg* expression (cyan) and *Tc-Tl10* expression (red) are shown in embryos spanning the stages of segment addition, from 8-22 hours AEL. Each embryo is labelled with its age AEL (within a 2 hour range, above) and with its staging moniker below (see text for explanation). Blue arrowheads mark *Tc-Wg* stripe W0, and red arrowheads mark *Tc-Tl10* stripe To1. Specific stripes are annotated in blue (*Tc-Wg*), red (primary stripes of *Tc-Tl10*) or pink (secondary stripes of *Tc-Tl10*). The inset at stage W5:To5(1-2) shows a close up on *Tc-Tl10* expression in the region of W1, indicating that the secondary *Tc-Tl10* stripe To1.5 has begun to form. Scale bar = 100 μM.

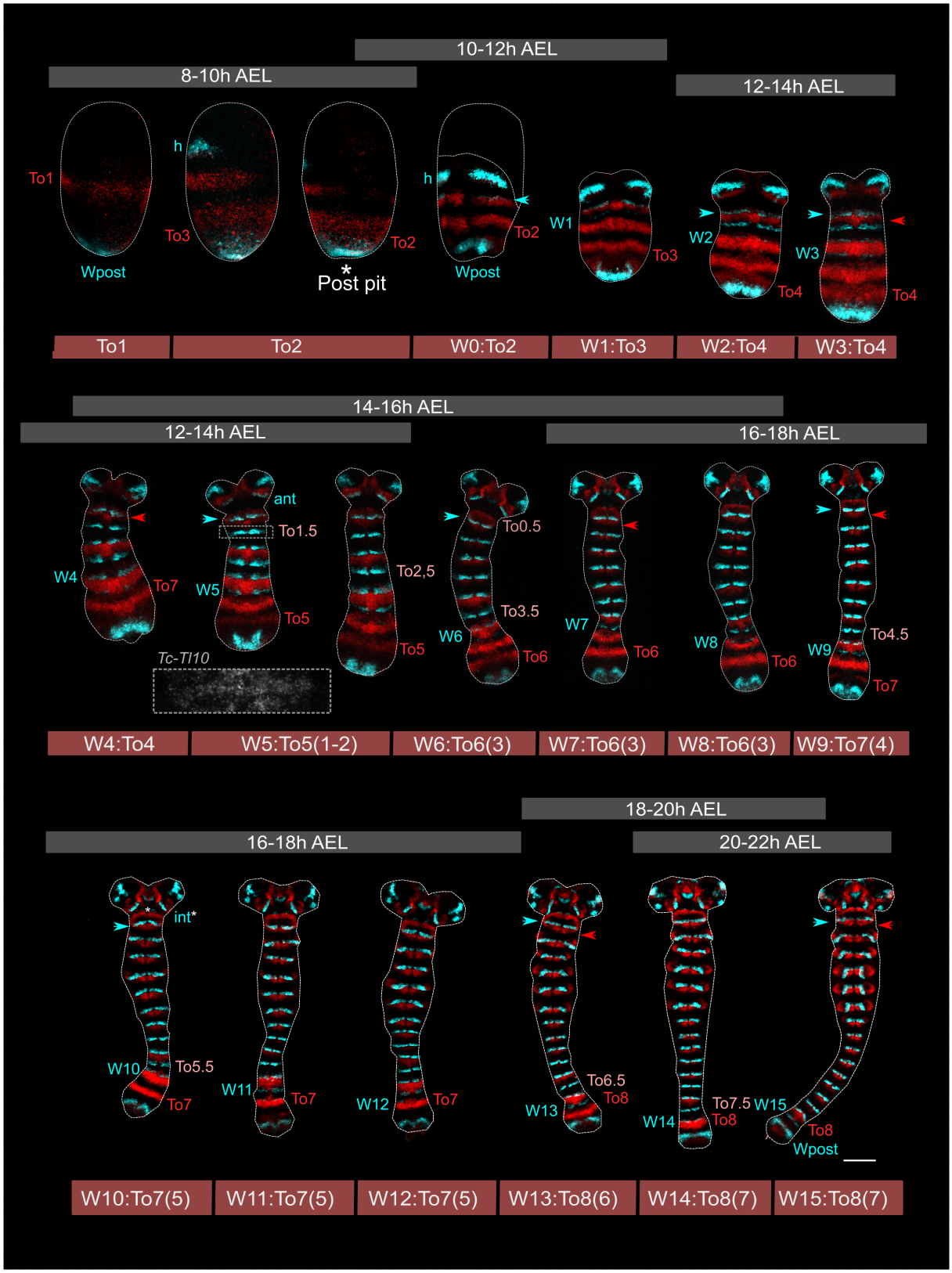
10-12h AEL
8-10h AEL
12-14h AEL
To1
h
To3
To2
Wpost
*
Post pit
h
To2
Wpost
W1
To3
W2
To4
W3
To4
To1
To2
W0:To2
W1:To3
W2:To4
W3:To4
14-16h AEL
12-14h AEL
16-18h AEL
W4
To7
ant
To1.5
W5
To5
Tc-Tl10
To2,5
To5
To0.5
To3.5
W6
To6
W7
To6
W8
To6
W9
To4.5
To7
W4:To4
W5:To5(1-2)
W6:To6(3)
W7:To6(3)
W8:To6(3)
W9:To7(4)
18-20h AEL
16-18h AEL
20-22h AEL
int*
W10
To5.5
To7
W11
To7
W12
To7
To6.5
To8
W13
W14
To7.5
To8
W15
To8
Wpost
W10:To7(5)
W11:To7(5)
W12:To7(5)
W13:To8(6)
W14:To8(7)
W15:To8(7)

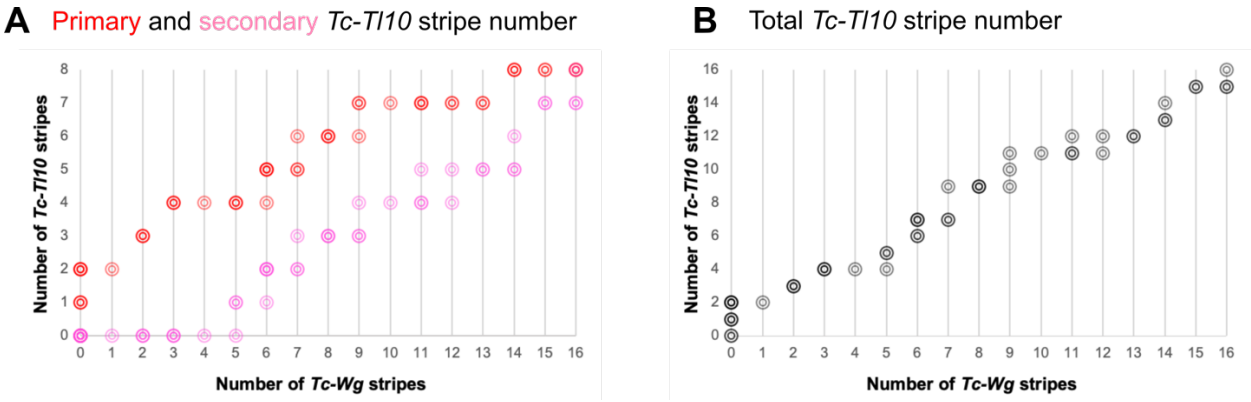

Figure 3.7. The number of primary (red) and secondary (pink) *Tc-Tl10* stripes (A) or total number of *Tc-Tl10* stripes (B) in an embryo compared to the number of *Tc-Wg* stripes (as a proxy for the progression of segmentation). Primary and secondary stripes are not added at a consistent rate, and there are therefore stages at which total *Tc-Tl10* stripe number does not vary between embryos with different numbers of parasegments (for example, embryos with 9-12 *Tc-Wg* stripes cannot consistently be distinguished). N = 51.

A staging system using *Tc-Wg* and *Tc-Tl10*

Fortunately, during my validation of *Tc-Tl10* as a possible marker gene, I discovered that it was actually possible to use two distinct marker genes in each of my HCR ISH reactions without 'wasting' a detection slot. Of the five fluorophores offered as hairpin tags by Molecular Instruments, two (Alexa Fluor 488 and 514) have significant overlap in their emission spectra, and using them together therefore risks signal bleed-through. After a long time avoiding using these tags together (and therefore limiting ourselves to four genes per HCR), we found that these tags could be used together reasonably effectively with some post-processing to eliminate some of the effects of bleed-through. I decided that *Tc-Wg* and *Tc-Tl10* have distinct enough expression patterns that they could be distinguished even using these tags, and so most of my thesis uses a staging system based on both genes, with *Tc-Wg* providing precise information about the progression of segmentation and *Tc-Tl10* supplementing this information (for example, providing staging before the emergence of the first *Tc-Wg* stripe, and occasionally allowing me to differentiate between embryos with the same number of *Tc-Wg* stripes). In this staging system, embryos are referred to using the number of the most recently formed *Tc-Wg* stripe, and the most recently formed *Tc-Tl10* stripe (Figure 3.6). For example, an embryo which has formed no *Tc-Wg* stripes and one *Tc-Tl10* stripe would be at stage To1; an embryo which has formed the first *Tc-Wg* stripe and the first *Tc-Tl10* stripe is at stage W0:T1; and an embryo which has formed 8 *Tc-Wg* stripes and six primary *Tc-Tl10* stripes is at stage W7:T6. Where relevant, I may distinguish otherwise identical stages based on the number of secondary stripes formed by writing this in brackets (*e.g.* W8:T6(2) would have only two secondary stripes formed, while W8:T6(3) would have 3 formed). This count will not include the most anterior secondary stripe that forms by splitting rather than *de novo.*

Tc-single-minded as a marker to highlight tissue boundaries

Segmentation in arthropods occurs initially in the ectoderm, with the mesoderm becoming secondarily segmented (Azpiazu et al., 1996; Green and Akam, 2013; Hannibal et al., 2012). I was therefore most interested in examining gene expression in the ectoderm of the embryo. *Single-minded* (*sim*) is a marker for mesectoderm (the tissue that lies at mesoderm/ectoderm border, and will give rise to the ventral midline) in the insects *Drosophila* (Thomas et al., 1988), *Apis mellifera* and *Tribolium* (Zinzen et al., 2006), the crustacean *Parhyale* (Vargas-Vila et al., 2010), and the myriapod *Strigamia* (Linne et al., 2012). I decided that this gene could serve as a useful boundary marker for the ectoderm, and have therefore included it in the same channel as *Tc-Wg* for many of my HCR ISHs. Appendix 2 provides relevant information on how the two genes overlap as a validation that they can be used together without losing spatial information. I summarise the expression of *Tc-sim* in Figure 3.8, in order to supplement the brief description already published for *Tribolium* (Zinzen et al., 2006).

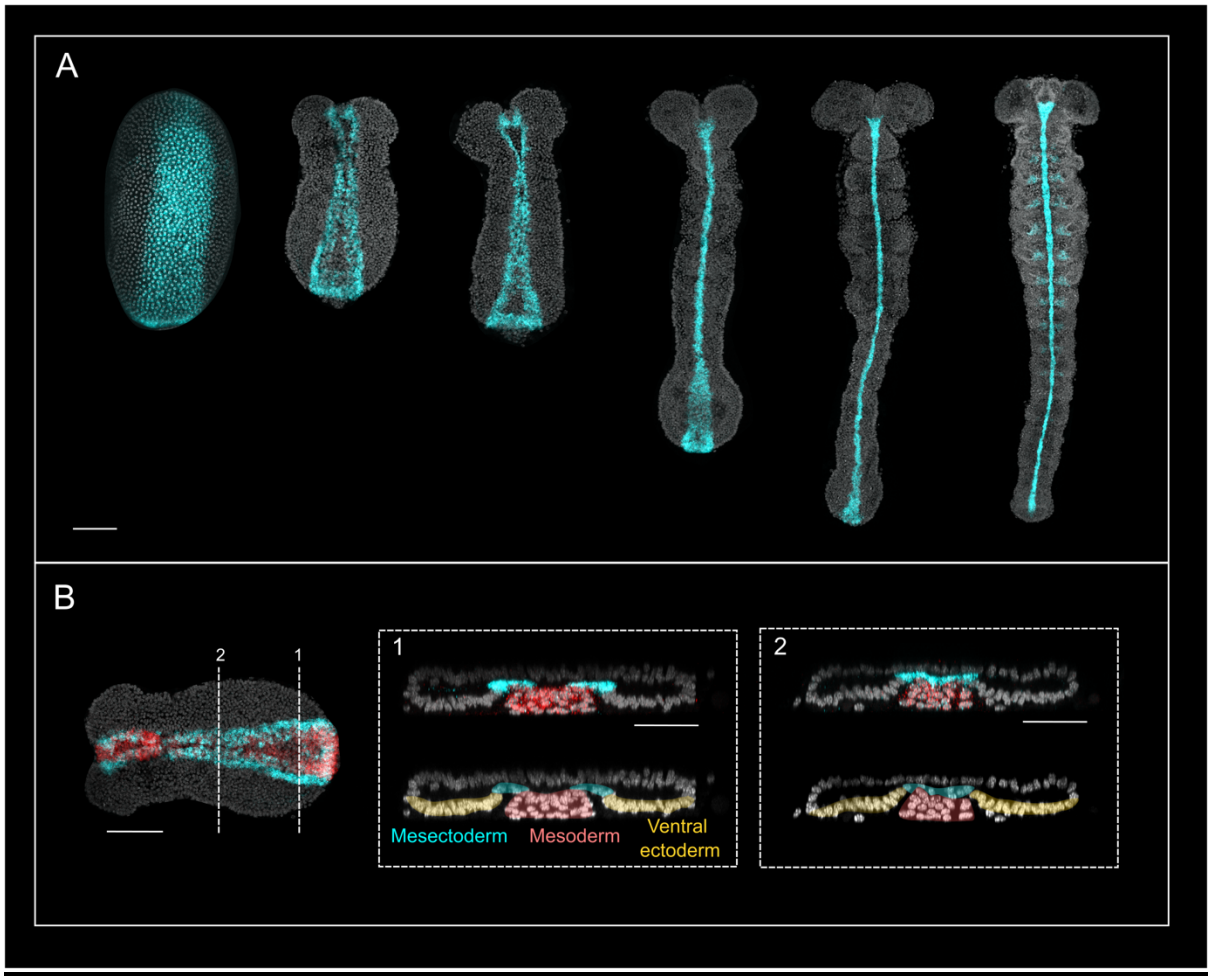

Figure 3.8. *Tc-single-minded (sim)* is expressed in the mesectoderm of *Tribolium* embryos throughout early development. **A|** *Tc-sim* (cyan) is expressed in the midline of the embryo in both the blastoderm and the germband. **B|** *Tc-sim* (cyan) is expressed specifically in the mesectoderm - the epithelial tissue immediately bordering or overlying the invaginating mesoderm (here marked by expression of *twist*, in red). Two transverse sections through a single embryo show how *sim* is initially expressed along the inner edge of the two ventral epithelial plates (1) and how these domains subsequently fuse to form a single midline overlying the invaginated mesoderm (2). Lower images in panels 1 and 2 are false coloured to show tissue layers. nuclei are detected using DAPI (grey). Scale bars for whole embryo images are 100 μM, and for insets in B are 50 μM.

3.2.2. Expression dynamics of individual gap genes

With a suitable spatial and temporal marker system established, I moved on to collecting data on canonical gap gene expression. I performed HCRs on *Tribolium* embryos covering the entire course of segmentation (from six hours AEL to 22 hours AEL). In each HCR, I included probes for *Tc-Wg*/*Tc-Sim* and *Tc-Tl10* as stage and spatial markers, and for three overlapping gap genes. All embryos were subsequently stained with DAPI to allow for visualisation of nuclei.

Using this dataset, I first examined the spatial and temporal dynamics of individual gap genes against *Tc-Tl10* an*d Tc-Wg*. I aimed to clarify and supplement previous descriptions of their expression, and to produce a comprehensive description of the expression of each gene against standardised markers as a resource for future study.

Expression dynamics of *Tc-hunchback (Tc-hb)*

Expression of *Tc-hb* has been previously described by Wolff et al. (1995). However, this description uses spatial markers in only a few select stages, and the marker used (the pair-rule gene *Tc-hairy*) has a complicated relationship with parasegment and segment boundaries, making the boundary estimates necessarily imprecise.

In *Drosophila* (Margolis et al., 1994), *Nasonia* (Pultz, 2005) and *Oncopeltus* (Liu and Kaufman, 2004a), *Dm-hb* mRNA is initially provided maternally; ovarian support cells known as 'nurse cells' synthesise and load it into developing oocytes as they mature. I show that the same is true in *Tribolium* by examining the expression of *Tc-hb* in ovarioles (the individual functional units of the ovary) dissected from adult females (Figure 3.9). Unlike *Drosophila*, which has polytrophic ovaries (in which nurse cells are bundled up with each oocyte), *Tribolium* has telotrophic ovaries, in which the nurse cells are clustered at the proximal end of the ovariole and RNA is shuttled to the oocyte through cytoplasmic 'nutritive' cords (Trauner and Büning, 2007), visible in Figure 3.9.

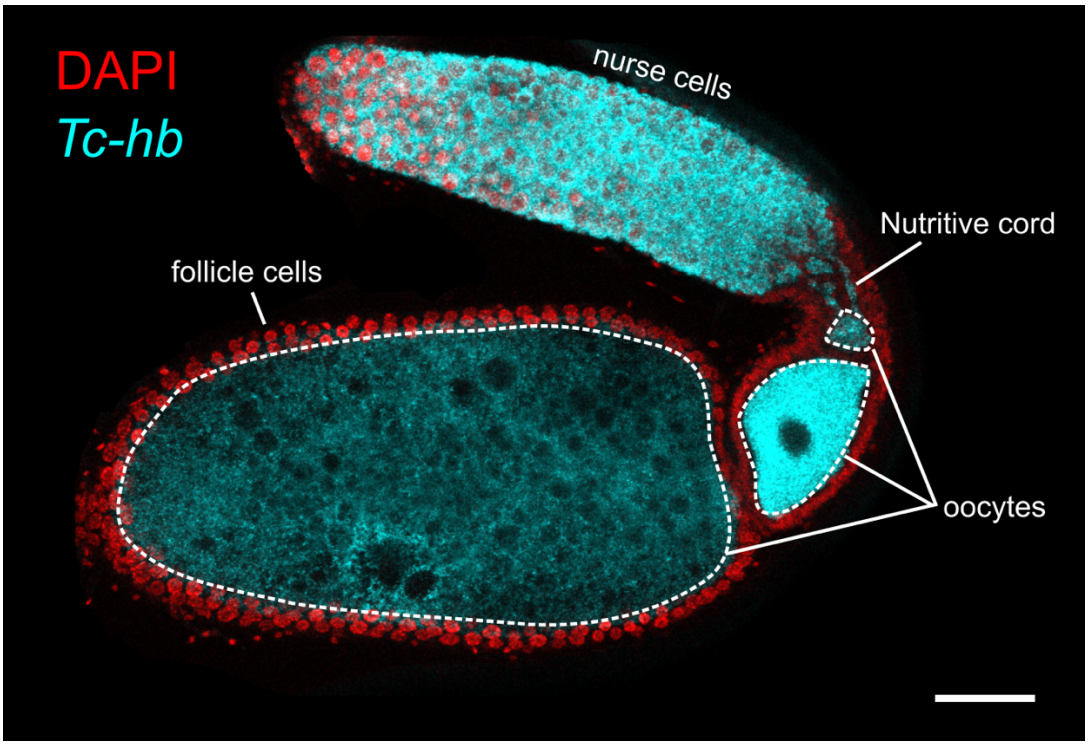

Figure 3.9. A single dissected ovariole showing that *Tc-hb* is expressed in nurse cells and provided to the developing oocytes through a nutritive cord. Maximum projection through the centre of a *Tribolium* ovariole, scale bar = 50 µM.

This maternal loading means that *Tc-hb* mRNA is ubiquitous in the early blastoderm (Figure 3.10, stage To0 and Wolff et al., 1995). *Tc-hb* expression remains ubiquitous until To1 begins to form (approximately 9 hours AEL, after the last synchronised mitosis of the blastoderm). At this stage, *Tc-hb* mRNA clears from the posterior tip of the embryo (Figure 3.10, stage To1 and Wolff et al., 1995). As reported by Wolff et al. (1995), expression subsequently intensifies in the cells of the serosa and, within the embryonic primordium, becomes restricted to a broad central band (Figure 3.10, stages T01-To2). This band spans from To1a-To2p, a region of the segment pattern that will give rise to PS1-3, and forms following loss of *Tc-hb* expression in the anterior and posterior regions of the embryo. Wolff et al. (1995) suggests that *Tc-hb* expression 'retracts' from the posterior of the embryo, but I have seen no evidence for this – instead, fading appears to occur simultaneously across the breadth of the domain. It may be that they interpreted the localised repression of *Tc-hb* at the posterior tip of the embryo as an early stage of retraction. I instead observe a two-stage clearance, firstly limited to the posterior tip of the embryo and then in a broader domain across the majority of the SAZ. Note that expression of *Tc-hb* is lost totally from the posterior of the embryo, but remains at a low level in the anterior for the remainder of segmentation.

In the SAZ, *Tc-hb* expression fades in PS1 and PS3, and finally in PS2, so that expression is uniform from the anterior of the embryo back to the posterior of PS3 (Figure 3.11, stages W1:To3-W5:To4(2)). *Tc-hb* then spreads from anterior to posterior in a segmental pattern, as parasegments mature (Figure 3.10, stage W6:To5(2) onwards, and Wolff et al., 1995). This expression is limited to the neurectoderm (Biffar and Stollewerk, 2014) and mesoderm (data not shown).

As reported by Wolff et al. (1995), a second domain of *Tc-hb* emerges in the posterior of the SAZ later in segmentation (Figure 3.10, stageW7:To6(3)). The anterior border of this domain shifts anteriorly in tandem with To7a (Figure 3.10, stages W9:To7(4)-W12:T07(5)), which will overlap with the anterior border of PS13 in the SAZ. The posterior border does not retract from the posterior SAZ, so that this domain of *Tc-hb* essentially spans from the anterior of PS13 to the terminus of the embryo.

Tc-hb is therefore expressed in two gap-like domains in the trunk – one spanning the primordia for PS1-PS3, and one spanning from the anterior of PS13 to the terminus of the embryo.

Figure 3.10 (overleaf). HCR showing *Tc-Tl10* (red) and *Tc-hb* (cyan or grey) expression in *Tribolium* embryos over the course of segment addition. Images are maximum projections through coronal optical sections (arrows indicate where the midline of the embryo is turned either to the left or to the right, *i.e.* where the optical sections are not perfectly perpendicular to the dorsoventral axis)). Germband stage embryos have been dissected away from the egg. Stage is given above each embryo according to the staging system I present in section 3.2.1. For simplicity, *Tc-Wg* expression is not shown, but the positions of selected *Tc-Tl10* and *Tc-Wg* stripes are indicated on greyscale images (in red and white respectively). The suffix 'a' refers to the anterior boundary of a stripe, while 'p' refers to the posterior boundary of a stripe. The asterisk marks the clearing of *Tc-hb* expression from the posterior terminus at stage To1. Scale bar = 100 μM.

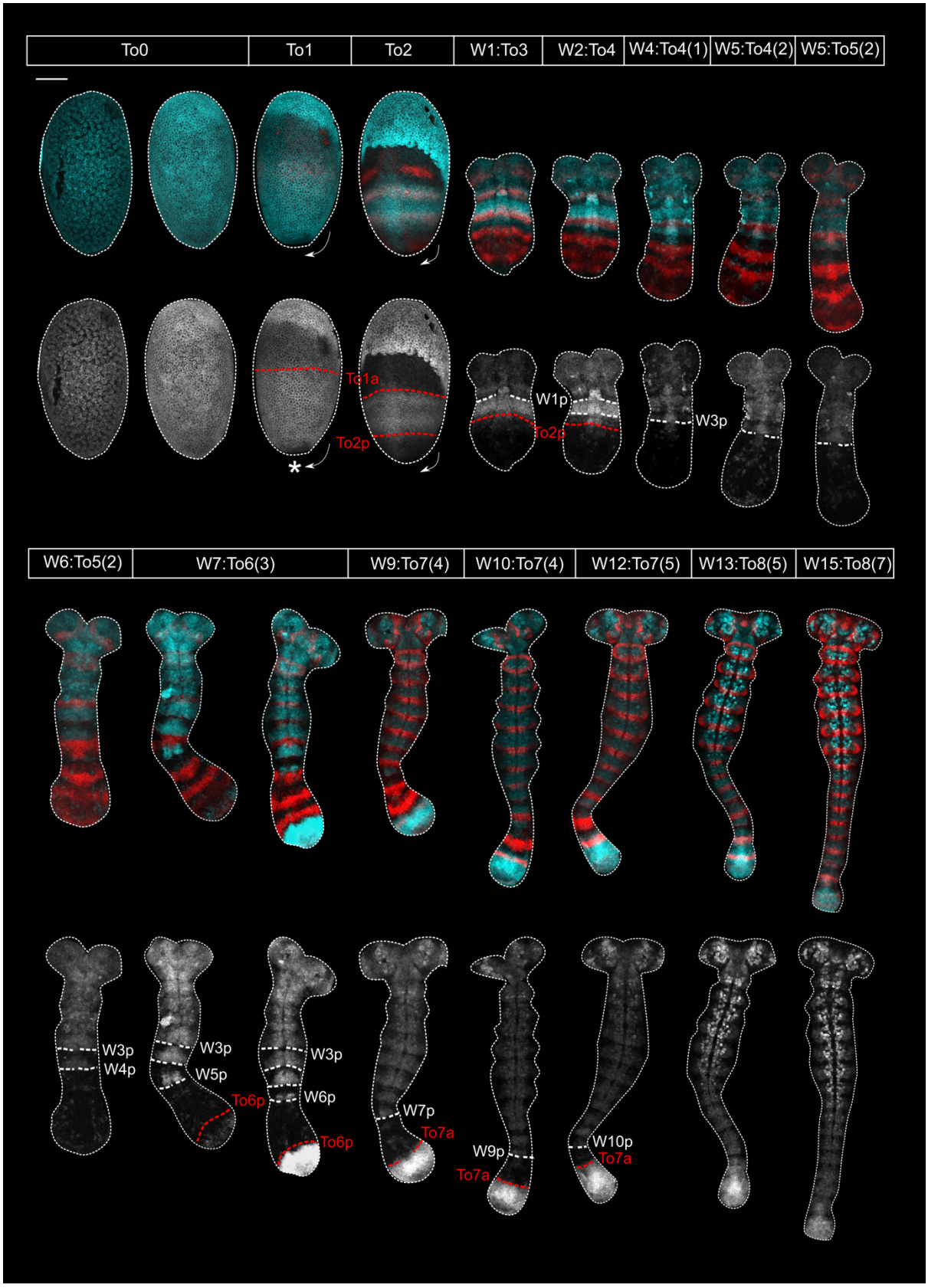
To0
To1
To2
W1:To3
W2:To4
W4:To4(1)
W5:To4(2)
W5:To5(2)
To1a
To2p
W1p
To2p
W3p
W6:To5(2)
W7:To6(3)
W9:To7(4)
W10:To7(4)
W12:To7(5)
W13:To8(5)
W15:To8(7)
W3p
W4p
W3p
W5p
To6p
W3p
W6p
To6p
W7p
To7a
W9p
To7a
W10p
To7a

Expression dynamics of *Tc-Krüppel (Tc-Kr)*

Tc-Kr expression has been previously described using single colorimetric ISHs by Sommer and Tautz (1993) and double colorimetric ISHs against *Tc-eve* Cerny et al. (2005). However, the temporal dynamics of early expression in particular have been poorly characterised.

Interestingly, *Tc-Kr* expression in the SAZ appears to be established in two steps – it is first activated in a small region at the posterior tip of the embryo (Figure 3.10, stage To0), and subsequently becomes expressed in a broad domain across the posterior SAZ, initially in a posterior to anterior gradient but subsequently becoming relatively uniform (Figure 3.10, stages To1-W0:To2). This seem to mirror the two-step clearance of *Tc-hb* observed in the posterior SAZ. The first phase of *Tc-Kr* emergence appears to have been missed by Cerny et al. (Cerny et al., 2005) or Sommer and Tautz (Sommer and Tautz, 1993), but is presented without comment in Zhu et al. (2017). These data suggest that there may be two distinct phases of regulation required to establish repression and activation, respectively, of *Tc-hb* and *Tc-Kr* in the SAZ.

The broad, posterior domain of *Tc-Kr* subsequently shifts anteriorly in tandem with the segment pattern, as is previously reported (Cerny et al., 2005). Previous descriptions consider the gap domain of *Tc-Kr* to cover T1-T3 precisely, in phase with the segmental, rather than parasegmental, pattern (Cerny et al., 2005). My data suggests that this domain instead initially covers PS3-PS5 in their entirety (spanning from the posterior compartment of the mandibular segment to the anterior compartment of T3) (Figure 3.11, stages W2:To4-W5:To5(2)). I suspect that the discrepancy between my own results and those and Cerny et al. (2005) are due to the difficulty of picking out overlaps in colorimetric ISHs, as it is ambiguous whether the boundaries of this *Tc-Kr* domain overlap or abut their spatial marker, *Tc-eve*.

A segmental pattern of *Tc-Kr* expression subsequently emerges in mature parasegments, likely related to a function of *Tc-Kr* in the neurectoderm (Biffar and Stollewerk, 2014). Late in segmentation, a new domain of *Tc-Kr* also appears in the primordia of the gut at the posterior end of the germband (Figure 3.11, stage W15:To8(7)). Both of these features have been previously reported by Cerny et al. (2005), but my data provides more precision as to the timing of their development for future reference.

Figure 3.11 (overleaf). HCR showing *Tc-Tl10* (red) and *Tc-Kr* (cyan or grey) expression in *Tribolium* embryos over the course of segment addition. Images are maximum projections through coronal optical sections (arrows indicate where the midline of the embryo is turned either to the left or to the right, *i.e.* where the optical sections are not perfectly perpendicular to the dorsoventral axis). Germband stage embryos have been dissected away from the egg. Stage is given above each embryo according to the staging system I present in section 3.2.1. For simplicity, *Tc-Wg* expression is not shown, but the positions of selected *Tc-Tl10* and *Tc-Wg* stripes are indicated on greyscale images (in red and white respectively). The suffix 'a' refers to the anterior boundary of a stripe, while 'p' refers to the posterior boundary of a stripe. Scale bar = 100 μM.

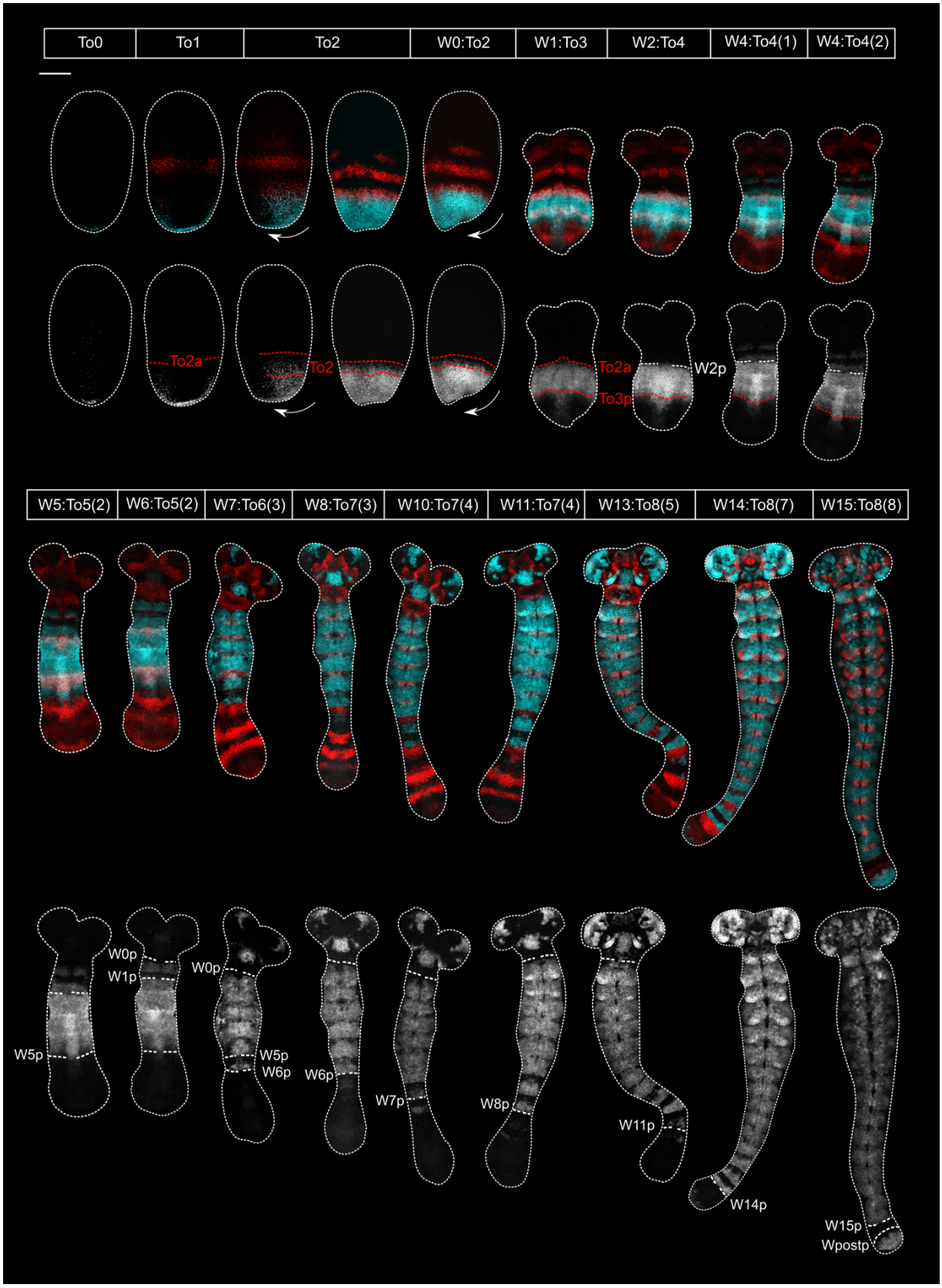
To0
To1
To2
W0:To2
W1:To3
W2:To4
W4:To4(1)
W4:To4(2)
To2a
To2
To2a
To3p
W2p
W5:To5(2)
W6:To5(2)
W7:To6(3)
W8:To7(3)
W10:To7(4)
W11:To7(4)
W13:To8(5)
W14:To8(7)
W15:To8(8)
W0p
W1p
W0p
W5p
W5p
W6p
W6p
W7p
W8p
W11p
W14p
W15p
Wpostp

Expression dynamics of *Tc-mille-pattes (Tc-mlpt)*

Tc-mlpt expression has been previously described in some detail by Savard et al. (2006). However, they relate *Tc-mlpt* expression only to the expression of a segment polarity gene (excluding dynamics within the SAZ) and this only at 5 distinct stages of development (none of them prior to germband formation). I therefore aim to flesh out this description here.

As reported by Savard et al. (2006), *Tc-mlpt* is first expressed in a broad domain in the presumptive head (Figure 3.12, stage To0). I found that this domain extends from the anterior of the embryo proper to To1p, subsequently fading within stripe To1 so that its posterior border sits at the back of PS0 (Figure 3.12, stages To1-W1:To3). The anterior of this head domain then fades, leaving a stripe of *Tc-mlpt* between To1a and W0p – *i.e.*, spanning PS0 (Figure 3.12, stages W2:4-W5:To4(2)). Savard et al. (2006) describe this stripe as instead precisely spanning the mandibular segment. This appears to result from a misunderstanding of their segment marker, the segment polarity gene *gooseberry*. *gooseberry* overlaps precisely with stripes of *Wg* (Li and Noll, 1993), so our results are directly comparable. Their data shows the anterior stripe of *Tc-mlpt* as abutting the anterior boundary of the first *gooseberry* stripe, equivalent to my results. The first *Tc-Wg* stripe, and therefore the first *Tc-gooseberry* stripe, formed in the trunk sits mid-way through the mandibular segment, and so their data also suggests a parasegmental rather than segmental stripe of expression. At later stages, the PS0 stripe fades and *Tc-mlpt* becomes expressed in specific neuroblasts of the head and anterior trunk (Figure 3.12, stages W7:To6(3)-W15:To8(8)).

Savard et al. (2006) report that two waves of *Tc-mlpt* emerge from the SAZ over the course of segment addition. In addition to these two, I detect a third, weaker domain which emerges near the end of segment addition (stage W13:To8(7)). Like *Tc-Kr*, the first domain of *Tc-mlpt* emerges in two phases – first, it is expressed in a small patch at the posterior tip of the embryo, overlapping with the posterior *Tc-Wg* domain, (Figure 3.12, stage To2), and then it becomes expressed in a broader domain across the posterior SAZ (Figure 3.12, stage To2). The weaker, anterior region of this domain fades rapidly, leaving a strong posterior domain that shifts anteriorly in tandem with the segment pattern (Figure 3.12, stages To2-W1:To3). The anterior boundary of this domain overlaps with To3a, and the posterior boundary overlaps with To5a, so that it later spans PS4-8 in the segmented germband (Figure 3.12, stages W1:To3-W8:To7(3)). The second wave of *Tc-mlpt* expression emerges in the posterior SAZ shortly after the patterning of PS6 (*i.e*. at the start of abdominal patterning) (Figure 3.12, stage W7:To6(3)). This domain also shifts anteriorly in tandem with the segment pattern, spanning

from To6p-To7p (later PS12-13) (Figure 3.12, stages W7:To6(3)-W13:To8(7)). Both of these descriptions are largely consistent with the results of Savard et al. (2006) (ignoring the fact that their descriptions do not match their data), save that they observe expression of the second domain only in PS12. Expression in PS13 fades rapidly compared to expression in PS12 (Figure 3.12, stages W13:To8(7) and W14:To8(7)), so it is not surprising that this may have been missed. The third and final burst of *Tc-mlpt* expression in the SAZ is weak and transitory, appearing across the entirety of the SAZ at stage W13:To8(7) (Figure 3.12). This domain was missed entirely by Savard et al. (2006), likely due to its transitory nature. It is expressed between To8a and the posterior of the *Tc-Wg* domain, indicating transient expression in at least the tissue that will give rise to PS15-16. *Tc-mlpt* is therefore expressed in the SAZ during the patterning of PS4-8, 12-13 and 15-16.

Each of these three domains of *Tc-mlpt* expression fade in the segmented germband at about the same time that secondary *Tc-Tl10* stripes begin to emerge in the relevant parasegments. *Tc-mlpt* subsequently becomes expressed ubiquitously across the embryo (Figure 3.12, stage W15(To8(8)). This ubiquitous expression may reflect a role in epidermal patterning (Ray et al., 2019).

Figure 3.12 (overleaf). HCR showing *Tc-Tl10* (red) and *Tc-mlpt* (cyan or grey) expression in *Tribolium* embryos over the course of segment addition. Images are maximum projections through coronal optical sections (arrows indicate where the midline of the embryo is turned either to the left or to the right, *i.e.* where the optical sections are not perfectly perpendicular to the dorsoventral axis). Germband stage embryos have been dissected away from the egg. Stage is given above each embryo according to the staging system I present in section 3.2.1. For simplicity, *Tc-Wg* expression is not shown, but the positions of selected *Tc-Tl10* and *Tc-Wg* stripes are indicated on greyscale images (in red and white respectively). The suffix ‘a’ refers to the anterior boundary of a stripe, while ‘p’ refers to the posterior boundary of a stripe. Scale bar = 100 μM.

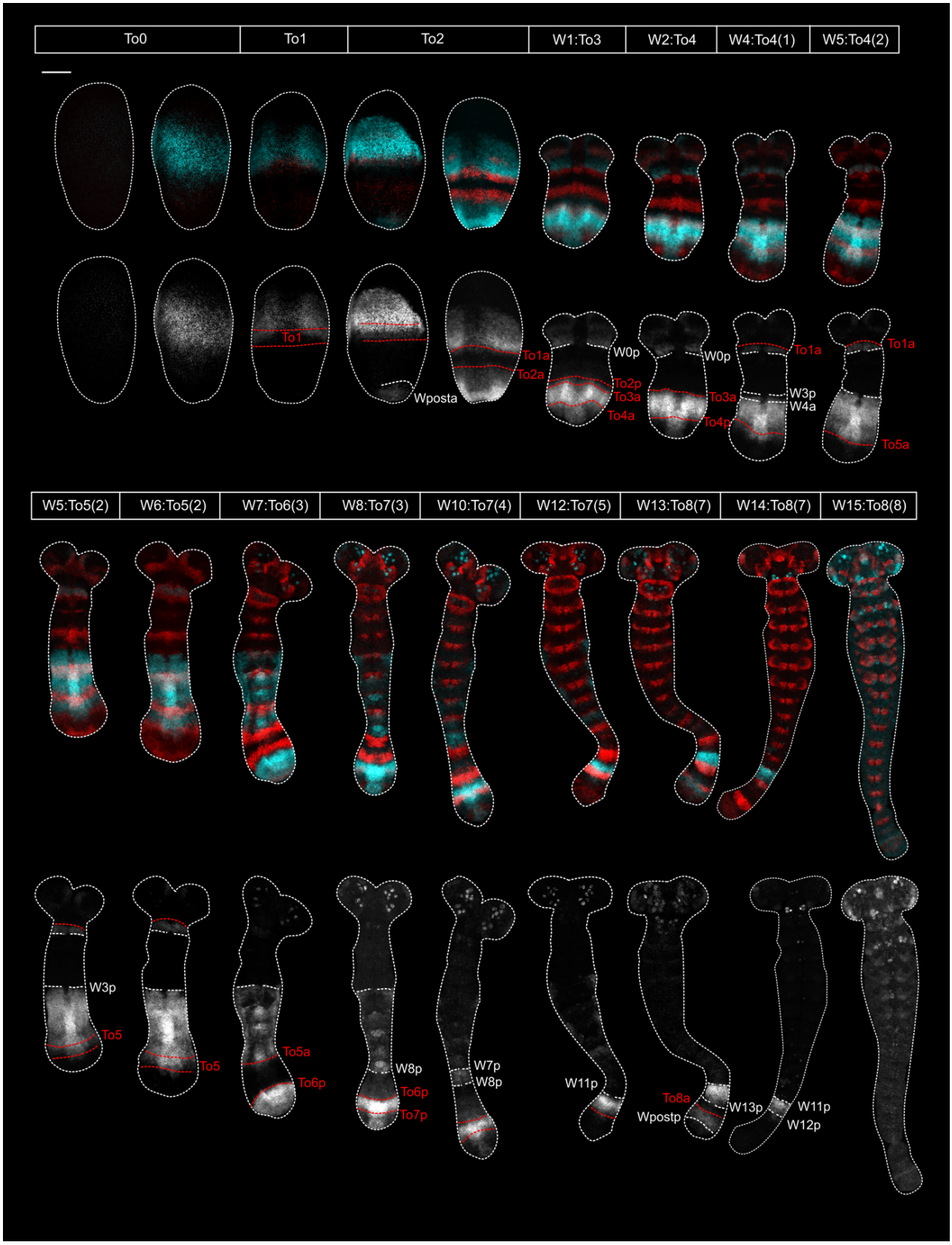
To0
To1
To2
W1:To3
W2:To4
W4:To4(1)
W5:To4(2)
To1
Wposta
To1a
To2a
W0p
To2p
To3a
To4a
W0p
To3a
To4p
To1a
W3p
W4a
To1a
To5a
W5:To5(2)
W6:To5(2)
W7:To6(3)
W8:To7(3)
W10:To7(4)
W12:To7(5)
W13:To8(7)
W14:To8(7)
W15:To8(8)
W3p
To5
To5
To5a
To6p
W8p
To6p
To7p
W7p
W8p
W11p
To8a
Wpostp
W13p
W11p
W12p

Expression dynamics of *Tc-shavenbaby (Tc-svb)*

Tc-svb expression has, prior to this work, been examined only in single colourimetric ISHs and in a limited range of stages (Ray et al., 2019). This is therefore the first description of its expression relative to a segment marker.

Tc-svb is expressed weakly but ubiquitously across the blastoderm during the formation of the first *Tc-Tl10* stripe (Figure 3.13, stage To1). This early expression was not described by Ray et al. (2019), and suggests that *Tc-svb* may have a more global role in early embryonic development. As To1 is refined, *Tc-svb* expression begins to fade in first the presumptive serosa, and then the anterior embryonic primordium, while it strengthens in the posterior third of the embryo (Figure 3.13, stage To1). The anterior boundary of this domain overlaps with To2a (Figure 3.13, stage To2), but the domain soon evolves into a strong stripe overlapping with To2 (Figure 3.13, stage W1:To3). This stripe is maintained for a short time in the germband, neatly overlapping with PS3 (Figure 3.13, stage W4:To4(1)). Shortly afterwards, a new domain of *Tc-svb* emerges in the posterior SAZ (Figure 3.13, stage W4:To4(1)). The anterior border of this domain abuts To5p (Figure 3.13, stage W5:To5(2)), and its posterior border eventually shifts forwards to rest just anterior of To7p (Figure 3.13, stage W8:To7(3)). This is equivalent to PS9-12, although by the time it reaches the segmented germband the anterior boundary of this domain is obscured by ubiquitous expression of *Tc-svb* (Figure 3.13, stage W13:To8(5)). Both of these domains have been described by Ray et al. (2019) without reference to spatial markers. However, as for *Tc-mlpt*, I also observe a third wave of *Tc-svb* in the SAZ that emerges near the end of segment addition (Figure 3.13, stage W13:To8(5)). This domain spans from To7p (eventually W14p) to the back of the posterior *Tc-Wg* domain.

In contrast to other gap genes, the expression of *Tc-svb* is seldom entirely lost in the SAZ – there are periods in which it is expressed at a lower level, or expressed in only the anterior SAZ, but it is always present to some extent (Figure 3.13). However, it is expressed most strongly during the patterning of PS5, PS9-12 and PS14-16.

Figure 3.13 (overleaf). HCR showing *Tc-Tl10* (red) and *Tc-svb* (cyan or grey) expression in *Tribolium* embryos over the course of segment addition. Images are maximum projections through coronal optical sections (arrows indicate where the midline of the embryo is turned either to the left or to the right, *i.e.* where the optical sections are not perfectly perpendicular to the dorsoventral axis). Germband stage embryos have been dissected away from the egg. Stage is given above each embryo according to the staging system I present in section 3.2.1. For simplicity, *Tc-Wg* expression is not shown, but the positions of selected *Tc-Tl10* and *Tc-Wg* stripes are indicated on greyscale images (in red and white respectively). The suffix 'a' refers to the anterior boundary of a stripe, while 'p' refers to the posterior boundary of a stripe. Scale bar = 100 μM.

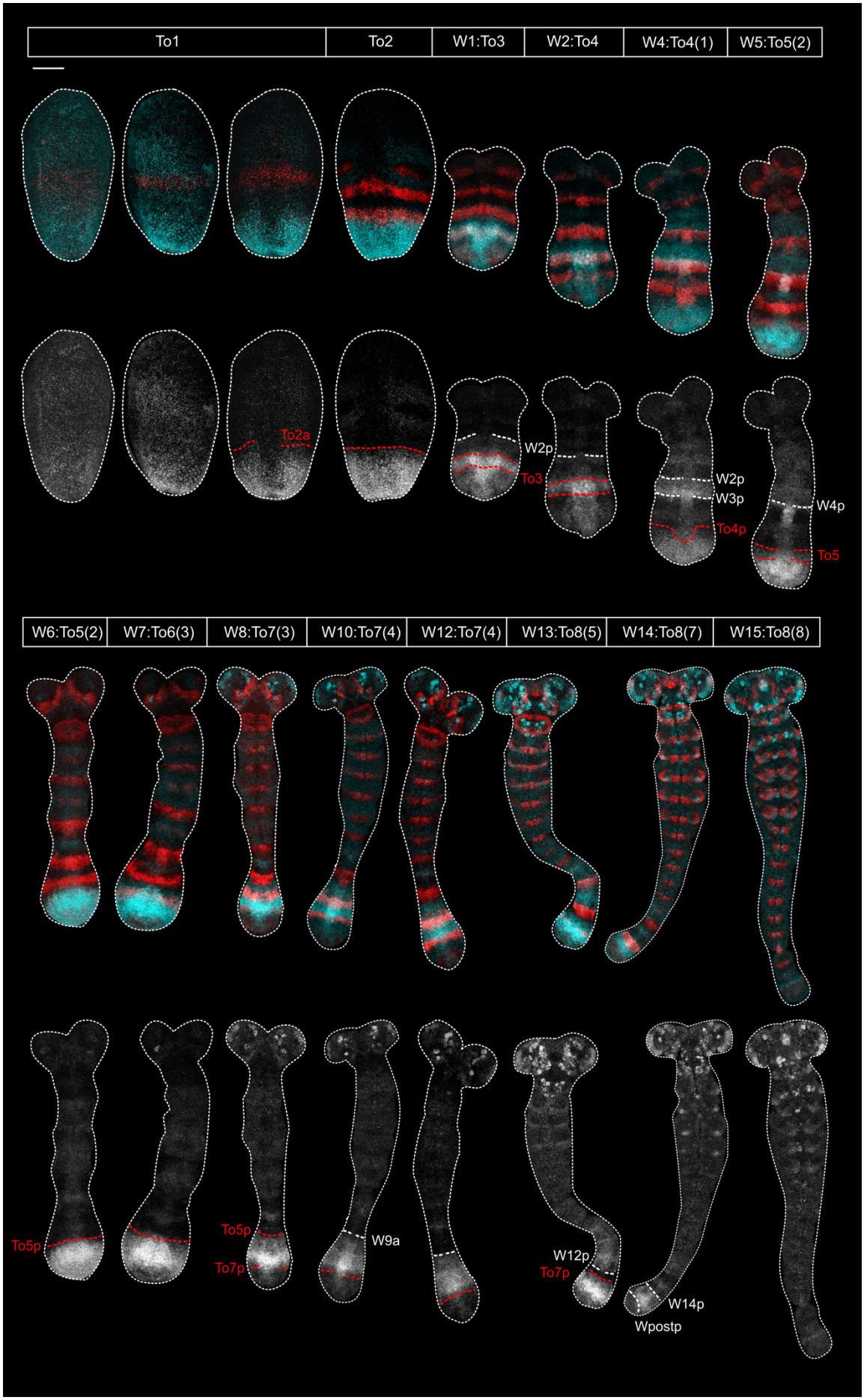
To1
To2
W1:To3
W2:To4
W4:To4(1)
W5:To5(2)
To2a
W2p
To3
W2p
W3p
To4p
W4p
To5
W6:To5(2)
W7:To6(3)
W8:To7(3)
W10:To7(4)
W12:To7(4)
W13:To8(5)
W14:To8(7)
W15:To8(8)
To5p
To5p
To7p
W9a
W12p
To7p
W14p
Wpostp

Expression dynamics of *Tc-giant (Tc-gt)*

Tc-gt expression has been described by Bucher and Klingler (2004). This description makes use of the pair-rule gene *Tc-eve* as a parasegmental/segmental marker, but again, only for a few select stages.

As in *Drosophila*, *Tc-gt* is provided maternally in *Tribolium* so the mRNA is initially ubiquitous (Figure 3.14, stage To0 and Bucher and Klingler (2004)). After the formation of the uniform blastoderm, however, mRNA is cleared anteriorly, from the presumptive serosa, and posteriorly, from a small patch at the terminus of the egg (Figure 3.14, stage To0 and Bucher and Klingler (2004)). The posterior third of the egg is then cleared of mRNA, leaving a broad domain of *Tc-gt* in the anterior embryo (Figure 3.14, stage To2 and Bucher and Klingler (2004)). Note that this repression of *Tc-gt* in the posterior of the embryo occurs in a two-step process, similar to *Tc-hb* and to the initial activation of *Tc-Kr* and *Tc-mlpt* in the SAZ. These similarities suggest that these four genes may be regulated by similar regulatory inputs and/or regulate each other.

Over time, the head domain of *Tc-gt* evolves into a stripe that is offset slightly posteriorly compared to To1, and spans from W0p to a short distance behind W1p (presumably overlapping with the first engrailed stripe, en1 - Figure 3.14, stages To2-W2:To3). Bucher and Klingler (2004) describe this head stripe as neatly overlapping the maxillary segment – my data, by contrast, suggest that this domain overlaps at least some of the mandibular segment as well as the entirety of the maxillary segment. The head stripe fades soon afterwards, such that *Tc-gt* is expressed at low levels across the head back to the posterior of PS1 (Figure 3.14, stage W5:To4(1)). Expression subsequently fades in PS1, and *Tc-gt* becomes expressed in specific neuroblasts in the head (Figure 3.14, stages W6:To5(2) onwards).

Shortly after maternal *Tc-gt* is cleared from the SAZ, the trunk gap domain emerges at the posterior-most tip of the embryo (Figure 3.14, stage To2). The anterior border of this expression domain shifts anteriorly (Bucher and Klingler, 2004) until it sits a short distance behind To3a (Figure 3.14, stage W1:To3). A strong stripe forms, spanning from this boundary back to abut To4a, and a second stripe subsequently forms spanning from a short distance behind To4a back to abut To5a (Figure 3.14, stages W1:To3-W6:To5(2)). In the segmented germband, these two stripes are refined to cover the majority of PS5 and the majority of PS7-8 (Figure 3.14, stages W6:To5(2)-W8:To7(3)). By contrast, Bucher and Klingler (2004) report that these two stripes neatly overlap with segments T3 and A1. It appears that the boundaries of these stripes may change as they emerge from the SAZ – the fact that their anterior

boundaries initially sit a short distance behind the anterior boundaries of *Tc-Tl10* stripes suggest that they are initially out of sync with the parasegmental pattern, but later come into sync as the pattern matures. Examination of *Tc-gt* expression with a segmental, rather than parasegmental, marker, may help to clarify this issue.

The two stripes of *Tc-gt* expression fade well before the end of segment addition, and expression is subsequently detected only in neuroblasts of the head (Figure 3.14, stage W10:To7(4) onwards).

Figure 3.14 (overleaf). HCR showing *Tc-Tl10* (red) and *Tc-gt* (cyan or grey) expression in *Tribolium* embryos over the course of segment addition. Images are maximum projections through coronal optical sections (arrows indicate where the midline of the embryo is turned either to the left or to the right, *i.e.* where the optical sections are not perfectly perpendicular to the dorsoventral axis). Germband stage embryos have been dissected away from the egg. Stage is given above each embryo according to the staging system I present in section 3.2.1. For simplicity, *Tc-Wg* expression is not shown, but the positions of selected *Tc-Tl10* and *Tc-Wg* stripes are indicated on greyscale images (in red and white respectively). The suffix 'a' refers to the anterior boundary of a stripe, while 'p' refers to the posterior boundary of a stripe. Scale bar = 100 μM.

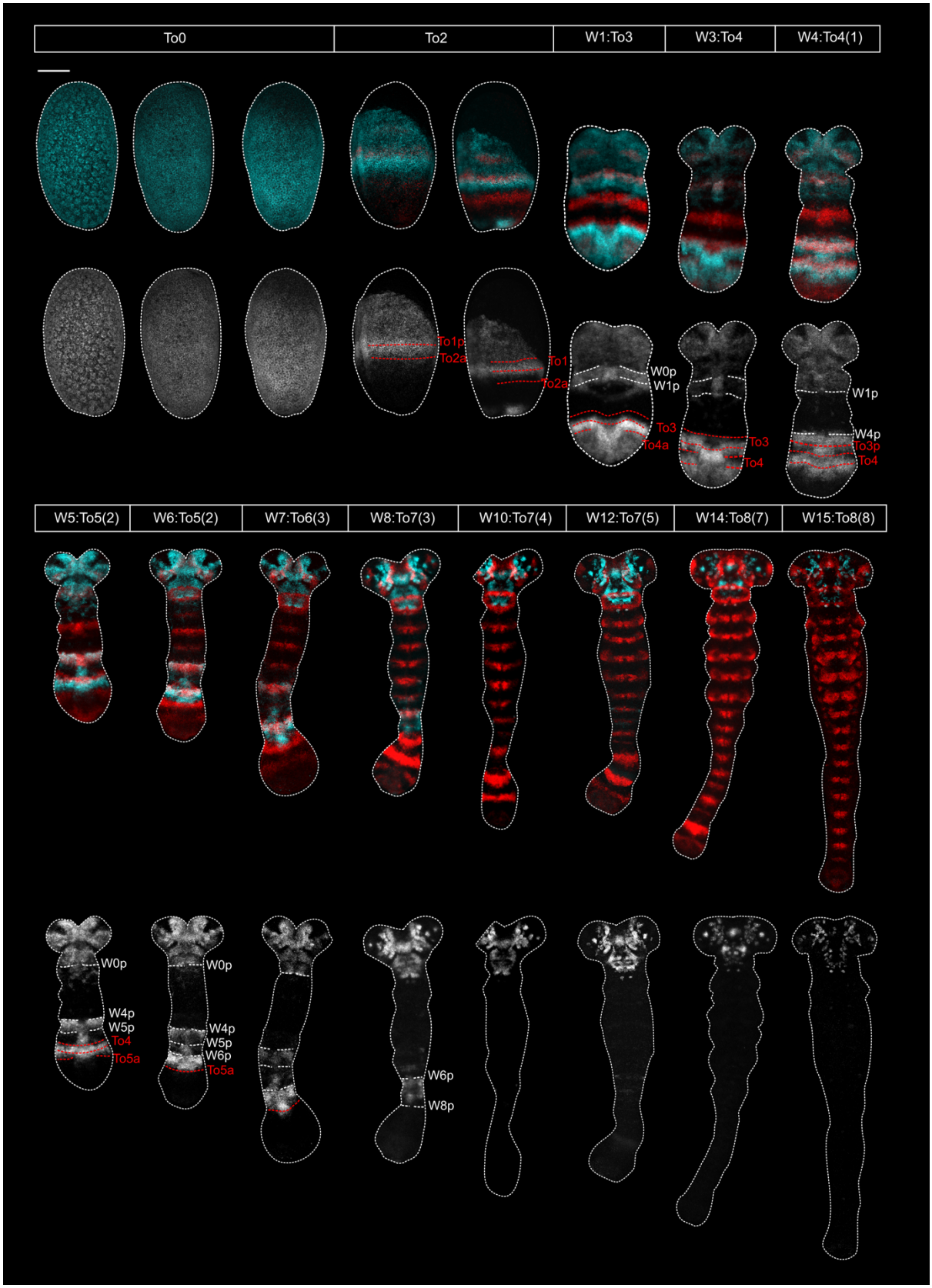
To0
To2
W1:To3
W3:To4
W4:To4(1)
To1p
To2a
To1
To2a
W0p
W1p
To3
To4a
To3
To4
W1p
W4p
To3p
To4
W5:To5(2)
W6:To5(2)
W7:To6(3)
W8:To7(3)
W10:To7(4)
W12:To7(5)
W14:To8(7)
W15:To8(8)
W0p
W4p
W5p
To4
To5a
W0p
W4p
W5p
W6p
To5a
W6p
W8p

Expression dynamics of *Tc-knirps (Tc-kni)*

Tc-kni expression has been described by Cerny et al. (2008) and Peel et al. (2013), but most focus has rested on the anterior domain, with no attempt made to map the posterior domain against segmental or parasegmental markers.

As reported by Cerny et al. (2008) and Peel et al. (2013), *Tc-kni* is first expressed in the early blastoderm in a broad head domain, excluding the differentiating serosa (Figure 3.15, stage To0). Within this domain, a stronger stripe of *Tc-kni* forms, spanning from the posterior boundary of the *Tc-Tl10* head stripe to To1a (Figure 3.15, stage To2). This is consistent with reports of the *Tc-kni* head stripe overlapping with PS0 (Peel et al., 2013). This stripe of *Tc-kni* is not maintained for long, and almost all head expression is gone by W6:To5(2) (Figure 3.15) save for an anterior region that marks the developing labrum (Figure 3.15, W6:To5(2) onwards and Cerny et al. (2008)).

The posterior domain of *Tc-kni* first emerges at the posterior pole of the embryo at stage To2 (Figure 3.15). Its anterior boundary then shifts anteriorly in tandem with *Tc-Tl10* stripes, abutting To3p (Figure 3.15, stages To2-W3:To4). This domain is strongest in a stripe spanning from To3p to To4a (later corresponding to PS6 - Figure 3.15, stage W3:To3). This stripe begins to fade soon after it emerges, faster than the remaining *Tc-kni* expression in the posterior SAZ (Figure 3.15, stage W4:To4(1)). After this posterior domain fades, expression is retained in the posterior mesoderm and mesectoderm (Figure 3.15, stages W5:To5(2)-W10:To7(4)). As reported by Cerny et al. (2008), I also observe expression of *Tc-kni* in the tracheal placodes (Figure 3.14, stage W8:To7(3) onwards) and overlapping with the posterior *Tc-Wg* domain at the end of segmentation, perhaps corresponding to a function in gut patterning (Figure 3.15, stages W13:To8(7) and W15:To8(7)).

Figure 3.15 (overleaf). HCR showing *Tc-Tl10* (red) and *Tc-kni* (cyan or grey) expression in *Tribolium* embryos over the course of segment addition. Images are maximum projections through coronal optical sections (arrows indicate where the midline of the embryo is turned either to the left or to the right, *i.e.* where the optical sections are not perfectly perpendicular to the dorsoventral axis). Germband stage embryos have been dissected away from the egg. Stage is given above each embryo according to the staging system I present in section 3.2.1. For simplicity, *Tc-Wg* expression is not shown, but the positions of selected *Tc-Tl10* and *Tc-Wg* stripes are indicated on greyscale images (in red and white respectively). The suffix 'a' refers to the anterior boundary of a stripe, while 'p' refers to the posterior boundary of a stripe. Scale bar = 100 μM.

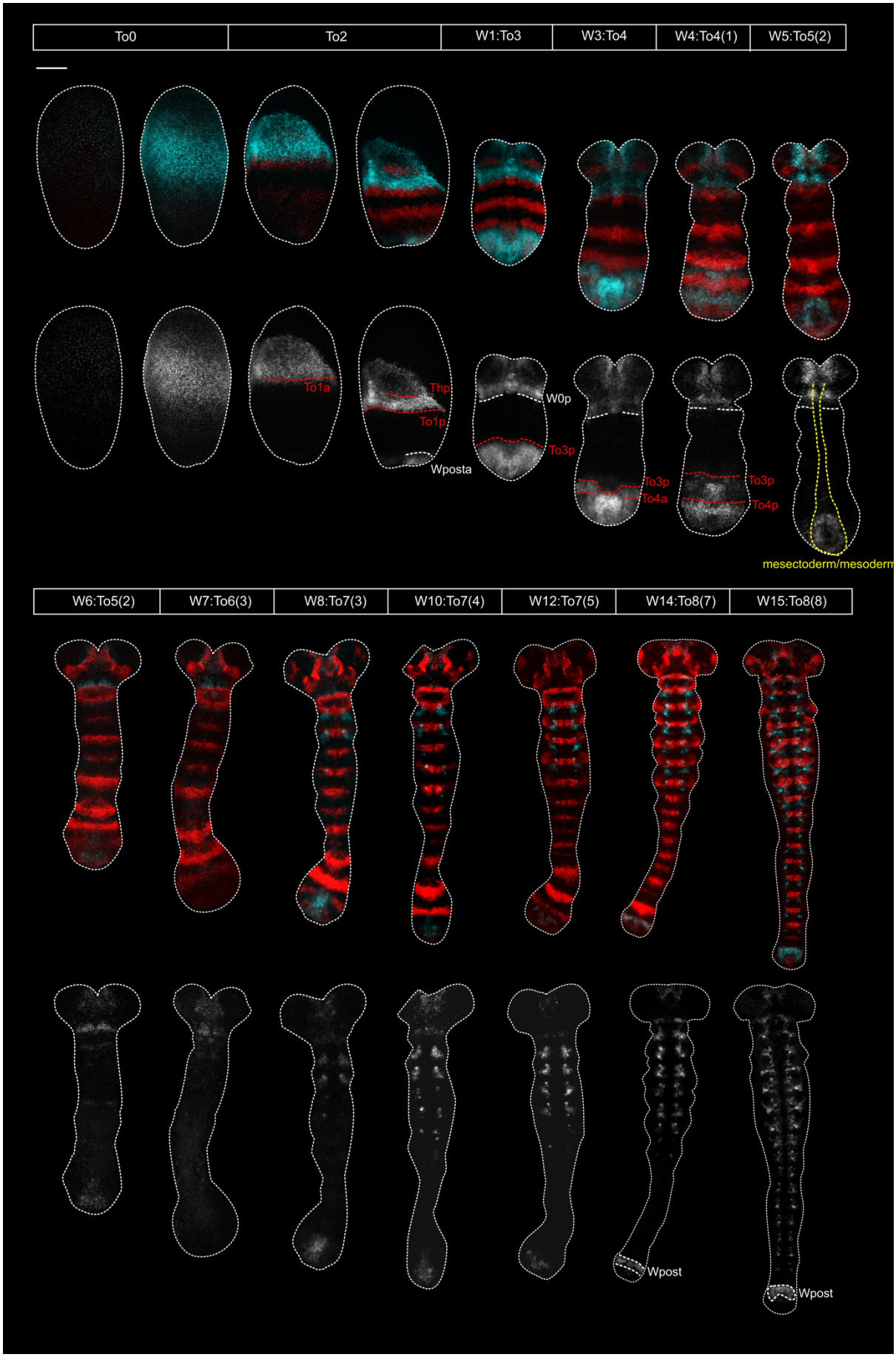
To0
To2
W1:To3
W3:To4
W4:To4(1)
W5:To5(2)
To1a
Thp
To1p
Wposta
W0p
To3p
To3p
To4a
To3p
To4p
mesectoderm/mesoderm
W6:To5(2)
W7:To6(3)
W8:To7(3)
W10:To7(4)
W12:To7(5)
W14:To8(7)
W15:To8(8)
Wpost
Wpost

3.2.3. Multiplexed expression analysis of gap gene dynamics

I next aimed to generate an integrated description of gap gene expression across the entire period of segment addition. I performed HCR ISHs against triplets of gap and gap-like genes (*Tc-hb*, *Tc-Kr*, *Tc-svb*, *Tc-mlpt*, *Tc-gt*, *Tc-kni* and/or *Tc-tll*) in addition to my three marker genes (*Tc-Tl10*, *Tc-Sim* and *Tc-Wg*). A representative series from each of three different triplet HCR ISHs is shown in Figure 3.16. Embryos at the same stage of development according to my staging system were pooled together, and information about the relative phasing of each gap or gap-like gene against my marker genes was abstracted into a graphical format as shown in Figure 3.17. The head was omitted from this abstraction for simplicity, although information on head expression is available in my dataset. In Figure 3.18 I show a condensed version of my full graphical dataset, focusing on expression of gap genes in the SAZ and newly formed parasegments over the course of segmentation. For simplicity, I have excluded the earliest stages of gap gene expression (prior to stage To1), and instead describe the relevant dynamics in the following text.

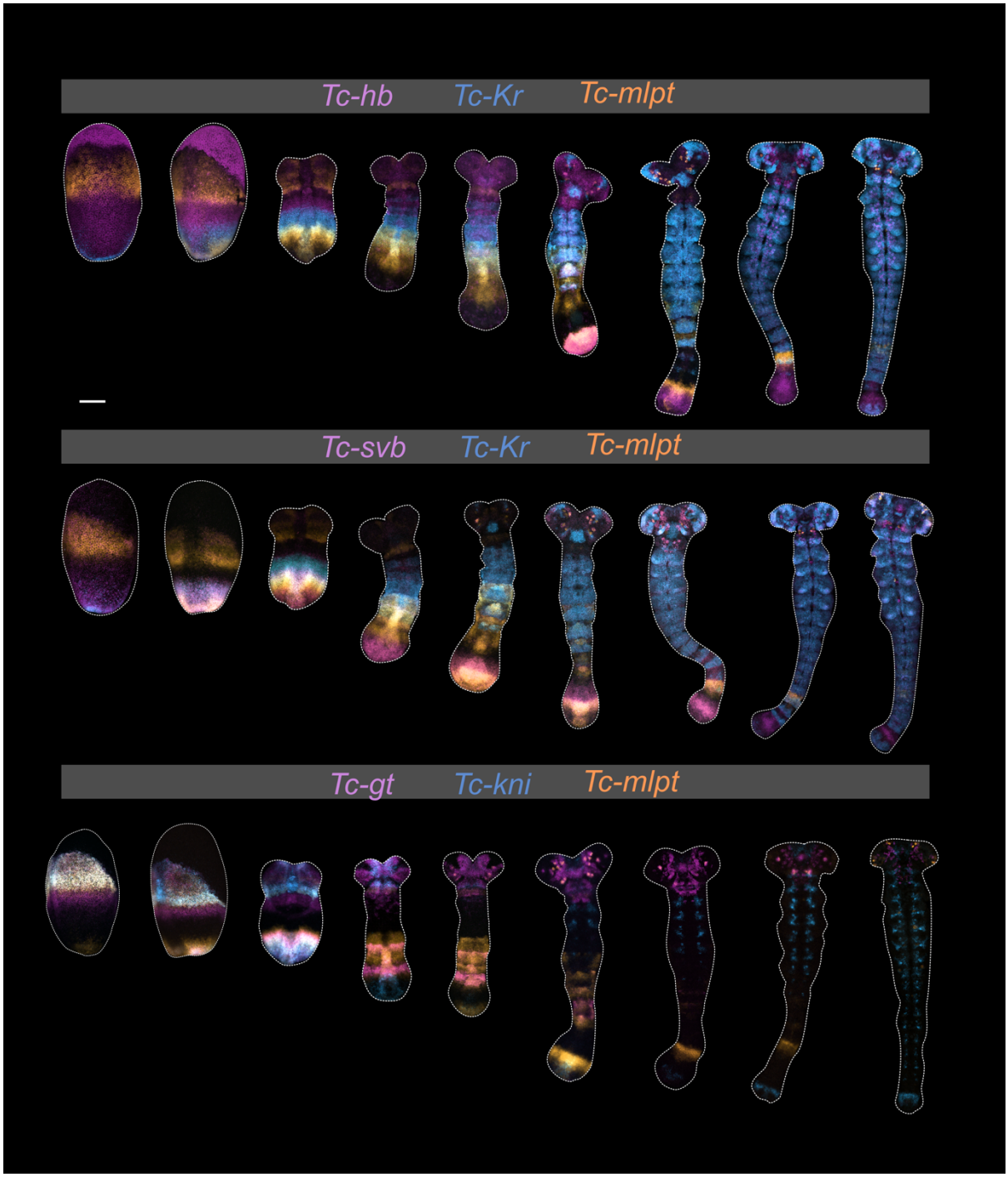

Figure 3.16. A selection of representative embryos from triplet HCR ISHs, spanning the course of segment addition. Each embryo contains information on the expression of three gap or gap-like genes, and my three marker genes (*Tc-Wg*, *Tc-Tl10* and *Tc-sim* – here excluded for simplicity). The triplet of gap or gap-like genes shown in each row are indicated above. Scale bar is 100 μM.

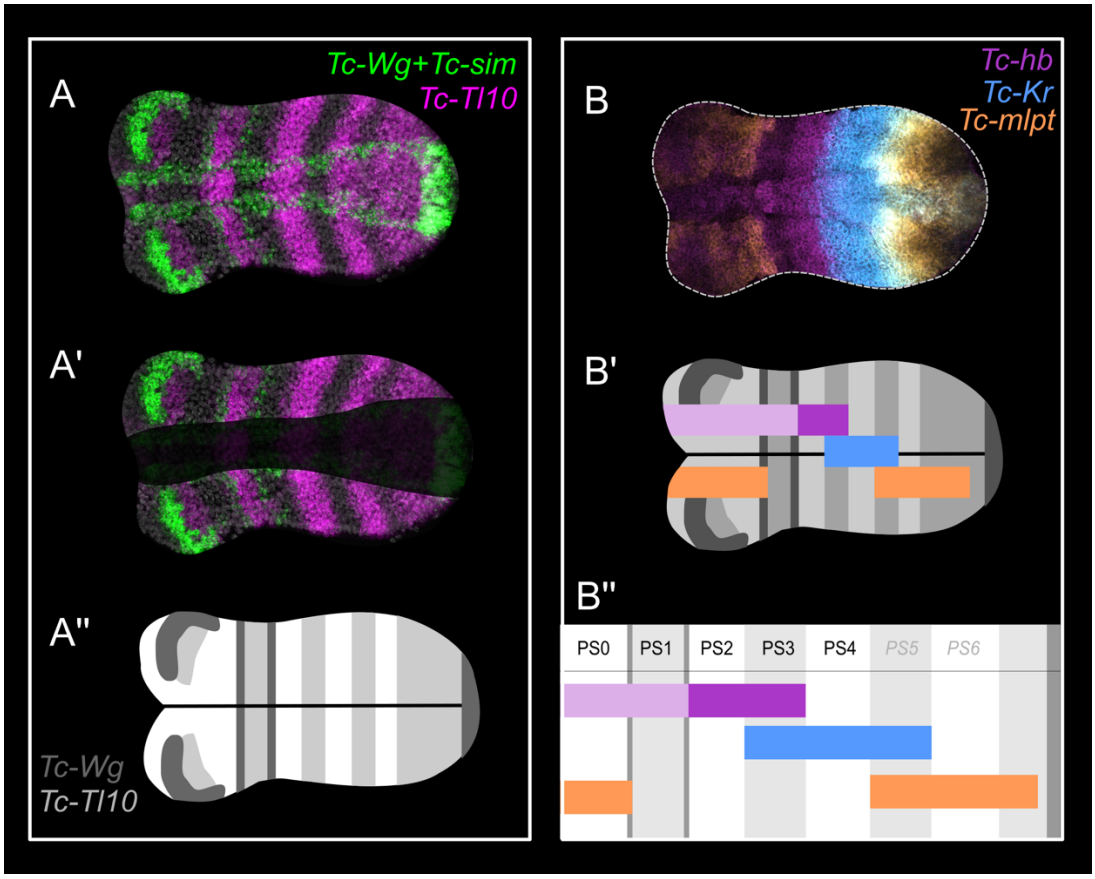

Figure 3.17. Compiling HCR data on canonical gap gene expression into a graphical abstract. **A|** A maximum projection through the ventral epithelium of a Tribolium embryo after HCR showing expression of *Tc-Wg* and *Tc-sim* (green) and *Tc-Tl10* (magenta) (A). *Tc-sim*-expressing tissue (mesectoderm) and the interior mesoderm are discounted from further analysis (A'). Information on *Tc-Wg* and *Tc-Tl10* expression in the ectoderm can be represented graphically as shown in A''. The central black line represents where mesectoderm and mesoderm have been 'excised'. **B|** HCR data on the expression of three gap genes from the same embryo as in A (B) can be represented graphically alongside *Tc-Wg* and *Tc-sim* expression as shown in B' (note that left-right differences are also discounted in my dataset, so position of stripes on the y axis is arbitrary). For my purposes, the shape of the embryo and expression of genes in the head is discounted so that the final dataset for this embryo appears as in B''.

Figure 3.18 (overleaf). Graphical representation of gap gene expression in the SAZ and newly formed parasegments at the indicated stages over the course of segment addition. Dark grey stripes indicate *Tc-Wg* stripes and the posterior *Tc-Wg* domain; light grey stripes indicate regions of the segment pattern that will give rise to odd-numbered parasegments in the SAZ (based on the boundaries of *Tc-Tl10* stripes) and odd-numbered parasegments in the segmented germband. The first column shows the trunk and posterior terminus in their entirety, while the subsequent columns show only the two most recently patterned parasegments and the SAZ for brevity. Segmentally repeated expression domains that emerge *de novo* in the segmented germband are excluded.

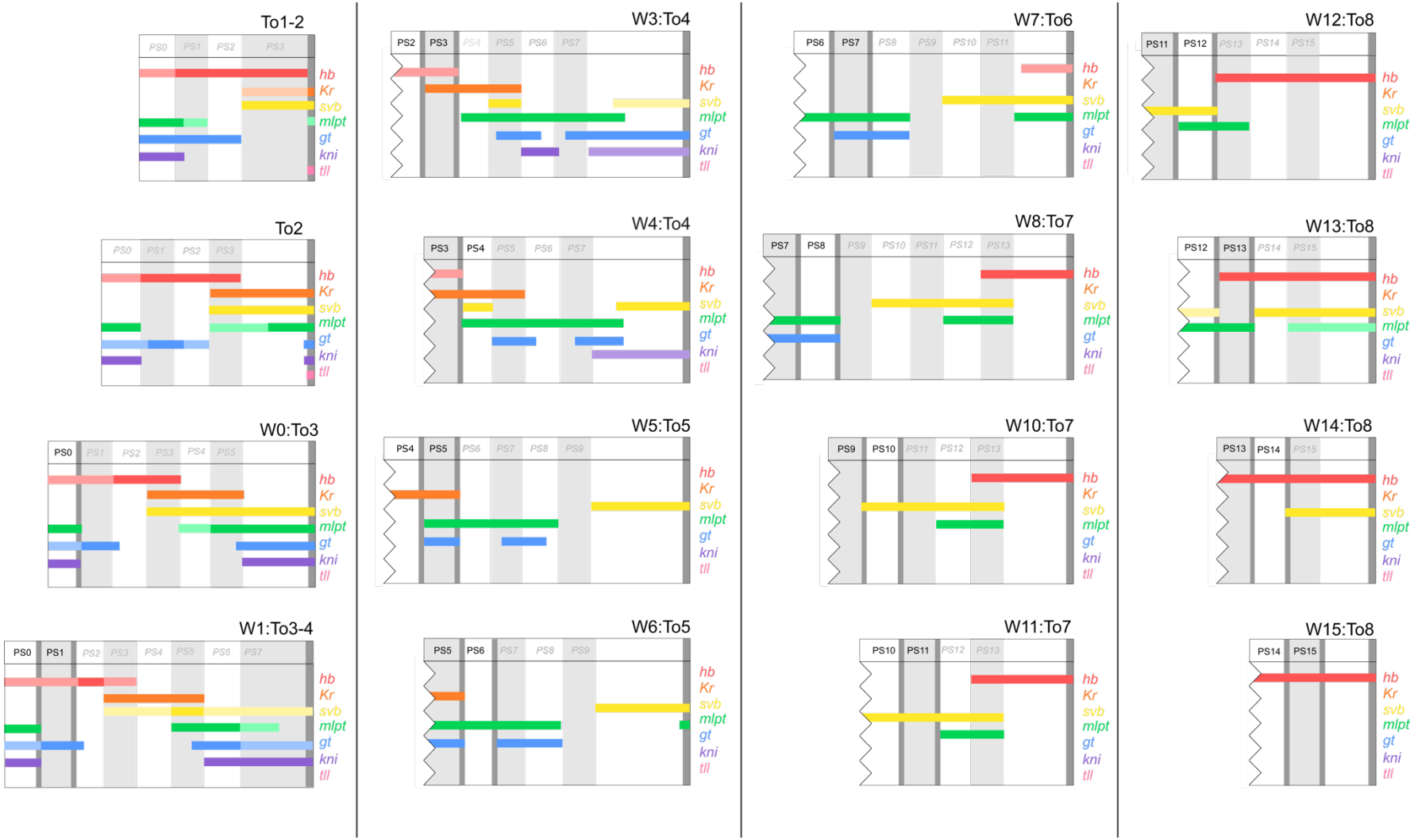
To1-2
PS0 PS1 PS2 PS3
hb Kr svb mlpt gt kni tll
To2
PS0 PS1 PS2 PS3
hb Kr svb mlpt gt kni tll
W0:To3
PS0 PS1 PS2 PS3 PS4 PS5
hb Kr svb mlpt gt kni tll
W1:To3-4
PS0 PS1 PS2 PS3 PS4 PS5 PS6 PS7
hb Kr svb mlpt gt kni tll
W3:To4
PS2 PS3 PS4 PS5 PS6 PS7
hb Kr svb mlpt gt kni tll
W4:To4
PS3 PS4 PS5 PS6 PS7
hb Kr svb mlpt gt kni tll
W5:To5
PS4 PS5 PS6 PS7 PS8 PS9
hb Kr svb mlpt gt kni tll
W6:To5
PS5 PS6 PS7 PS8 PS9
hb Kr svb mlpt gt kni tll
W7:To6
PS6 PS7 PS8 PS9 PS10 PS11
hb Kr svb mlpt gt kni tll
W8:To7
PS7 PS8 PS9 PS10 PS11 PS12 PS13
hb Kr svb mlpt gt kni tll
W10:To7
PS9 PS10 PS11 PS12 PS13
hb Kr svb mlpt gt kni tll
W11:To7
PS10 PS11 PS12 PS13
hb Kr svb mlpt gt kni tll
W12:To8
PS11 PS12 PS13 PS14 PS15
hb Kr svb mlpt gt kni tll
W13:To8
PS12 PS13 PS14 PS15
hb Kr svb mlpt gt kni tll
W14:To8
PS13 PS14 PS15
hb Kr svb mlpt gt kni tll
W15:To8
PS14 PS15
hb Kr svb mlpt gt kni tll

Early repression of *Tc-hb* and *Tc-gt*, and activation of *Tc-Kr*, occurs in a region overlapping with *Tc-tll* expression

A homologue of the terminal gap gene *Dm-tll* is expressed at the posterior pole of the *Tribolium* embryo prior to gastrulation (Schröder et al., 2000). The relationship between this domain of *Tc-tll* and other gap gene domains suggests that it does not play a similar role to its homologue in *Drosophila* (for example, it is expressed well before the formation of the terminal *hb* stripe, which it plays a role in repressing in *Drosophila*) (Schröder et al., 2000). The role of *Tc-tll* has therefore been proposed to be limited largely to pre-patterning of the embryonic terminus, with little or no involvement in the gap gene cascade (Schröder et al., 2000).

I theorised that the posterior domain of *Tc-tll* might be involved in the initial, localised phase of repression of *Tc-hb* and *Tc-gt* at the posterior pole. To investigate this hypothesis further, I examined the expression of *Tc-tll* alongside *Tc-hb*, *Tc-gt* and/or *Tc-Kr* in blastoderm stage embryos (Figure 3.19).

I found that the expression of *Tc-tll* precedes the localised loss of expression of *Tc-hb* and *Tc-gt* in the posterior terminus of the embryo, and that its expression domain neatly overlaps the region of degradation (Figure 3.19, A-B'). *Tc-Kr* expression emerges at the same time as the expression of *Tc-hb* and *Tc-gt* is lost at the posterior pole (Figure 3.19, A-B'). In *Drosophila*, *Dm-tll* is able to repress *Dm-hb* and *Dm-gt* (reviewed in Jaeger, 2011), so a causative relationship is plausible. Confirming this will, of course, require functional analysis.

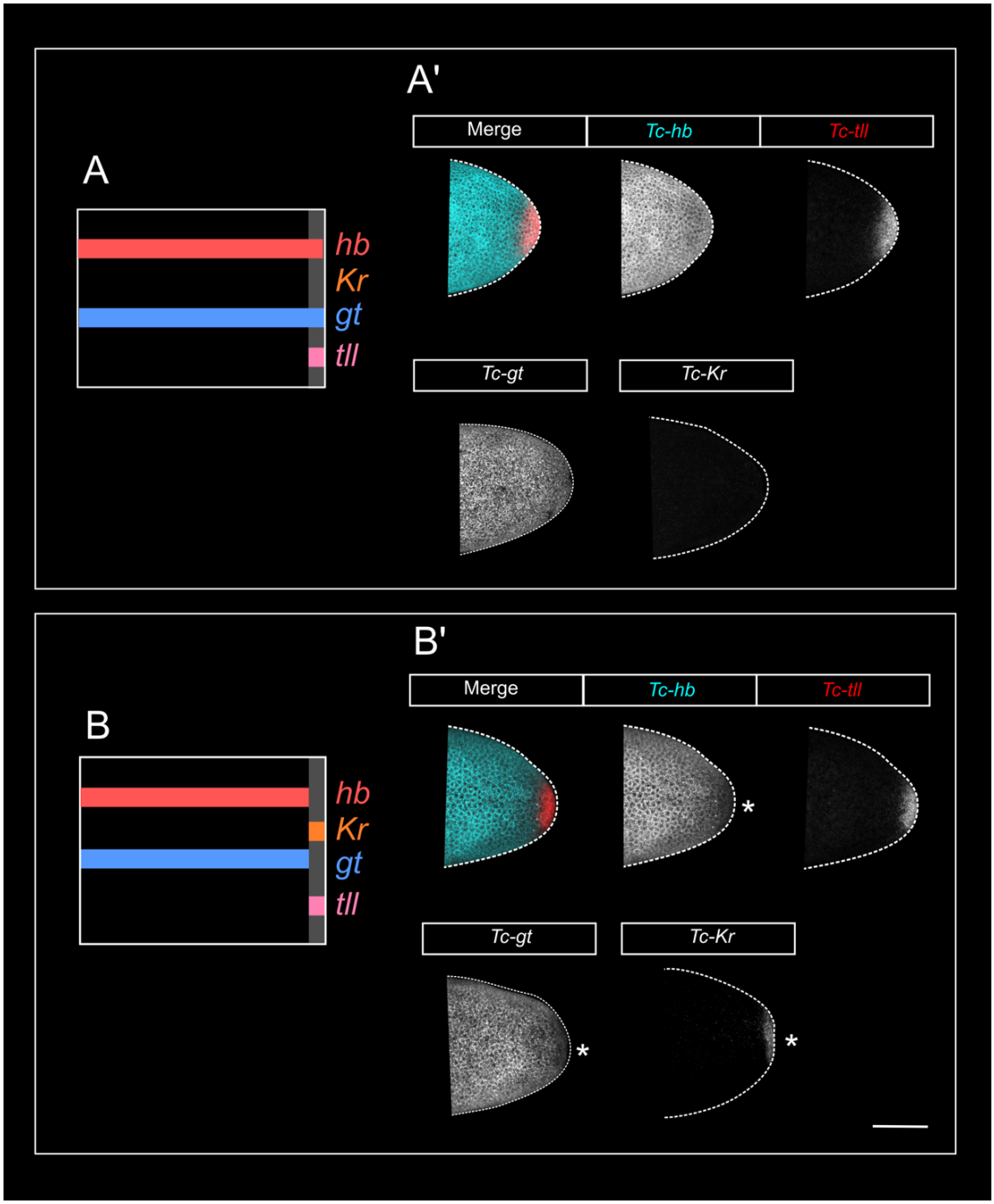

Figure 3.19. *Tc-tll* expression prefigures terminal repression of *Tc-hb* and *Tc-gt*. A| *Tc-tll* is expressed at the posterior terminus, initially overlapping *Tc-hb* and *Tc-gt*. At this stage both of the latter genes reach all the way to the posterior terminus and *Tc-Kr* is not expressed. B| *Tc-hb* and *Tc-gt* expression are subsequently lost in the region in which *Tc-tll* is expressed. *Tc-Kr* expression then emerges overlapping with *Tc-tll*. Note that in both panels, *Tc-gt* and *Tc-Kr* images are from different embryos than *Tc-hb* and *Tc-tll* (and each other) but have been determined to be an equivalent age using DAPI staining. Scale bar is 100 µM.

Tc-svb fills the gap gene gap

My multiplexed data confirms previous observations that the gap and gap-like genes are expressed in densely overlapping but staggered domains in the SAZ during patterning of the anterior regions of the embryo (from PS0-7, spanning from the mandibular segment back to encompass the anterior compartment of A2), and more sparsely during the patterning of posterior regions (Figure 3.19). A key observation is that the candidate gap gene *Tc-svb* is expressed in the 'gap gene gap', being the sole gap gene expressed in the SAZ during the patterning of much of the posterior abdomen (~PS9-12) (Figure 3.19). However, as noted earlier, the expression of *Tc-svb* is far from typical for a canonical *Tribolium* gap gene. Rather than being expressed in one or two contiguous blocks of segments, *Tc-svb* is expressed in the SAZ for almost the entire course of segmentation, although it is lost from the posterior SAZ just after the beginning of abdominal segmentation (Figure 3.19, stages W3:To4-W8:To7) and lost entirely from the SAZ just before the end of segment addition (Figure 3.19, stage W12:To8).

The switching of Tc-Svb protein to an active from correlates temporally and spatially with the emergence of posterior *Tc-gt, Tc-kni* and *Tc-hb* domains

Given the unusual expression dynamics of *Tc-svb*, I decided to investigate how its expression relates to that of its proposed 'co-factor', *Tc-mlpt*. Based on their analysis of single colorimetric ISHs, Ray et al. (2019) report that the expression patterns of *Tc-mlpt* and *Tc-svb* are most likely mutually exclusive for the majority of segment addition, save for one short period just prior to gastrulation. Using multiplexed data, I show that the expression of *Tc-mlpt* and *Tc-svb* overlaps extensively in the SAZ three times during segment addition – firstly, as previously described, in the blastoderm prior to gastrulation, in a region covering the primordia PS5-7; secondly, midway through segment addition, in the primordia for PS12-13; and finally at the end of segment addition, in the primordia for PS15-16 (Figure 3.19 and Figure 3.20).

As discussed in the introduction, *mlpt* peptides are able to trigger transformation of Svb protein from a repressor to an activator (Kondo et al., 2010). The interactions observed between *Tc-mlpt* and other gap genes (Savard et al., 2006) are therefore likely to be indirect, mediated through its interaction with Tc-Svb. I wondered whether changes in the form of the Svb TF, as predicted by co-expression (or lack thereof) with *mlpt*, might correlate with changes in gap gene expression in the SAZ.

The first burst of *Tc-mlpt* expression, and presumably the switching of Tc-Svb to an active form, precedes the emergence of the posterior *Tc-gt* and *Tc-kni* domains (Figure 3.21). We know from previous work (Savard et al., 2006) that *Tc-mlpt* is required for the emergence of at least the posterior *Tc-gt* domain – it seems feasible that the interaction between *Tc-mlpt* and *Tc-gt* is mediated through Tc-Svb and its switch into an activator. Whether *Tc-mlpt* or *Tc-svb* knockdown impacts the expression of *Tc-kni* has not been tested. As *Tc-mlpt* expression fades in the SAZ, and Tc-Svb presumably returns to a repressive form, *Tc-gt* and *Tc-kni* expression also fade (Figure 3.19), suggesting that they might be repressed by *Tc-svb* in the absence of *Tc-mlpt*. *Tc-svb* then remains expressed alone in the SAZ until the second burst of *Tc-mlpt*, which directly precedes the emergence of the posterior *Tc-hb* domain (Figure 3.22)..

Together, these expression data suggest that *Tc-mlpt* and *Tc-svb* may play important roles in co-ordinating the activation and repression of different gap genes.

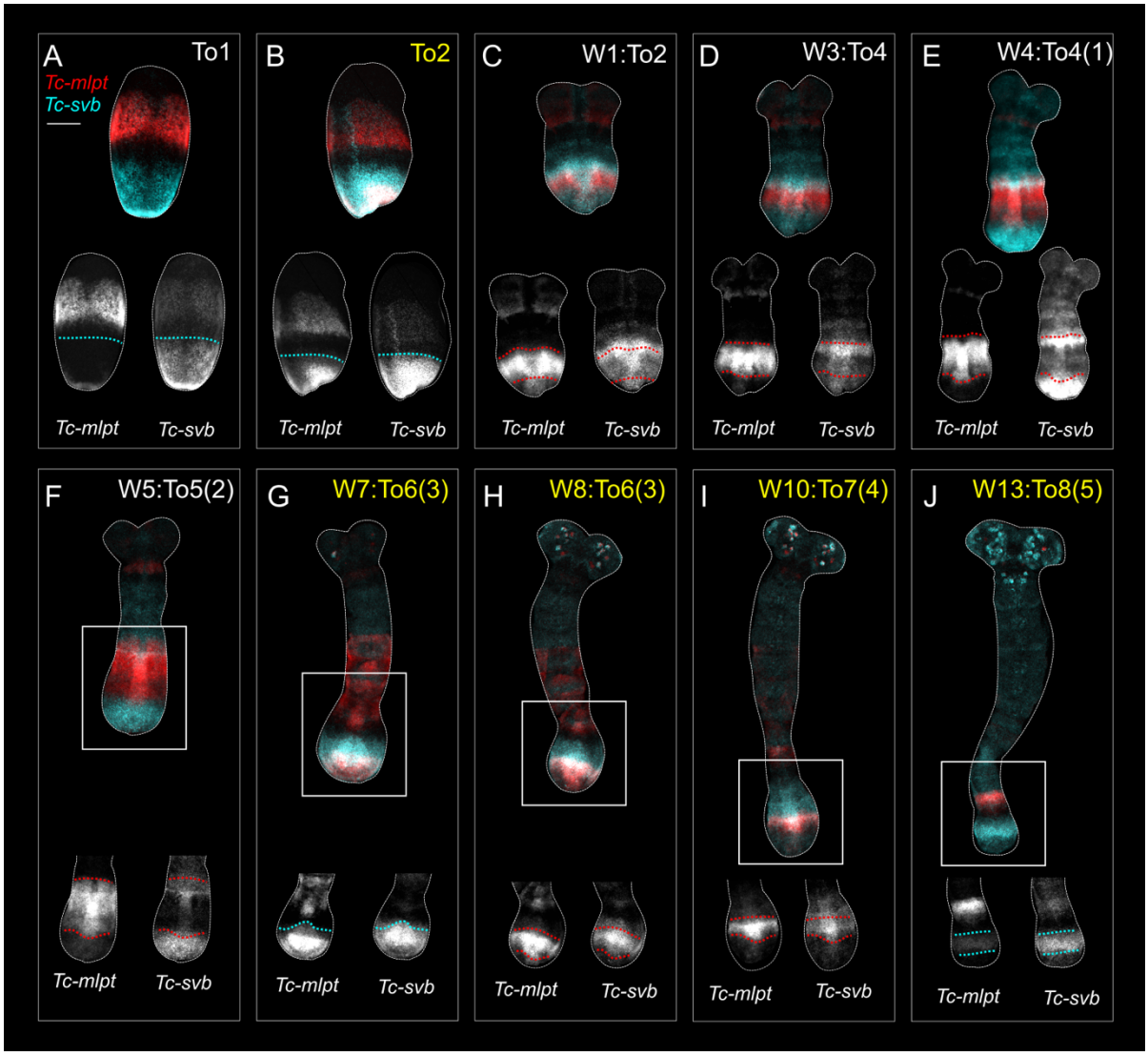

Figure 3.20. *Tc-svb* (cyan) and *Tc-mlpt* (red) expression over the course of segment addition. Dotted lines in greyscale images mark the same boundary in each pair of images, allowing easier comparison of overlap. Yellow stage names are used to indicate where there is extensive overlap of *Tc-mlpt* and *Tc-svb* expression. Scale bar is 100 μM.

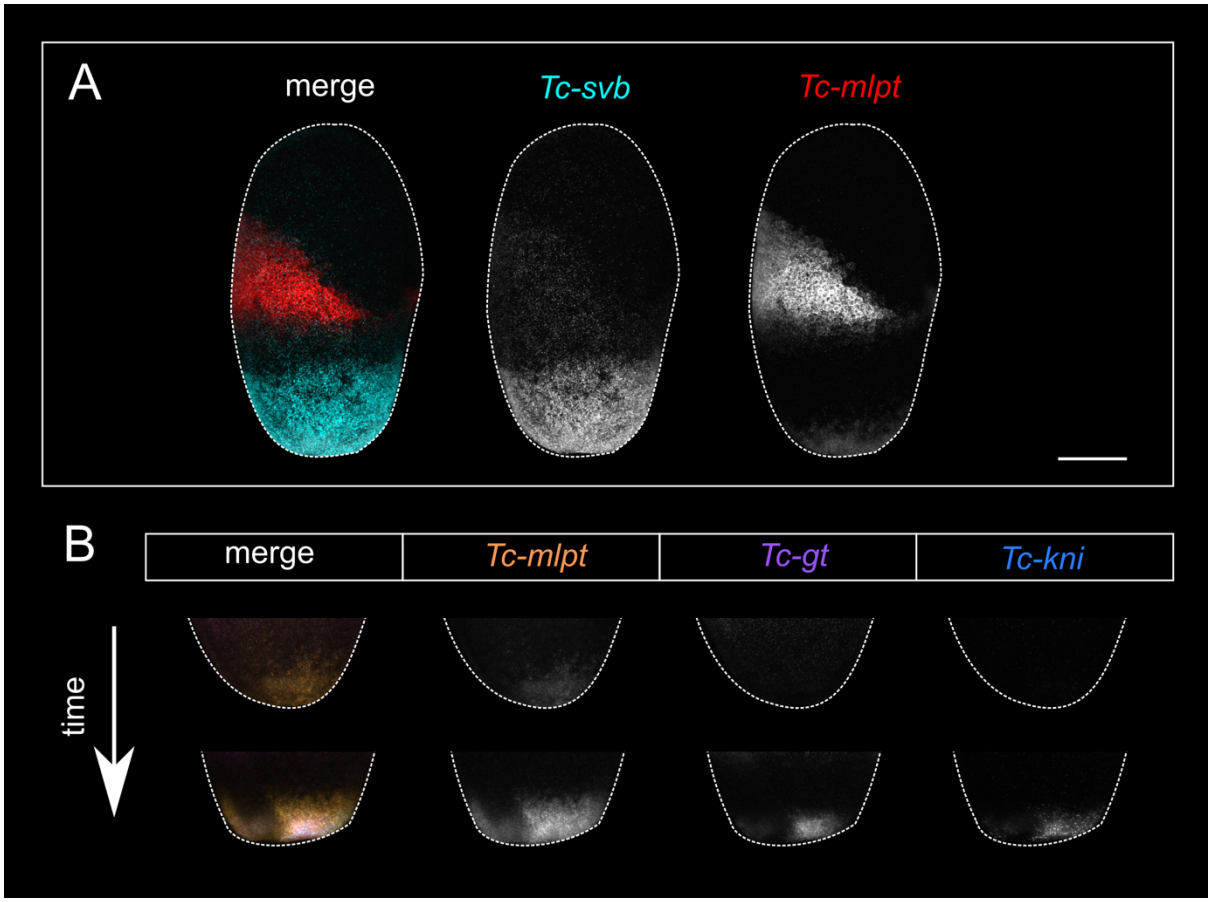

Figure 3.21. *Tc-mlpt* and *Tc-svb* are co-expressed shortly before the emergence of posterior *Tc-gt* and *Tc-kni*. **A|** A blastoderm stage embryo at the same stage as that in B (staged using *Tc-Wg*, *Tc-Tl10* and DAPI) showing the emergence of *Tc-mlpt* within the posterior *Tc-svb* domain. **B|** Cropped images of the posterior terminus of two embryos after the emergence of the posterior domain of *Tc-mlpt*, showing that this prefigures the emergence of posterior *Tc-gt* and *Tc-kni*. Scale bar is 100 μM.

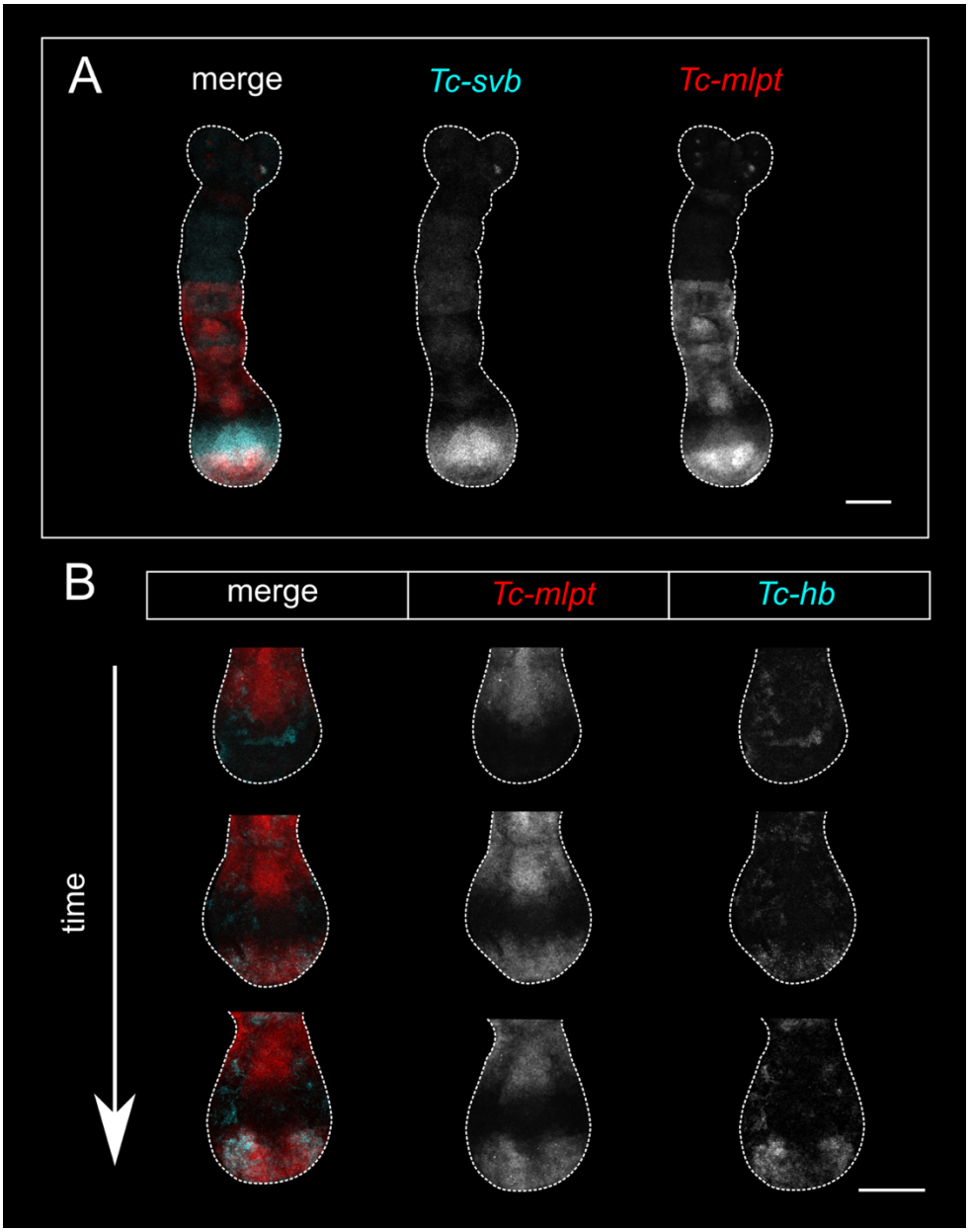

Figure 3.22. *Tc-mlpt* and *Tc-svb* are co-expressed shortly before the emergence of posterior *Tc-hb*. **A|** A mid-segmentation embryo at a similar stage to those in B showing that *Tc-mlpt* is co-expressed with *Tc-svb* at this stage. **B|** Cropped images of the posterior terminus of three embryos before and during the emergence of the posterior domain of *Tc-mlpt*, showing that this prefigures the emergence of posterior *Tc-hb*. Scale bar is 50 µM.

3.3. DISCUSSION

In this chapter I have established a spatial and temporal marker system to use for my analyses going forward. In doing so, I have validated *Tc-Tl10* as a spatial marker that combines useful features of both segment polarity and pair-rule gene markers and provided the first description of *Tc-sim* in a sequentially-segmenting insect. I then present a thorough description of the expression of each of the canonical and candidate gap genes in *Tribolium* against my standardised marker set. The greater level of precision and temporal coverage in my HCR dataset compared to previous colorimetric datasets has allowed me to pinpoint boundaries or domains previously missed, and also to correct some errors in published work. Notably, this is the first description of *Tc-svb* expression against a segment marker of any kind. Finally, I compared the expression of the gap genes in multiplexed HCR datasets in order to compile an abstracted summary of gap gene expression in the SAZ across the course of segment addition. This will present a useful resource to anyone studying gap genes, but has also generated some novel observations that are discussed below.

3.3.1. *Tc-Tl10* can be used as a spatial marker across the SAZ and germband

My results indicate that the relationship between *Tc-Tl10* and the segmental pattern is slightly more complex than previously understood (Benton et al., 2016). In the SAZ, a weak leading edge is detected at the anterior of primary *Tc-T10* stripes, which must be discounted if one wants to use the anterior boundary as an indicator for future parasegment boundaries. Furthermore, the secondary stripes of *Tc-Tl10* initially overlap with *Tc-Wg* stripes before taking on their final position directly behind them, so that one must differentiate between immature and mature stripes in order to relate them to the parasegment pattern. If I had known that I would be able to use two spatial markers from the beginning of my PhD, I may instead have chosen to use *Tc-Wg* and *Tc-eve* as a dual spatial marker system, as *Tc-eve* does not appear to have a leading edge in the SAZ, and its secondary stripes do not shift relative to the segment pattern during maturation. However, I believe the validation of *Tc-Tl10* as a spatial marker suitable for standalone use will be useful to those who are unable to perform highly multiplexed reactions, or those who do not have access to a confocal microscope with a broad range of lasers.

3.3.2. The terminal system and activation of *Tc-Kr*

One of the key early events in the gap gene series in *Tribolium* is the degradation of maternally provided *Tc-hb* and *Tc-gt* at the posterior pole, and the subsequent emergence of *Tc-Kr* expression in this region. Schmitt-Engel et al. (2012) propose that the repression of both genes is mediated through the activity of the products of the posteriorly-localised mRNA *Tc-nanos* and its co-factor, *Tc-pumilio.* When one or both of these genes are knocked down by pRNAi, Tc-Hb and Tc-Gt fail to retract from the posterior pole, and the posterior domains of *Tc-Kr*, *Tc-gt*, *Tc-mlpt* and *Tc-kni* never arise (Schmitt-Engel et al., 2012). In *Drosophila*, Dm-Hb is translationally repressed by Dm-Nanos and Dm-Pumilio, resulting in loss of autoactivation and subsequently loss of expression; however, there is no evidence that they interact with *Dm-gt* in this way (Hülskamp et al., 1989; Irish et al., 1989b). *Tc-gt* may differ from *Dm-gt* in that it appears to contain a Nanos Response Element (NRE) sequence, like *Dm-hb* and *Tc-hb* (Schmitt-Engel et al., 2012).

Another way in which Nanos may influence *Tc-hb* and *Tc-gt* expression is through the terminal gene *Tc-tll*. In *Drosophila*, Dm-Nanos promotes the expression of *Dm-tll* at the posterior pole (Cinnamon et al., 2004), and *Dm-tll* is able to repress *Dm-gt* and *Dm-hb* in order to repress them from the terminus of the embryo (reviewed in Jaeger, 2011). The distribution of *Tc-nanos* mRNA or protein has not yet been examined in *Tribolium* embryos (Schmitt-Engel et al., 2012), but if it is similar to its *Drosophila* homologue, then we might expect the protein to be distributed in a broad posterior-anterior gradient (Wang et al., 1994). If this is the case, then perhaps *Tc-hb* and *Tc-gt* are repressed at the very terminus of the embryo by localised Tc-Tll protein, and subsequently repressed in a broad posterior domain by the gradient of Tc-Nanos protein. To dissect which aspects of the terminal patterning network are, indeed, required for regulating gap gene expression in *Tribolium*, more functional tests will be required – in particular, no-one has yet examined gap gene expression in a *Tc-tll* knockdown.

3.3.3. The expression dynamics of *Tc-mlpt* and *Tc-svb* correlate with activation and repression of other gap genes

My expression data suggests that both activation and repression by Tc-Svb may be required for transitions in gap gene expression over the course of segmentation.

I have shown that co-expression of *Tc-mlpt* and *Tc-svb* (and so presumably the switching of *Tc-svb* to an active form) correlates with the switching on of posterior *Tc-gt* and *Tc-kni* domains. *Tc-mlpt* has previously been shown to be required for activation of the posterior *Tc-gt* domain (Savard et al., 2006), and I propose that this activation is mediated through its interaction with Tc-Svb. Both *Tc-mlpt* and *Tc-svb* knockdowns show homeotic transformation of abdominal segments towards a thoracic fate (Ray et al., 2019; Savard et al., 2006), a phenotype that is not observed in *Tc-gt* knockdowns (Bucher and Klingler, 2004). It therefore seems likely that they have at least one more target in the abdomen. *Tc-kni* knockdowns also show no abdominal transformations (Cerny et al., 2005). However, in *Drosophila*, *Tc-gt* and *Tc-kni* seem to act redundantly to prevent expansion of *Tc-Kr* into the abdomen (Kraut and Levine, 1991). If this redundant repression is conserved in *Tribolium*, then the abdominal phenotype of *Tc-mlpt* and *Tc-svb* knockdowns could result from loss of both *Tc-gt* and *Tc-kni* expression. This could be confirmed by examining *Tc-kni* expression in *Tc-mlpt* knockdowns, and performing double knockdowns for *Tc-gt* and *Tc-kni* (see Chapter 5).

I also show that co-expression of *Tc-mlpt* and *Tc-svb* prefigure the emergence of the posterior *Tc-hb* domain. In *Drosophila*, the formation of the posterior *Dm-hb* domain requires terminal *Dm-tll* expression, although it is likely that this regulation is indirect, through repression of *Dm-kni* (reviewed in Jaeger, 2011). It has therefore been somewhat of a mystery how the posterior domain of *Tc-hb* is regulated, given that it is expressed well after both *Tc-tll* and *Tc-kni* have faded from the SAZ. The correspondence in timing and location of this domain with the emergence of the second wave of *Tc-mlpt* seems too exact to be a coincidence. Knockdown of *Tc-mlpt* does seem to delay the expression of this domain; however, it still forms eventually (Savard et al., 2006), suggesting Tc-Svb cannot be the sole activator for this domain, if it does indeed act as an activator.

To dissect how Tc-Mlpt and Tc-Svb interact with the gap gene network, it would be interesting to compare gap gene expression in both knockdowns, given that knockdown of the former should result in a loss of only the activator function of Tc-Svb, while knockdown of the latter should result in loss of activating and repressing functions. This is, of course, assuming

that Tc-Mlpt does not also have roles independent of Tc-Svb, which its homologues certainly do outside of segment patterning (Pueyo and Couso, 2008).

This work demonstrates how analyses of multiplexed gene expression can provide an invaluable supplement to the information gleaned from knockdown experiments. Based on knockdown alone, it is not possible to determine whether a protein interacts directly or indirectly with the genes that become misexpressed. Examining the temporal and spatial dynamics of gene expression can then provide evidence for or against hypotheses about direct interactions between genes. My dataset will, I hope, remain useful for future studies that wish to further investigate the interactions between gap genes.

3.3.4. Do *Tc-mlpt* and *Tc-svb* have a distinct role compared to other gap genes?

In this chapter, I show that *Tc-mlpt* and *Tc-svb* together almost entirely fill the so-called 'gap gene gap' – one or both of them are expressed in the SAZ throughout the course of abdominal segment formation (Figure 3.23). However, as discussed in the results, *Tc-svb* is expressed in the SAZ for the majority of segment addition, in contrast to any other gap gene. Given the relationship between the expression of *Tc-mlpt*, *Tc-svb* and other gap genes, I propose that the role of *Tc-svb* and *Tc-mlpt* may be more akin to an ON/OFF switch that regulates the gap gene state of the SAZ. To understand this, it may be helpful to visualise the experience of a single cell in the SAZ (Figure 3.24). As it cycles through the expression of different gap genes, it is also oscillating between two states, determined by the activity of Tc-Svb; either Tc-Svb is co-expressed with *Tc-mlpt*, in which case it acts as an activator (Svb-A), or it is not, and it acts as a repressor (Svb-R). The state of this switch seems to be under the control of the rest of the gap gene network to at least some extent, as the first burst of *Tc-mlpt* is lost in *Tc-Kr* knockdowns and expanded in *Tc-gt* knockdowns (Savard et al., 2006). However, how the second *Tc-mlpt* burst is triggered is as yet unknown.

A striking observation when viewing the gap gene network from this perspective is that although *Tc-svb* is co-expressed with other gap genes for almost the entirety of development, no other gap gene is expressed between the turning off of *Tc-gt* and *Tc-kni* and the turning on of *Tc-hb*. I therefore remain unconvinced that *Tc-svb* presents an answer to the issue of the gap gene gap. It is entirely possible that there are additional candidate gap genes that are expressed during the patterning of the abdominal segments, and I will present my examination of three candidates in the next results chapter.

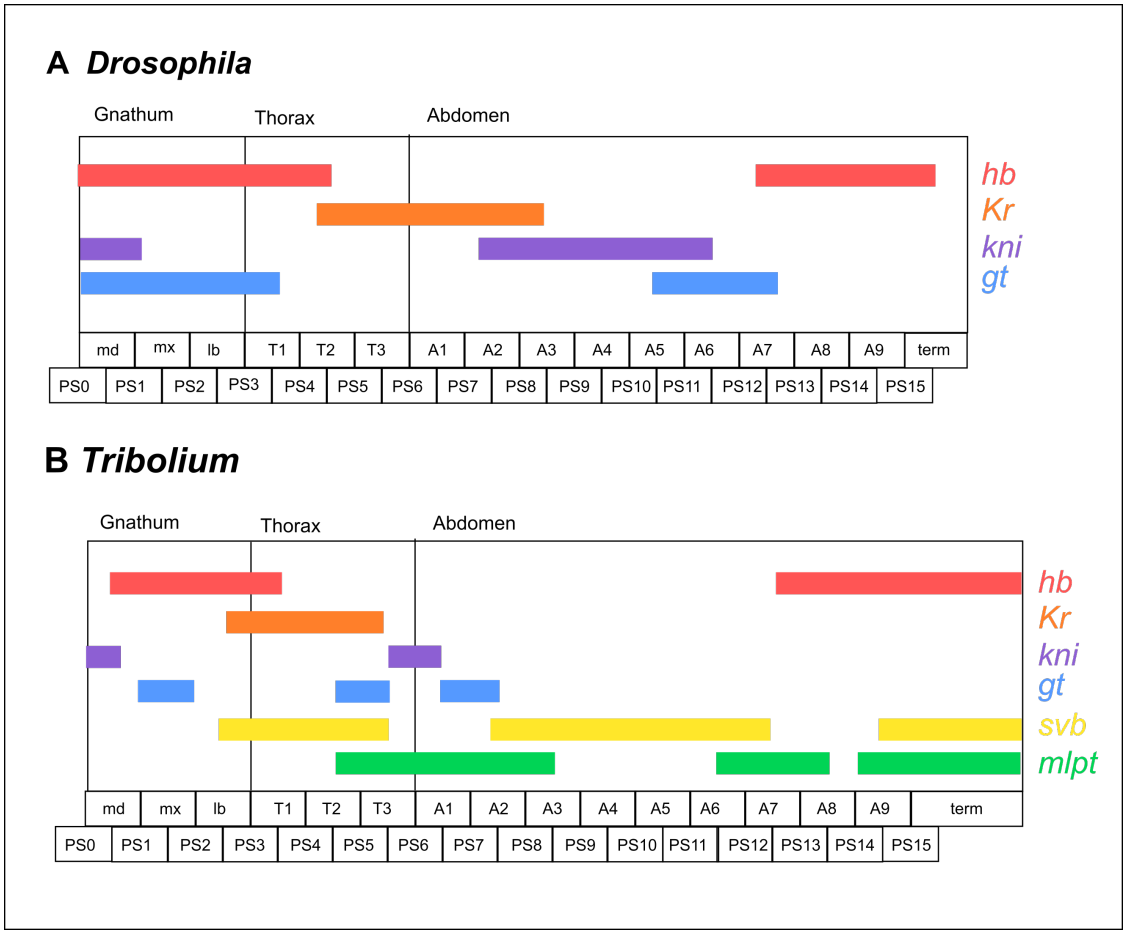

Figure 3.23. Summary of the gap genes expressed by trunk (para)segments as they are specified (*i.e.* at the time that segmental *Wg* stripes first emerge) in *Drosophila* (A) and *Tribolium* (B). Note that the pattern is compressed anteriorly in *Tribolium*, with much of the abdominal segments expressing only *Tc-mlpt* and/or *Tc-svb*. Term = terminus of the embryo.

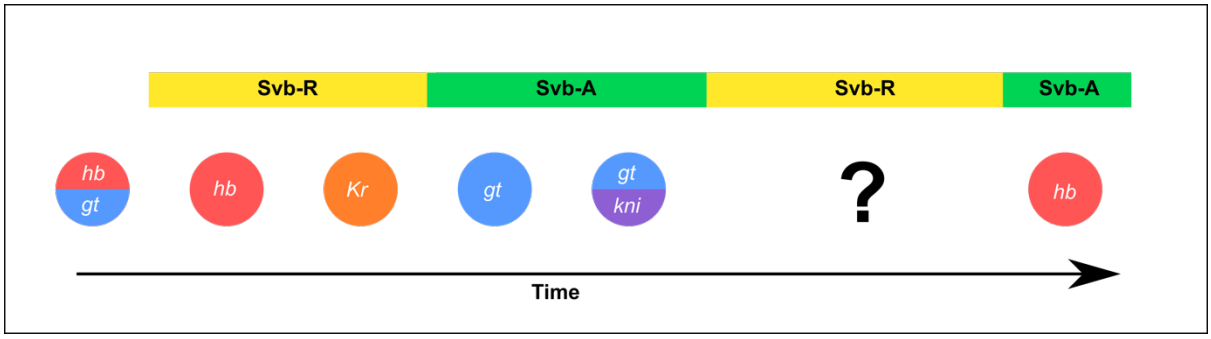

Figure 3.24. Representation of gap genes expressed by a single cell in the SAZ over the course of segment addition. In this model, *Tc-svb* and *Tc-mlpt* expression are externalised into an ON/OFF switch, the output of which is whether Tc-Svb is acting as an activator (co-expressed with *Tc-mlpt* – Svb-R) or as a repressor (not co-expressed with *Tc-mlpt* – Svb-A). See text for more details.

4. INVESTIGATING CANDIDATE GAP GENES FROM THE NEUROBLAST TIMER SERIES

4.1. INTRODUCTION

4.1.1. The neuroblast timer series is a source of gap gene candidates for *Tribolium*

Homologues of all four of the canonical trunk gap genes from *Drosophila* (*Dm-hb*, *Dm-Kr*, *Dm-gt* and *Dm-kni*) have been shown to regulate segment patterning and/or identity in *Tribolium* (Bucher and Klingler, 2004; Cerny et al., 2005; Cerny et al., 2008; Marques-Souza et al., 2008; Peel et al., 2013). However, unlike in *Drosophila*, the expression domains of these genes are insufficient to cover the length of the trunk during segment addition, resulting in a period during which the SAZ expresses no canonical gap genes and creating 'a gap gene gap' (Cerny et al., 2008). Although *Tc-mlpt* and *Tc-svb* are expressed in the SAZ during this period, I have argued in the previous chapter that their expression patterns are more consistent with their acting as regulators of the gap gene network than as gap genes themselves. If this is the case, then it suggests that there are additional gap genes yet to be identified in *Tribolium*.

One promising source of gap gene candidates is the neuroblast timer series in *Drosophila*. Of the four core neuroblast timer genes, two (*hb* and *Kr*) are also canonical gap genes, and two others (*nub* and *cas*) are regionally expressed along the AP axis of the blastoderm in the same manner as the gap genes (Isshiki et al., 2001; Jaeger, 2011; Peel et al., 2005). In addition to these four core genes, the TF *grainyhead* (*grh*), may act as a fifth timer gene in certain neuroblast lineages (Baumgardt et al., 2009; Brody and Odenwald, 2000; Brody and Odenwald, 2002; Cenci and Gould, 2005); however, at least in *Drosophila*, its expression during segment patterning is less suggestive of a role in AP patterning (Dynlacht et al., 1989; Huang et al., 1995).

Save for a brief description of the expression of *nub* and *cas* in neuroblasts (Biffar and Stollewerk, 2014) and unpublished preliminary work of our collaborator's student, E. Raymond, on the same genes, the expression and function of *Tc-nub*, *Tc-cas* and *Tc-grh* have yet to be characterised in *Tribolium* embryos. Below, I describe these genes and their roles in development in more detail, and assess their potential as candidate gap genes.

4.1.2. *Nubbin* (*nub*) as a candidate gap gene

nub encodes a class II POU domain transcription factor that shares homology with the mammalian Oct factors Oct1 and Oct2 (Billin et al., 1991; Dick et al., 1991; Lloyd and Sakonju, 1991; Prakash et al., 1992). *Nub* exists as a single copy in most arthropods (Li and Popadić, 2004), but in *Drosophila* this gene has undergone a duplication to produce the two linked genes *pdm1* (**P**OU **d**omai**n** protein **1** - also referred to as *nub*) and *pdm2* (Billin et al., 1991; Cockerill et al., 1993; Dick et al., 1991; Lloyd and Sakonju, 1991). These genes are expressed in almost identical patterns during development (Cockerill et al., 1993; Dick et al., 1991; Lloyd and Sakonju, 1991), and are largely functionally redundant (Yeo et al., 1995). Henceforth, *nub* will be used to refer to both the ancestral gene and *pdm1* in *Drosophila*, with the assumption that *pdm2* expression and function is very similar or identical. *Pdm1/pdm2* double mutants will be referred to as *nub* mutants for simplification.

Like other Oct genes, *nub* plays a broad range of roles in development, tissue homeostasis and regeneration, most of which have been investigated functionally only in *Drosophila*. *Nub* is expressed in the developing nervous system in a range of insects (Biffar and Stollewerk, 2014; Li and Popadić, 2004) as well as in spiders and crustaceans (Damen et al., 2002). Functional studies in *Drosophila* indicate that its expression is necessary in developing neuroblasts for the formation of daughter cells with mid/late neural fates (Grosskortenhaus et al., 2006; Isshiki et al., 2001) and in a subset of neurons for axonal pathfinding later in development (Yeo et al., 1995).

Also deeply conserved is the expression of *nub* in developing arthropod appendages. It is expressed in rings along the length of the limbs in crustaceans, spiders and various insect species (Abzhanov and Kaufman, 2000; Averof and Cohen, 1997; Damen et al., 2002; Prpic and Damen, 2005; Prpic and Damen, 2009; Turchyn et al., 2011). In insects, at least, this expression seems to be regulated by Notch signaling and is required for proper formation of the leg joints (Turchyn et al., 2011). *Nub* is also commonly expressed in derivatives of limbs or of parts of limbs, for example in the wing imaginal disc of *Drosophila* (where it is required for proximal-distal patterning) (Cifuentes and García-Bellido, 1997; Ng et al., 1995), and the spinnerets, book gills and tracheae of spiders (Damen et al., 2002).

nub has also been shown to be required post-embryonically in *Drosophila* to regulate the activity of the immune system in the gut (Dantoft et al., 2013; Dantoft et al., 2016) and of intestinal stem cells for gut homeostasis and repair (Lindberg et al., 2018; Tang et al., 2018). Interestingly, in these contexts, alternative splicing of *Dm-nub* has been suggested to be

important for its function. Alternative transcripts of *Dm-nub* give rise to one of two protein products (NUB-PD or NUB-RD) which differ in their N-terminal sequences and play opposite roles in the gut (Lindberg et al., 2018). One promotes maintenance of pluripotency and division of intestinal stem cells, while the other promotes differentiation (Tang et al., 2018) and likewise, one promotes immune repression in the gut and the other activation (Lindberg et al., 2018).

Of the neuroblast timer genes, *nub* is certainly the most promising gap gene candidate. It is expressed in a gap-like domain in the abdomen during segment specification in *Drosophila* (Billin et al., 1991; Cockerill et al., 1993; Dick et al., 1991; Lloyd and Sakonju, 1991; Prakash et al., 1992), in the hemipteran *Oncopeltus* (Hrycaj et al., 2008) and in the house cricket *Acheta* (Turchyn et al., 2011). Preliminary evidence also suggests that it is expressed during the patterning of abdominal segments in *Tribolium* (Biffar and Stollewerk, 2014 and E. Raymond, unpublished). Ectopic expression of *Dm-nub* generates classical gap gene phenotypes; specifically, deletion of the first two abdominal segments and occasionally deletion or fusion of T2 and T3 (Cockerill et al., 1993). At the molecular level, this is reflected in fusion or deletion of pair-rule gene stripes (Cockerill et al., 1993). *nub* mutants show less obvious segmentation defects, with only occasional and partial fusion of pair-rule stripes in the abdomen (although this is exacerbated in *Dichaete* mutants) (Ma et al., 1998). The expression of *Dm-nub* in the abdomen is regulated by other gap genes – it is repressed by *Dm-hb, Dm-kni* and the terminal gap gene *Dm-tll* (Cockerill et al., 1993). However, *Dm-nub* is first expressed a short time after the other trunk gap genes become expressed, and does not seem to regulate any of them itself (Cockerill et al., 1993). For this reason, it is thought to occupy a space somewhere between the gap gene network and the pair-rule gene network in the segmentation hierarchy (Cockerill et al., 1993), hence the title of a ‘gap-like’ gene.

Interestingly, *nub* appears to play different roles in segment patterning in different insect species. While *nub* mutation in *Drosophila* primarily impacts segment boundary formation (Cockerill et al., 1993), with no effect on Hox gene patterning (Hrycaj et al., 2008), *nub* RNAi in *Oncopeltus* leaves segment patterning intact but results in homeotic transformation of abdominal segments towards a more thoracic fate (Hrycaj et al., 2008). Specifically, expression of the Hox gene *abdA* in the abdomen is repressed, resulting in the formation of ectopic legs on segments A2-A6 (Hrycaj et al., 2008). By contrast, RNAi against *nub* in the house cricket *Acheta* affects the development of limb joints but has no impact on segment patterning or identity in the abdomen, despite its prominent expression domain here during segment addition (Turchyn et al., 2011). As a non-Drosophilid holometabolous insect,

and a representative of the extremely diverse Coleoptera, *Tribolium* represents a useful additional datapoint to aid in determining which aspects of *nub*'s activity are conserved across the insects.

4.1.3. *Castor* (*cas*) as a candidate gap gene

cas (or *ming*) encodes a zinc finger transcription factor (Cui and Doe, 1992; Mellerick et al., 1992) homologous with the gene *Casz1* (or *Cst*) in vertebrates (Christine and Conlon, 2008; Vacalla and Theil, 2002). Casz1 plays varied roles in cell fate specification and differentiation – for example, it is required for the formation of mid/late born neurons in the retina (Mattar et al., 2015), function of rod photoreceptors in the eye (Mattar et al., 2018) and for heart and vascular development (Charpentier et al., 2013, 1; Christine and Conlon, 2008; Dorr et al., 2015; Liu et al., 2014). In arthropods, the expression and function of *cas* has been examined only in *Drosophila,* but it appears to regulate cell fate decisions in at least two contexts; in neuroblasts, where it is essential for the formation of daughter cells with mid/late born fates (Cui and Doe, 1992; Isshiki et al., 2001; Mellerick et al., 1992); and in the ovary, where it is required for the maintenance of follicle stem cells and their differentiation into polar and stalk cells (Chang et al., 2013).

Like *Dm-nub*, it is also expressed at the blastoderm stage in a broad, gap-like domain in the presumptive abdomen of *Drosophila* (Isshiki et al., 2001; Mellerick et al., 1992). However, this domain is limited to the ventral, presumably neurogenic, ectoderm, and *Dm-cas* null mutants do not display any overt defects in segmentation or in segment identity (Mellerick et al., 1992). There is, as yet, no evidence for its regulating the expression of any canonical gap gene, although it is able to repress *Dm-nub* (Kambadur et al., 1998). Given these observations, *Tc-cas* is a less promising gap gene candidate than *Tc-nub*, but it does appear to be expressed at the right place and time to contribute to filling the gap gene gap; preliminary descriptions suggest that it is expressed in the SAZ during the patterning of the mid/posterior abdomen (Biffar and Stollewerk, 2014 and E. Raymond, unpublished). Additionally, if the role of *nub* in the gap gene network is more prominent in *Tribolium* than in *Drosophila*, then it could be that repression of *nub* by *cas* is also required for correct abdominal patterning. Regardless of whether it plays a role in segment patterning, examination of *cas* expression and function in another insect will also help to broaden our understanding of its role in development.

4.1.4. *Grainyhead* (*grh*) as a candidate gap gene

Grh encodes a transcription factor also known as Elf-1 or NTF-1 (Bray and Kafatos, 1991). Elf-1 belongs to the LSF/GRH family of transcription factors, which is conserved across the animal kingdom (Traylor-Knowles et al., 2010). The GRH members of this family are primarily expressed in epithelial tissues and involved in epithelial organogenesis and epidermal wound repair (Frisch et al., 2017; Wang and Samakovlis, 2012). It is the least promising of the neuroblast timer genes as a gap gene candidate, as it does not have an obvious gap-like expression domain in the *Drosophila* blastoderm – instead, it is expressed in specific neuroblasts and more broadly across the epidermis of the later embryo (Bray et al., 1989; Dynlacht et al., 1989). In the former context, it acts as a determinant of late-born neural fates (Baumgardt et al., 2009) as well as regulating the regional activity of post-embryonic neuroblasts in tandem with Hox gene expression (Almeida and Bray, 2005; Cenci and Gould, 2005; Khandelwal et al., 2017). Its roles in the epidermis are varied; it is a key regulator of the planar cell polarity system (Lee and Adler, 2004); required for tracheal morphogenesis (Hemphälä, 2003); and required for epithelial differentiation and wound healing (Gangishetti et al., 2012; Mace, 2005). Accordingly, *grh* null mutants present with issues in cuticle formation and patterning but no defects in segment patterning or identity (Bray and Kafatos, 1991).

However, Grh displays some properties that could make it a plausible gap gene candidate in the right context. *In vitro* studies indicate that it is a direct regulator of both a pair-rule gene (*Ftz*) and a Hox gene (*Ubx*) (Biggin and Tijan, 1988; Dynlacht et al., 1989), although its deletion does not seem to affect their expression in the epidermis or CNS (Bray and Kafatos, 1991; Cenci and Gould, 2005). In neuroblasts, it is required for maintenance of expression of the Hox gene *abdA* (Cenci and Gould, 2005). Grh also interacts with the terminal gap gene *tll*, acting to repress it in the absence of terminal torso signaling (Liaw et al., 1995), and is able to repress *Dm-cas* in neuroblasts (Baumgardt et al., 2009). Because *grh* expression has not been studied in any insects outside of *Drosophila*, I decided to include it in my investigation of potential gap gene candidates from the neuroblast timer series.

4.1.5. Specific aims

In this chapter, I aim to determine whether *Tc-nub*, *Tc-cas*, or *Tc-grh* have a detectable role in axial patterning in *Tribolium*. In section 4.2.1, I present descriptions of the expression patterns of *Tc-nub*, *Tc-cas* and *Tc-grh* against my temporal and spatial mapping system, and confirm that the former two genes (but not the latter) display gap-like expression domains. In section 4.2.2, I examine the expression of *Tc-nub* and *Tc-cas* in relation to the expression of other gap genes using multiplexed HCR ISH; firstly, to determine if the order of expression of the neuroblast timer series (*hb*, *Kr*, *nub*, *cas*) is conserved along the length of the axis of *Tribolium*, as it is in *Drosophila*; secondly, to determine whether *Tc-nub* and *Tc-cas* are expressed within the gap gene gap; and thirdly, to predict plausible interactions between *Tc-nub*, *Tc-cas* and other gap genes. In section 4.2.3, I perform RNAi against *Tc-nub* and *Tc-cas* to determine whether they have a detectable role in axial patterning in *Tribolium*.

4.2. RESULTS

4.2.1. Expression of candidate gap genes from the neuroblast timer series

Expression of *Tc-nubbin (Tc-nub)*

Tc-nub expression during segment addition has been briefly examined in Biffar and Stollewerk's (2014) work on insect neuroblasts, and in more depth by a student of our collaborator, Andrew Peel (E. Raymond, unpublished). Both studies found that, as in *Drosophila*, this gene is expressed in a gap-like domain for at least some of the period of segment addition. However, my work here presents the first detailed description of *Tc-nub* expression against parasegmental markers covering the entire period of segment addition.

Like *Dm-nub*, *Tc-nub* has been annotated as producing two transcripts (TC032751-RA and -RB), both transcribed from the same strand. However, these transcripts have not been verified experimentally, and pooled RNA-Seq data suggests that at least one of two TC032751-RB-specific exons is not expressed at any stage during development (Beetlebase website: http://www.Beetlebase.org, Official Gene Set 3 of *Tribolium castaneum* GA2 strain). In addition, previous manual annotations of the gene predict only one transcript, TC032751-RA (E. Raymond, unpublished). Given these conflicting reports, I chose to order probes against the verified and manually annotated transcript, TC032751-RA.

I first examined *Tc-nub* expression in an ovariole dissected from an adult female ovary, to determine whether mRNA might be provided maternally to the egg. *Tc-nub* is expressed in the nurse cells at the proximal end of the tropharium, but not provided to the oocytes (Figure 4.1A). Interestingly, this domain overlaps with a region of weakened *Tc-hb* expression (Figure 4.1A').

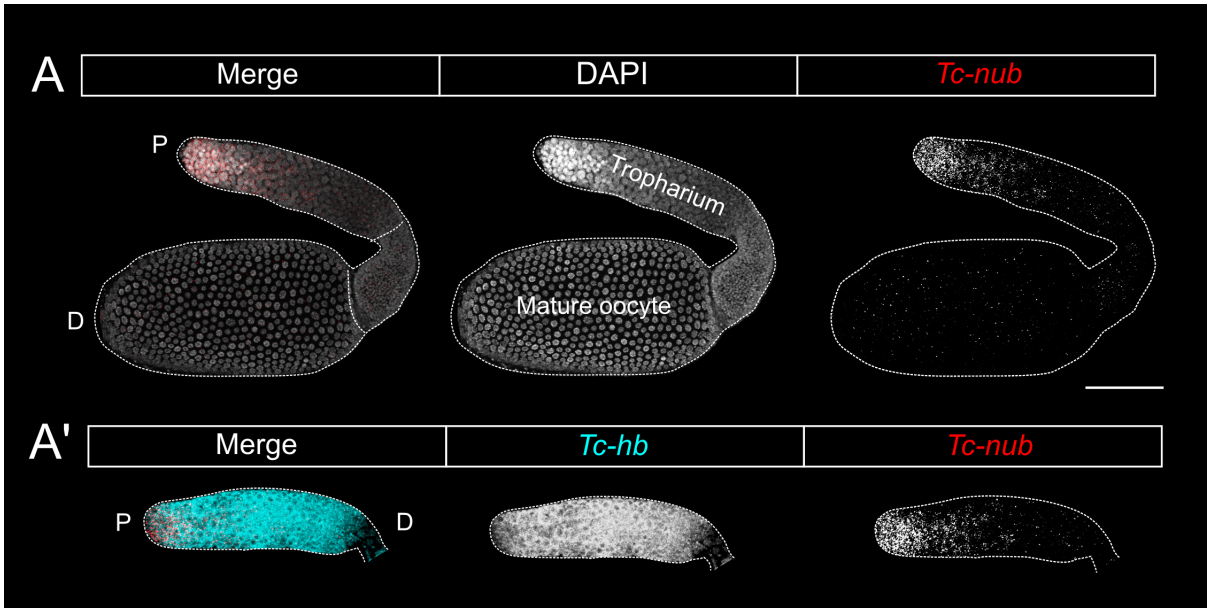

Figure 4.1. HCR ISH showing expression of *Tc-nub* in an ovariole dissected from an adult female ovary. A' shows the expression of *Tc-hb* and *Tc-nub* in the tropharium. P = proximal end of ovariole, D = distal end of ovariole. Scale bar is 100 μM.

Next, I examined *Tc-nub* expression in embryos spanning the period of segment addition. *Tc-nub* is first expressed in the blastoderm as the serosa begins to differentiate. At this stage, it is expressed weakly across the entire embryonic primordium but largely excluded from the serosa (Figure 4.2, stage T0). Expression gradually strengthens in the anterior of the embryo, spanning from the junction with the serosa back to the posterior of To0 (Figure 4.2, stages To1-2 and W0:To2). This head domain therefore covers the entirety of the head lobes back to the posterior of the primordium for PS0. In *Drosophila*, *nub* is also expressed in the head early in development, but this is limited to the primordium of the clypeolabrum (the fused product of the clypeus – a facial sclerite – and labrum) (Lloyd and Sakonju, 1991). *Tc-nub* expression in the *Tribolium* head appears to specifically exclude the region of the developing labrum (Figure 4.2, stage W1:To3-4).

By stage W0:To2, a new domain of *Tc-nub* has emerged in the posterior-most region of the embryo, overlapping with the posterior *Tc-Wg* domain (Figure 4.2). This anterior border of this domain shifts anteriorly as To3 is formed. Expression is strongest in the posterior of the SAZ, behind To3, and fades towards the anterior of the SAZ until it is almost undetectable anterior to To2p (Figure 4.1, stage W1:To3-4). This domain displays gap-gene-like dynamics, with the anterior border shifting anteriorly in tandem with dynamic *Tc-Tl10* stripes and the

posterior border retracting from the back of the SAZ (Figure 4.2, stages W1:To3-4-W4:To5(1)). As the parasegments at the anterior edge of this domain mature, the weakly expressed region resolves into an early neuroectodermal pattern (Figure 4.2, stage W5:To5(2)). Neuroectodermal expression is initially detected in only parasegments 2 and 3 (Figure 4.2, stage W5:To5(2)) but it rapidly spreads anteriorly until it is present in all mature parasegments (Figure 4.2, stage W7:To6(3)). Neuroectodermal expression of *Tc-nub* fades in the regions overlapping with *Tc-Wg* stripes (Figure 4.2, stages W5:To5(2)-W10:To7(4)), suggesting a possible interaction. During this period, the posterior border of the *Tc-nub* domain continues to shift anteriorly, away from the posterior of the SAZ, in tandem with shifts in the segment pattern. This border abuts the anterior of the To7 stripe (Figure 4.2, stage W12:To7(5)). *Tc-nub* is therefore strongly expressed in the SAZ during the patterning of approximately PS5-12, comprising the posterior compartment of T2 through to the anterior compartment of A7. There is some uncertainty in interpreting the precise borders of *Tc-nub* expression. The anterior border is initially located a short distance behind W4p (Figure 4.2, stage W4:To5(1)), which is consistent with it abutting the back of en4, and therefore the back of the T2 segment, as reported by E. Raymond (unpublished)). However, shortly afterwards, it appears to directly abut W4p (Figure 4.2, stage W5:T05(2)). In addition, although the posterior border initially abuts To7a (Figure 4.2, stage W12:To7(5)) (which marks the future anterior border of PS13), it subsequently appears to sit a short distance anterior of this, abutting W12a (Figure 4.2 stage W14:To8(7)). Both phenomena may be related to regulation of *Tc-nub* by *Tc-ftz* – in *Drosophila*, *Dm-ftz* is responsible for promoting parasegmental stripes of *Dm-nub* out of phase with the *Dm-Wg* stripes (Lloyd and Sakonju, 1991), an interaction that may come into effect only outside of the SAZ. I will continue to use the PS5-PS12 approximation when discussing regions of the axis potentially affected by *Tc-nub* expression, but these subtleties are worthy of further investigation.

By the end of segment addition, *Tc-nub* is expressed in the developing appendages, in neuroblasts within the head and across the length of the segmented germband, and also in the lateral part of the posterior *Tc-Wg* domain (Figure 4.2, stage W15:To8(8)). These domains will not be described here in more detail, as they are not relevant to my primary research questions.

Figure 4.2 (overleaf). HCR showing *Tc-Tl10* (red) and *Tc-nub* (cyan or grey) expression in *Tribolium* embryos over the course of segment addition. Images are maximum projections through coronal optical sections (arrows indicate where the midline of the embryo is turned either to the left or to the right, *i.e.* where the optical sections are not perfectly perpendicular to the dorsoventral axis). Germband stage embryos have been dissected away from the egg. Stage is given above each embryo according to the staging system I present in section 3.2.1. For simplicity, *Tc-Wg* expression is not shown, but the positions of selected *Tc-Tl10* and *Tc-Wg* stripes are indicated on greyscale images (in red and white respectively). The suffix 'a' refers to the anterior boundary of a stripe, while 'p' refers to the posterior boundary of a stripe. The asterisk in the embryo at stage W1:To3-4 marks the absence of *Tc-nub* expression in the tissue that will give rise to the labrum. Scale bar = 100 μM.

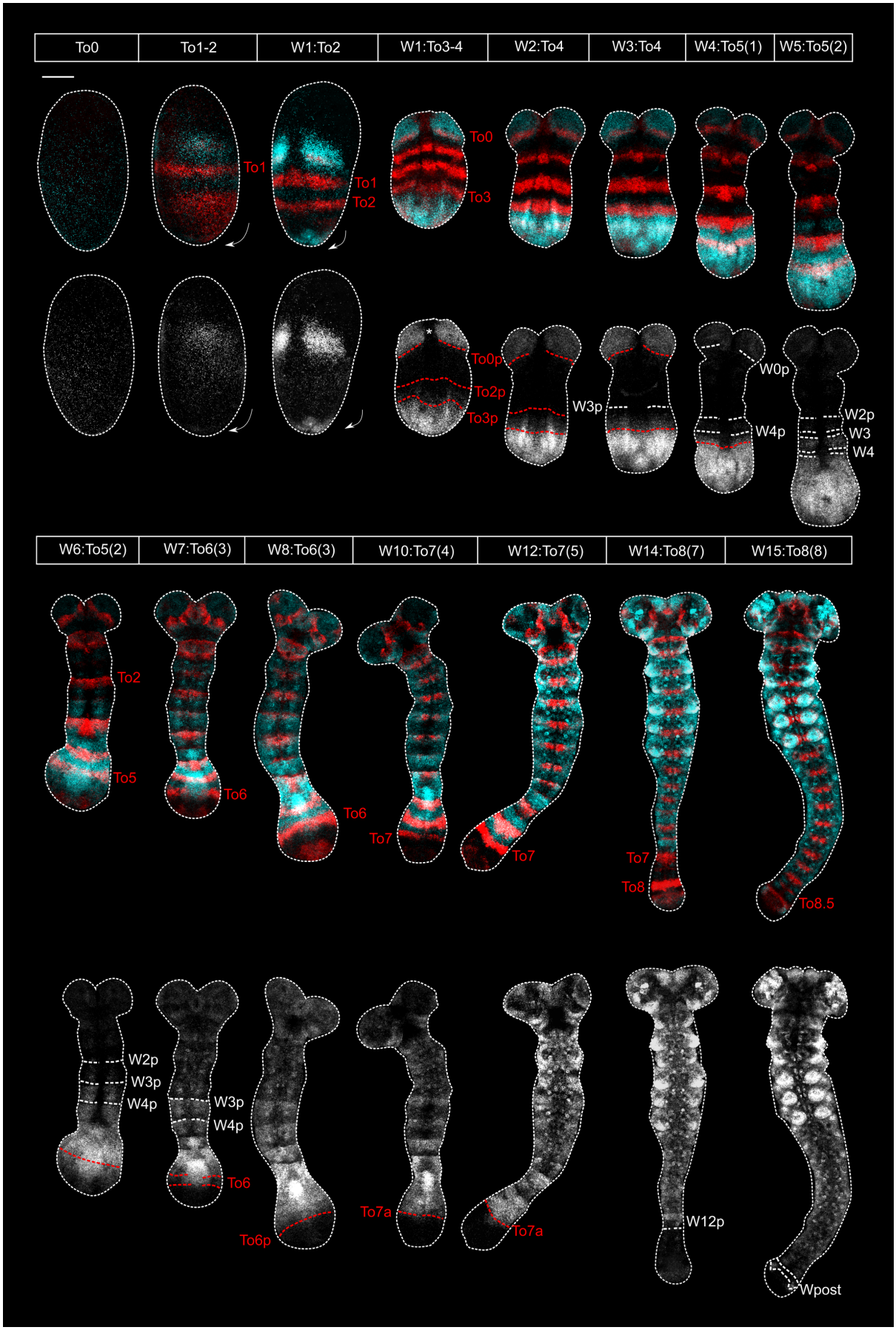
To0
To1-2
W1:To2
W1:To3-4
W2:To4
W3:To4
W4:To5(1)
W5:To5(2)
To1
To1
To2
To0
To3
To0p
To2p
To3p
W3p
W0p
W4p
W2p
W3
W4
W6:To5(2)
W7:To6(3)
W8:To6(3)
W10:To7(4)
W12:To7(5)
W14:To8(7)
W15:To8(8)
To2
To5
To6
To6
To7
To7
To7
To8
To8.5
W2p
W3p
W4p
W3p
W4p
To6
To6p
To7a
To7a
W12p
Wpost

Expression of *Tc-castor (Tc-cas)*

Preliminary examination of *Tc-cas* expression by Biffar and Stollewerk (2014) indicates that it is also expressed in the SAZ during the patterning of abdominal segments. E. Raymond and A. Peel determined that this abdominal expression overlaps with that of *Tc-nub*, but did not determine its exact positioning (unpublished data). I therefore show here the first in depth description of *Tc-cas* expression, representing the first thorough description in any arthropod other than *Drosophila*.

Tc-cas is expressed in the follicular cells surrounding mature oocytes in the ovary (Figure 4.3), consistent with the role of its homologue in regulating follicular cell development in *Drosophila* (Chang et al., 2013). However, *Tc-cas* mRNA is not present in the oocyte itself, and is not present in the embryo until after the germband has formed (data not shown and Figure 4.4).

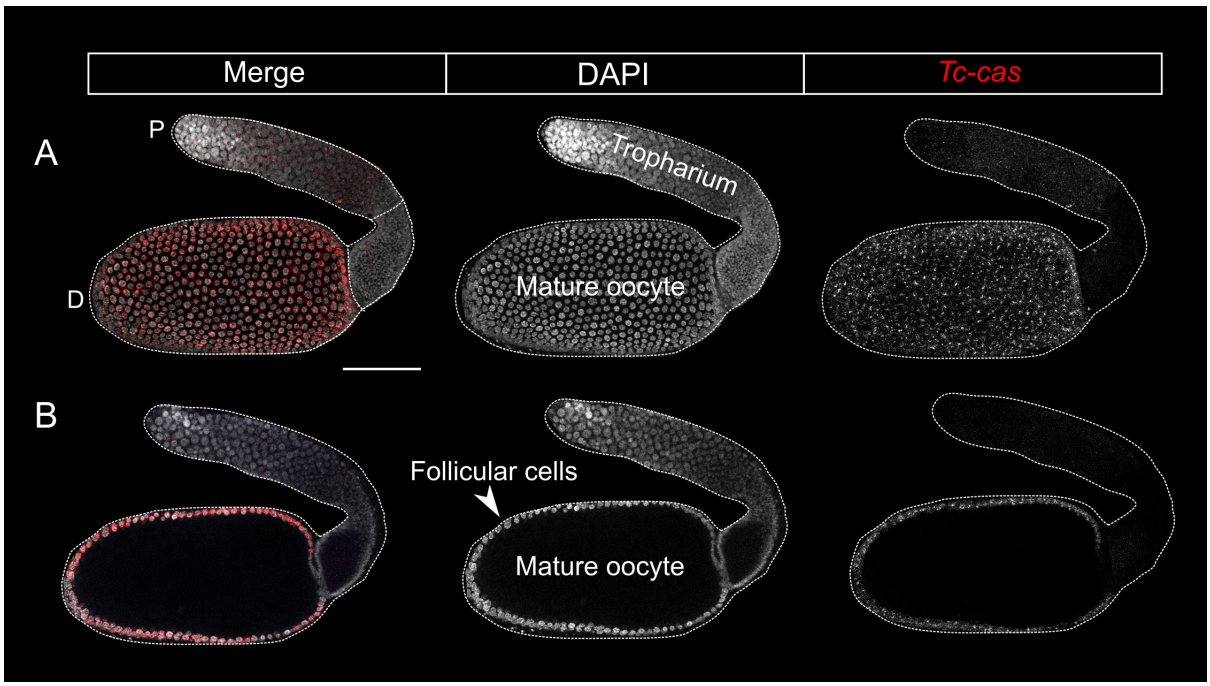

Figure 4.3. HCR ISH showing expression of *Tc-cas* in an ovariole dissected from an adult female ovary. **A** shows a projection through the entire ovariole, indicating that expression is localised to the mature distal oocyte; and **B** shows a projection through the centre of the ovariole, indicating that expression is limited to the outer layer of follicular cells and mRNA is not present in the oocyte itself. P = proximal end of ovariole, D = distal end of ovariole. Scale bar is 100 μM.

During embryonic development, *Tc-cas* expression is initially detected in the developing labrum (Figure 4.4, stage W3:To4). Expression is initially faint, but becomes stronger at the end of segment addition (Figure 4.4, stage W15:To8(8)). There is no obvious parallel to this expression in *Drosophila – Dm-cas* is expressed in the head, but this expression is limited to small neurogenic cell clusters, none of them in the developing clypeolabrum (Mellerick et al., 1992).

Expression in the SAZ is first detected faintly at stage W4:To4 (Figure 4.4). Expression at this stage is punctate and patchy. The anterior border eventually aligns with To4a (and with W6p, when this parasegment boundary becomes patterned), and the posterior border does not quite reach the back of the SAZ. This singular weak domain resolves into several subdomains over the course of segment addition. Each of these subdomains begins as strongly expressed in the lateral ectoderm of the SAZ, and then fades as the pattern moves into the segmented germband (Figure 4.4, stages W8:To6(3)-W12:To7(5)). One of these subdomains forms in each of PS9-12. Throughout mid-late segment addition, *Tc-cas* is also expressed in the posterior of the SAZ, in two lateral domains that overlap with posterior *Tc-Wg* (Figure 4.4, stages W8:To6(3)-W14:To8(7))). This domain expands anteriorly slightly at the end of segment addition to cover part of the SAZ during patterning of PS15 (Figure 4.4, W14:To8(7)).

Figure 4.4 (overleaf). HCR showing *Tc-Tl10* (red) and *Tc-cas* (cyan or grey) expression in *Tribolium* embryos over the course of segment addition. Images are maximum projections through coronal optical sections. All embryos have been dissected away from the egg. Stage is given above each embryo according to the staging system I present in section 3.2.1. For simplicity, *Tc-Wg* expression is not shown, but the positions of selected *Tc-Tl10* and *Tc-Wg* stripes are indicated on greyscale images (in red and white respectively). The suffix ‘a’ refers to the anterior boundary of a stripe, while ‘p’ refers to the posterior boundary of a stripe. Scale bar = 100 μM.

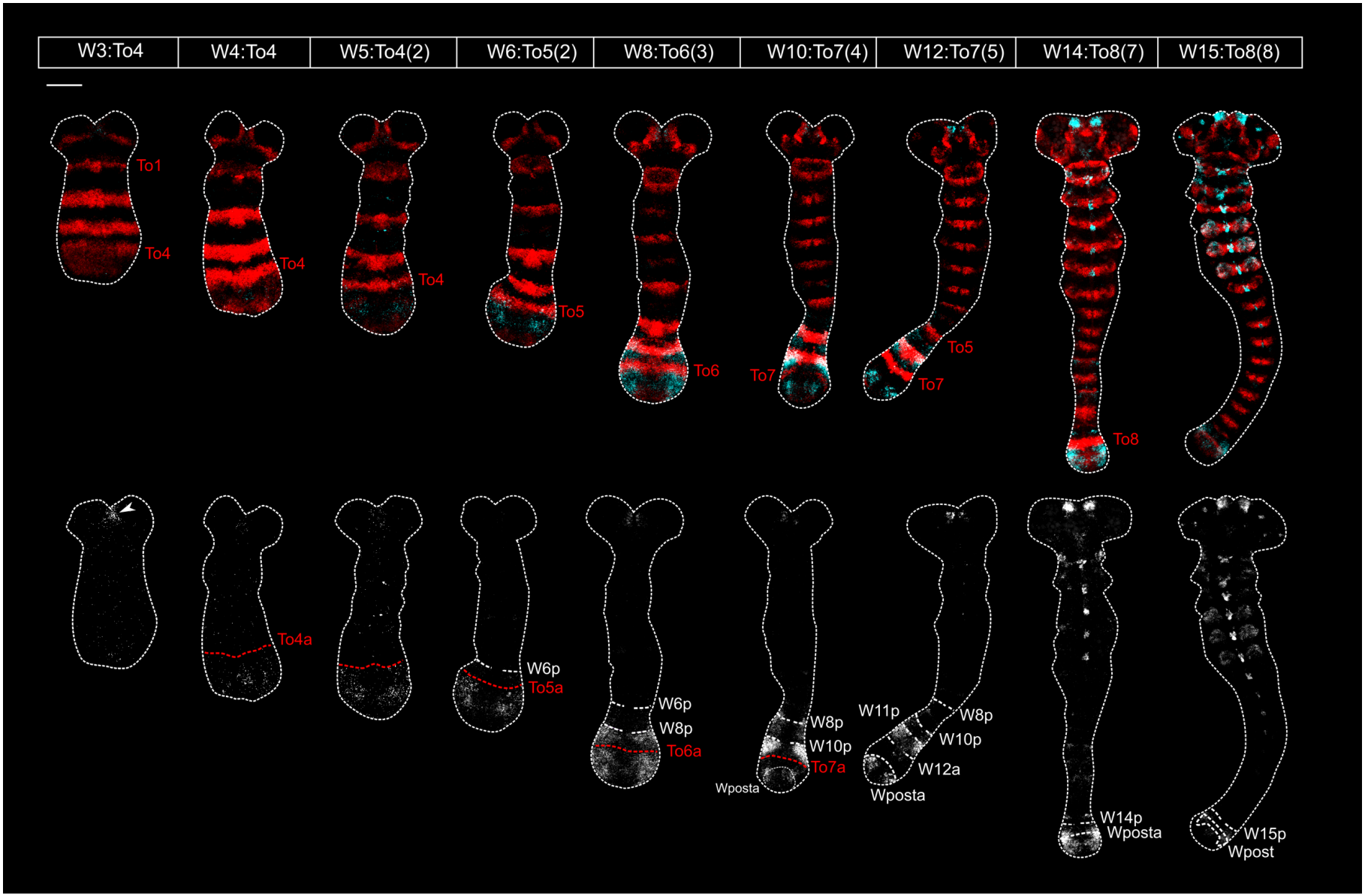
W3:To4
W4:To4
W5:To4(2)
W6:To5(2)
W8:To6(3)
W10:To7(4)
W12:To7(5)
W14:To8(7)
W15:To8(8)
To1
To4
To4
To4
To5
To6
To7
To5
To7
To8
To4a
W6p
To5a
W6p
W8p
To6a
W8p
W10p
To7a
Wposta
W11p
W8p
W10p
W12a
Wposta
W14p
Wposta
W15p
Wpost

This means that Tc-cas is expressed in the SAZ weakly during the patterning of PS6-7, and more strongly during the patterning of PS9-12 (and perhaps some of PS15). In *Drosophila,* the exact boundaries of *Dm-cas* expression have not been determined; however, my data suggests some other deviations in expression of *Tc-cas* compared to its *Drosophila* homologue. *Dm-cas* expression is restricted to the ventral ectoderm and mesoderm, supporting the idea that is not required for patterning of non-neural ectoderm (Mellerick et al., 1992). By contrast, *Tc-cas* is expressed in ventral, lateral and dorsal ectoderm in the SAZ of *Tribolium*, and is instead excluded from the mesoderm (Figure 4.5). This is more suggestive of a potential role in segmental patterning than the expression pattern observed in *Drosophila*. Note that other gap genes, and *Tc-nub*, are similarly expressed in dorsal, lateral and ventral ectoderm, but are also typically expressed in the mesoderm (Figure 4.5).

At the end of segment addition, *Tc-cas* becomes expressed in neuroblasts in the head and along the midline, and in developing gnathal and thoracic appendages (stage W15:To8(8) and E. Raymond, unpublished). These domains will not be described here in more detail, as they are not relevant to my primary research questions.

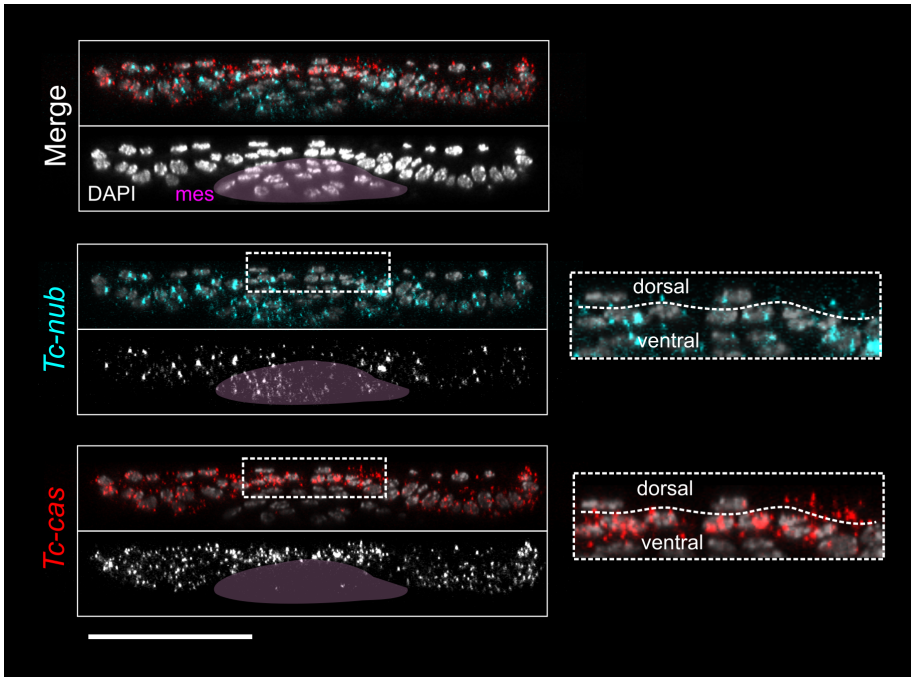

Figure 4.5. Expression of *Tc-nub* and *Tc-cas* in a transverse section through the SAZ, indicating that *Tc-nub* but not *Tc-cas* is expressed in the mesoderm. Mes = mesoderm, shaded pink. Insets show a close up on apposing dorsal and ventral ectoderm cells, showing that *Tc-nub* and *Tc-cas* are expressed in both. Scale bar = 50 μM.

Expression of *Tc-grainy-head (Tc-grh)*

Tc-grh expression has not previously been examined, and my work here represents the first description of its expression in any insect species outside of *Drosophila*. I found no evidence for a broad, gap-gene-like expression domain in the SAZ during segment addition (Figure 4.6). *Tc-grh* can first be detected in the blastoderm, when it is expressed broadly in the embryonic ectoderm but excluded from the developing serosa and mesoderm (Figure 4.6, stage To1-2). *Tc-grh* is then expressed broadly across the germband throughout segment addition, becoming excluded from the brain and central nervous system at later stages (Figure 4.6). This expression pattern is consistent with its playing a role in epithelial development, as in *Drosophila* (Gangishetti et al., 2012). Due to its unpromising expression pattern and my time limitations, *Tc-grh* was excluded from further analysis.

Figure 4.6. HCR showing *Tc-Tl10* (red) and *Tc-grh* (cyan or grey) expression in *Tribolium* embryos over the course of segment addition. Images are maximum projections through coronal optical sections. Germband stage embryos have been dissected away from the egg. Stage is given above each embryo according to the staging system I present in section 3.2.1. Scale bar = 100 μM.

4.2.2. Expression of *Tc-nub* and *Tc-cas* relative to other gap genes

Having confirmed that both *Tc-nub* and *Tc-cas* have gap-gene-like expression domains, I wanted to investigate how these domains relate to those of other gap genes in *Tribolium*. In particular, I wanted to understand how the expression domains of the four neuroblast timer genes related to one another, and whether the expression patterns of *Tc-nub* and *Tc-cas* are suggestive of interactions with gap genes outside of this series.

The neuroblast timer genes *Tc-hb, Tc-Kr, Tc-nub* and *Tc-cas* are expressed in a conserved spatiotemporal order in the SAZ of *Tribolium*

I first investigated whether the temporal order of expression of the four core neuroblast timer genes (*Tc-hb*, *Tc-Kr*, *Tc-nub* and *Tc-cas*) was reflected in their order of expression along the anterior-posterior axis of *Tribolium*, as in *Drosophila*. To do this, I performed multiplexed HCR ISH against these four genes in embryos spanning the course of segment addition.

As in *Drosophila*, the four neuroblast timer genes are expressed in a conserved spatial order along the length of the anterior-posterior axis of *Tribolium* (Figure 4.7A). This spatial order is established by sequential expression of *Tc-hb*, *Tc-Kr*, *Tc-nub* and *Tc-cas* in the SAZ (Figure 4.7B), so that the cells of the SAZ experience the same sequence of these genes as neuroblasts do (Figure 4.7C). However, unlike in neuroblasts, *Tc-hb* becomes expressed again in the SAZ at the end of segment addition, abutting the back of the *Tc-nub* and *Tc-cas* domains (Figure 4.8 and Figure 4.7B). Together, the expression domains of these four genes are sufficient to cover the length of the segmented trunk.

I also noticed that all four neuroblast timer genes are expressed in nested domains in the posterior gut tissue at the end of segment addition. On closer inspection, the spatial order of these domains is the same as along the anterior-posterior axis, but in reverse order (*i.e. Tc-cas* is most anterior, *Tc-hb* most posterior) (Appendix 3). This additional example strengthens the theory that the four neuroblast timer genes might have been redeployed as a network for use in other developmental scenarios.

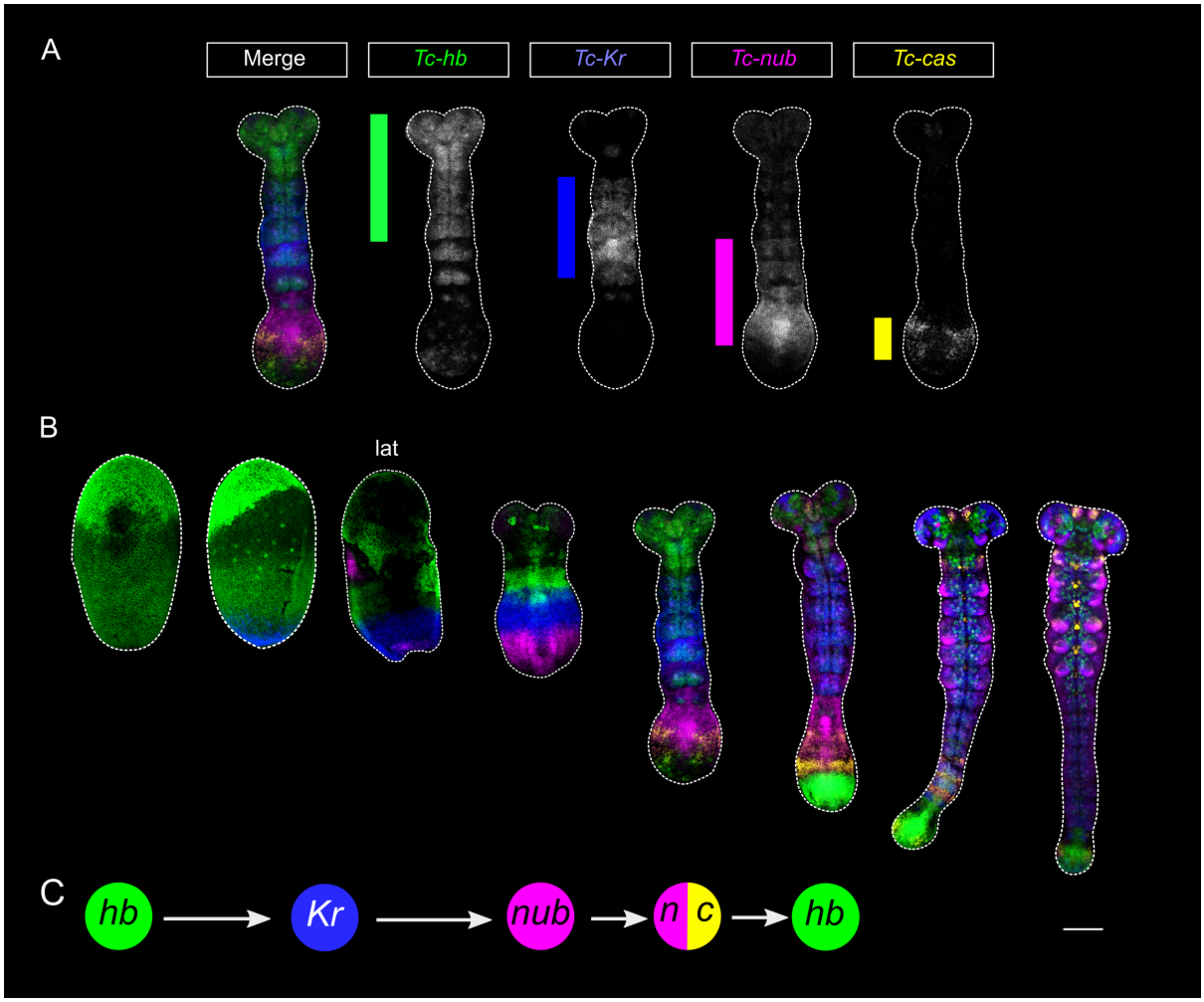

Figure 4.7. HCR ISH showing expression of the four core neuroblast timer genes, *Tc-hb*, *Tc-Kr*, *Tc-nub* and *Tc-cas*, in *Tribolium* embryos during segment addition. A) shows that the four genes are expressed in sequential spatial order along the anterior-posterior axis of the embryo during mid-segmentation. B) and C) show that this spatial order is established by sequential temporal expression in the posterior SAZ. Images of blastoderm stage embryos are maximum projections through the ventral (or lateral where labelled) half of the embryo. Images of germband stage embryos are maximum projections through the sections that contain *Tc-Wg*-expressing epithelium (*i.e.* the ectoderm proper). All images are orientated with anterior at the top. Scale bar is 100 μM.

Tc-nub and *Tc-cas* are expressed in the gap gene gap

Tc-nub and *Tc-cas* are both expressed within the 'gap gene gap' that spans approximately from PS8 to PS12 (Figure 4.8). The anterior portion of the *Tc-nub* domain also overlaps with the dense field of gap gene domains straddling the thoracic-abdominal boundary. In particular, the posterior domains of *Tc-nub*, *Tc-gt* and *Tc-kni* all overlap extensively in PS5-8 (T2p-A3a), and in fact emerge at almost the same time (Figure 4.8, stage To2 onwards).

Figure 4.8, overleaf. Expression of *Tc-nub* and *Tc-cas* compared to other gap genes in *Tribolium*. Parasegments (in the segmented germband), and the patterning units that will later specify parasegments (in the SAZ), are labelled in normal text or in italics, respectively. Odd-numbered parasegments/parasegment patterning units, which express *Tc-Tl10/Tc-eve*, are marked by light grey bands. *Tc-Wg* stripes are marked by dark grey bands. After the first column, the anterior of the embryo is cut off and only the most recent two mature parasegments are represented, for optimal use of space.

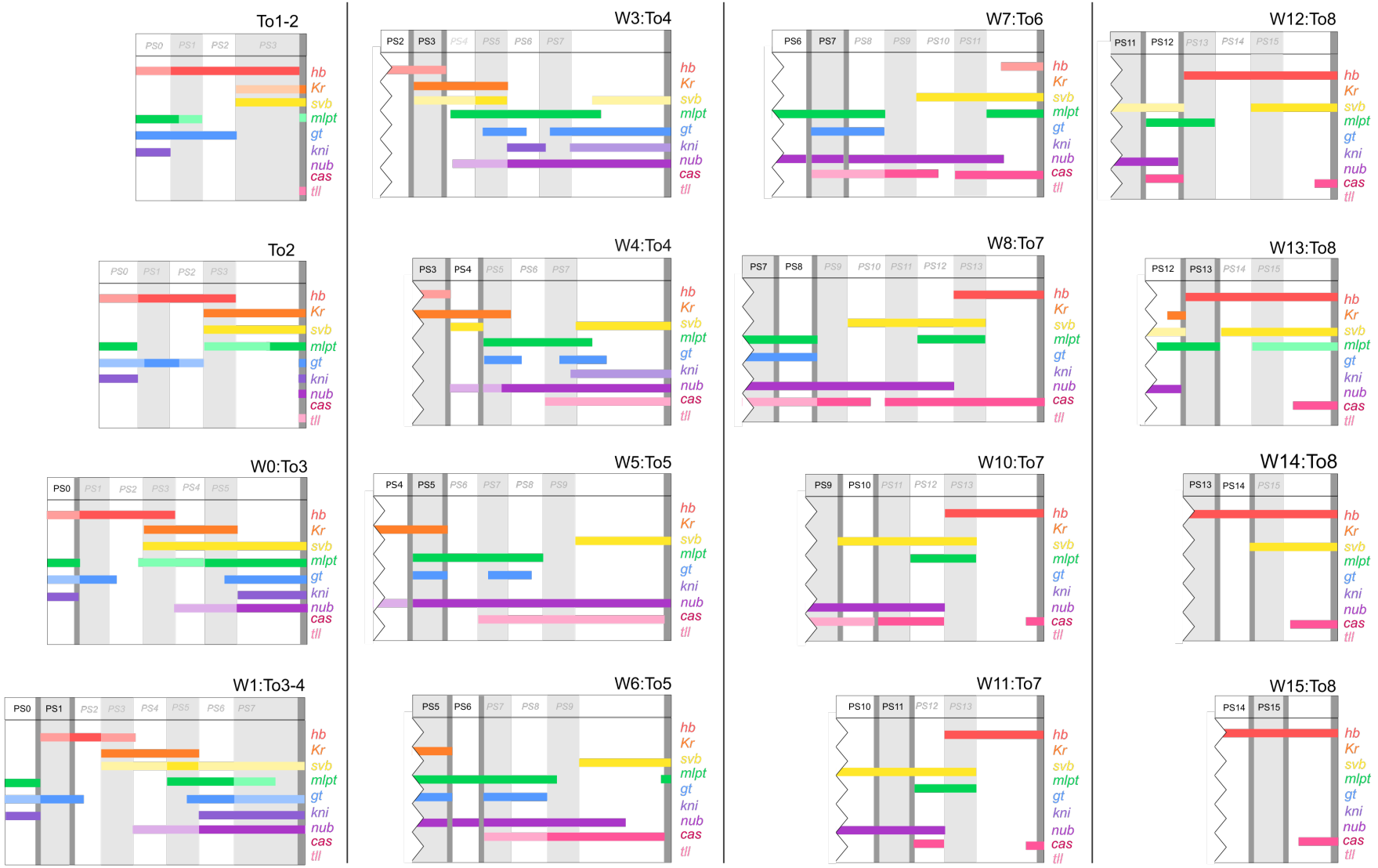
To1-2
PS0 PS1 PS2 PS3
To2
PS0 PS1 PS2 PS3
W0:To3
PS0 PS1 PS2 PS3 PS4 PS5
W1:To3-4
PS0 PS1 PS2 PS3 PS4 PS5 PS6 PS7
W3:To4
PS2 PS3 PS4 PS5 PS6 PS7
W4:To4
PS3 PS4 PS5 PS6 PS7
W5:To5
PS4 PS5 PS6 PS7 PS8 PS9
W6:To5
PS5 PS6 PS7 PS8 PS9
W7:To6
PS6 PS7 PS8 PS9 PS10 PS11
W8:To7
PS7 PS8 PS9 PS10 PS11 PS12 PS13
W10:To7
PS9 PS10 PS11 PS12 PS13
W11:To7
PS10 PS11 PS12 PS13
W12:To8
PS11 PS12 PS13 PS14 PS15
W13:To8
PS12 PS13 PS14 PS15
W14:To8
PS13 PS14 PS15
W15:To8
PS14 PS15
hb
Kr
svb
mlpt
gt
kni
nub
cas
tll

The expression dynamics of *Tc-nub* and *Tc-cas* relative to other gap genes suggest that they may interact in the process of segment addition

Previous research has identified several likely interactions between *nub*, *cas* and other gap genes in the context of neuroblast development and segment patterning in *Drosophila*. My expression analyses suggest that many of these interactions may be conserved in the context of axial patterning in *Tribolium*.

***Tc-nub*:** Dm-Hb appears to be a potent repressor of *Dm-nub*, both in neuroblasts (Kambadur et al., 1998) and in the process of segment patterning (Cockerill et al., 1993; Lloyd and Sakonju, 1991). In the latter context, at least, this interaction appears to be direct (Kambadur et al., 1998). The dynamics of *Tc-nub* expression are consistent with this interaction being conserved during axial patterning in *Tribolium*. *Tc-nub* expression first emerges in the SAZ shortly after *Tc-hb* expression fades (Figure 4.8, stage W0:To3). Its expression is strong where there is no detectable *Tc-hb* mRNA, and weaker where low levels of *Tc-hb* are detected (Figure 4.7, stage W0:To3). Although *Tc-nub* expression in the SAZ begins to fade before the posterior domain of *Tc-hb* emerges (Figure 4.8, stage W7:To5), the two genes neatly abut for the remainder of segment addition (Figure 4.8, stage W9:To7 onwards and Figure 4.9). It therefore seems likely that Tc-Hb plays an important role in setting or maintaining the anterior and posterior boundaries of *Tc-nub* expression.

The terminal system, and *tll* in particular, is also thought to be required to repress *nub* in *Drosophila* (Cockerill et al., 1993). Indeed, the emergence of the abdominal *Tc-nub* domain correlates with the fading of *Tc-tll* expression in the terminus of the embryo (Figure 4.8, stage To2). However, this could be an indirect effect, resulting from repression of *Tc-hb* by Tc-Tll.

In *Drosophila*, Kni also has a repressive effect on *nub* expression, resulting in the splitting of the *nub* domain into two stripes (Cockerill et al., 1993). By contrast, in *Tribolium*, *Tc-nub* and *Tc-kni* domains overlap extensively, and there is no evidence that the latter represses the former (Figure 4.8).

Interestingly, the emergence of the posterior *Tc-nub* domain correlates closely with the emergence of the posterior *Tc-gt* and *Tc-kni* domains. It is worth considering that these three genes may share some elements of regulation, whether this be repression by *Tc-tll* or activation by *Tc-mlpt* and *Tc-svb*, as proposed in the previous chapter.

Dm-nub itself is thought to repress *Dm-Kr* in the context of neuroblast patterning (Grosskortenhaus et al., 2006; Isshiki et al., 2001; Tran and Doe, 2008), although no evidence of this interaction has been found in axial patterning (Cockerill et al., 1993). Such an interaction

is certainly plausible in *Tribolium*, based on the expression dynamics of *Tc-nub* and *Tc-Kr*. *Tc-nub* expression emerges within the *Tc-Kr* domain, and where it is expressed strongly, *Tc-Kr* expression subsequently fades (Figure 4.8).

***Tc-cas*:** There is less known about interactions of *cas* with gap and gap-like genes. Like *Dm-nub*, *Dm-cas* appears to be repressed by Dm-Hb in neuroblasts (Isshiki et al., 2001). As for *Tc-nub*, the posterior boundary of the gap-like *Tc-cas* domain neatly abuts the posterior domain of *Tc-hb* (Figure 4.8, Figure 4.9), so it is plausible that Tc-Hb represses *Tc-cas* in this context too.

The activation of *Tc-cas* in the SAZ is harder to explain. In neuroblasts, *Dm-cas* is thought to become expressed due to a combination of activation via Dm-Nub and derepression as expression of *Dm-hb* and *Dm-Kr* fades (Isshiki et al., 2001). In *Tribolium*, *Tc-cas* first becomes expressed some time after *Tc-hb* and *Tc-Kr* expression fades, and after *Tc-nub* first becomes expressed, suggesting that these interactions are less important for establishing the gap-like domain of *Tc-cas* expression. The emergence of this domain does correlate well with fading of *Tc-gt* and *Tc-kni* in the SAZ (Figure 4.8, stage W5:To4), so perhaps one or both of these genes acts a repressor of *Tc-cas* to control the timing of its expression.

Note that it was my intention to test many of these interactions as a part of my PhD, but unfortunately, the COVID-19 pandemic cut some of my experiments short. However, some of these interactions are tested in this and the next chapter.

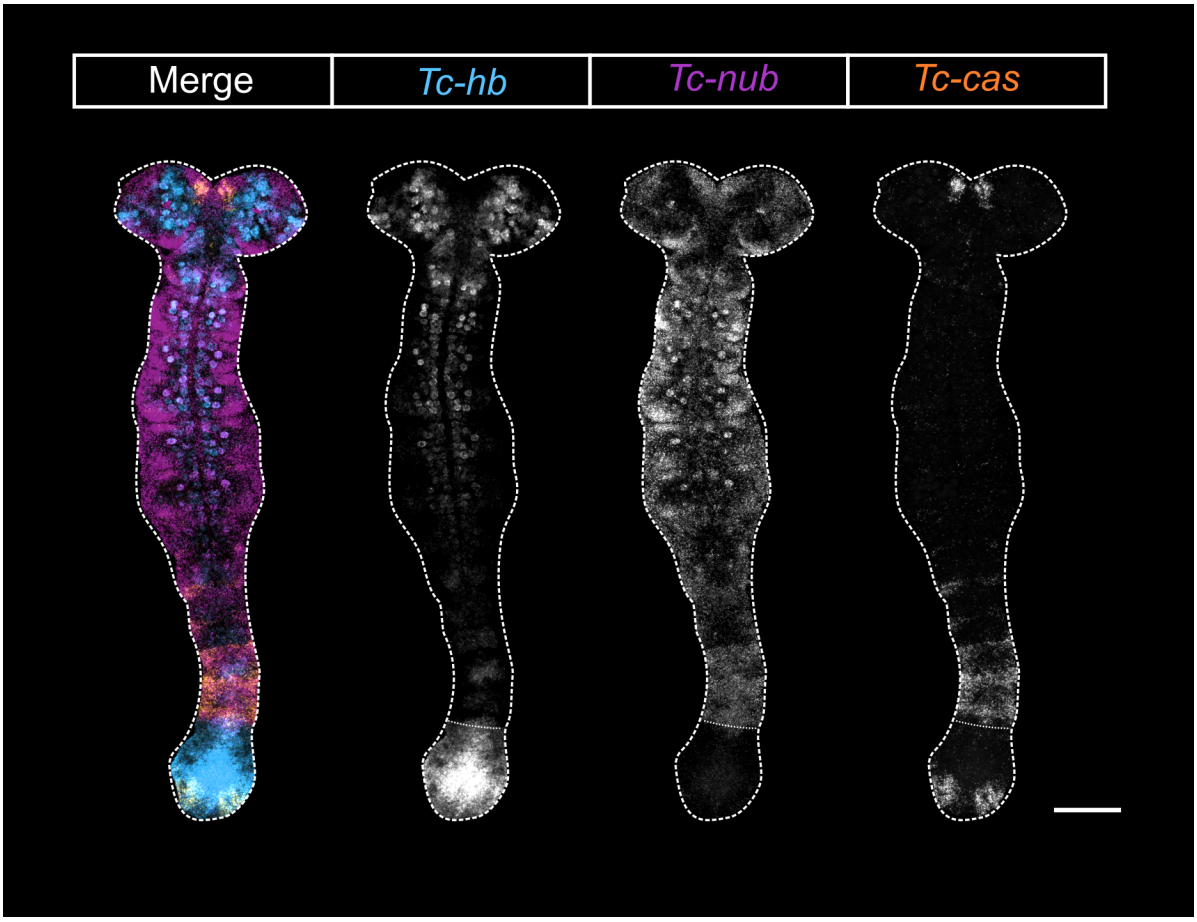

Figure 4.9. Expression of *Tc-hb, Tc-nub* and *Tc-cas* in a mid-elongation germband. The anterior boundary of the posterior *Tc-hb* domain is marked with a dotted line. Scale bar is 100 μM.

4.2.3. Investigating the function of *Tc-nub* and *Tc-cas* in axial patterning using RNAi

The expression patterns of *Tc-nub* and *Tc-cas* are consistent with their playing a role in axial patterning, in particular during abdominal segment formation. I next aimed to investigate the role of each gene in axial patterning using parental RNAi (pRNAi) and embryonic RNAi (eRNAi).

Both *Tc-nub* and *Tc-cas* pRNAi reduce viability and hatching rate

For my first pRNAi experiment, I injected females with 1 µg/µL GFP dsRNA as a negative control (N=32), *Tc-odd* dsRNA as a positive control (N=16), or *Tc-nub* dsRNA (N=31) or *Tc-cas* dsRNA (N=31). Eggs were collected every 2-3 days for a period of four weeks and left to develop into larvae for cuticle preparation. Survival of injected females after two days was high for all treatments (93-100%).

As expected, injection of GFP dsRNA had no noticeable effect on cuticle formation or hatching in offspring compared to uninjected controls (data not shown). Injecting *Tc-odd* dsRNA also had the expected effect on offspring, with just over half of embryos failing to form cuticles (counted as 'empty eggs') and the remaining embryos displaying distinctive truncation phenotypes in line with those described by Choe et al. (2006) (Table 4.1).

Injection with either *Tc-nub* or *Tc-cas* dsRNA led to an increase in the number of empty eggs compared to negative controls (55-60% compared to 17% for the GFP treatment) (Figure 4.1). I hypothesise that this early mortality might be related to an early role of *Tc-nub* and *Tc-cas* in ovary function. Those embryos that did form cuticle did not display any overt morphological defects. However, although 40-45% of embryos laid by *Tc-nub* or *Tc-cas* injected mothers had normal cuticles, only 3-5% of embryos succeeded in hatching, compared to 78.5% for the GFP treatment (Table 4.1). The failure of otherwise 'normal' larvae to hatch could be a result of defects in the nervous system. Both *Tc-nub* and *Tc-cas* are expressed in neuroblasts in *Tribolium* (Biffar and Stollewerk, 2014), and *Dm-cas* mutation has been shown to prevent hatching of *Drosophila* embryos with otherwise normal cuticles, presumably because of disruption to the nervous system (Mellerick et al., 1992).

Table 1. Cuticle phenotypes of offspring produced by mothers injected with 1 µg/µL GFP, *Tc-nub* or *Tc-cas* dsRNA. N = number of eggs examined; WT = wild type; 'other' refers to offspring that produced a non-wild-type cuticle.

Treatment (1 µg/µL)	**N**	**% WT cuticles**	**% empty eggs**	**% other**	**% hatching**
GFP dsRNA (-)	404	83.2	16.8	0	78.5
odd dsRNA (+)	116	0	57.8	42.2	0
nub dsRNA	447	44.3	55.7	0	3.6
cas dsRNA	167	40.7	59.2	0	4.8

To confirm that RNAi was working as expected, I examined *Tc-nub* expression in 24-27 hour old embryos from water- or 1 µg/µL *Tc-nub* dsRNA-injected mothers. (Note that this and the following pRNAi trials use water as a negative control, as I had been advised and tested for myself that injections with water and with GFP dsRNA give similar outcomes to no-injection controls (data not shown)). Interestingly, in this experiment, the percentage of empty eggs was very similar to that observed in the water control treatment, although hatching rate remained low (data not shown) – I surmise that the dose of *Tc-nub* received by parents may have been lower than in my initial experiments, with hatching being more sensitive to knockdown than the early viability phenotype.

I found that expression of *Tc-nub* was reduced in extended germband embryos after *Tc-nub* pRNAi, and the remaining expression was limited mainly to distinct punctae (Figure 4.12). These punctae likely represent sites of nascent transcription in nuclei, which are not impacted by RNAi. *Tc-nub* mRNA in the cytoplasm therefore seems to be effectively degraded after pRNAi, even at 1 µg/µL. It would be useful to investigate the extent of knockdown in several replicates at this concentration using qPCR, to better understand where the variability in the viability phenotype comes from.

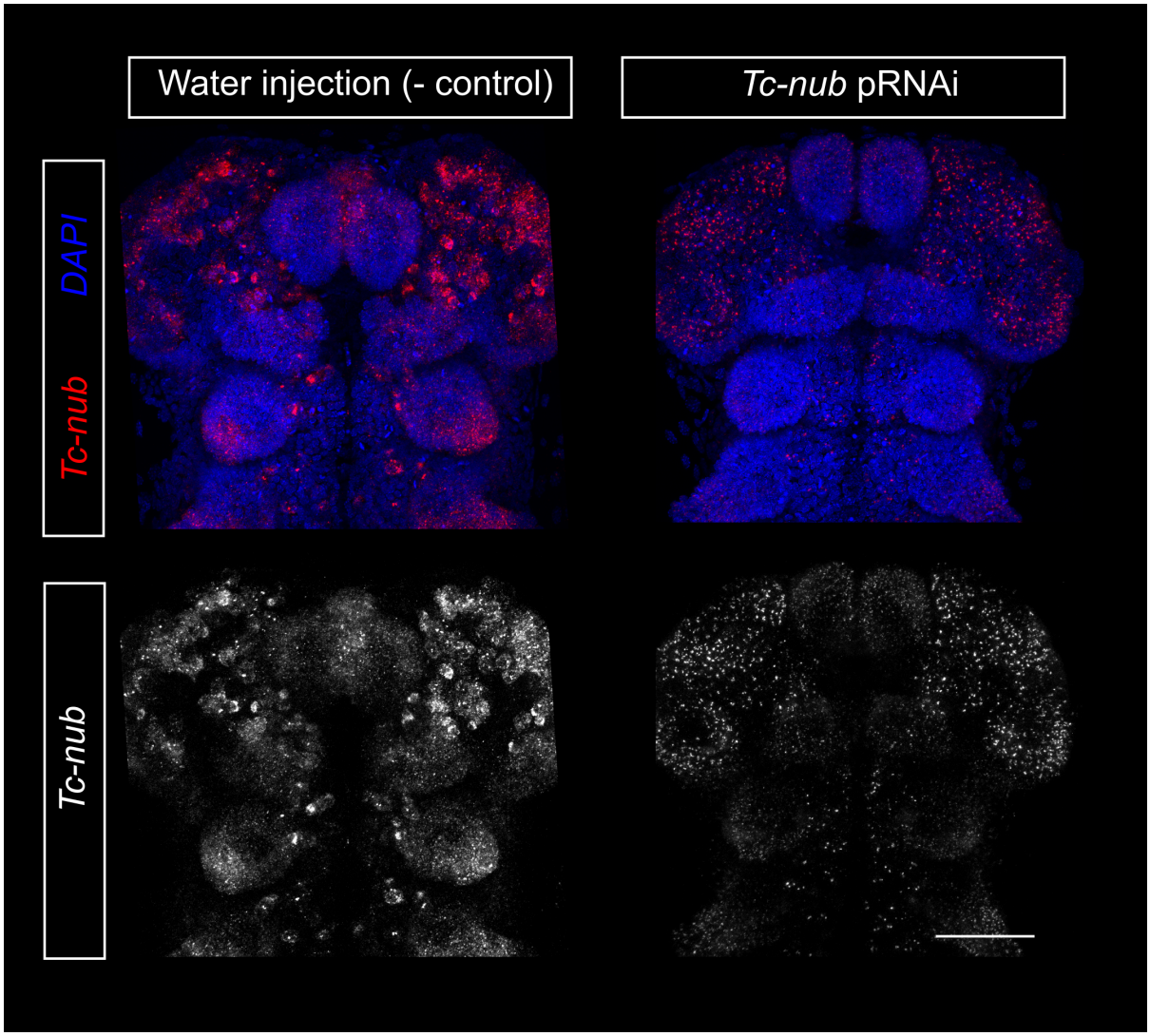

Figure 4.12. Expression of *Tc-nub* in embryos laid by mothers injected with either water (negative control) or 1 μg/μL *Tc-nub* dsRNA. Note that there is little detectable cytoplasmic transcript in the latter, with expression instead limited primarily to punctae that likely mark nuclear transcription. Embryos are 24-27h AEL. Each panel shows just the head of a single embryo with anterior at the top. Scale bar is 50 μM.

Increasing the concentration of *Tc-nub* dsRNA results in the appearance of abdominal phenotypes at low penetrance

Increasing the concentration of *Tc-nub* or *Tc-cas* dsRNA to 2 μg/μL resulted in the emergence of a very small number of unusual phenotypes in offspring cuticles (Table 4.2). Again, close to half of the eggs produced by mothers injected with *Tc-nub* or *Tc-cas* dsRNA failed to form cuticle, compared to 17% of GFP control embryos, and the rate of hatching was markedly reduced. Of the embryos examined after *Tc-nub* pRNAi, 8/120 (6.7%) contained cuticles with defects in abdominal patterning. Specifically, five embryos had abdominal truncations (missing from 1-4 segments and the terminus of the embryo); one had disorganised segment boundaries in the anterior abdomen; and two had small cuticular protrusions growing out of segments A1 and/or A2 (Figure 4.13). Increasing the concentration of *Tc-nub* dsRNA to 3 μg/μL did not increase the frequency of axial phenotypes further (data not shown).

Increasing the dose of *Tc-cas* dsRNA to 2 μg/μL resulted in the appearance of one unusual cuticle (with an ectopic leg on T2) (Table 4.2) – however, this phenotype was not observed again and so likely represents a chance disruption of embryogenesis, unrelated to my RNAi treatment.

Table 4.2. Cuticle phenotypes of offspring produced by mothers injected with water or 2 μg/μL *Tc-nub* or *Tc-cas* dsRNA. N = number of eggs examined; WT = wild type; 'other' refers to offspring that produced a non-wild-type cuticle.

Treatment	N	% WT cuticles	% empty eggs	% other	% hatching
Water	100	83	17	0	82
nub dsRNA (2 μg/μL)	120	50	43.3	6.7	2.5
cas dsRNA (2 μg/μL)	116	37.9	61.2	0.9	3.4

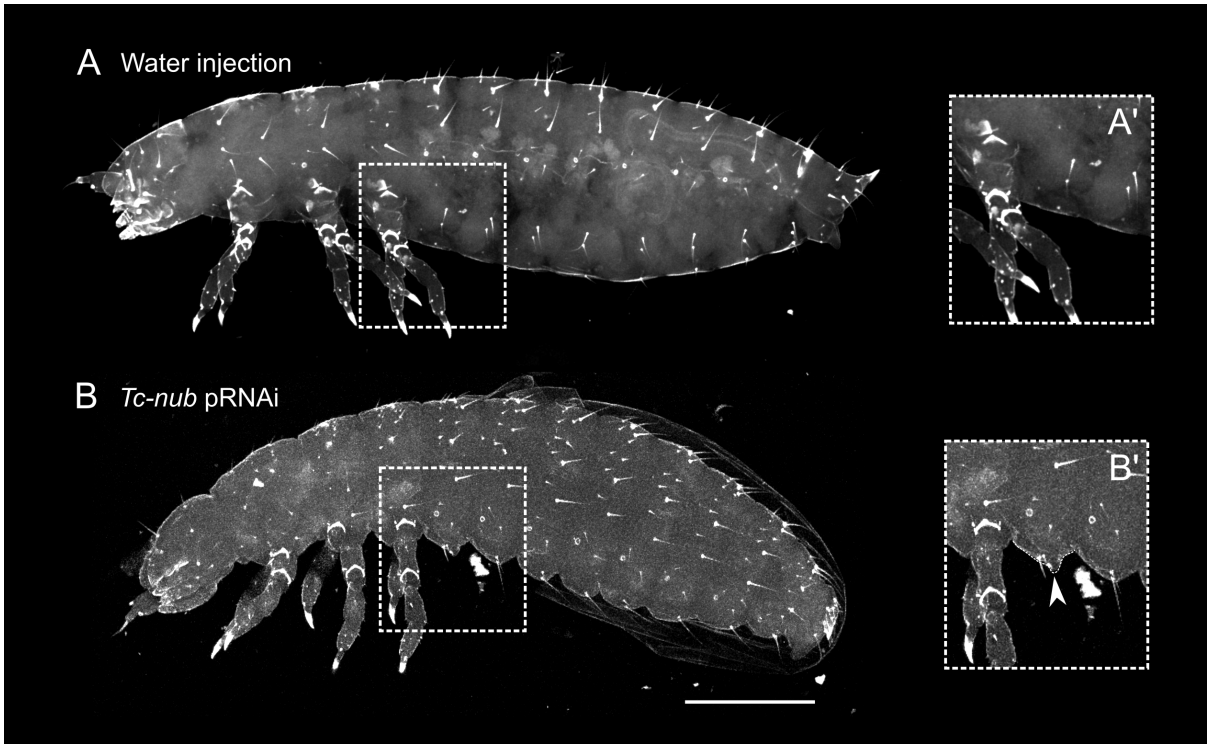

Figure 4.13. Cuticles of larvae produced by mothers injected with water (negative control) (A-A') or with 2 μg/μL *Tc-nub* dsRNA (B-B'). Insets A' and B' show a close up on the regions indicated in A and B, respectively. The white arrowhead indicates a cuticular 'nub' growing on segment A1. Scale bar is 200 μM.

Tc-nub eRNAi circumvents early embryo death and results in a higher proportion of abdominal phenotypes

In parallel, I performed knockdowns using eRNAi to validate my results. Because it involves mechanical disruption of the egg, eRNAi is more disruptive to embryonic development than pRNAi, and the percentage of injected embryos surviving to make cuticles is therefore much lower (~50-60% for eRNAi in my hands, c.f. ~80-83% after pRNAi,). eRNAi has also been observed to produce more non-specific phenotypes than pRNAi, often related to the injection site (M. Benton, personal communication, and my own observations). I, for example, was injecting into the anterior of the embryo, in order to leave the posterior SAZ intact, and observed many embryos with disfigured or missing heads even in control treatments (usually varying between 0-20% in frequency). However, as long as these effects are controlled for, eRNAi provides a useful alternative to pRNAi that circumvents possible roles of genes in oogenesis.

In contrast to my observations using pRNAi, embryos injected with 2 μg/μL *Tc-nub* or *Tc-cas* dsRNA formed cuticles at comparable rates to those injected with GFP dsRNA (Table 4.3). This suggests that the high proportion of empty eggs laid by mothers injected with *Tc-nub* or *Tc-cas* dsRNA results from the effects of knockdown on either oogenesis or very early embryogenesis. Given that neither gene is expressed strongly in the oocyte or early embryo, but is expressed in the ovary (see section 4.5), I would suggest that it is the former. Determining whether *Tc-nub* and *Tc-cas* play roles in ovary function and oogenesis will require more investigation, however (for example, examining the phenotype of ovaries and oocytes after knockdown).

In addition, I observed a higher frequency of unusual abdominal phenotypes specific to the *Tc-nub* eRNAi treatment (Table 4.3). Minor abdominal truncations were observed at a low frequency in all treatments, with only a marginal increase in the *Tc-nub* treatment. Abdominal segment boundaries were disrupted in 6.5% of cuticles arising from *Tc-nub* eRNAi, but in none of the other treatments. Most notably, 10% of the cuticles arising from *Tc-nub* eRNAi displayed cuticular 'nubs' on segment A1 (Figure ZF), a phenotype never observed in the other two treatments. Use of a higher dose of *Tc-nub* dsRNA (4 μg/μL) increased the penetrance of the 'nub' phenotype to 30%, although no truncations or segment boundary disruptions were observed in this treatment (Table 4.4).

No unusual phenotypes were observed to be specific to *Tc-cas* dsRNA-injected embryos using eRNAi.

Table 4.3. Cuticle phenotypes of embryos injected with 2 µg/µL GFP, *Tc-nub* or *Tc-cas* dsRNA. N = number of eggs injected; 'No. (%) cuticles' refers to the number (%) of injected embryos going on to form cuticles; 'boundary' refers to segment boundary disruptions; and 'nubs' refers to small, bilateral cuticular protrusions on the abdominal segments.

Treatment (2 µg/µL)	N	No. (%) cuticles	% abdominal phenotype		
			% truncation	% boundary disruption	% 'nubs'
GFP dsRNA	94	53 (56.4)	1.9	0	0
nub dsRNA	148	91 (61.4)	5.4	6.5	12.1
cas dsRNA	89	43 (48.3)	2.3	0	0

Table 4.4. Cuticle phenotypes of embryos injected with 4 µg/µL GFP or *Tc-nub*. N = number of eggs injected; 'No. (%) cuticles' refers to the number (%) of injected embryos going on to form cuticles; 'boundary' refers to segment boundary disruptions; and 'nubs' refers to small, bilateral cuticular protrusions on the abdominal segments.

Treatment (4 µg/µL)	N	No. (%) cuticles	% abdominal phenotype		
			% truncation	% boundary disruption	% 'nubs'
GFP dsRNA	49	31 (63.2)	3.2	0	0
nub dsRNA	49	25 (51.0)	0	0	32

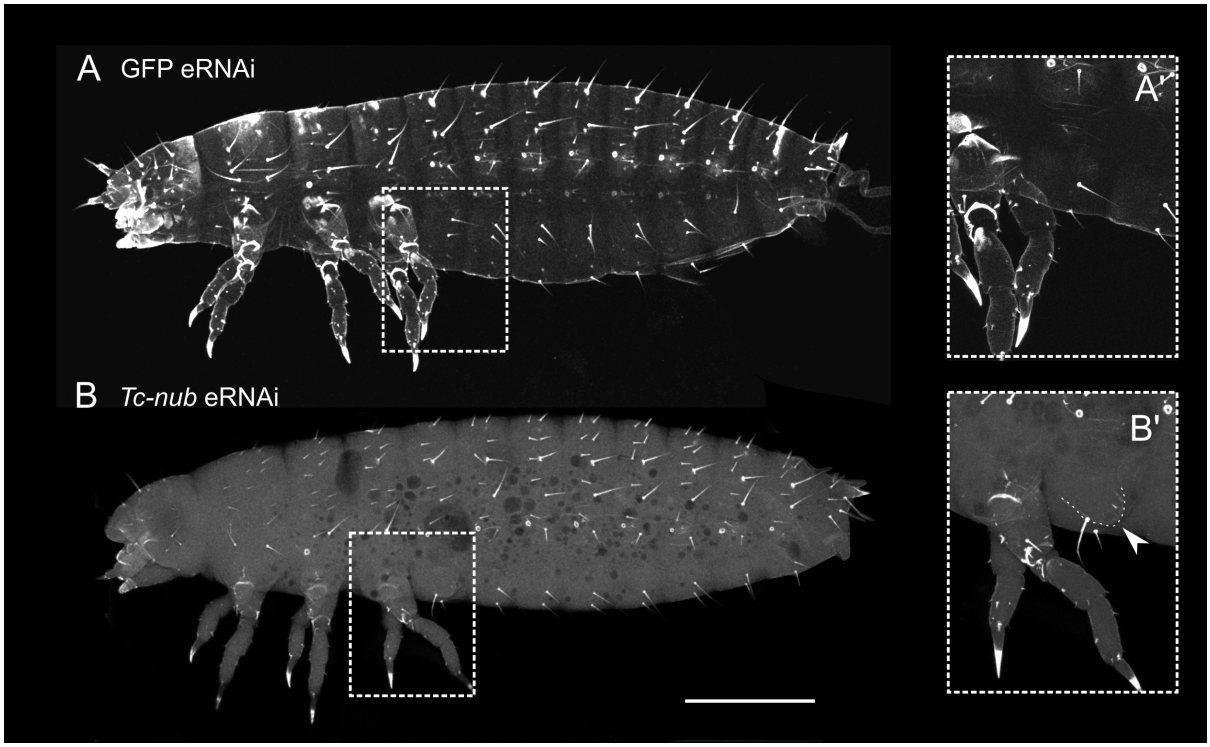

Figure 4.14. Cuticles produced by embryos injected with 2 µg/µL *GFP* dsRNA (negative control) (A-A') or with 2 µg/µL *Tc-nub* dsRNA (B-B'). Insets A' and B' show a close up on the regions indicated in A and B, respectively. The white arrowhead indicates a cuticular 'nub' growing on segment A1. Scale bar is 200 µM.

Tc-nub knockdown results in misexpression of the Hox gene *Tc-abdA*

The formation of a cuticular protrusion in the posterior compartment of A1 suggests a subtle homeotic transformation. *Tc-abdA* mutants display similar protrusions along the length of the abdomen (Stuart et al., 1993), so I hypothesised that the phenotype observed after *Tc-nub* pRNAi might result from repression of *Tc-abdA* in PS7 (A1p-A2a). In the absence of *Tc-abdA*, abdominal parasegments take on the fate of PS6 (T3p-A1a), therefore forming the posterior portion of a T3 leg on each segment (Lewis et al., 2000; Stuart et al., 1993). The cuticular 'nubs' observed could therefore represent partial thoracic appendages.

To investigate this hypothesis, I examined *Tc-abdA* expression in extended germband embryos produced by mothers injected with 2 μg/μL *Tc-nub* dsRNA. In accordance with my hypothesis, I frequently observed a reduction in *Tc-abdA* expression in the anterior portion of PS7 (Figure 4.15). The percentage of embryos showing some degree of *Tc-abdA* repression in PS7 (7/9, or 77.8%) was vastly higher than the percentage of cuticles displaying the 'nub' phenotype after pRNAi (2%). It may be that I have missed subtler phenotypes in cuticles produced after pRNAi in my earliest experiments, so that the actual percentage of embryos with the phenotype is higher. Alternatively, it may be that embryos are usually able to recover from this degree of misexpression and pattern their abdomens correctly. (Note that the number of embryos examined for this experiment was low as it was performed while I was trouble-shooting how to effectively collect small batches of embryos. I had meant to repeat this experiment for confirmation, but work on this was truncated by COVID-19).

I observed normal expression of three potential regulators of *Tc-abdA* - *Tc-hb*, *Tc-Kr* and *Tc-gt* - in 14-17h embryos laid by mothers injected with 2 μg/μL *Tc-nub* dsRNA (data not shown). *Tc-Kr* abuts the anterior of the *Tc-nub* domain, and its expansion in *Tc-gt* knockdowns appears to promote ectopic appendage development (Cerny et al., 2005), and *Dm-Kr* and *Dm-gt* regulate *Dm-abdA* expression in *Drosophila* (Casares and Sánchez-Herrero, 1995). It is possible that any changes in the expression of these gap genes is only transient and not visible at the stage I observed. Alternatively, *Tc-nub* may be directly required for activation of *Tc-abdA* in the anterior of PS7.

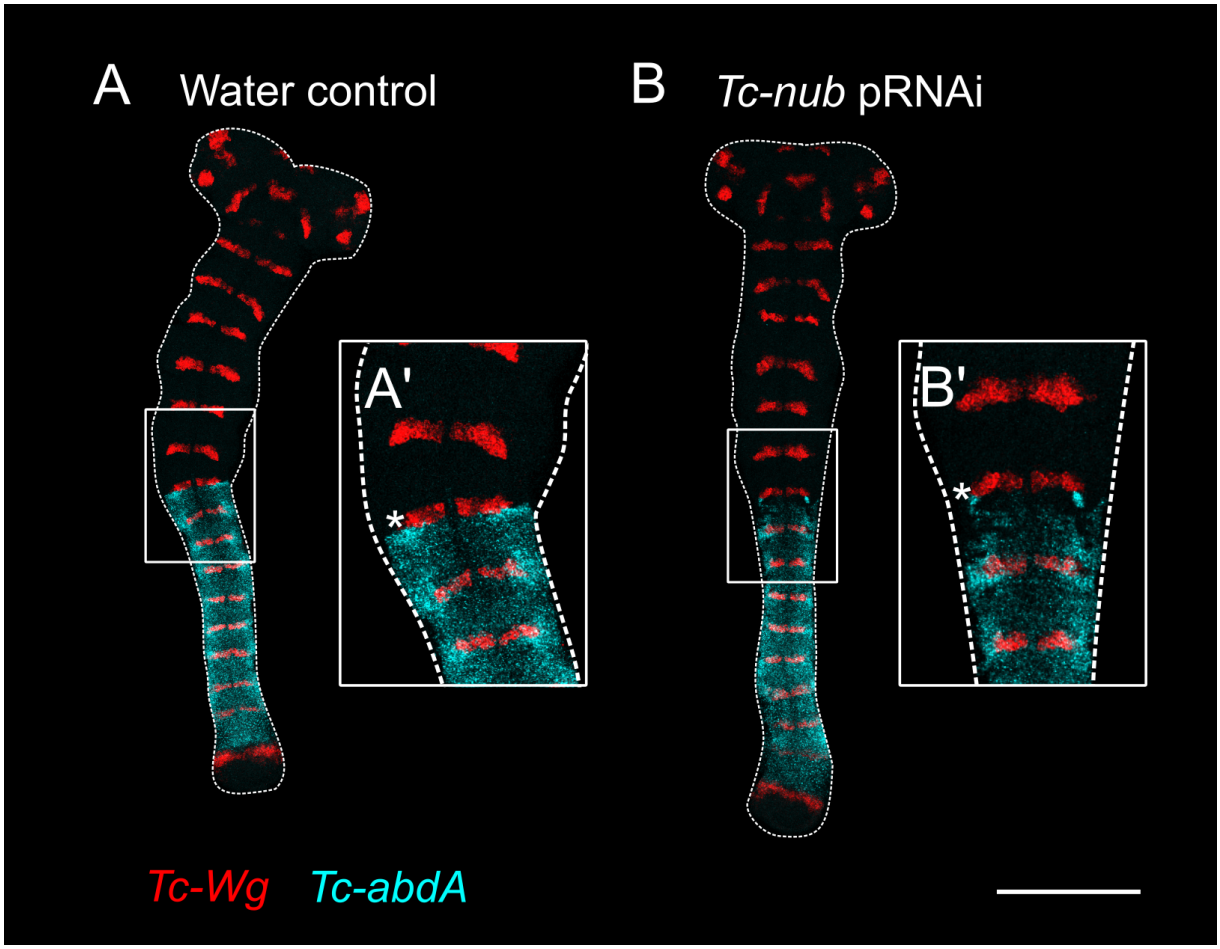

Figure 4.15. Expression of *Tc-nub* in stage-matched embryos laid by mothers injected with either water (negative control) or 2 µg/µL *Tc-nub* dsRNA. Insets A' and B' show close ups on the regions indicated in A and B, respectively, highlighting the reduced expression of *Tc-abdA* in the anterior of PS7 (Wg6 is marked with an asterisk). Scale bar is 200 µM.

Contrary to previous reports, *Dm-nub* may be required for proper expression of *Dm-abdA*

Previous reports have found that *Drosophila Dm-nub* mutants show normal *Dm-abdA* expression (Hrycaj et al., 2008). Given the subtlety of the effect of *Tc-nub* knockdown on *Tc-abdA* expression in *Tribolium*, I decided to re-examine this claim using two different mutant lines; DfGR4, used by Hrycaj et al. (2008) to examine effects on *Dm-abdA* expression, and DfED769, which has a smaller deletion which still removes both *pdm1* and *pdm2*.

I found subtle effects on *Dm-abdA* expression in both mutant lines (results for Df760 shown in Figure 4.16). Specifically, *Dm-abdA* expression is repressed at the edges of its normal domain in embryos lacking *Dm-nub* expression (Figure 4.16). It seems as if *Dm-abdA* expression is normal in the region where *Dm-nub* is not normally expressed (in the central dip which overlaps with *Dm-kni* expression), but is repressed in regions where *Dm-nub* should normally be expressed (PS7 and PS9). However, by the end of segmentation, *Dm-abdA* expression has recovered and is identical in mutants and non-mutants (data not shown). Together, these observations suggest that *Dm-nub* may have a role in initiating *Dm-abdA* expression, but is not necessary for the final elaboration of the *Dm-abdA* domain.

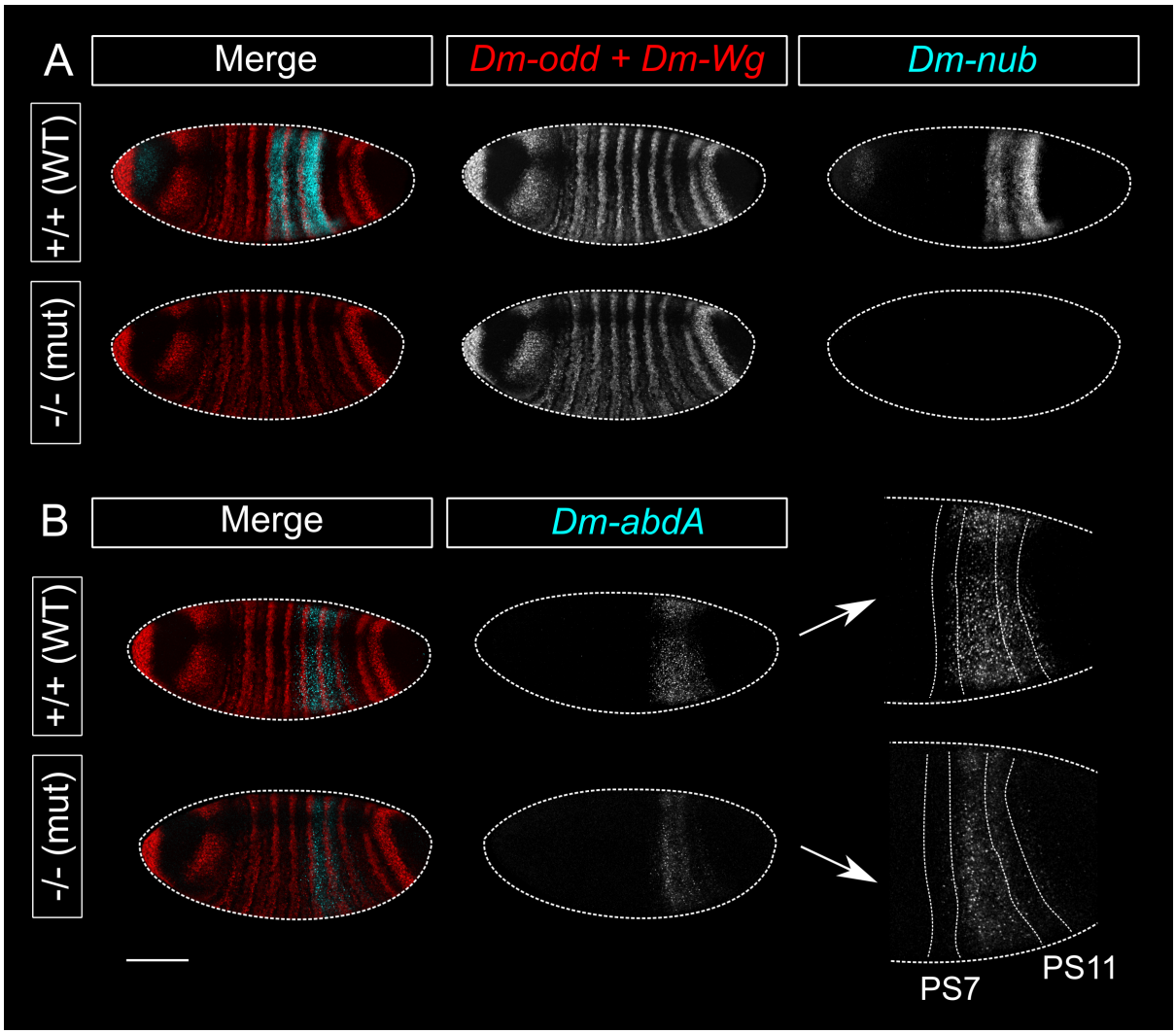

Figure 4.16. Expression of *Dm-nub* and *Dm-abdA* in stage-matched wild type *Drosophila* embryos (+/+ (WT)) and *nub* mutants (-/- (mut), mutant line Df760). Note that in the *nub* mutant, *Dm-abdA* expression is reduced at the lateral edges of its domain, in particular in PS7 and PS11 where *Dm-nub* is usually expressed. Scale bar is 100 μM.

4.3. DISCUSSION

In this chapter, I have shown that the neuroblast timer genes *Tc-nub* and *Tc-cas* are expressed in broad, gap-like domains during segment patterning. The four genes of the neuroblast clock (*Tc-hb*, *Tc-Kr*, *Tc-nub* and *Tc-cas*) are expressed in temporal series in the SAZ, generating ordered expression domains along the AP axis (similar to what is observed in *Drosophila*). I additionally show that *Tc-nub* is required for normal expression of *Tc-abdA* in PS7, but that *Tc-cas* knockdown has no obvious effect on segmental patterning. Together, these results have interesting implications for the evolution of the gap gene network and its relation to the neuroblast timer series.

4.3.1. The SAZ of *Tribolium* expresses the neuroblast timer genes in the same order as neuroblasts themselves

I show here that the neuroblast timer genes are expressed in the same temporal order in the SAZ of *Tribolium* as they are in neuroblasts themselves. Sequential expression of *Tc-hb*, *Tc-Kr*, *Tc-nub* and *Tc-cas* in the SAZ results in these genes forming an ordered series of domains that covers the length of the AP axis (Figure 4.17). It is possible that some remnant of this temporal order exists in *Drosophila* – although no single cell will cycle through expression of all four genes, maternal *Dm-Hb* is certainly present before *Dm-Kr* becomes expressed, and *Dm-nub* is first expressed a cell cycle later than either of these genes (Cockerill et al., 1993). However, overall, the process by which expression domains of *Tc-hb*, *Tc-Kr*, *Tc-nub* and *Tc-cas* are established in *Tribolium* is much more obviously analogous to the process of sequential fate assignment in neuroblasts. Similar to neuroblasts, the undifferentiated cells in the SAZ express each of these genes in order until they 'mature' (in this case, move into the segmented germband), at which point they cease to cycle through the timer series.

In neuroblasts, the function of this sequential expression is to allow the production of different daughter cell types in a stereotyped order (Isshiki et al., 2001). It is easy to imagine how such a function would be usefully co-opted for axial patterning; the SAZ has to generate segments in a stereotyped order, with the earliest-maturing cells contributing to the gnathal segments; those maturing slightly later, to the thorax; and the latest-maturing contributing to the abdomen. My work and others' (Hrycaj et al., 2008) suggest that *nub* may be required to some extent for full realisation of abdominal fates (discussed further in section 4.3.4).

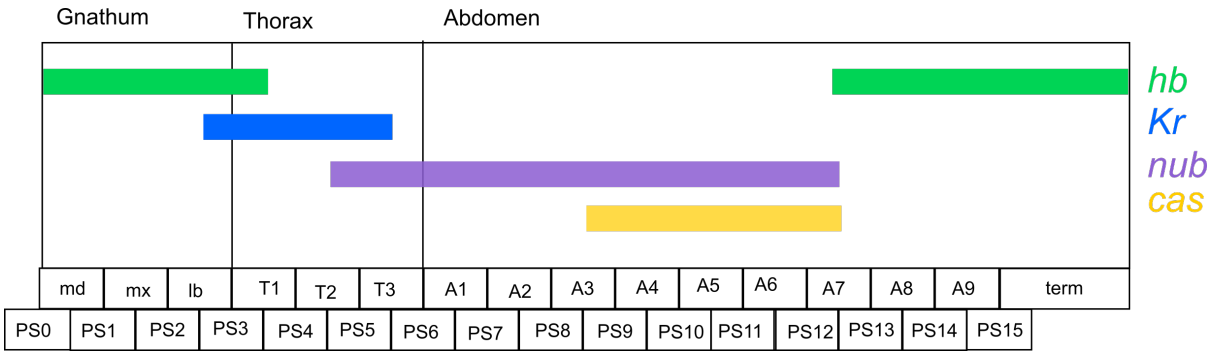

Figure 4.17. Summary of the expression of the four neuroblast timer genes in trunk (para)segments as they are specified (*i.e.* at the time that segmental *Wg* stripes first emerge) in *Tribolium*. Term = terminus of the embryo.

4.3.2. *Tc-nub* and *Tc-cas* are expressed in the ovary and are likely to function during oogenesis

I found that both *Tc-nub* and *Tc-cas* are expressed in the ovaries of *Tribolium*. The fact that eRNAi results in fewer 'empty eggs' than pRNAi also suggests that these two genes may play an active role in oogenesis. Such a finding is not surprising for *Tc-cas*; as mentioned in the results, *Dm-cas* is also required for ovary function in *Drosophila* (Chang et al., 2013). The iBeetle screen reports that pRNAi against *Tc-cas* results in a reduction in the number of previtellogenic egg chambers and the size of the tropharium (Dönitz et al., 2018). These results pertain to only 2 individuals, so further investigation is warranted, but support the theory that *Tc-cas* plays an active role in ovary function in *Tribolium* as in *Drosophila*.

This is, by contrast, the first report of a *nub* homologue being expressed in the ovary of any arthropod. It is interesting that *Tc-nub* should mark out a distinct population of nurse cells. In the late pupal stage, 'pro-nurse' cells at the proximal end of the tropharium undergo polyploidisation, subsequently allowing the expansion of the nurse cell syncytium (Trauner and Büning, 2007). It is possible that this proliferative activity continues into adulthood, in which case *Tc-nub* may be a marker for pro-nurse cells. Such a role would be consistent with *nub*'s role in regulating proliferation in other contexts, such as the adult intestine of *Drosophila* (Tang et al., 2018).

4.3.3. RNAi against *Tc-nub* and *Tc-cas* does not affect leg development, despite their expression in developing limb buds

Tribolium provides an advantage for studying appendage development compared with *Drosophila*, as like most arthropods, the limbs are patterned in the embryo; by contrast, the limbless *Drosophila* larva delays appendage patterning until pupation. I show here that both *Tc-nub* and *Tc-cas* are expressed in the developing gnathal and thoracic appendages of *Tribolium* embryos. *nub* is expressed in the appendage buds of diverse arthropods (Abzhanov and Kaufman, 2000; Averof and Cohen, 1997; Damen et al., 2002; Prpic and Damen, 2005; Prpic and Damen, 2009; Turchyn et al., 2011), but this is the first known example of *cas* being expressed in appendage buds.

Despite their expression in appendage buds, knockdown of neither *Tc-nub* nor *Tc-cas* had any obvious effect on the limb development. Knockdown or knockout of *nub* has been shown to cause defects in leg formation in a range of different insects (Cifuentes and García-Bellido, 1997; Hrycaj et al., 2008; Turchyn et al., 2011), so this is an unusual observation. The concentrations of *nub* dsRNA that I have used (2-2.5 μg/μL) are within the ranges employed by Hrycaj et al. (2008) and Turchyn et al. (2011), but it is possible that the efficacy of RNAi was lower in my experiments. This could result from intrinsic differences in the RNAi machinery of *Tribolium* compared to other insects, or from differences in injection volume or post-injection leakage. I find it unlikely that experimental error explains the discrepancy, as my positive control (*Tc-odd*) as well as RNAi trials for other previously described gap genes (*Tc-hb*, *Tc-Kr* and *Tc-mlpt*) worked well in my hands. Perhaps the role of *Tc-nub* has recently diverged so that its expression, but not its function, in limbs is maintained. Alternatively, perhaps its role has become redundant with some other protein in *Tribolium* (see Chapter Five for more on this).

4.3.4. *nub* regulates *abdA* gene expression in disparate insect groups

I found little evidence for a role of *Tc-cas* in segment patterning. By contrast, I did observe a subtle impact of *Tc-nub* pRNAi and eRNAi on segment identity. Specifically, partial loss of *Tc-abdA* expression in PS7 in *Tc-nub* knockdowns leads to the formation of cuticular 'nubs', which I have proposed are partially formed thoracic legs, on the first abdominal segment. I have also shown, contrary to previous reports (Hrycaj et al., 2008) that *Dm-abdA* expression is subtly disrupted in *Drosophila nub* mutant embryos. It has previously been

reported that in *Oncopeltus*, knockdown of *Of-nub* leads to repression of *Of-abdA* across the length of the abdomen (Hrycaj et al., 2008). There are therefore now three examples of *nub* regulating *abdA* expression in three disparate insect groups. In all of these cases, knockdown or loss of *nub* leads to loss of *abdA* expression, suggesting either that *nub* acts as an activator of *abdA* or that it represses a repressor of *abdA*. Regulation of the infraabdominal regions in *Drosophila* (the regulatory regions that drive *Dm-abdA* and *Dm-AbdB* expression in specific parasegments) is thought to be accomplished through a combination of general activation, and specific repression by gap genes (specifically *Dm-Hb* and *Dm-Kr*) (Casares and Sánchez-Herrero, 1995). *Tc-Kr* is also likely to repress *Tc-abdA* in *Tribolium* – after *Tc-mlpt* RNAi, embryos display expanded expression of *Tc-Kr* and concomitant repression of *Tc-abdA* expression in the abdomen (Savard et al., 2006). Combined with the fact that *Tc-nub* and *Tc-Kr* abut at a sharp boundary, and that *Dm-nub* is able to repress *Dm-Kr* (Grosskortenhaus et al., 2006), derepression of *Tc-Kr* seems a plausible explanation to explain the repression of *Tc-abdA* in *Tc-nub* knockdowns. I failed to observe any impact of *Tc-nub* knockdown on *Tc-Kr* expression, but given the subtlety of the effects on *Tc-abdA* expression I cannot rule out having missed equally subtle and/or transient effects on *Tc-Kr* expression. Detailed examination of *Kr* expression after *nub* mutation or knockdown in *Tribolium*, *Drosophila* and *Oncopeltus* would be a useful next step.

It is worth asking why I might have observed such a mild phenotype in *Tribolium* compared to another sequentially-segmenting insect like *Oncopeltus*. Knockdown of *Of-nub* leads to abdominal transformations with greater severity (A2-A9 segments are all transformed into appendage bearing segments, with many of these appendages being close to normal thoracic legs) and high penetrance (~90-100% of *Oncopeltus* embryos display abdominal transformations, compared to only 10-30% of treated *Tribolium* embryos) (Hrycaj et al., 2008). Difference in experimental methods might account for this discrepancy, if I exposed my beetles to a lower total dose of *nub* dsRNA, but I find this an unconvincing explanation; my HCRs indicate that *Tc-nub* is effectively knocked down, and as discussed above, RNAi experiments using dsRNAs with known effects worked as expected, arguing against any consistent experimental bias. In addition, I performed several experiments using even higher concentrations of *Tc-nub* dsRNA, and although they increased the penetrance of the 'nub' phenotype somewhat, they did not impact the severity.

Another possible explanation is that the relative importance of *nub* for abdominal Hox regulation varies between different insect species. I show here that *Dm-nub* has only subtle effects on *abdA* expression, and *nub* seems to have no impact on abdominal identity in the

house cricket *Acheta* (Turchyn et al., 2011). Clearly, the relative importance of *nub* for patterning the abdomen varies between different insect groups.

Given that *Tc-nub* expression overlaps extensively with other gap genes in the anterior abdomen, I wondered whether its subtle effect here might result from functional redundancy with one or more of these genes. This possibility is discussed in more detail, and investigated, in Chapter Five.

5. REDUNDANT ACTIVITY OF ABDOMINAL GAP GENES

5.1. INTRODUCTION

5.1.1. Redundancy in the gap gene network

I have shown in Chapter Four that *Tc-nub* knockdowns in *Tribolium* result in weak abdominal transformations with low penetrance, in contrast to the strong abdominal transformations observed in *Of-nub* knockdowns in *Oncopeltus* embryos (Hrycaj et al., 2008). As discussed at the end of that chapter, there are several reasons why *Tc-nub* may have a weaker RNAi phenotype than *Of-nub*. One of the most intriguing is that *Tc-nub* may be acting redundantly with other abdominal gap genes to fulfil a function in axial patterning.

In *Drosophila*, strong, mutual repression between non-overlapping pairs of gap genes (*Dm-hb/Dm-kni* and *Dm-Kr/Dm-gt*) is sufficient to establish staggered, static gap gene domains, but dynamic anterior shifts are produced by weaker, asymmetric repression between overlapping pairs of gap genes (Dm-Kr⊣*Dm-hb*, Dm-Kni⊣*Dm-Kr* and Dm-Gt⊣*Dm-kni*) (reviewed in Jaeger, 2011) (Figure 5.1A). Where these two spatial systems meet, they often generate some degree of redundancy; for example, although Dm-gt is a strong repressor of *Dm-Kr*, *Dm-gt* mutants show almost normal *Dm-Kr* expression as its boundaries are maintained via repression by Dm-Hb (anteriorly) and Dm-Kni (posteriorly) (Kraut and Levine, 1991).

By contrast, current models of the gap gene network in *Tribolium* include very little redundancy (Figure 5.1B). The low redundancy postulated in this network is at odds with the large number of overlapping gap and gap-like gene domains in the posterior thorax and anterior abdomen. In particular, PS5-PS7 (T2p-A2a) express *Tc-mlpt* + *Tc-svb*, *Tc-gt* and *Tc-kni* in addition to *Tc-nub* during their early specification (Chapters 3 and 4). It has been proposed that the large number of overlapping gap gene domains in this region might be necessary for pair-rule patterning to be maintained during the transition from blastoderm to germband, with the staggered boundaries of these gap genes directing the formation of specific pair-rule gene stripes (Cerny et al., 2008). However, neither *Tc-nub* nor *Tc-kni* knockdowns show any disruptions in segment patterning at the thorax-abdomen transition (Chapter 4 and Cerny et al.,

2008; Peel et al., 2013). As of yet, no-one has carried out double or triple knockdowns in *Tribolium* to investigate whether these genes may act redundantly.

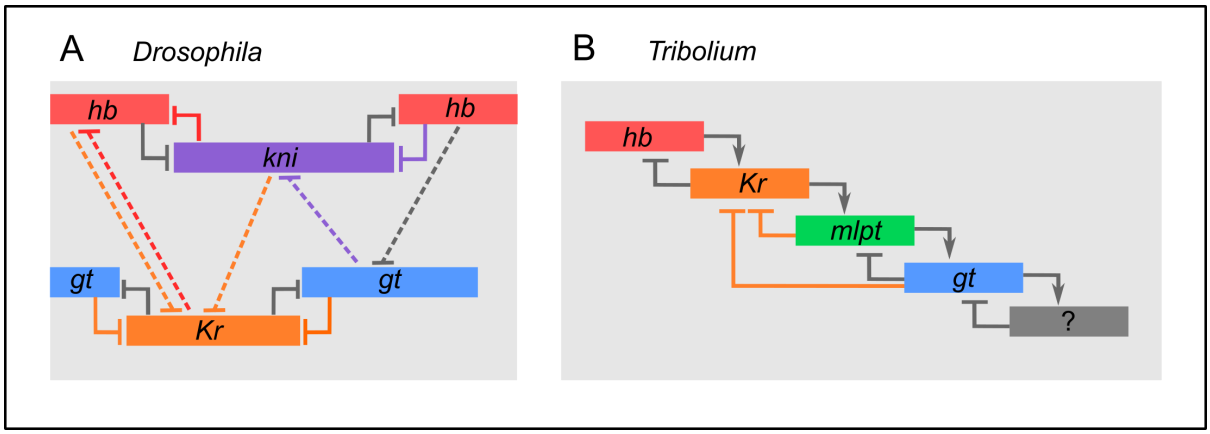

Figure 5.1. Core interactions between gap genes in the *Drosophila* (A) and *Tribolium* (B) gap gene networks. Panel A is adapted from Jaeger (2011) and panel B is adapted from Zhu et al. (2017). In A, solid lines indicate strong repression, while dotted lines indicate weak repression. Where functional data has indicated some degree of redundancy in an interaction, those interactions are highlighted in the same colour as the target gene. For example, the posterior border of *Dm-Kr* (orange) is set via repression from both Dm-gt and Dm-kni, so the lines corresponding to these interactions are coloured orange.

5.1.2. Does Tc-Nub act redundantly with Tc-Gt and/or Tc-Kni to repress *Tc-Kr* in the abdomen?

Interestingly, all of the gap genes expressed in the posterior thorax and anterior abdomen of *Tribolium* are able to repress *Kr* expression in some context in *Tribolium* and/or *Drosophila* (Table 5.1). However, knocking down *Tc-nub* or *Tc-gt* has no obvious impact on the posterior border of *Tc-Kr* expression (Chapter 4 and Cerny et al., 2005), and *Tc-kni* knockdowns show no anterior abdominal phenotype, indicating that this is probably also the case for *Tc-kni*. If the posterior boundary of *Tc-Kr* is set via repression by *Tc-gt*, *Tc-kni* and *Tc-nub* this would explain why knockdown of any one of these genes has little or no impact on *Tc-Kr* expression. There is, as of now, only one gene which has been shown to repress *Tc-Kr* in the abdomen in *Tribolium* – *Tc-mlpt* (Savard et al., 2006). I have discussed earlier how the co-expression of *Tc-mlpt* and *Tc-svb* precede the emergence of the abdominal *Tc-gt*, *Tc-kni* and *Tc-nub* domains in the SAZ, and how this might indicate co-ordinated activation of some or all

of the three genes by Tc-Svb in its activator form (Chapters 3 and 4). This could explain why *Tc-mlpt* knockdowns might have a more pronounced effect on *Tc-Kr* expression than any one of *Tc-nub*, *Tc-gt* or *Tc-kni*.

Table 5.1. Effects of *mlpt/svb*, *nub*, *gt* or *kni* misexpression on *Kr* expression during neuroblast (NB) and/or axial patterning in *Drosophila* or *Tribolium*. All have been shown to repress *Kr* expression in one context or another (evidence against their acting as repressors of *Kr* are highlighted in red).

Gene	***Drosophila***		***Tribolium***	
mlpt/svb	_	_	*Tc-mlpt* knockdowns show posterior expansion of *Tc-Kr* gap domain. *Tc-svb* knockdowns show same homeotic transformations as *Tc-mlpt.*	(Savard et al., 2006) (Ray et al., 2019)
nub	Repression or ectopic expression in NBs leads to extended or abolished expression of *Dm-Kr*, respectively. Mutants show normal *Dm-Kr* gap gene domain.	(Grosskortenhaus et al., 2006; Tran and Doe, 2008) (Cockerill et al., 1993)	Knockdowns exhibit no obvious effect on *Tc-Kr* expression.	Chapter 4, E. Raymond (unpublished)
gt	Ectopic expression represses *Dm-Kr* gap domain.	(Kraut and Levine, 1991)	Knockdowns show anterior expansion of *Tc-Kr* gap domain.	(Cerny et al., 2005)
kni	Mutants show posterior expansion of *Dm-Kr* gap gene domain.	(Jäckle et al., 1986)	_	_

5.1.3. Potential redundancy of *Tc-nub* and *Tc-cas* in the posterior abdomen

As discussed in the previous chapter, knockdown of *Tc-cas* has no obvious effect on abdominal segmentation or segment identity, despite its prominent expression domain in the SAZ during posterior abdominal segment patterning. However, the gap-like domain of *Tc-cas* expression entirely overlaps with the posterior of the abdominal *Tc-nub* expression domain (Chapter 4). This raises the question of whether these two genes may also play a redundant role in the abdomen.

5.1.4. Specific aims

In this chapter, I aimed to determine whether *Tc-nub* might be acting redundantly with *Tc-gt* and/or *Tc-kni* in the anterior abdomen, and with *Tc-cas* in the posterior abdomen, to influence axial patterning. To do this, I performed double and triple knockdowns of these genes in *Tribolium* embryos using eRNAi, and analysed the resulting phenotypes using cuticle preparations and HCRs against Hox and other gap genes. I also examined gene expression in *Tc-svb* knockdowns to investigate whether the resulting abdominal transformations are related to misexpression of *Tc-nub*.

5.2. RESULTS

5.2.1. Validation of *Tc-kni* and *Tc-gt* dsRNA: *Tc-gt* knockdown generates abdominal transformations with low penetrance

I first aimed to validate the dsRNA I had synthesised for *Tc-gt* and *Tc-kni* by performing eRNAi against both genes individually. dsRNA injected at 1 μg/μL was sufficient to generate phenotypes consistent with those previously described for *Tc-gt* and *Tc-kni* knockdowns (Bucher and Klingler, 2004; Cerny et al., 2008; Peel et al., 2013) (Tables 5.1 and 5.2 and Figure 5.2).

***Tc-kni*:** Approximately 90% of cuticles formed in eggs injected with *Tc-kni* dsRNA lacked one or both antennae, and 25% displayed disruptions in posterior abdominal segment boundaries (Figure 5.2B). Most of the cuticles lacking antennae also lacked or displayed only remnants of the mandibles, although this was not quantified. Injecting *Tc-kni* dsRNA at a higher concentration (2 μg/μL) resulted in a similar number of cuticles lacking antennae (~83%) but no disruptions in abdominal segment boundaries. Cerny et al. (2008) describe this phenotype as displaying lower and variable penetrance than the head phenotype, so I am not overly concerned about this discrepancy. Previous studies indicate that increasing the concentration of dsRNA up to 4 μg/μL does not qualitatively affect the resulting phenotypes (Cerny et al., 2008; Peel et al., 2013), so we can be reasonably confident in saying that knockdowns of *Tc-kni* do not affect anterior abdominal segment patterning or identity despite its expression in this region.

***Tc-gt*:** All of the cuticles formed in eggs injected with 1 or 2 μg/μL *Tc-gt* dsRNA displayed canonical phenotypes associated with *Tc-gt* knockdown, in particular truncation (*i.e.,* a lower total number of segments than the wild type cuticles) and transformation of the maxilla and labium into thoracic legs (Figure 5.2C) (Bucher and Klingler, 2004). However, I also observed an additional phenotype, not reported by Bucher and Klingler (2004). Cuticles formed after *Tc-gt* eRNAi typically display 5 pairs of legs, representing those on the two transformed gnathal segments and the three thoracic segments. In addition, 11% of cuticles injected with 1 μg/μL *Tc-gt* dsRNA, and 17% of cuticles injected with 2 μg/μL *Tc-gt* dsRNA, developed a pair of partial or complete legs on the following segment, which in a wild type embryo would represent segment A1 (Figure 5.2D, Table 5.2).

Table 5.1. Cuticle phenotypes of embryos injected with 2 µg/µL *GFP* dsRNA, 1 µg/µL *Tc-kni* dsRNA + 1 µg/µL *GFP* dsRNA or 2 µg/µL *Tc-kni* dsRNA. N = number of eggs injected; 'No. (%) cuticles' refers to the number (%) of injected embryos going on to form cuticles; 'lost antenna' refers to cuticles which lack one or both antennae; and 'boundary disrupted' refers to cuticles displaying partial fusions and/or deletions of segments in the abdomen.

Treatment	Conc	N	No. (%) cuticles	% lost antenna	% boundary disrupted
GFP dsRNA	2 µg/µL	94	53 (56.4)	0	0
Tc-kni dsRNA	1 µg/µL (+1 µg/µL GFP)	45	28 (62.2)	89.3	25
	2 µg/µL	45	30 (66.7)	83.3	0

Table 5.2. Cuticle phenotypes of embryos injected with 2 µg/µL *GFP* dsRNA, 1 µg/µL *Tc-gt* dsRNA + 1 µg/µL *GFP* dsRNA or 2 µg/µL *Tc-gt* dsRNA. N = number of eggs injected; 'No. (%) cuticles' refers to the number (%) of injected embryos going on to form cuticles; 'gnathal trans' refers to cuticles with maxillary and labial segments transformed to leg-bearing thoracic segments; 'extra 'legs'' refers to cuticles in which at least one abdominal segment has been transformed to bear a pair of complete or partial legs (this is in addition to the transformed gnathal segments).

Treatment	Conc	N	No. (%) cuticles	% gnathal trans	% truncation	% extra 'legs'
GFP dsRNA	2 µg/µL	94	53 (56.4)	0	1.2	0
Tc-gt dsRNA	1 µg/µL (+1 µg/µL GFP)	45	28 (62.2)	100	100	11.1
	2 µg/µL	45	30 (66.7)	100	100	17.4

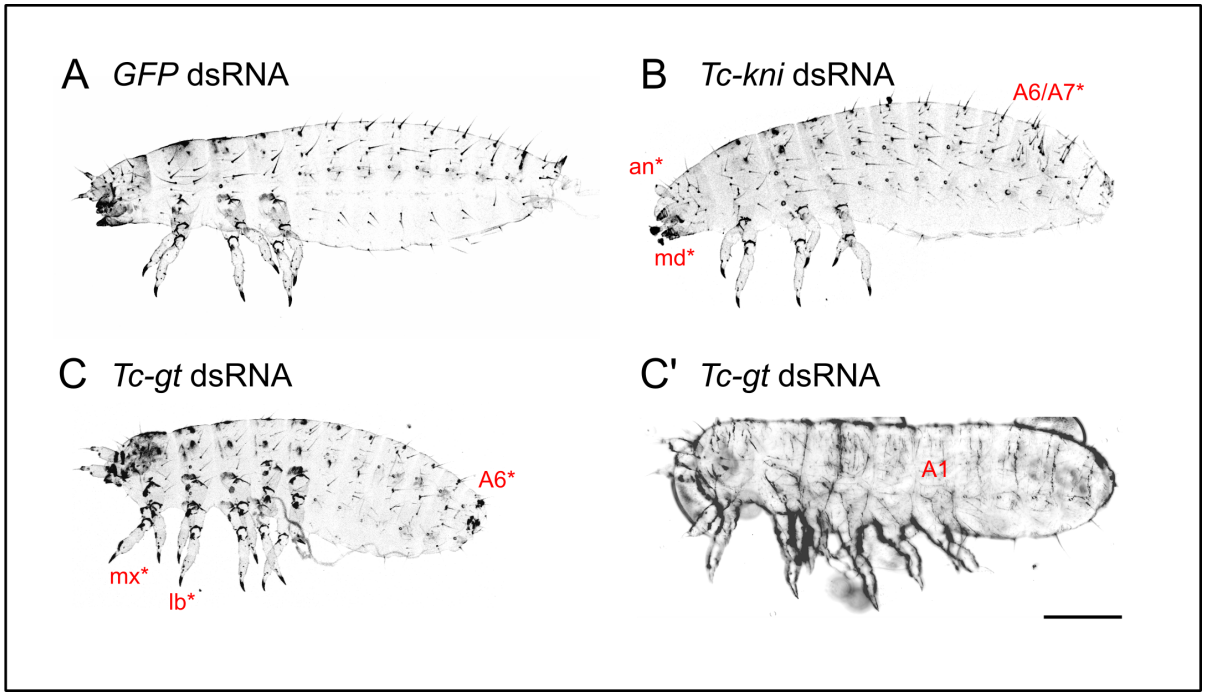

Figure 5.2. Cuticles from eggs injected with 2 µg/µL *GFP*, *Tc-kni* or *Tc-gt* dsRNA. Red annotations indicate characteristic phenotypes in B and C (an*, md*, mx* and lb* = deletion of antennae, mandibles maxilla and labium, respectively; A6/A7* = partial fusion of segments A6 and A7; A6* truncation after segment A6) and a novel phenotype for *Tc-gt* eRNAi in panel C' (formation of an ectopic leg on segment A1). Note that the *GFP* dsRNA image in A is re-used in several eRNAi figures in this thesis, but is representative of experiments carried out in parallel to each eRNAi knockdown. The image in panel C' was taken on a compound instead of a confocal microscope, and is from a poorer quality cuticle preparation – with more time, this experiment would have been repeated to gather higher quality images. Scale bar is 200 µM.

The reason for the discrepancy between my results and those of Bucher and Klingler (2004) is not immediately clear. They performed eRNAi against *Tc-gt* using dsRNA prepared from the same gene fragment, and using the same concentration as me (up to 2 µg/µL). However, dsRNA concentration is not always an effective predictor of knockdown strength, as this can be impacted by the quality of the dsRNA preparation or the volume of dsRNA injected. It is possible that the strength of the knockdowns performed by Bucher and Klingler (2004) was slightly under the threshold required to generate partial legs. Regardless, it seems that *Tc-gt* has a role in regulating abdominal segment identity in segment A1. The fact that both *Tc-nub* and *Tc-gt* knockdowns generate homeotic transformations of segment A1 at low penetrance supports the hypothesis that the two genes may have partially redundant roles in regulating anterior abdominal segment identity.

5.2.2. Knockdown of *Tc-nub* with *Tc-gt* and/or *Tc-kni* results in stronger and more penetrant abdominal transformations

Having established that *Tc-nub* and *Tc-gt* knockdowns affect anterior abdominal identity in a small percentage of cuticles, and that *Tc-kni* has no apparent role in the anterior abdomen, I set out to determine whether knocking combinations of these genes out together might increase the penetrance or severity of the phenotypes observed. Indeed, I observed that knocking down *Tc-nub* with *Tc-kni* and/or *Tc-gt*, or *Tc-kni* with *Tc-gt*, increased the severity and penetrance of abdominal segment transformation compared to knocking down any of these genes singly (Figures 5.3, Table 5.3 and Figure 5.4).

At 1 μg/μL, *Tc-gt* knockdown alone results in the formation of partial or complete legs on segment A1 in ~10% of cuticles; at the same concentration, *Tc-nub* knockdown alone results in the formation of nubs on segment A1 at a similar frequency; and *Tc-kni* knockdown has no obvious homeotic effect on the abdomen. Knocking *Tc-nub* and *Tc-kni* down together, however, increases the frequency of cuticles with only weak abdominal transformations to 40%, and additionally results in strong transformations in ~24% of cuticles (Figure 5.3B, Table 5.3, Figure 5.4). These transformations, unlike those observed in single *Tc-nub* knockdowns, often affect both segment A1 and A2. Likewise, knocking *Tc-gt* down in tandem with *Tc-kni* more than doubles the frequency of weak transformations to ~25%, with an additional ~46% of cuticles displaying at least one segment with a strong transformation (Figure 5.3C, Table 5.3, Figure 5.4). Again, unlike *Tc-gt* knockdowns, both A1 and A2 are often affected. In both of these double knockdowns, transformations of A1 are more likely to be weak, and those on A2 to be strong (Figure 5.3B and C), so that the average number of additional pairs of legs in cuticles displaying transformations is 1 (Table 5.3).

If the effect of knockdown of *Tc-nub* and *Tc-gt* was simply additive, we would expect the double knockdown to result in ~10% of cuticles displaying a weak transformation (nubs) and ~10% displaying strong transformations (partial or complete legs). Instead, weak transformations are observed in ~30% of cuticles, and an additional 50% show at least one strongly transformed segment (Figure 5.3D, Table 5.3, Figure 5.4). *Tc-nub/Tc-gt* knockdowns are more likely to have strong transformations of both A1 and A2 than *Tc-nub/Tc-kni* or *Tc-gt/Tc-kni* double knockdowns, and so have a slightly higher average number of additional leg pairs (1.3 - Table 5.3).

Finally, knocking down all three genes together produces the most severe and penetrant phenotype of all (Figure 5.3E, Table 5.3, Figure 5.4). Specifically, ~95% of cuticles developing

from embryos injected with all three dsRNAs have strong transformation of at least one abdominal segment towards a thoracic fate. These cuticles have an average of 4 extra pairs of legs (not including the maxillary legs induced by *Tc-gt* knockdown), and a maximum of seven extra pairs (Table 5.3), indicating transformation of up to seven abdominal segments. The legs are also often fully formed, rather than the partial legs observed commonly in double knockdowns (Figure 5.3). Weaker triple knockdowns display fully formed thoracic legs on the anterior abdominal segments, and 'nubs' or partial legs on the more posterior segments (data not shown), indicating that the anterior abdomen is more sensitive to knockdown.

Triple knockdown experiments also produced a higher percentage of empty eggs. Around 60-70% of embryos in single knockdown treatments, but only 25% of those in triple knockdown treatments, went on to form cuticle (Table 5.3). Two of the double knockdowns (*Tc-nub/Tc-kni* and *Tc-nub/Tc-gt*) also had a slightly reduced frequency of cuticle formation compared to single knockdowns (~45%; Table 5.3).

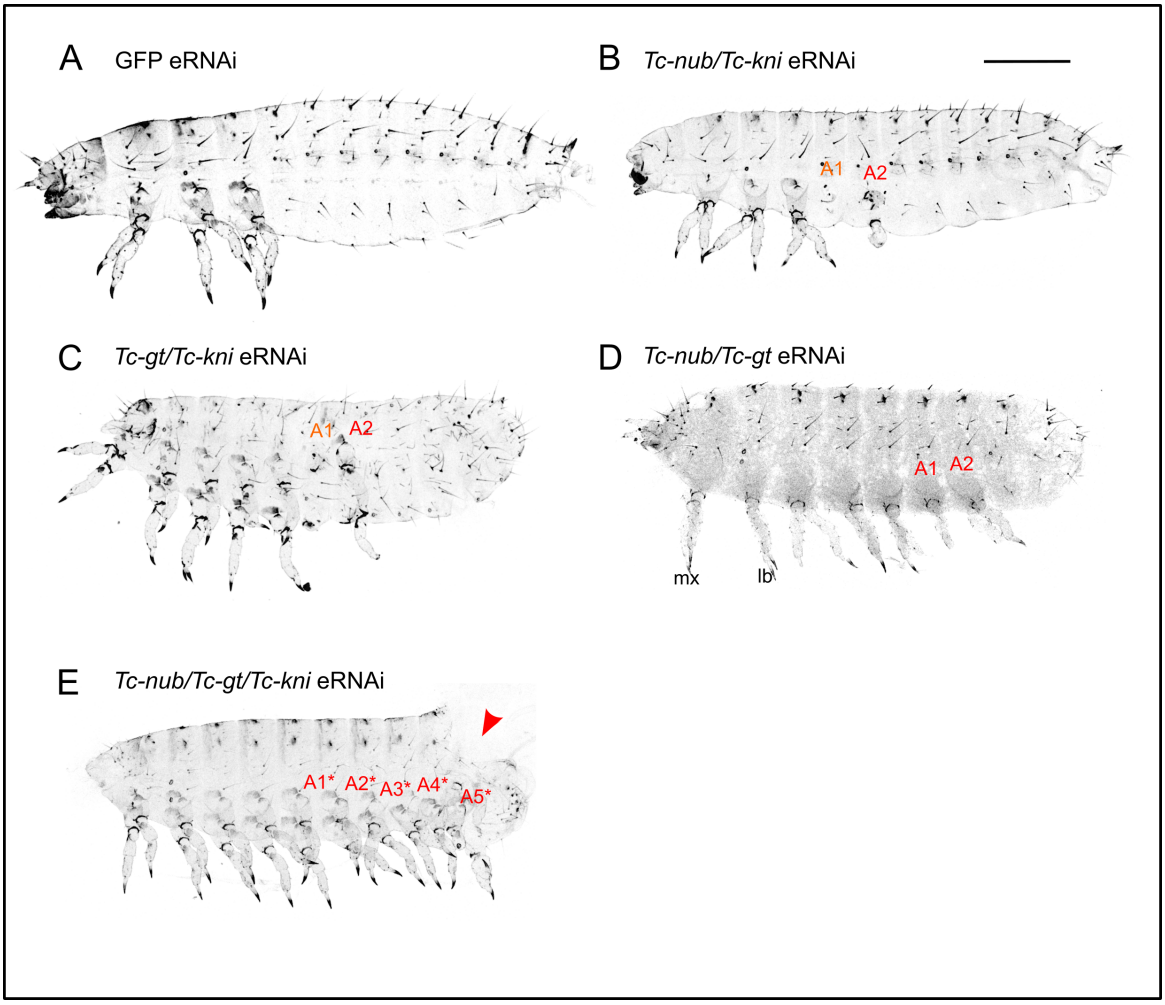

Figure 5.3. Cuticles from eggs injected with 2 µg/µL *GFP* dsRNA, or with mixtures 1 µg/µL of *Tc-nub*, *Tc-kni* and/or *Tc-gt* dsRNA. Abdominal segments displaying ectopic 'nubs' or partial/complete legs are labelled in orange or red, respectively. Triple knockdown segment annotations, marked with an asterisk, represent my best guess of wild type segment identity, assuming that the first leg-bearing segment represents the maxillary segment. The arrowhead in E indicates damage to the cuticle. Scale bar is 200 µM.

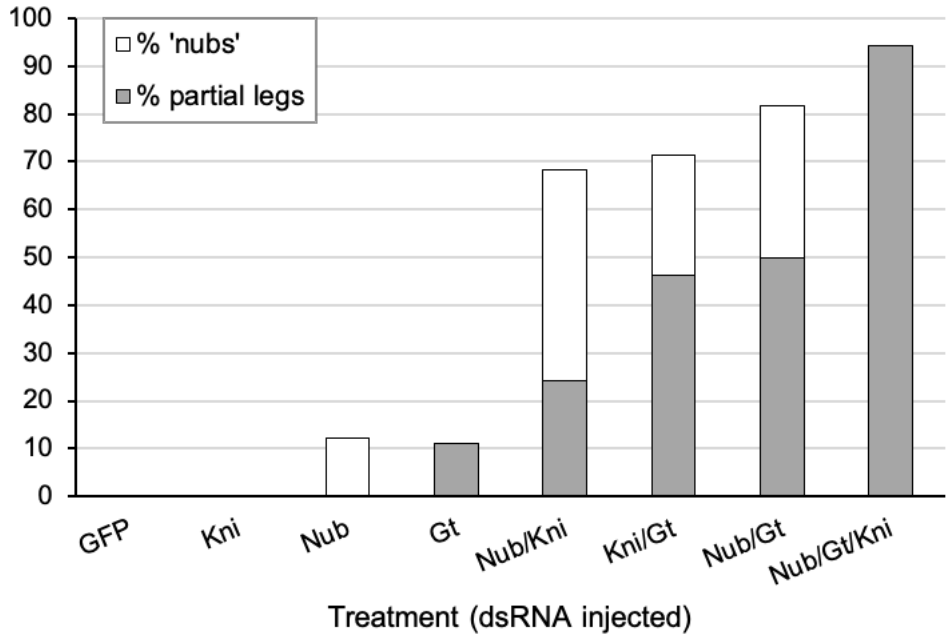

Figure 5.4. The percentage of cuticles displaying transformations of abdominal segments is increased in double or triple knockdowns of *Tc-nub*, *Tc-gt* and/or *Tc-kni* compared to single knockdowns of any one of these genes. Cuticles with abdominal transformations are split into those that display only 'nubs' (white) – weaker abdominal transformations - or at least one partial or complete leg (gray) – stronger abdominal transformations.

Table 5.3. Cuticle phenotypes of embryos injected with *GFP* dsRNA compared to single, double and triple knockdowns of *Tc-nub*, *Tc-gt*, and *Tc-kni* (single knockdowns were carried out using 2 μg/μL of dsRNA, while all doubles and triple knockdowns used the component dsRNAs mixed to a final concentration of 1 μg/μL each). N = number of eggs injected; 'No. (%) cuticles' refers to the number (%) of injected embryos going on to form cuticles; 'abdominal transformations' refers to cuticles in which abdominal segments have been transformed towards a thoracic fate; 'nubs' and 'legs' refer to 'nubs' or partial/complete legs, respectively, formed on abdominal segments; 'Av(max) # extra leg pairs' refers to the average (or maximum) number of pairs of legs presumed to have formed through homeotic transformation of an abdominal segment.

Treatment (dsRNA injected)		N	No. (%) cuticles	% abdominal transformations			Av(max) # extra leg pairs
				% 'nubs'	% legs	Total %	
Singles	*GFP*	266	171 (63.9)	0	0	0	0
	Tc-nub	148	91 (61.5)	12.1	0	**12.1**	0
	Tc-kni	45	28 (62.2)	0	0	0	0
	Tc-gt	50	36 (72)	0	11	**11**	**1 (1)**
Doubles	*Tc-nub* + *Tc-kni*	93	41 (44.0)	43.3	24.3	**67.6**	**1 (1)**
	Tc-gt + *Tc-kni*	49	28 (57.1)	25	46.4	**71.4**	**1 (1)**
	Tc-nub + *Tc-gt*	95	38 (45.9)	31.6	50	**81.6**	**1.3 (2)**
Triple	*Tc-nub* + *Tc-gt* + *Tc-kni*	136	35 **(25.7)**	0	0	**94.3**	**4.0 (7)**

Interestingly, knocking down *Tc-gt* in addition to *Tc-kni* and/or *Tc-nub* does not appear to impact the penetrance or severity of embryonic truncations. *Tc-gt* knockdowns result in truncations of the posterior abdomen with a very high penetrance, usually affecting 4 segments (Table 5.4). *Tc-nub/Tc-gt* and *Tc-nub/Tc-gt/Tc-kni* knockdowns both generate a similar frequency and severity of truncations (Table 5.4). In contrast, *Tc-nub/Tc-kni* knockdown results in a very low number and severity of truncations, similar to what is observed in GFP controls (Table 5.4). These data suggest that the truncations observed in *Tc-nub/Tc-gt* or *Tc-nub/Tc-gt/Tc-kni* knockdowns result primarily from loss of *Tc-gt,* and that neither *Tc-nub* nor *Tc-kni* play any substantial role in maintaining the segmentation clock.

Table 5.4. Cuticle phenotypes of embryos injected with *GFP* dsRNA compared to single, double and triple knockdowns of *Tc-nub*, *Tc-gt*, and *Tc-kni* (single knockdowns were carried out using 2 µg/µL of dsRNA, while all doubles and triple knockdowns used the component dsRNAs mixed to a final concentration of 1 µg/µL each). N (cuticles) = number of cuticles; % truncated = % of cuticles that have lost one or more segment.

Treatment (dsRNA injected)		N (cuticles)	% truncated	No. segments deleted (Max (mode))
Singles	*GFP*	42	0.2%	1 (0)
	Tc-gt	35	**94%**	**7 (4)**
Doubles	*Tc-nub* + *Tc-kni*	43	0.7%	1 (0)
	Tc-nub + *Tc-gt*	22	**95%**	**7 (3)**
Triple	*Tc-nub* + *Tc-gt* + *Tc-kni*	19	**95%**	**7 (3)**

Tc-nub, *Tc-gt* and *Tc-kni* do not have redundant functions in the head

Several of the head and gnathal appendages are deleted or transformed in *Tc-gt* and *Tc-kni* knockdowns ((Bucher and Klingler, 2004; Cerny et al., 2008; Peel et al., 2013). In the former, the maxillary and labial appendages are transformed into thoracic legs, while the anterior head appendages (the mandibles, antennae and labrum) are left intact (Bucher and Klingler, 2004). In contrast, in *Tc-kni* knockdowns, the antennae and often mandibles are lost, due to issues with segment boundary patterning (Cerny et al., 2008; Peel et al., 2013). Although *Tc-nub* is expressed in the head, it does not display any overt head phenotypes. I wondered whether, as in the abdomen, these three genes may have partially or fully overlapping roles which might be revealed by double or triple knockdown. However, knocking *Tc-nub* down in tandem with *Tc-kni* or *Tc-gt* does not worsen their effects on head and gnathal segment formation (Figure 5.5B and C). Likewise, knocking down *Tc-gt* and *Tc-kni* together (with or without *Tc-nub*) results in a phenotype equivalent to the sum of their effects - loss of the antennae and mandibles, and transformation of the maxillary and labial segments into thoracic legs, leaving the labrum unaffected (Figure 5.5D). We can conclude that *Tc-nub* is not acting redundantly with these other gap genes in the head, at least with respect to visible aspects of cuticle morphology.

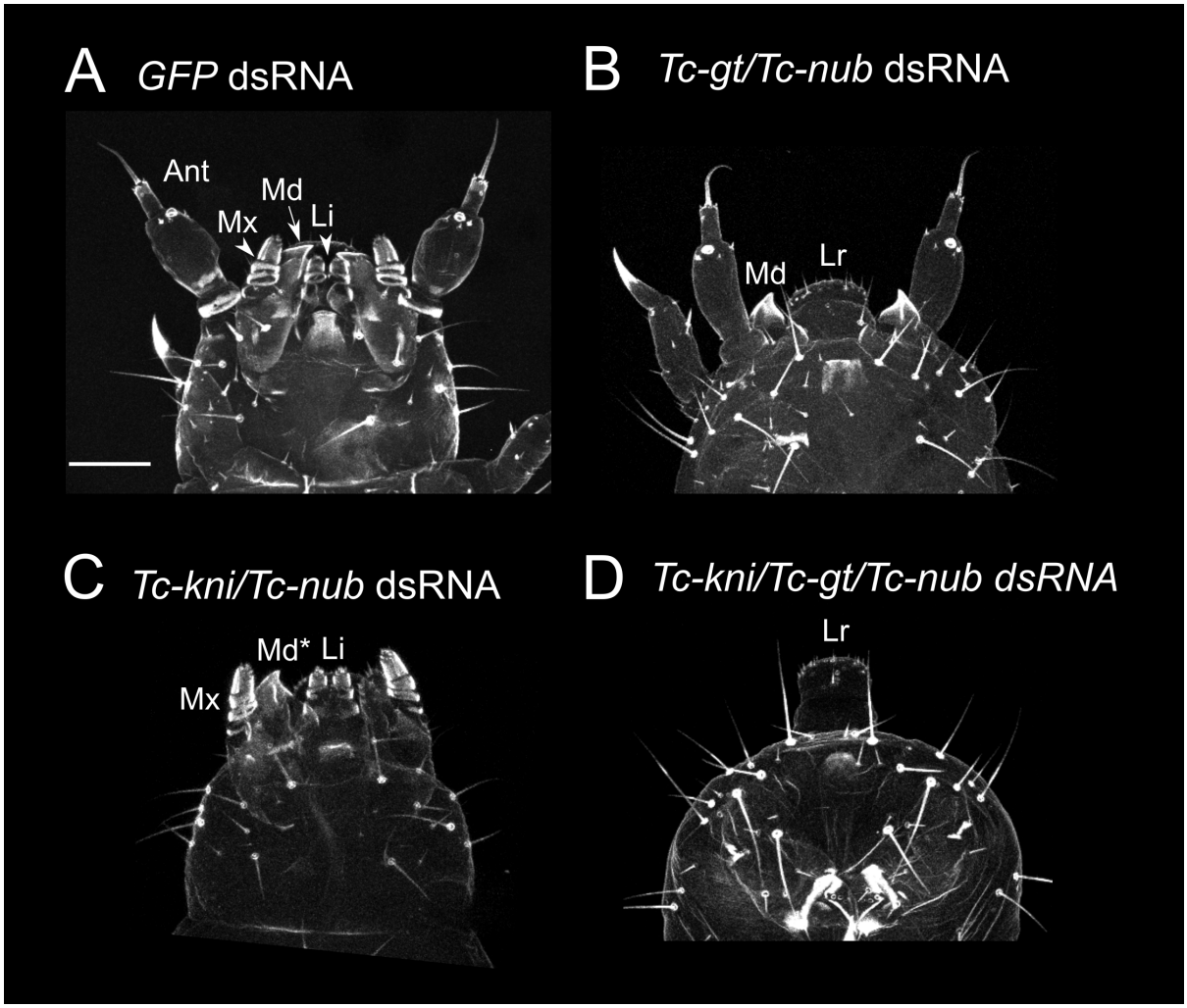

Figure 5.5. Close ups on the heads of cuticles from eggs injected with 2 µg/µL *GFP* dsRNA, or with mixtures of 1 µg/µL *Tc-nub*, *Tc-kni* and/or *Tc-gt* dsRNA. An = antenna; Md = mandible; Mx = maxilla; Li = labium; Lr = labrum. In C, Md* indicates the single remaining mandible (the second mandible is lost in this knockdown). Scale bar is 50 µM.

5.2.3. Double or triple knockdowns of *Tc-nub*, *Tc-gt* and/or *Tc-kni* misexpress abdominal and thoracic Hox genes

The homeotic transformation of abdominal segments into thoracic segments that results from double and triple knockdowns of *Tc-nub*, *Tc-gt* and *Tc-kni* suggest that these genes may regulate Hox gene expression. To determine whether Hox genes are misexpressed in double and triple eRNAi embryos, I performed HCR ISH against the thoracic Hox gene *Tc-Antp* and the abdominal Hox genes *Tc-abdA* and *Tc-Ubx* in 16-17 hour old embryos (mid segment-addition).

I used *Tc-Wg* as a marker to track the progress of segmentation in each embryo (Figure 5.5B, 5.6B, 5.7B). Uninjected embryos have anywhere between 8 and 13 *Tc-Wg* stripes when they are 16-18 hours old, with the average being 10 and the mode being 11 (Chapter 1). Embryos injected with *GFP* dsRNA are slightly developmentally delayed, showing an average and mode of 7 *Tc-Wg* stripes at 16-17 hours. Embryos injected with any combination of *Tc-nub*, *Tc-kni* and *Tc-gt* dsRNA have even fewer stripes at 16-17 hours, with averages of 4-6 (data not shown). This could represent developmental delays, segment deletion, or posterior truncation. *Tc-kni* knockdown is known to result in loss of the antennal and deterioration of the mandibular segment polarity stripes (Peel et al., 2013), and this is often observed in *Tc-gt/Tc-kni* knockdowns (Figure 5.5B). *Tc-gt* knockdown has also been shown to result in disruption of pair-rule patterning across the thorax and abdomen (Bucher and Klingler, 2004), and I observed similar defects in many knockdowns involving *Tc-gt* dsRNA (Figure 5.5B). In order to compare embryos at similar stages of segment development, I chose those with milder segmentation phenotypes (*i.e.* with 5-7 *Tc-Wg* stripes) for display in Figure 5.5 (with the exception of one example of a severe triple knockdown).

I found that expression of the abdominal Hox gene *Tc-abdA* is repressed or lost during anterior abdominal patterning in all double or triple knockdowns (Figure 5.5). In double knockdowns, *Tc-abdA* is still expressed in the SAZ, but with reduced intensity, in particular in the anterior of its usual domain (Figure 5.5). This likely corresponds to reduced expression in the tissue that will give rise to PS6 and perhaps PS7. Note that expression of *Tc-abdA* in the germ cells, which at this stage are migrating over the ventral surface of the SAZ, is unaffected (data not shown). Finally, triple knockdowns display total loss of *Tc-abdA* expression in the SAZ (Figure 5.5).

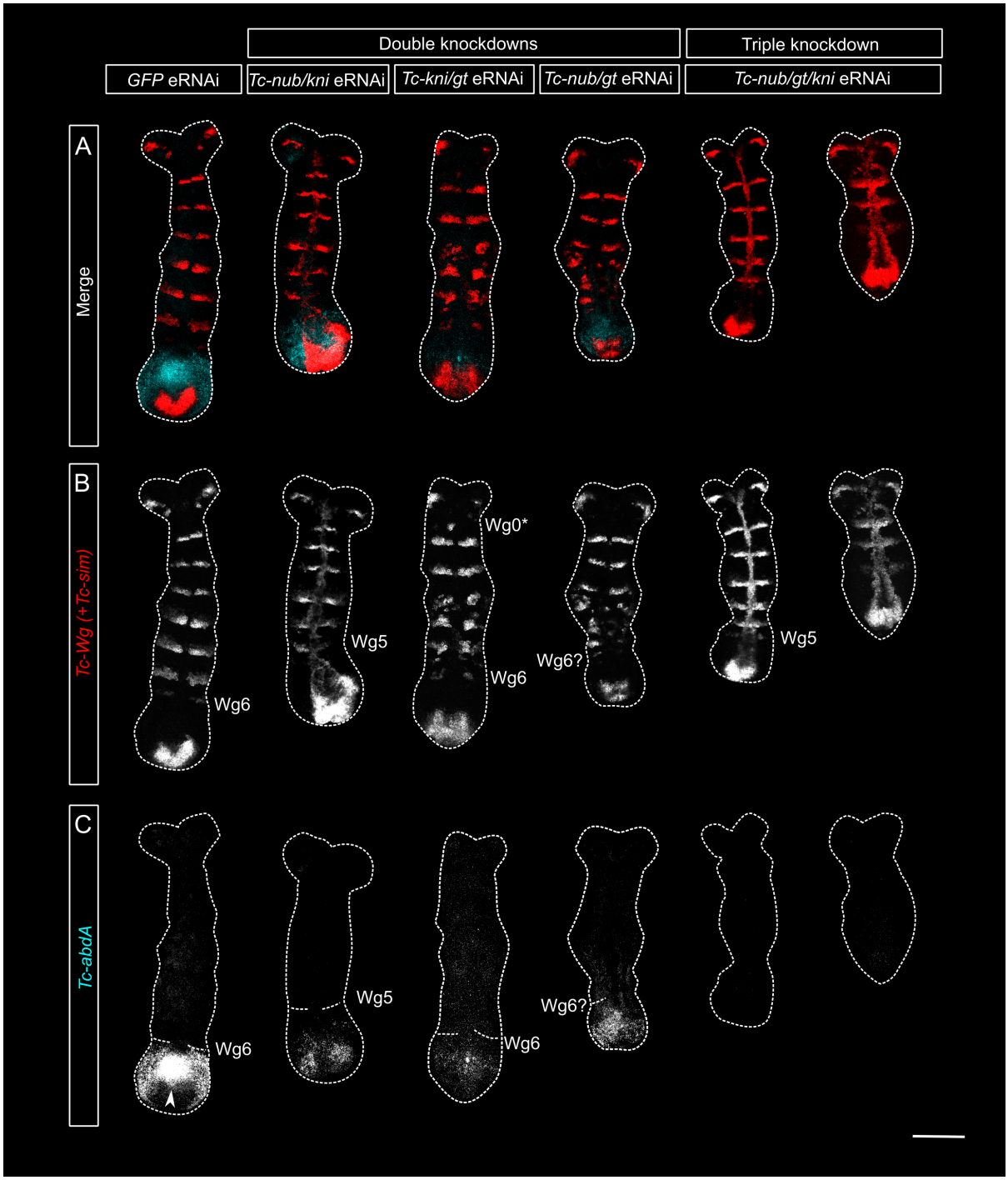

Figure 5.5. Expression of *Tc-Wg* (and sometimes *Tc-sim*) (B) and *Tc-abdA* (C) in representative embryos injected with 2 µg/µL *GFP* dsRNA or with mixtures of 1 µg/µL *Tc-nub*, *Tc-kni* and/or *Tc-gt* dsRNA. Specific *Tc-Wg* stripes are annotated. Note the deteriorated Wg1 stripe in *Tc-kni/Tc-gt eRNAi* embryos. The white arrow in C indicates the germ cells, which express *Tc-abdA* and were unable to be removed from the optical section. Germ cells are frequently lost during the dissection process after eRNAi. Scale bar is 100 µM.

Previous research indicates that knockdown of *Tc-abdA* alone results in the formation of small cuticular protrusions ('nubs'), rather than fully formed thoracic legs; to achieve the latter phenotype, loss of both *Tc-abdA* and *Tc-Ubx* is required (Lewis et al., 2000). This suggests that *Tc-Ubx* expression is likely also affected in many of my knockdowns.

All knockdowns showed reduced intensity of *Tc-Ubx* expression in the majority of embryos examined, with triple knockdowns showing the greatest reduction in intensity (Figure 5.6). The spatial distribution of *Tc-Ubx* transcript in *Tc-nub/Tc-kni* double knockdowns was normal; however, in any knockdown including *Tc-gt* dsRNA, the anterior border of *Tc-Ubx* was shifted anteriorly to encompass at least PS3 and PS4 (Figure 5.6). This is likely related to the anterior expansion of *Tc-Kr* in *Tc-gt* knockdowns , and the subsequent transformation of gnathal to thoracic segments (Bucher and Klingler, 2004).

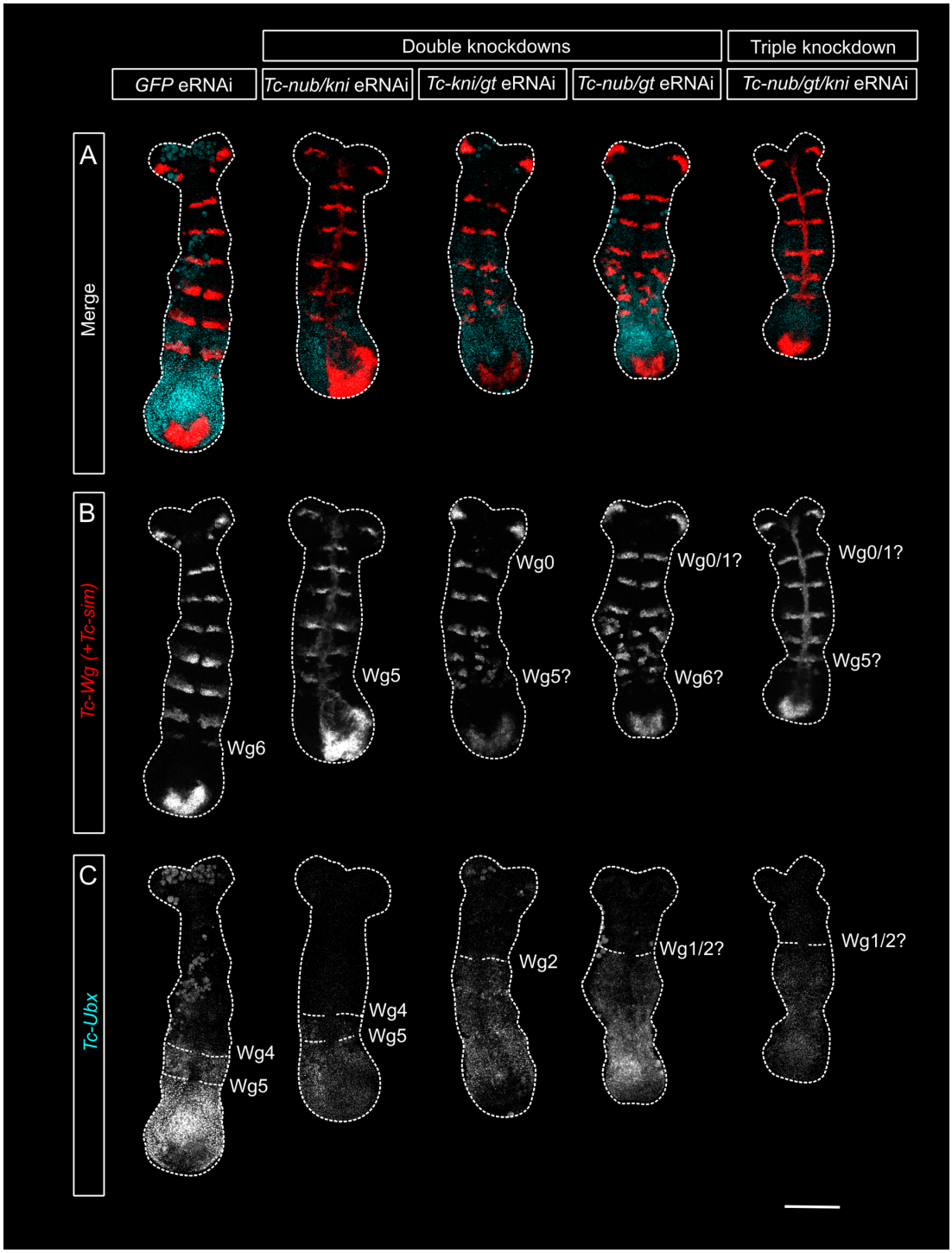

Figure 5.6. Expression of *Tc-Wg* (and sometimes *Tc-sim*) (B) and *Tc-Ubx* (C) in representative embryos injected with 2 µg/µL *GFP* dsRNA or with mixtures of 1 µg/µL *Tc-nub*, *Tc-kni* and/or *Tc-gt* dsRNA. Specific *Tc-Wg* stripes are annotated. Scale bar is 100 µM.

Lastly, I examined the expression of the thoracic Hox gene *Tc-Antp*. Many Hox genes display a regulatory feature known as posterior prevalence, whereby more posterior Hox genes repress those normally expressed in the anterior of the embryo (reviewed in Duboule and Morata, 1994; Morata, 1993). We might then expect that loss or repression of *Tc-abdA* and *Tc-Ubx* in the abdomen would allow *Tc-Antp* to expand posteriorly, subsequently promoting the development of segments towards a thoracic fate. At stage W6, Tc-*Antp* is usually expressed most strongly in PS3-6, with weaker expression in the anterior SAZ (Figure 5.7). Double *Tc-nub/Tc-kni* knockdown embryos exhibit a similar pattern of expression, but in triple knockdowns, *Tc-Antp* expression is expanded anteriorly (to encompass PS0-PS2) and expanded posteriorly and intensified in the SAZ (Figure 5.7). Anterior expansion of *Tc-Antp* following *Tc-gt* knockdown has been reported by Cerny et al. (2005), and presumably underlies the transformation of gnathal segments into thoracic legs observed in these knockdown treatments. The posterior expansion of *Tc-Antp* in triple knockdown embryos likely contributes to the high frequency of 'complete' thoracic legs formed in the abdomen, compared to double knockdowns where 'nubs' or partial legs are more common.

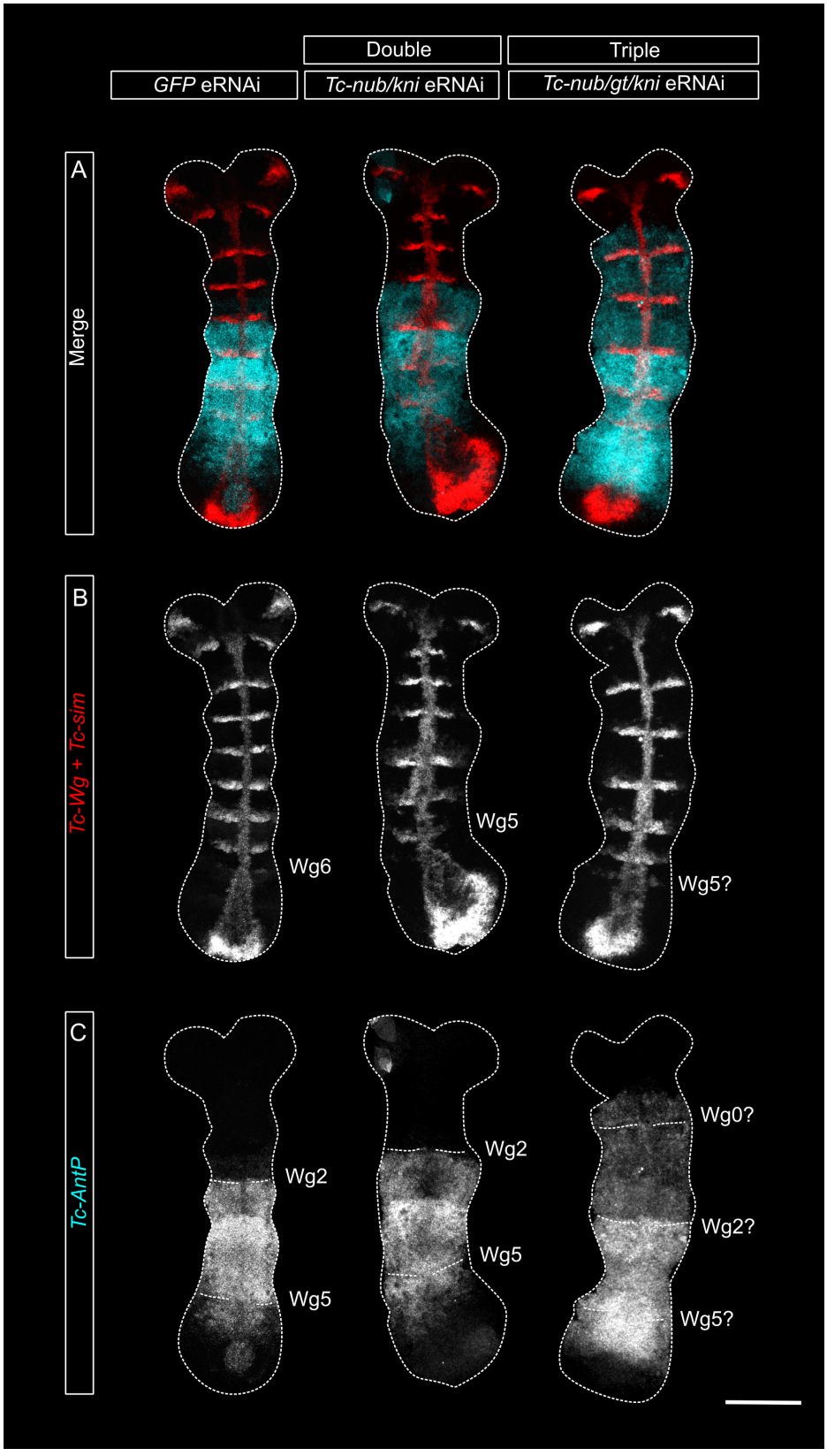

Figure 5.7. Expression of *Tc-Wg* and *Tc-sim* (B) and *Tc-Antp* (C) in representative embryos injected with 2 µg/µL *GFP* dsRNA or with mixtures of 1 µg/µL *Tc-nub* and *Tc-kni* (double kmockdowns) or 1 µg/µL of *Tc-nub*, *Tc-kni* and *Tc-gt* dsRNA (triple knockdowns). Specific *Tc-Wg* stripes are annotated. Scale bar is 100 µM.

5.2.4. *Tc-Kr* expression is expanded into the abdomen in double and triple knockdowns

I next aimed to better determine the cause of Hox gene misexpression by examining the expression of other gap genes. The anterior borders of *Dm-Ubx* and *Dm-abdA* in *Drosophila* are set primarily via direct repression by Dm-Hb and Dm-Kr, respectively (Casares and Sánchez-Herrero, 1995; White and Lehmann, 1986). I examined the expression of both genes in embryos following double or triple knockdowns.

I did not observe any expansion of *Tc-Hb* expression in triple knockdown embryos, despite the reduced intensity of *Tc-Ubx* staining – indeed, in several instances, anterior *Tc-hb* expression was itself reduced in intensity (data not shown). However, *Tc-Kr* expression is very obviously expanded posteriorly in both double and triple knockdowns, with a more pronounced expansion in the latter (Figure 5.8C). In control embryos at stage W5, *Tc-Kr* is usually expressed strongly in PS1-5, and more weakly in PS6 (Figure 5.8C, *GFP* dsRNA-injected embryos). In *Tc-nub/Tc-gt* and *Tc-gt/Tc-kni* double knockdowns at the same stage, by contrast, *Tc-Kr* expression is extended posteriorly, beyond the posterior border of PS6 and into the SAZ (Figure 5.8C). This aligns well with the repression of *Tc-abdA* that is observed in the anterior SAZ at this stage (Figure 5.5C). I was unable to perform an HCR ISH against *Tc-Kr* in *Tc-nub/Tc-kni* double knockdowns due to time constraints, but I assume that they exhibit a posterior expansion of *Tc-Kr* expression similar to the other two double knockdowns. In triple knockdowns, *Tc-Kr* expression is expanded all the way to the back of the SAZ (Figure 5.8C), which aligns with the total loss of *Tc-abdA* expression observed in the SAZ at similar stages (Figure 5.5C).

Tc-Kr expression in the head indicates that both *Tc-nub/Tc-gt* and *Tc-gt/Tc-kni* knockdown embryos may be more advanced in head development than the GFP controls (Figure 5.8C), despite their similar progress through segmentation (Figure 5.8B). Both of the former exhibit paired head domains of *Tc-Kr* which usually do not emerge until at least stage W7 (Chapter 3). *Tc-Kr* expression is also expanded anteriorly into at least PS0 in these double knockdowns. This does not usually occur at all in wild type embryos (Chapter 3). I propose that this is likely due to the actions of *Tc-gt* alone; if *Tc-gt* has a more prominent role in repressing *Tc-Kr* anteriorly, then the expansion of the latter in *Tc-gt* knockdowns would explain the transformation of gnathal to thoracic segments. I am not certain why anterior expansion of *Tc-Kr* is not observed in triple mutants. Examination of additional gap and Hox genes, and a detailed description of segment patterning, in triple knockdowns may be required to understand the fate of the head segments.

Figure 5.8. Expression of *Tc-Wg* (B) and *Tc-Kr* (C) in representative embryos injected with 2 µg/µL *GFP* dsRNA or with mixtures of 1 µg/µL *Tc-nub*, *Tc-kni* and/or *Tc-gt* dsRNA. Specific *Tc-Wg* stripes are annotated. Note the deteriorated W0 stripe in *Tc-kni/Tc-gt eRNAi* embryos. Scale bar is 100 µM.

5.2.5. Tc-Svb is not required for *Tc-nub* expression

Tc-mlpt and *Tc-svb* knockdowns also result in transformations of anterior abdominal segments to a thoracic fate (Ray et al., 2019; Savard et al., 2006), similar in severity to any of the three double knockdowns tested here, but less severe than those observed in triple knockdowns. I wondered whether this might indicate that *Tc-mlpt/Tc-svb* (i.e. Tc-Svb in its activator form) might be required for the expression of at least two of *Tc-nub*, *Tc-gt* and *Tc-kni*. *Tc-mlpt* is certainly required for expression of *Tc-gt* (Savard et al., 2006), and my multiplexed expression analysis suggests that all three genes are first expressed shortly after *Tc-mlpt* and *Tc-svb* are co-expressed in the posterior SAZ (Chapters 3 and 4). To investigate this hypothesis, I examined the effects of *Tc-svb* knockdown on gene expression in the embryo (in hindsight, *Tc-mlpt* is the more obvious choice, as knocking it down should remove only the 'activating' function of Tc-Svb – knocking *Tc-svb* down will remove its activity as an activator or a repressor. However, I was keen to confirm that the phenotype in *Tc-svb* knockdowns had the same etiology as in *Tc-mlpt* knockdowns, and this seemed a good chance to do that).

I first confirmed that *Tc-Kr* is posteriorly expanded in *Tc-svb* knockdown embryos (Figure 5.9), as it is after *Tc-mlpt* knockdown (Savard et al., 2006). Knockdown efficacy was assayed by examining *Tc-svb* expression in HCR ISHs and also by comparing cuticle preparations to those described in previous publications. At stage W7, *Tc-Kr* is expressed strongly as far back as PS5 and weakly in PS6 (Figure 5.9A). By contrast, *Tc-svb* knockdowns with the same number of *Tc-Wg* stripes show *Tc-Kr* expression spanning back into the SAZ, beyond PS7 (Figure 5.9A). This means that *Tc-Kr* is ectopically expressed throughout the entirety of PS6 and PS7 (T3p-A2a), and to some extent in PS8. As in double *Tc-nub/Tc-kni*, *Tc-nub/Tc-gt* or *Tc-kni/Tc-gt* knockdowns, this expansion is associated with repression of *Tc-abdA* expression in these parasegments (Figure 5.9B).

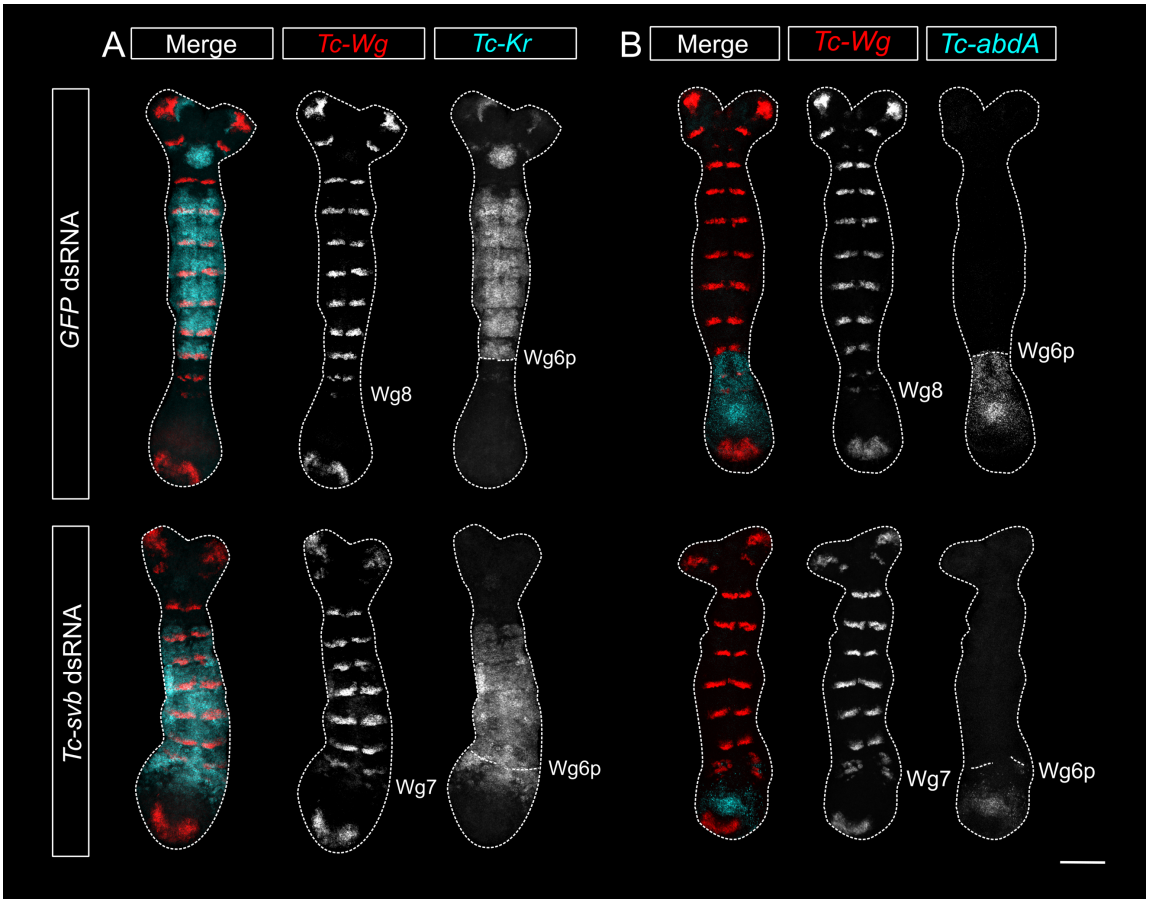

Figure 5.9. Expression of *Tc-Wg* and *Tc-Kr* (A) or *Tc-abdA* (B) in representative embryos injected with 2 µg/µL *GFP* OR *Tc-svb* dsRNA. Scale bar is 100 µM.

Next, I confirmed that posterior *Tc-gt* expression was disrupted after *Tc-svb* knockdown. In *Tc-mlpt* knockdowns, the abdominal domain of *Tc-gt* is lost entirely (Savard et al., 2006). If this is due to a loss of activated *Tc-svb*, we might expect *Tc-svb* knockdowns to give a similar phenotype. Indeed, *Tc-gt* expression is almost entirely lost in *Tc-svb* knockdowns (Figure 5.10A). However, *Tc-nub* expression is not abolished, instead remaining expressed in the SAZ while being repressed in the segmented germband (Figure 5.10B). These results suggest either that Tc-Svb is not strictly required for expression of *Tc-nub*. It would be useful to examine *Tc-nub* expression in *Tc-mlpt* knockdowns to confirm whether Tc-Svb is able to regulate *Tc-nub* in its repressor form.

If *Tc-svb* does not interact with *Tc-nub* in the SAZ, then *Tc-kni* becomes an attractive alternative target to explain the homeotic transformations observed in the anterior abdomen following *Tc-svb* or *Tc-mlpt* knockdown. Unfortunately, I did not have time to examine *Tc-kni* expression in *Tc-svb* knockdowns. This is a promising avenue for anyone aiming to gain a deeper understanding of the roles of *Tc-mlpt* and *Tc-svb* in segment patterning.

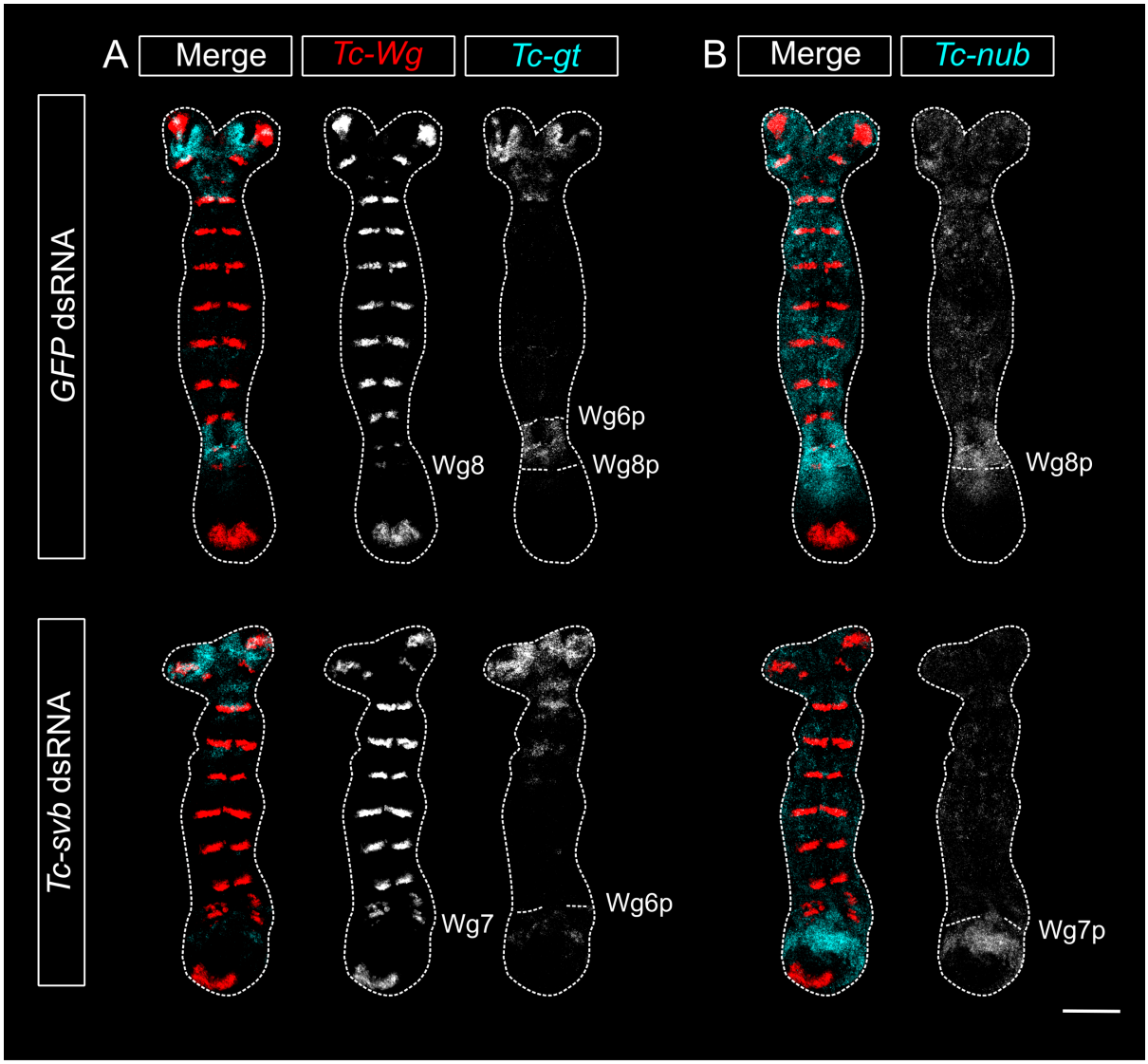

Figure 5.10. Expression of *Tc-Wg*, *Tc-gt* (A) and *Tc-nub* (B) in representative embryos injected with 2 µg/µL *GFP* OR *Tc-svb* dsRNA. Scale bar is 100 µM.

In order to better understand the regulation of *Tc-nub*, I additionally examined its expression in *Tc-hb* knockdowns. Research in the context of the neuroblast timer series (Kambadur et al., 1998) and the gap gene network (Cockerill et al., 1993) indicates that *Dm-hb* is able to repress *Dm-nub*. In contrast to this, I found that knocking down *Tc-hb* results in loss of *Tc-nub* expression entirely (data not shown). However, *Tc-hb* knockdown also results in loss of *Tc-Kr* expression (Cerny et al., 2005) and subsequently *Tc-mlpt* expression (Savard et al., 2006). Given that Tc-Svb is not apparently required for *Tc-nub* expression, I would propose that it is likely that *Tc-Kr* is required for *Tc-nub* activation, as it appears to be in neuroblasts (Isshiki et al., 2001).

5.2.6. Double knockdowns of *Tc-nub* and *Tc-cas* show no abdominal phenotype but show leg patterning defects

In addition to double and triple knockdowns of *Tc-nub* with *Tc-gt* and/or *Tc-kni*, I also carried out knockdowns of *Tc-nub* and *Tc-cas* to determine whether they might play a redundant role in the posterior abdomen. Double *Tc-nub/Tc-cas* knockdowns do not appear to display any posterior abdominal phenotypes, but 52% of cuticles examined exhibit defects in leg formation. Specifically, the pretarsus, or claw, is almost entirely abolished (Figure 5.11). I examined the expression of *Tc-nub* and *Tc-cas* in 1-3 day old wild-type *Tribolium* embryos to determine how they might influence leg development in this way. As in most sampled insects, *Tc-nub* is expressed in rings around each thoracic appendage, likely corresponding to the future leg joints (Li and Popadić, 2004; Turchyn et al., 2011) (Figure 5.12). Consistent with a role in pretarsus formation, *Tc-cas* is expressed at the terminus of each developing thoracic appendage (Figure 5.12). Given that *Tc-nub* is not even expressed in the pretarsus itself, it is not clear why these two genes would have redundant functions in pretarsus development.

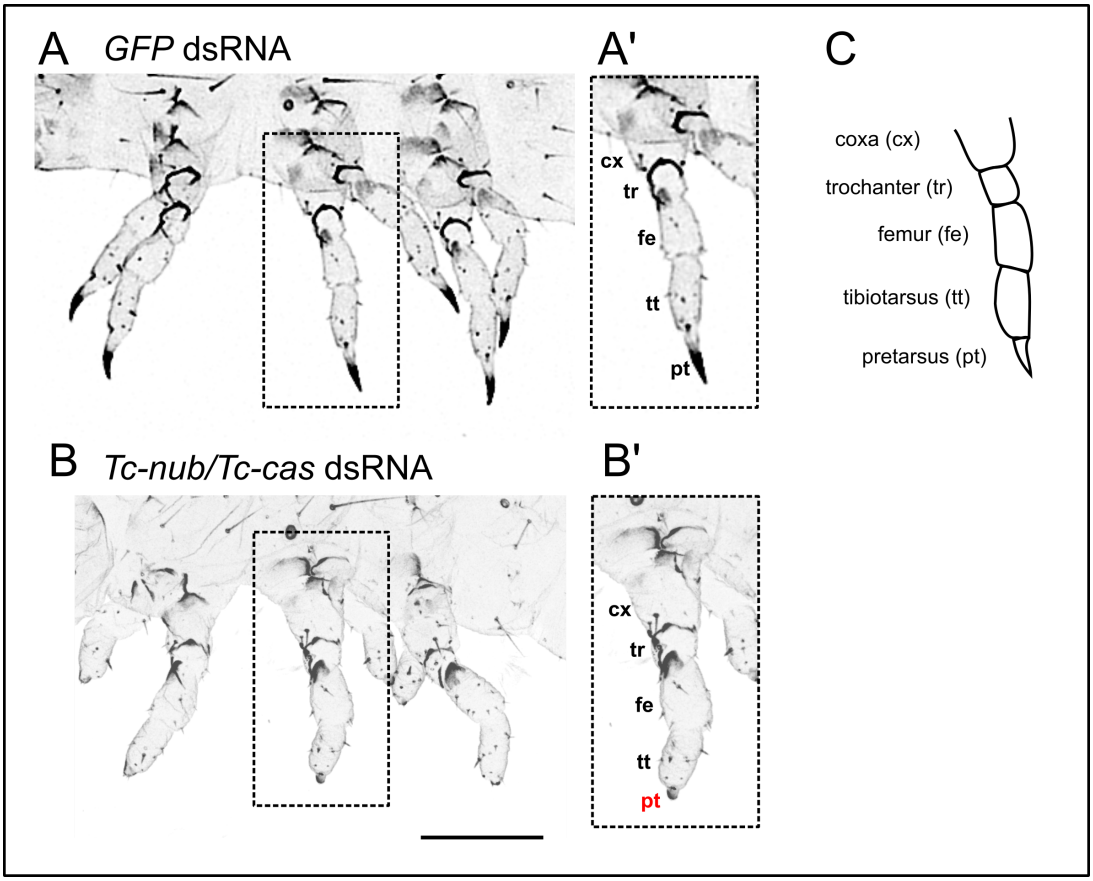

Figure 5.11. Close ups on the thoracic legs of cuticles from eggs injected with 2 µg/µL *GFP* dsRNA (A-A'), or with a mixture of 1 µg/µL *Tc-nub* and *Tc-cas* dsRNA (B-B'). Panel C illustrates the components of a normal larval leg. Note that the pretarsus (pt) is significantly reduced after *Tc-nub/Tc-cas* dsRNA (B'). Scale bar is 100 µM.

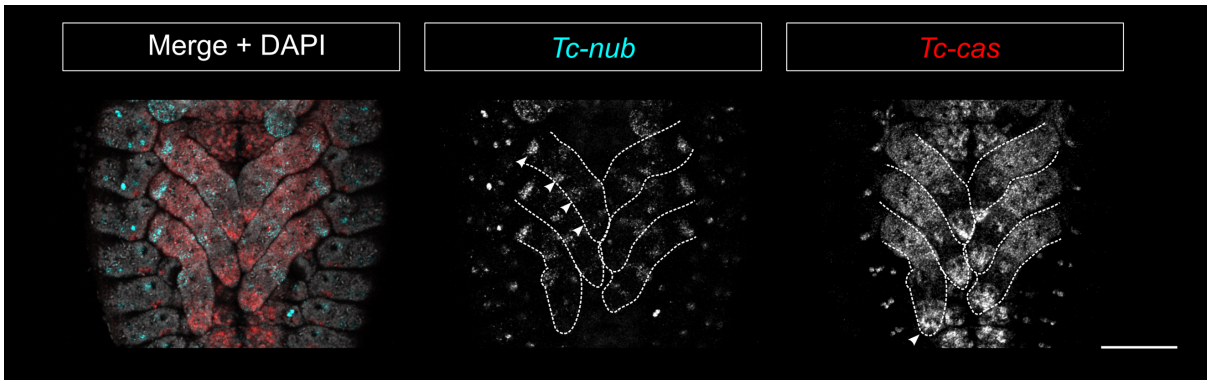

Figure 5.12. *Tc-nub* and *Tc-cas* expression in the thoracic legs of a *Tribolium* embryo (post-segmentation). *Tc-nub* is expressed in rings, marked by arrowheads (likely corresponding to the future joints) and *Tc-cas* is expressed in a broad domain at the base of the leg, and at the leg tip (marked by an arrowhead). Scale bar is 100 µM.

5.3. DISCUSSION

In this chapter, I have shown that at least three genes – *Tc-nub*, *Tc-gt* and *Tc-kni* – play semi-redundant roles in repressing *Tc-Kr* expression in the SAZ of *Tribolium* during abdominal segment patterning. In their absence, *Tc-Kr* becomes expressed in the abdominal segment primordia, and these segments are transformed into thoracic segments due to misexpression of the Hox genes *Tc-Antp*, *Tc-Ubx* and *Tc-abdA*. This has several interesting implications for the structure and evolution of the gap gene network, and also for the regulation of Hox genes by this network, as discussed in the following sections.

5.3.1. *Tc-kni* and *Tc-nub* act as trunk gap genes in *Tribolium*

Although its homologue, *Dm-kni*, plays a significant role in the gap gene network of *Drosophila* (reviewed in Jaeger, 2011), *Tc-kni* is not considered to act as a trunk gap gene in *Tribolium* (Cerny et al., 2008), leading to its exclusion from recent analyses of the gap gene network (for example, Zhu et al., 2017). *Dm-nub* is considered to act at a level below the canonical trunk gap genes, as although it is regulated by other gap genes, it does not apparently regulate any itself (Cockerill et al., 1993). Similarly, in *Tribolium*, knockdowns of *Tc-nub* alone do not result in misexpression of other gap genes (Chapter 4). However, my work in this chapter indicates that both *Tc-kni* and *Tc-nub* are able to regulate the gap gene *Tc-Kr*, and through this regulation play an essential role in establishing Hox gene domains in the abdomen. I would therefore propose that both genes should be considered components of the trunk gap gene network in *Tribolium*.

It is possible that redundancy may have led to the roles of these genes being overlooked in the gap networks of other insect species. For example, the fact that *Dm-nub* mutants have normal *Dm-Kr* expression may result from redundant repression by Dm-Gt and/or Dm-Kni, as I have observed in *Tribolium*. Indeed, similar redundancy between Dm-Gt and Dm-Kni nearly excluded the former from consideration as a gap gene during the early investigations of this network (Kraut and Levine, 1991). Two experiments would be particularly useful to further investigate the role of *Dm-nub* in axial patterning: firstly, driving ectopic expression of *Dm-nub* with a heat shock line, and seeing whether this is sufficient to repress *Dm-Kr* expression; and secondly, knocking down the expression of *Dm-gt* and/or *Dm-kni* in *Dm-nub* mutants, to see if these genes act redundantly in *Drosophila* too. (I had already synthesised dsRNA for this

latter experiment and begun eRNAi trials, but unfortunately COVID-19 lockdown truncated this experiment).

The degree of redundancy between *nub* and other abdominal genes may also vary between insect species. For example, in *Oncopeltus*, *Oc-nub* knockdown is sufficient to generate transformations of most abdominal segments towards a thoracic fate (Hrycaj et al., 2008). Given my observations from *Tribolium*, I would hypothesise that this phenotype results from overexpression of *Oc-Kr*, suggesting that *Oc-nub* plays a more central role in *Kr* repression than *Tc-nub* does. Indeed, knocking down *Oc-gt* or *Oc-kni* has no impact on segment identity in the anterior abdomen (Ben-David and Chipman, 2010; Liu and Patel, 2010). The differences between *Oncopeltus* and *Tribolium* highlight the importance of examining a variety of short germ species if we are to understand the evolution of the gap gene network in insects.

5.3.2. Similarities between the axial patterning network and the neuroblast timer series

The finding that *Tc-nub* acts as a trunk gap gene lends further support to the idea that the same basic gene network (*Hb*, *Kr*, *nub* and *cas*) has been deployed both for neuroblast fate determination and axial patterning in insects. Some of the interactions between neuroblast timer genes are also displayed by the trunk gap genes; for example, *Tc-hb* is required for expression of *Tc-Kr*, and *Tc-Kr* represses *Tc-hb* (Marques-Souza et al., 2008). I have not yet obtained a clear picture of *Tc-nub* regulation, but it is plausible from my results that *Tc-nub* is activated by *Tc-Kr*, and it is almost certain that *Tc-nub* is able to repress *Tc-Kr*. It seems that the similarities between the axial patterning network and the neuroblast timer series may go beyond the identity and order of genes expressed, into the interactions between the genes themselves. If this series forms a stand-alone module of the gap gene network, it begs the question of how additional genes such as *Tc-mlpt*, *Tc-svb*, *Tc-gt* and *Tc-kni* have been integrated. Studying when and how these components were assembled into different gap gene network topologies will bring us towards a deeper understanding of the evolution of axial patterning in insects.

I have been unable to uncover any obvious function for the abdominal domain of *Tc-cas*. It is possible that its role in *Tribolium* is limited to neural patterning, in contrast to the first three neuroblast timer genes. It is also possible that it plays a role in segment patterning in other species that has been lost in *Tribolium*. Currently, data on the expression and function of *cas* in insects outside of *Drosophila* are sorely lacking, and I look forward to seeing more studies on the topic.

5.3.3. Redundant repression of *Kr* in the abdomen is a conserved feature of *Drosophila* and *Tribolium* gap gene networks

As described in the introduction, repression of *Dm-Kr* in the abdomen of *Drosophila* relies on the activity of both Dm-Gt and Dm-Kni (Figure 5.13A). I have shown that redundant repression of *Tc-Kr* is also an important feature of abdominal patterning in *Tribolium* (Figure 5.13B). In *Drosophila*, this redundancy is likely to be a consequence of the requirement to set up staggered gap gene domains but also to drive expression domains anteriorly over the course of segmentation (Jaeger, 2011). However, in *Tribolium*, both of these features have been proposed to be driven by a simple network in which each gap gene promotes the expression of the next, and represses the expression of the one before (Zhu et al., 2017) (Figure 5.1). In the presence of a graded activator (*Tc-cad*), these interactions are proposed to be sufficient to drive the sequential expression of gap genes (Zhu et al., 2017). This raises the question of what the role of such redundancy might be in a short germ insect like *Tribolium*.

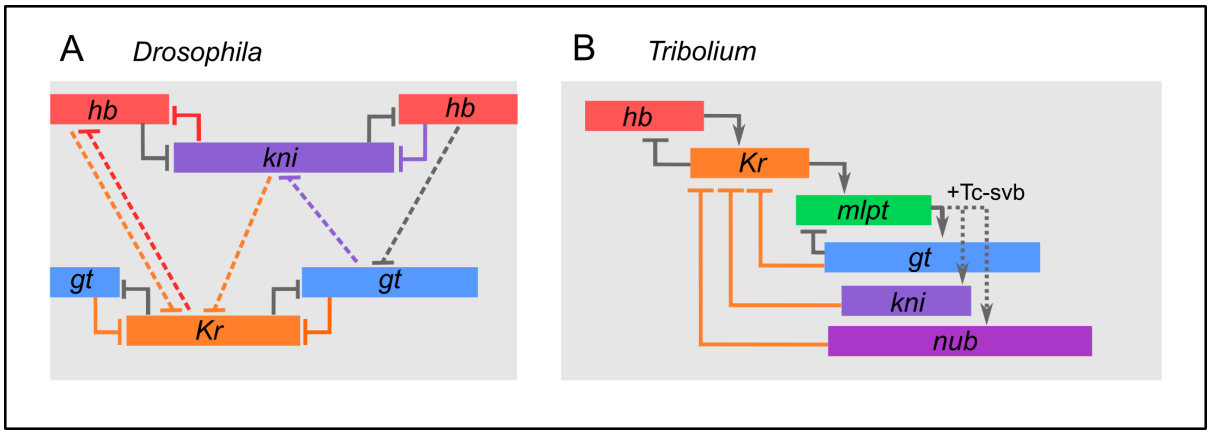

Figure 5.13. The core interactions of the gap gene network in *Drosophila* (A) compared to my updated model of gap gene interactions in *Tribolium* (B). Where functional data has indicated some degree of redundancy in an interaction, those interactions are highlighted in the same colour as the target gene. For example, the posterior border of *Dm-Kr* (orange) is set via repression from both Dm-gt and Dm-kni, so the lines corresponding to these interactions are coloured orange. Note that in both networks, *Kr* is repressed posteriorly by multiple gap proteins.

One benefit that redundancy in gene networks provides is robustness. The containment of *Kr* expression to the centre of insect embryos plays a crucial role in establishing the tagma of the adult. *Kr* is typically expressed in segments that are destined to form part of the thorax

(Cerny et al., 2005; Knipple et al., 1985; Liu and Kaufman, 2004b; Mito et al., 2006). Here, it represses more anterior, gnathal Hox genes (such as *sex combs reduced (scr)* and *deformed (dfd)*) (Cerny et al., 2005; Lavore et al., 2014; Liu and Kaufman, 2004b; Riley et al., 1987) and more posterior, abdominal Hox genes (such as *abdA*) (Casares and Sánchez-Herrero, 1995). It follows from this that misexpression of Kr can have disastrous effects on axial patterning. For example, expansion of *Tc-Kr* into the anterior of the embryo leads to repression of *Tc-scr* and *Tc-dfd* and subsequent transformation of gnathal appendages to legs (this chapter and Cerny et al., 2005), while expansion into the abdomen leads to repression of *Tc-abdA* and transformation of legless segments into leg-bearing segments (this chapter). These drastic transformations will almost certainly be lethal, and so robust mechanisms for regulating *Kr* expression are essential. It makes sense, then, that there may be several genes with a role in repressing *Tc-Kr* expression in overlapping domains in the abdomen. This explanation is, however, at odds with the comparatively un-robust repression of *Tc-Kr* in the anterior of the embryo, where knockdown of *Tc-gt* alone is sufficient to allow expansion of *Tc-Kr* expression and homeotic transformation (Cerny et al., 2005). It is possible that subtle differences in the timing and distribution of expression, or strength of repression, between *Tc-gt*, *Tc-kni* and *Tc-nub* are important for fine-tuning *Tc-Kr* expression at the border between the thorax and abdomen, where multiple segment identities can be found in close contact.

5.3.4. *Tc-nub* and *Tc-kni* have no obvious effect on the segmentation clock

I observe truncations of the embryo only in double or triple knockdown experiments that include knockdown of *Tc-gt.* Furthermore, knocking down *Tc-nub* and/or *Tc-kni* does not appear to increase the severity or penetrance of truncations in *Tc-gt* knockdowns. These results suggest that of the three genes, only *Tc-gt* has any significant role in regulating the activity of the segmentation clock. If this is the case, then a dual role in segment formation and diversification is not necessarily a characteristic feature of individual gap genes in *Tribolium*, as it is in *Drosophila*. Indeed, my results suggest that the role of Tc-Nub in segment patterning may be limited to its redundant repression of *Tc-Kr*, with no obvious direct interaction with Hox genes or the segmentation clock.

Overall, my findings suggest that the gap gene network of *Tribolium* is not as conceptually simple as once thought. Instead, it displays redundancy, and different elements appear to be specialised towards different tasks (simply regulating other gap genes,

maintenance of the segmentation clock and/or Hox regulation). Determining how these functions are distributed over the network will be an important future endeavour.

6. GENERAL DISCUSSION

In this thesis, I have shown that the genes of the neuroblast timer series are expressed in the same temporal order in the SAZ of *Tribolium* as they are in insect neuroblasts. Furthermore, I have demonstrated that the neuroblast timer gene *nub* plays an active role in segment patterning in *Tribolium*. These findings bolster the theory that a modified version of the neuroblast timer network may form a module of the gap gene network. I have additionally proposed in Chapter 3 that *mlpt* and *svb* together form an on/off switch that acts to modulate the expression of other gap genes.

One of the overarching themes of my thesis is therefore a reimagining of the gap gene network as consisting of several interlocking modules, with different evolutionary origins and, potentially, varying purposes. In the following discussion, I will go into some more detail about my hypotheses regarding the functions and evolutionary origins of the neuroblast timer, *mlpt/svb* and *gt/kni* modules, and how this might impact our understanding of gap genes and the gap gene network as a whole.

6.1. The neuroblast timer module and Hox gene regulation

As discussed in the introduction, homeotic transformations have been considered a defining phenotypic trait of gap gene mutants or knockdowns across the insects. In *Drosophila*, all four of the trunk gap genes (*hb*, *Kr*, *kni* and *gt*) regulate Hox genes directly, by binding to associated cis-regulatory regions (Casares and Sánchez-Herrero, 1995; Irish et al., 1989a; Qian et al., 1991; Shimell et al., 2000). This is therefore a shared molecular feature of the canonical *Drosophila* gap genes. By contrast, it is not clear whether this is a shared feature of all of the genes making up the *Tribolium* gap gene network. At least Tc-Hb and Tc-Kr are thought to regulate Hox genes directly in *Tribolium*, as they play similar roles in Hox gene regulation to their *Drosophila* counterparts (Cerny et al., 2005; Marques-Souza et al., 2008). I have shown in this thesis that although Tc-Nub, Tc-Gt and Tc-Kni all play a role in establishing abdominal Hox gene expression in *Tribolium*, this can most parsimoniously be explained as an indirect effect of their interaction with *Tc-Kr*. The homeotic transformations observed in the gnathal segments of *Tc-gt* knockdowns can also be explained by *Tc-Kr* expansion (Bucher and Klingler, 2004). Likewise, the role of *Tc-mlpt/Tc-svb* in establishing abdominal Hox gene expression can be explained via indirect regulation of *Tc-Kr* (most likely through *Tc-gt* and *Tc-kni*). Of course, it is possible that Tc-Nub, Tc-Kni, Tc-Gt and/or Tc-Mlpt/Tc-Svb regulate Hox

genes directly in addition to indirect regulation via *Tc-Kr*. Determining this will require more detailed analysis of the cis-regulatory regions of the Hox cluster. If direct regulation of Hox genes is, however, limited to Tc-Hb and Tc-Kr, then this can hardly be considered a shared molecular function of the gap genes.

The first three genes in the neuroblast timer series (*Tc-hb*, *Tc-Kr* and *Tc-nub*) have an intriguing relationship to Hox gene expression and regulation. The expression domains of *Tc-hb*, *Tc-Kr* and *Tc-nub* all broadly align with the three trunk tagma (gnathum, thorax and abdomen, respectively) in *Tribolium*, save that they are shifted anteriorly to align with parasegment boundaries, and *nub* covers most but not all of the abdominal parasegments (Figure 6.1A). Furthermore, each of these genes plays an active role in specifying its particular tagma; Tc-Hb appears to repress thoracic (central) and abdominal (posterior) Hox genes to allow gnathal (anterior) Hox genes to be expressed; Tc-Kr represses gnathal and abdominal Hox genes to allow the thoracic Hox gene *Antp* to be expressed; and Tc-Nub appears to indirectly promote the expression of abdominal Hox genes by repressing *Tc-Kr* (Figure 6.1B). This minimal network therefore, in theory, provides enough information to lay down the basic functional divisions of the insect axis (although not, of course, the fine details of individual segment identity).

As discussed in Chapter 5, it is easy to see a parallel between sequential specification of neural identities and sequential specification of segmental identities. The indirect regulation of cell fate by Tc-Nub also has a parallel in certain neuroblast lineages. In NB3-1 neuroblasts, Dm-Hb and Dm-Kr play an active role in defining the identities of cells produced during the first and second temporal identity windows; loss of either gene results in a loss of the cell types usually produced during those windows (Tran and Doe, 2008). By contrast, loss of *Dm-nub* delays the onset of the third temporal identity window, but does not prevent the relevant cell types from being produced (Tran and Doe, 2008). This means that rather than being required to drive the identity of third-born neurons, Dm-Nub is simply required to close the second temporal identity window by repressing *Dm-Kr* (Tran and Doe, 2008). This may be either because there is an additional factor that is required to specify the third temporal identity window (Tran and Doe, 2008), or, alternatively, because this identity is the default state, usually repressed by earlier temporal factors such as Dm-Hb and Dm-Kr. During segmental patterning in *Drosophila* and vertebrates, the posterior Hox genes are able to repress anterior and middle Hox genes by posterior prevalence. This provides a possible explanation for how Tc-Nub might be able to drive posterior fates simply by repressing *Tc-Kr* - in the absence of a

repressor, the interactions between the Hox genes automatically output posterior fates (Figure 6.1B).

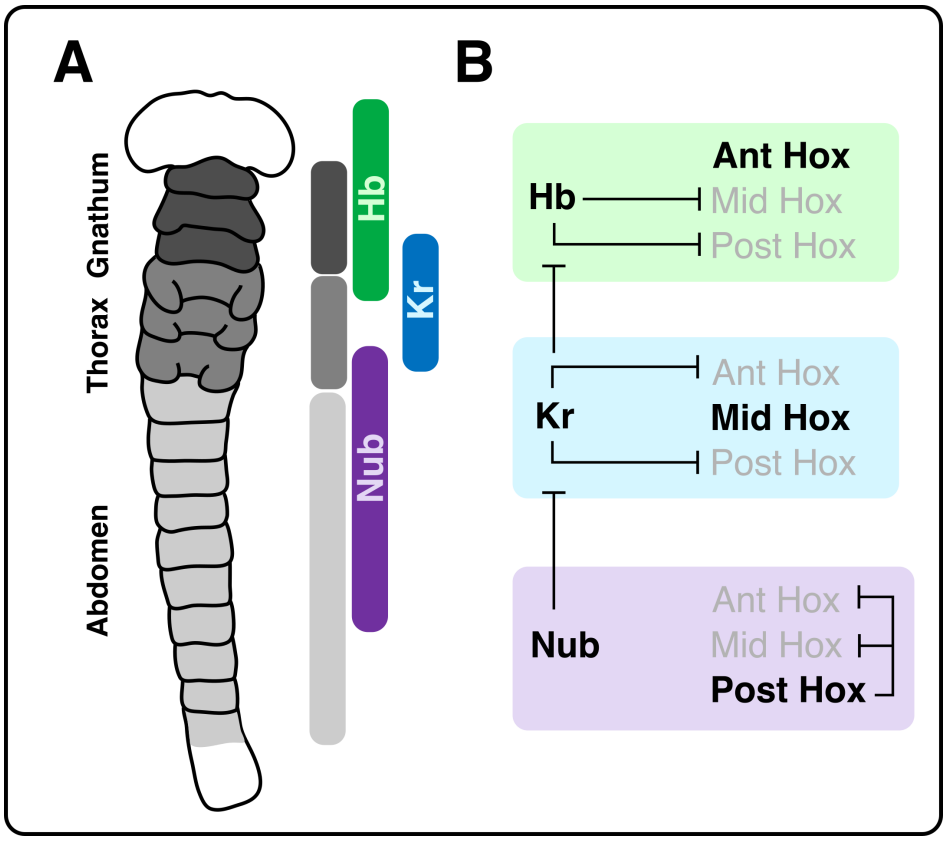

Figure 6.1. The neuroblast timer module as a core regulator of axial fates. A| The first three neuroblast timer genes are expressed in domains (green, blue and purple) that broadly overlap the three tagma of the insect embryo – the head/gnathum, the thorax and the abdomen (represented in the context of the embryo and as simplified grey bars). B| These same three genes interact with Hox genes and with each other in such a way as to drive a 'minimal network' to lay down anterior, middle and posterior Hox gene expression. Each box represents a different region of the embryo, expressing a different neuroblast timer gene (shown as non-overlapping for simplicity).

My model has little to say about the restriction of *Tc-AbdB*, the posterior-most Hox gene, to the posterior of the abdomen. Obvious candidates for regulating this gene are the overlapping domains of *Tc-cas* and *Tc-hb*. As discussed in Chapters 4 and 5, I have not found any obvious role for *cas* in segment patterning. There are tantalising links between *Dm-cas* and *Dm-AbdB* in *Drosophila* neuroblasts – for example, Dm-AbdB protein activates the expression of *Dm-cas* in posterior neuroblasts (Ahn et al., 2010; Kim and Yoo, 2014). However, there is thus far no evidence for regulation in the other direction. The function of the posterior domain of *Tc-hb* is yet to be tested directly, but this domain is interesting for several reasons. Firstly, *Dm-hb* expression never follows *Dm-cas* expression in neuroblasts; its expression in the SAZ therefore represents a departure from the linear progression of the neuroblast timer series, and suggests the possibility of cyclic expression. In addition, the posterior domain of *hb* is thought to be linked to the termination of segmentation in some way, at least in *Bombyx* (Nakao, 2016). Posterior Hox genes can terminate axial elongation in vertebrates (Denans et al., 2015; Young et al., 2009), so perhaps this role of *hb* is mediated through regulation of *AbdB*. It is, of course, possible that the restriction of *AbdB* expression to the posterior abdomen does not depend on gap genes. Given these uncertainties, the regulation of Hox genes in the posterior abdomen of sequentially-segmenting insects represents a compelling topic for further investigation.

Given that the role of Hb, Kr and Cas in neural specification appears to pre-date their expression during/function in segment patterning, it seems likely that the neuroblast timer network was co-opted for use in segment patterning, rather than vice versa (reviewed in the General Introduction). If this is the case, then the neuroblast timer network must have at some point been altered to regulate Hox gene expression. Although Hox genes are expressed in neuroblasts (for example, Bello et al., 2003; Tsuji et al., 2008), there is no evidence that they are regulated by genes of the neuroblast timer series in this context. A better understanding of the gene networks acting downstream of the neuroblast timer series in neuroblasts, and of how exactly the neuroblast timer genes interact with Hox genes during segment patterning, might shed light on this question.

6.2. The *mlpt/svb* module - a link to segment patterning?

In addition to direct regulation of Hox genes, the four *Drosophila* trunk gap genes also share the ability to directly bind to stripe-specific cis-regulatory enhancers of pair-rule gene expression (Schroeder et al., 2011). However, as discussed in the Introduction, gap genes have not been shown to regulate specific pair-rule gene stripes in *Tribolium*, and in selected other sequentially-segmenting insects; instead, their knockdown leads to early termination of segmentation and axial elongation. This suggests that one or more of them are required for the ongoing activity of the pair-rule oscillator in the SAZ. I argue in this section that there is an obvious candidate for this role – the *Tc-mlpt/Tc-svb* module – and that the truncations observed in various gap gene knockdowns might all be explained through their interactions with this module.

Like many other gap gene knockdowns, *mlpt/svb* knockdowns result in early termination of segmentation and axial elongation in several different insect species (Ray et al., 2019), including *Tribolium* (Ray et al., 2019; Savard et al., 2006). Ray et al. (2019) have proposed that Mlpt and Svb may directly regulate segment addition through an interaction with Notch signaling. Notch signaling is thought to be required to co-ordinate pair-rule gene oscillations between cells in many different arthropod species (reviewed in Introduction). Mlpt peptides are known to regulate Notch signaling in many different developmental contexts in *Drosophila* - for example, in sensory organ specification, patterning of veins and the dorsoventral boundary of the wing, and in leg joint formation (Pi et al., 2011; Pueyo and Couso, 2011). In the leg joints, Mlpt peptides trigger the transformation of Svb to an activator, and Svb subsequently drives the (presumably indirect) repression of the Notch ligand Delta, creating a sharp Dl+/Dl- boundary at the future joint position (Pueyo and Couso, 2011). Comparative expression patterns suggest that the role of *mlpt/svb* in regulating Notch signaling in the leg may be deeply conserved within the arthropods (Pueyo and Couso, 2011). Svb, furthermore, seems to have a very ancient association with Notch – indeed, a homologue of the Svb gene regulates Notch signaling during vertebrate hair development (Wells et al., 2009). If *mlpt/svb* are able to regulate Notch signaling in the SAZ, then disruption of their expression might also lead to loss of co-ordination in pair-rule gene oscillations and subsequent breakdown in segment patterning.

Several gap gene knockdowns (at least *Tc-hb*, *Tc-Kr*, *Tc-gt* and *Tc-mlpt*) result in early termination of truncation and segment addition in *Tribolium* (Bucher and Klingler, 2004; Cerny et al., 2005; Marques-Souza et al., 2008; Savard et al., 2006), and all of these knockdowns also

result in misexpression of *mlpt* (Savard et al., 2006). The extent of truncation in these knockdowns shows some relation to the nature of *mlpt* misexpression; in *Kr* knockdowns, where *mlpt* expression is lost (Savard et al., 2006), truncations occur just posterior to the normal domain of *mlpt* expression (between the thorax and abdomen) (Cerny et al., 2005), whereas in *gt* knockdowns, where *mlpt* expression is expanded anteriorly (Savard et al., 2006), truncations occur from the anterior thorax backwards (Bucher and Klingler, 2004). If the effects of Hb, Kr and Gt on segment addition and elongation were indeed mediated via *mlpt/svb* in sequentially-segmenting insects, this would have two important implications. Firstly, in this case, a direct role in regulating segment addition/elongation would not be a feature shared by most gap gene homologues in sequential segmentation. This would align with the proposal that the ancestral role of gap genes was to regulate Hox gene expression, rather than to regulate segment formation (Peel et al., 2005). Secondly, it would suggest that interactions between the *mlpt/svb* module and the neuroblast timer module may be key to co-ordinate segment formation (regulated primarily by the former) and segment diversification (regulated primarily by the latter).

There are two major caveats to this theory. Firstly, Ray et al.'s (2019) model of Mlpt/Svb function suggests that the two genes interact to form a retreating wavefront of active Svb, which is able to stabilise Notch oscillations much as the SAZ timer gene *opa* stabilises pair-rule gene oscillations (Clark and Peel, 2018). This is based on what is known of the role of *Mlpt/Svb* in Notch regulation in the leg (Pueyo and Couso, 2011). However, the expression patterns that I report for *Tc-mlpt* and *Tc-svb* are incompatible with such a theory, as the expression domains of both genes move anteriorly in tandem with the segment pattern (and therefore do not form a retreating wavefront) (Chapter 3). *Tc-mlpt* is also expressed in bursts that have no obvious relationship to the periodicity of segmentation (Chapter 3). It is not clear how these patterns could contribute to co-ordination of Notch signals across the tissue of the SAZ. Furthermore, it is not clear that Notch signaling is even required for segmentation in many sequentially-segmenting insects, including *Tribolium*; for example, the Notch ligand *Delta* is not expressed in the SAZ of *Tribolium*, *Oncopeltus* or *Gryllus* (Aranda, 2006; Aranda et al., 2008; Auman et al., 2017; Kainz et al., 2011). The absence of *Delta* does not necessarily rule out a role for Notch in segment patterning (Clark et al., 2019), but if Notch signaling is not required to co-ordinate pair-rule gene oscillations, then it becomes harder to explain why *mlpt/svb* knockdowns would lead to truncations.

I am, of course, open to the idea that other genes from the gap gene network may regulate segment patterning and/or axial elongation in addition to, or instead of, *Tc-mlpt* and

Tc-svb. There is certainly evidence that components of this network can influence the balance of cell division and differentiation in neuroblasts. Extended expression of *Dm-nub* in specific neuroblast lineages is sufficient to delay quiescence and maintain cell division, while expression of *Dm-cas* triggers quiescence and termination of mitoses (Tsuji et al., 2008). *Dm-cas* is also able to downregulate the expression of *Dm-Dichaete* (a SAZ timer gene) in neuroblasts (Maurange et al., 2008), suggesting the possibility that it might do something similar in the SAZ as part of the termination of segmentation. Neither *nub* nor *cas* RNAi produces any defects in segment patterning or elongation in *Tribolium*, but it is worth investigating the possibility that they might in other insects and non-insect arthropods.

The observation that *Tc-gt* and *Tc-kni* are both transiently expressed in pair-rule stripes in *Tribolium* (Bucher and Klingler, 2004; Cerny et al., 2008; Peel et al., 2013), might be taken to suggest that these genes play a role in regulating segmentation. However, this is thought to be as a result of regulation of these genes by pair-rule genes, rather than vice versa (A. Peel, pers. comm.). *Tc-kni* is certainly regulated by the pair-rule gene *Tc-eve* in the head (Peel et al., 2013).

6.3. *gt* and *kni* – an intermediate module?

My outline of the two modules above raises the question of why *Tc-gt* and *Tc-kni* may have been recruited to segment patterning in the trunk. One possibility, represented in Figure 6.2, is that *Tc-gt* and *Tc-kni* may act as a key link between the neuroblast timer and *Tc-mlpt/Tc-svb* module. Several genes, including *Tc-gt* (but not including *Tc-nub*), are misexpressed following *Tc-mlpt* or *Tc-svb* knockdown (Chapter 5 and Savard et al., 2006). However, my expression analysis suggests that the strongest candidates for direct regulation by Tc-Svb are *Tc-gt* and *Tc-kni* (Chapter 3). I have also shown that both Tc-Gt and Tc-Kni feed back onto the neuroblast timer module through their repression of *Tc-Kr* (Chapter 5). Both genes are expressed during the transition from thoracic segment patterning (carried out largely in the blastoderm, during cellularisation) to abdominal segment patterning (carried out in the SAZ, following cellularisation). Perhaps co-ordination between the networks driving segment formation and diversification is especially important during this handover period.

It is also feasible that they are required to ‘fine-tune’ the timing and distribution of *Tc-Kr* expression in the posterior thorax and abdomen in order to promote segment-specific differences in identity. It may be useful to examine larval morphology beyond the cuticle in *Tc-gt* and *Tc-kni* knockdowns to see whether finer-scale segment identity is maintained.

6.4. A revised understanding of the gap gene network in *Tribolium* (and beyond)

I present a visual summary of my hypotheses regarding the interactions of the "gap genes" in *Tribolium* in Figure 6.2. Interactions have been inferred or predicted based on the work in this thesis, previous analyses of the gap gene network in *Tribolium*, and extrapolations from what we know of the neuroblast timer network (in particular, see Averbukh et al., 2018) and the *Drosophila* gap gene network (reviewed in Jaeger, 2011). Previous models of the gap gene network in *Tribolium* emphasise direct activation as being the driving force for sequential gene activation, with repression mainly acting to turn off the previous gene in the series (Zhu et al., 2017) (see Figure 5.1 in Chapter 5). By contrast, my model borrows from updated models of the neuroblast timer network in proposing a central role for repressor decay in driving sequential gene activation (Averbukh et al., 2018). This is thought to generate a more robust network and can better explain experimental data from neuroblasts (Averbukh et al., 2018). All of these interactions are predictions based on knockdown or mutant data, rather than representations of direct interactions – I have made some guesses as to which interactions are likely to be direct (non-dotted lines) and which indirect (dotted lines), but these guesses will need to be tested by analysis of binding in the cis-regulatory regions of each gene.

A takeaway from my work is that the most functionally precise definition of a "gap gene"– a gene that directly regulates both Hox gene and pair-rule gene expression, as well as the expression of other gap genes - is not usefully applied outside of *Drosophila*. Savard et al. (2006) have proposed an updated definition to account for differences in function between the gap genes in *Drosophila* and their homologues in sequentially-segmenting insects - "a gene that shows early contiguous expression domains and whose loss leads to a loss of adjacent segments and the transformation of segments". Because it makes no reference to function at the molecular level, this definition is extremely broad, encompassing a range of genes that likely have different molecular functions and share a phenotypic class simply because they interact as part of a network. There is certainly an argument to be made that gap genes might be defined by the output of their network, rather than by any one gene individually, but referring to the complicated series of modules in Figure 6.2 as a single network seems to be an oversimplification. I believe that it will be more useful, going forward, to use the term "gap gene" in a highly contextual way, referring specifically to *Drosophila hb*, *Kr*, *gt*, *kni*, *tll* and *hkb*, with the "gap network" comprising the well-described interactions between these genes in *Drosophila*. When discussing the evolution of the gap gene network, it may be more useful

instead to discuss the evolution of specific interacting modules (such as the neuroblast timer and *mlpt/svb* modules) that co-ordinate Hox gene expression and segment patterning.

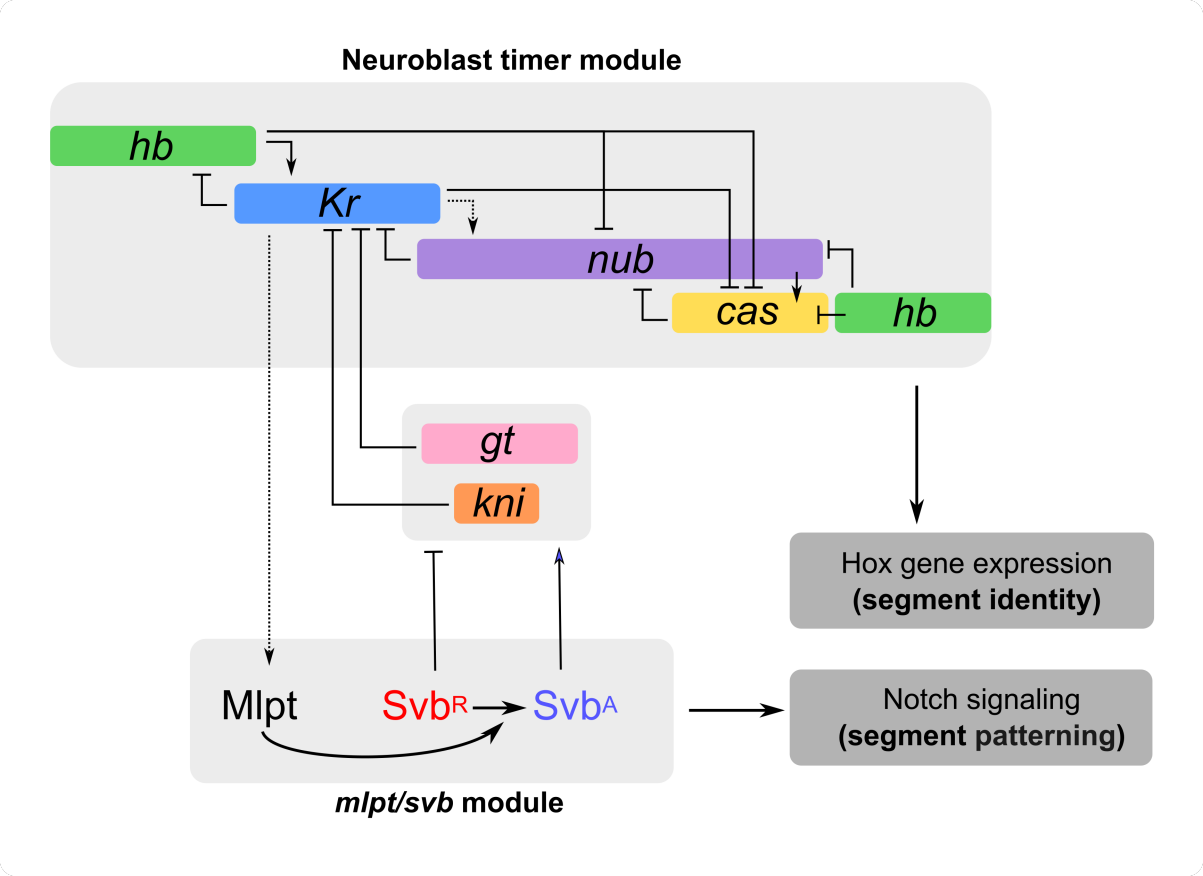

Figure 6.2. A revised model of the *Tribolium* gap gene network. The relative expression domains of the genes of the neuroblast timer module, and *gt* and *kni*, are indicated by the extent of their coloured bars. The width of the grey box surrounding the neuroblast timer module indicates the extent of the segmented trunk region. The expression domains of the *mlpt/svb* genes are not shown, as I believe they play a role in regulating gap gene expression over the entire course of segment addition. The interactions between genes are indicated by unbroken lines (predicted direct interactions) or dotted lines (predicted indirect interactions). The major outputs of each module are indicated in dark grey boxes on the right.

6.5. Future directions

My work has opened up several lines of enquiry that I think will be promising to pursue in the future. The deployment of the neuroblast timer module during segment patterning in *Tribolium*, some 300 million years diverged from *Drosophila*, suggests that this may be a more widely conserved feature of the insects, and perhaps even of the arthropods. Examining the expression and function of these four genes in a range of species will be crucial to confirm that this network initially evolved in the context of neural patterning, and to determine when and how it was co-opted for segment patterning. Note that my work highlights the importance of considering redundancy in any mutant or knockdown studies. It is therefore worth revisiting the function of *nub* (and *kni*) in other species where they are thought to have little or no role in segment patterning (including *Drosophila*).

Existing models of the gap gene network in *Tribolium* are based almost entirely on the results of knockdown studies. My thesis highlights how multiplexed expression analyses can provide a useful supplement for predicting (or ruling out) genetic interactions, and can therefore help to build more robust network models. Approaches such as HCR ISH can also be applied broadly, even to experimentally intractable species, making them well-suited for making evolutionary comparisons. However, confirming how gap genes truly interact with each other, and with other segmentation genes, during sequential segmentation can only result from more intensive study of their regulation at the molecular level. Analysing the cis-regulatory sequences associated with pair-rule, gap and Hox genes (for example, looking for consensus binding sequences and driving expression from specific enhancers using enhancer traps), and what is bound to them at different stages of development (for example, using ChIP-Seq), would provide a deeper understanding of how the 'gap gene network' in *Tribolium* relates to genes at other levels of the segmentation hierarchy. In particular, I would be interested to know how many of the proposed gap genes in *Tribolium* are actually able to bind to regulatory elements associated with pair-rule or Hox genes, like the gap genes in *Drosophila.*

Finally, I would note that the neuroblast timer network represents just one of many elements that are shared between neural and segment patterning. I hope that further comparison of the two systems will help to illuminate exactly how the complex process of segmentation evolved in arthropods.

7. APPENDICES

Appendix 1. A list of genes that were cloned but not used in experiments in this thesis. The primers used for each gene are also provided. The final column lists whether probes were synthesised (Y) or not.

Gene	Significance	Primers (5'-3')	Probes
Tc-chinmo	Associated with neuroblast timer series	F:TGCAACATCGTTCAGCAACC R:GTTCGTGGAGAGTCTCGCTG	Y
Tc-Wnt5	SAZ signaling factor	F:GTTCGTGGAGAGTCTCGCTG R:ACTGATCGCACACACGTCTT	
Tc-Wnt8	SAZ signaling factor	F:AAGAGCGGTCTCTTTGTCGG R:GAGCATCGCTGCTTTCTTCG	Y
Tc-WntA	SAZ signaling factor	F: TTTGCTTCCGTCGCTTTGTG R:GCACAACAATCTGCAACCGT	Y
Tc-fgf8	SAZ signaling factor	F: CGCTTATCCGCTCTCCATGT R: AGTCATCGTCCGGCAGAAAG	
Tc-trithorax	Trithorax group gene (Hox regulation?)	F: GTGATTGCGAGAATGACGGC R: TCCAAGGCTCGACAGTTGAC	
Tc-Ash1	Trithorax group gene (Hox regulation?)	F: CGCAACTGACGTTTCGTACA R: GTCCGAGCTGGAATAGGTCG	
Tc-E(Z)	Polycomb group gene (Hox regulation?)	F: CCCTTCCCTCAGTTCGCATT R: ACACGCTTGAAGACCTTGCT	Y
Tc-myoglianin	Homolog of mammalian *GDF11* (posterior Hox regulation?)	F: AGGAGGAGGACGACTACCAC R: ATCGGGTCGATTACGAGCAC	Y

Appendix 2. Expression of *Tc-sim* and *Tc-Wg* at selected stages of segment addition.

In order to determine whether *Tc-Wg* and *Tc-sim* could be visualised in the same channel without losing informative aspects of expression for either gene, I examined their expression in double HCRs across the course of segment addition. In particular, I wanted to ensure that that anterior and posterior boundaries of the *Tc-Wg* domain could be detected, as I planned to use these landmarks in my analyses.

The posterior *Tc-Wg* domain first appears as a ring around the posterior-most tip of the blastoderm (Figure 7.1, A, A', C and C'). *Tc-Sim* is strongly expressed in the presumptive mesoderm and mesectoderm, and overlaps with the ventral half of the *Tc-Wg* ring (Figure 7.1, A-B'). The two genes share a posterior boundary, and the (fuzzy) anterior boundary of the *Tc-Wg* domain is clearly distinguishable in the ventral and dorsal ectoderm.

Interestingly, the cells at the posterior tip of the embryo, which express neither gene, form a morphologically distinct 'pocket' (Figure 7.1, D), and almost certainly include the primordial germ cells given what we know of their behaviour and the expression of the primordial germ cell marker *vasa* in *Tribolium* (Schröder, 2006). As the germband forms, these cells will detach from the epithelium and begin to migrate along the ventral surface (Schröder, 2006).

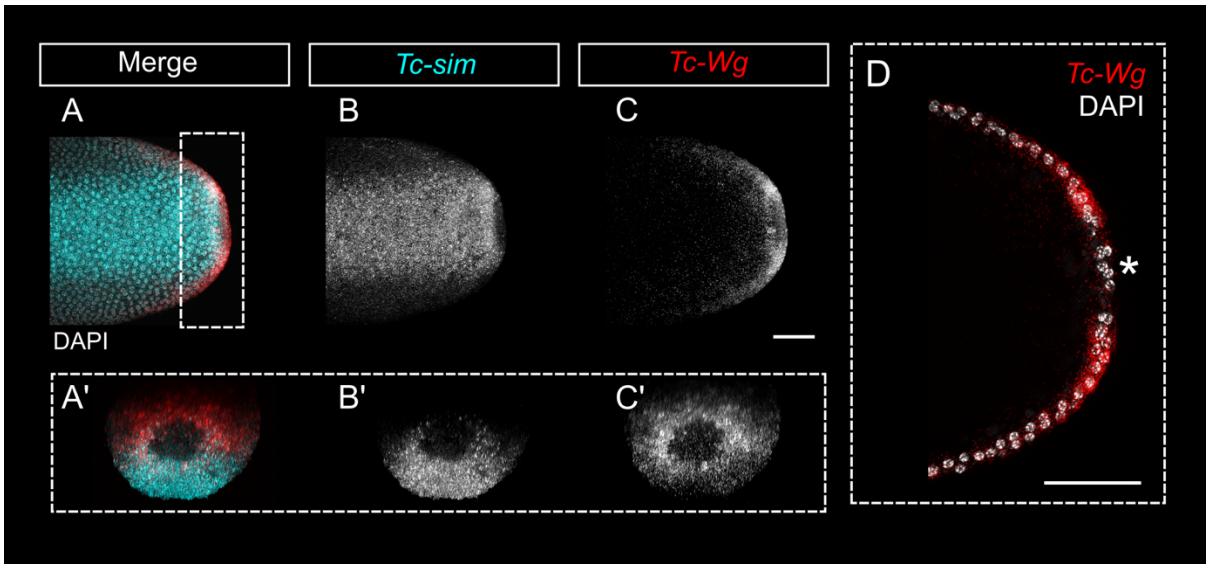

Figure 7.1. Posterior *Tc-Wg* and *Tc-sim* expression in the early blastoderm (stage To1). **A-C** show expression of *Tc-sim* (cyan) and *Tc-Wg* (red) in the posterior half of a blastoderm stage embryo (maximum projection through coronal sections). **A'**, **B'** and **C'** show the posterior of the same embryo (maximum projection through transverse sections), illustrating the ventral arc of *Tc-sim* and ring of *Tc-Wg*. **D** shows a sagittal section through the same embryo illustrating the morphologically distinct pocket of cells sitting within the *Tc-Wg* ring. Scale bar = 50 μM.

By stage W2, *Tc-Sim* expression has almost entirely faded from the central mesoderm and is retained in what is presumably mesectoderm (Figure 7.2, A, A', B and B'). The ring of *Tc-Wg* has now evolved into an arc – given that it overlaps with *Tc-sim* expression, this may be the ventral half of the ring, suggesting that *Tc-Wg* is repressed in the dorsal ectoderm at some point before this stage. The arcs of *Tc-sim* and *Tc-Wg* overlap extensively, but they share an anterior border, and the region posterior to the *Tc-Wg* arc expresses *Tc-sim* at a much lower intensity.

Note that if the *Tc-Wg* arc here does indeed represent the ventral part of the ring observed at the blastoderm stage, then either the domain has shifted across the tissue, or the tissue has shifted posteriorly and dorsally so that the arc now has its posterior border in the dorsal ectoderm (Figure 7.2, B and B''). This observation highlights the importance of using a patterning marker rather as a posterior boundary for the SAZ, rather than simply the posterior of the embryo.

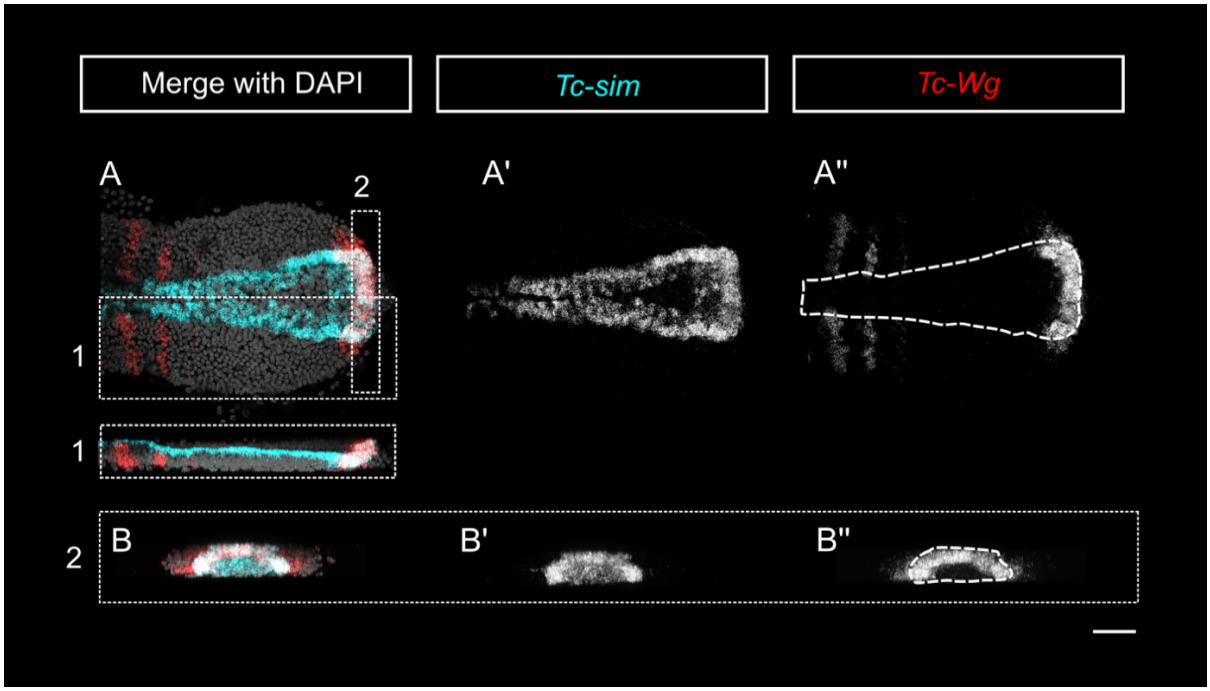

Figure 7.2. Posterior *Tc-Wg* and *Tc-sim* expression in the early germband (stage W2). A-A' show expression of *Tc-sim* (cyan) and *Tc-Wg* (red) in the posterior half of an early germband stage embryo (maximum projection through coronal sections). Insets 1 and 2 show different sections through the same embryo. 1 shows a maximum projection through sagittal sections, illustrating how the posterior boundary of *Tc-sim* and *Tc-Wg* has sits in the dorsal epithelium. 2 (**B-B''**) shows a maximum projection through transverse sections of the posterior-most tip of the embryo. Note the overlapping arc of *Tc-sim* and *Tc-Wg*. Scale bar = 50 µM.

The posterior domain of *Tc-Wg* continues to overlap with *Tc-sim* into mid-elongation (Figure 7.3, stage W7). Both still have their posterior borders in the dorsal ectoderm, although the posterior border of *Tc-Wg* is now more dorsal than that of *Tc-sim* (Figure 7.3, 1 and 3). Within the ventral epithelium, *Tc-Wg* overlaps expression of *Tc-sim* in the medial mesectoderm but also extends laterally into the ventral ectoderm proper (Figure 7.3, 2).

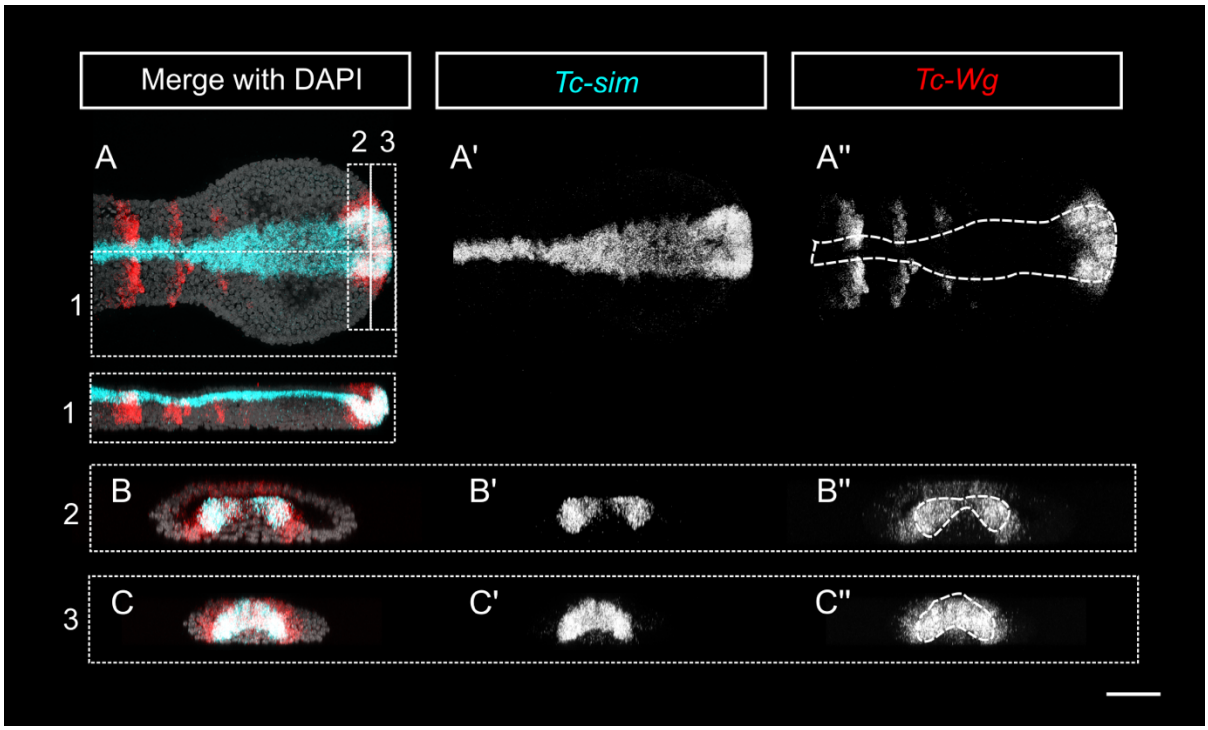

Figure 7.3. Posterior *Tc-Wg* and *Tc-Sim* expression in a germband embryo during mid-elongation (stage W7). A-A' show expression of *Tc-sim* (cyan) and *Tc-Wg* (red) in the posterior of a mid-elongation germband stage embryo (maximum projection through coronal sections). Insets 1, 2 and 3 show different sections through the same embryo. 1 shows a maximum projection through sagittal sections, highlighting how the posterior boundary of both genes still sits on the dorsal surface. 2 and 3 show maximum projections through transverse sections; 2 (**B-B''**) in a region close to the posterior of the embryo, highlighting the lateral domains of *Tc-Wg* in the ectoderm; and 3 (**C-C''**) at the posterior tip of the embryo, showing the overlapping arcs of *Tc-sim* and *Tc-Wg*, again with protruding lateral domains of *Tc-Wg*. Scale bar = 50 μM.

By stage W12, the posterior domain of *Tc-Wg* has evolved dramatically, now sitting as a stripe across the ventral ectoderm (Figure 7.4, A-A'' and 1). This may be through shifting of the domain itself, or through movement of the tissues at the posterior terminus. Interestingly, the posterior of the Tc-sim domain does not undergo a similar ventral shift, now marking the midline back to the posterior terminus of the embryo (Figure 7.4, A-A''). Within its posterior domain, *Tc-Wg* expression is beginning to fade in the mesectoderm but is strong in the ventral and lateral ectoderm (Figure 7.4, 2). From this stage onwards, the anterior and posterior boundaries of the *Tc-Wg* stripe remain distinct relative to *Tc-sim* expression.

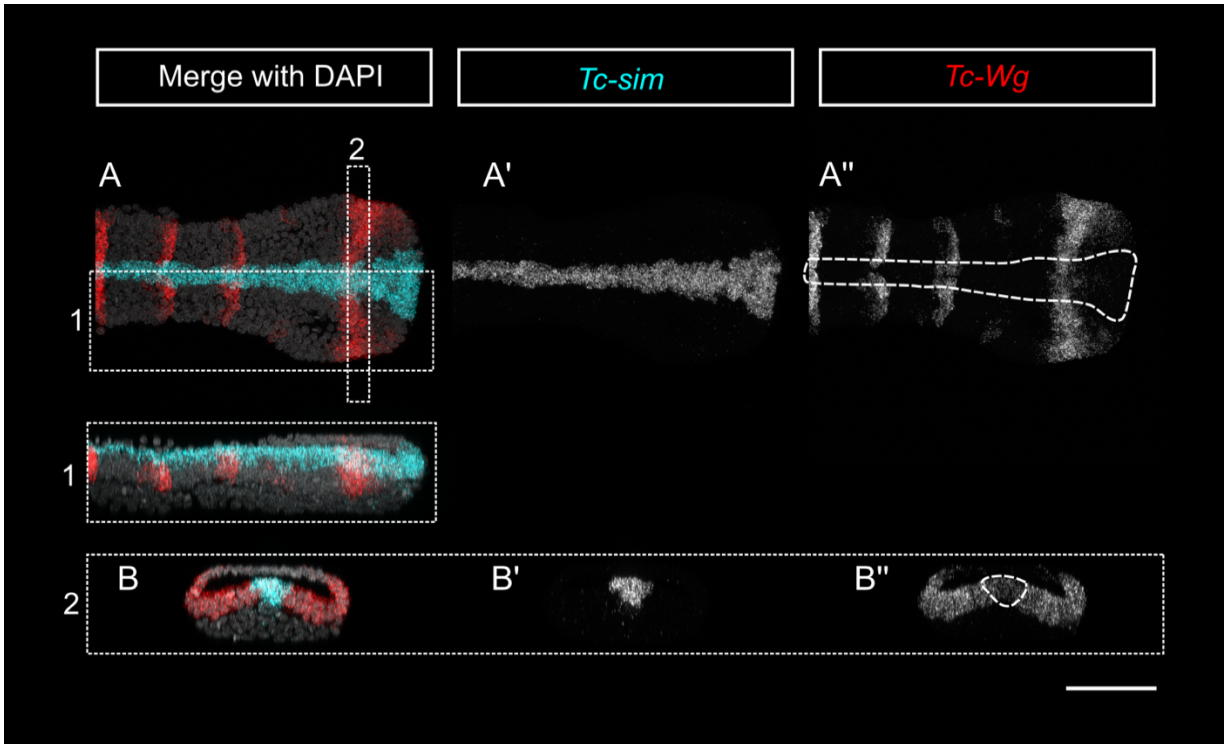

Figure 7.4. *Tc-Wg* and *Tc-Sim* expression in the SAZ of a *Tribolium* during late elongation (stage W12). A-A' show expression of *Tc-sim* (cyan) and *Tc-Wg* (red) in the posterior of a mid/late-elongation germband stage embryo (maximum projection through coronal sections). Insets 1 and 2 show different sections through the same embryo. 1 shows a maximum projection through sagittal sections, highlighting how the posterior domain of *Tc-Wg* has shifted to sit in the ventral ectoderm. 2 (**B-B''**) shows a maximum projection through transverse sections at the level of the posterior *Tc-Wg* stripe, illustrating how *Tc-Wg* is expressed in the ventral ectoderm but not in the dorsal ectoderm, mesoderm or mesectoderm. (where *Tc-sim* is still expressed). Scale bar = 50 µM.

Appendix 3. *Tc-hb*, *Tc-Kr*, *Tc-nub* and *Tc-cas*) are expressed in spatial order in the gut primordium (from posterior to anterior) at the end of segment addition in *Tribolium*.

A) shows a maximum projection through coronal sections of the entire terminus of the embryo, while B) shows maximum projections of transverse sections through the regions indicated. *Tc-cas* is expressed in the most anterior section, section 1; *Tc-nub* is expressed in the ectoderm in section 2; and *Tc-hb* and *Tc-Kr* are co-expressed in the ectoderm in the most posterior section, section 3. Scale bar = 50 μM.

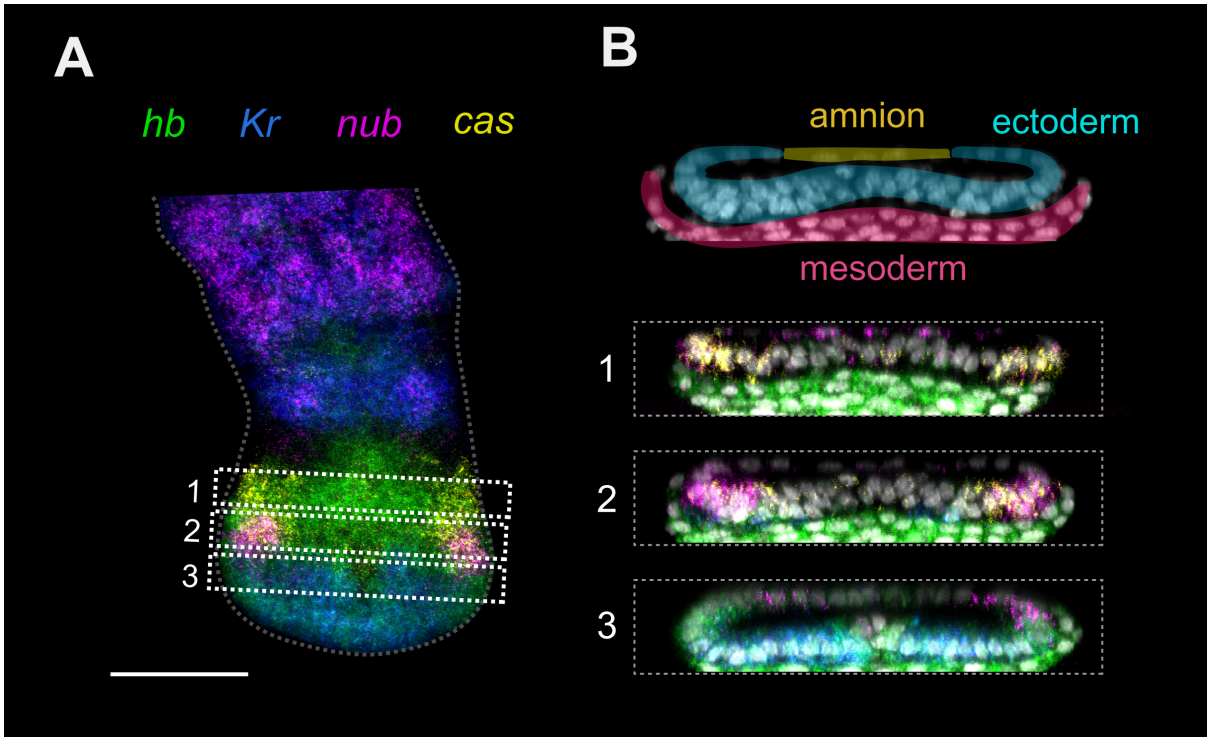

8. BIBLIOGRAPHY

Abzhanov, A. and Kaufman, T. C. (2000). Homologs of Drosophila appendage genes in the patterning of arthropod limbs. *Dev. Biol.* **227**, 673–689.

Ahn, J.-H., Yoo, S., Park, H.-J., Jung, K.-I., Kim, S.-H. and Jeon, S.-H. (2010). Drosophila castor is regulated negatively by the Ubx and abdA genes, but positively by the AbdB gene. *Int. J. Dev. Biol.* **54**, 1251–1258.

Akam, M. (1987). The molecular basis for metameric pattern in the Drosophila embryo. *Development* **101**, 1–22.

Akam, M. (1998a). Hox genes: from master genes to micromanagers. *Curr. Biol.* **8**, R676-8.

Akam, M. (1998b). Hox genes, homeosis and the evolution of segment identity: no need for hopeless monsters. *Int. J. Dev. Biol.* **42**, 445–451.

Almeida, M. S. and Bray, S. J. (2005). Regulation of post-embryonic neuroblasts by Drosophila Grainyhead. *Mech. Dev.* **122**, 1282–1293.

Alsiö, J. M., Tarchini, B., Cayouette, M. and Livesey, F. J. (2013). Ikaros promotes early-born neuronal fates in the cerebral cortex. *Proc. Natl. Acad. Sci.* **110**, E716–E725.

Aranda, M. (2006). Functional analysis of a homolog of the pair-rule gene hairy in the short-germ beetle Tribolium castaneum.

Aranda, M., Marques-Souza, H., Bayer, T. and Tautz, D. (2008). The role of the segmentation gene hairy in Tribolium. *Dev. Genes Evol.* **218**, 465–477.

Auman, T. and Chipman, A. D. (2018). Growth zone segmentation in the milkweed bug Oncopeltus fasciatus sheds light on the evolution of insect segmentation. *BMC Evol. Biol.* **18**, 1–16.

Auman, T., Vreede, B. M. I., Weiss, A., Hester, S. D., Williams, T. A., Nagy, L. M. and Chipman, A. D. (2017). Dynamics of growth zone patterning in the milkweed bug *Oncopeltus fasciatus*. *Development* **144**, 1896–1905.

Averbukh, I., Lai, S.-L., Doe, C. Q. and Barkai, N. (2018). A repressor-decay timer for robust temporal patterning in embryonic Drosophila neuroblast lineages. *eLife* **7**, e38631.

Averof, M. and Cohen, S. M. (1997). Evolutionary origin of insect wings from ancestral gills. *Nature* **385**, 627–630.

Azpiazu, N., Lawrence, P. A., Vincent, J. P. and Frasch, M. (1996). Segmentation and specification of the Drosophila mesoderm. *Genes Dev.* **10**, 3183–3194.

Baumgardt, M., Karlsson, D., Terriente, J., Díaz-Benjumea, F. J. and Thor, S. (2009). Neuronal Subtype Specification within a Lineage by Opposing Temporal Feed-Forward Loops. *Cell* **139**, 969–982.

Bello, B. C., Hirth, F. and Gould, A. P. (2003). A Pulse of the Drosophila Hox Protein Abdominal-A Schedules the End of Neural Proliferation via Neuroblast Apoptosis. *Neuron* **37**, 209–219.

Ben-David, J. and Chipman, A. D. (2010). Mutual regulatory interactions of the trunk gap genes during blastoderm patterning in the hemipteran Oncopeltus fasciatus. *Dev. Biol.* **346**, 140–149.

Benton, M. A., Pechmann, M., Frey, N., Stappert, D., Conrads, K. H., Chen, Y. T., Stamataki, E., Pavlopoulos, A. and Roth, S. (2016). Toll Genes Have an Ancestral Role in Axis Elongation. *Curr. Biol.* **26**, 1609–1615.

Berghammer, A. J., Weber, M., Trauner, J. and Klingler, M. (2009). Red Flour Beetle (Tribolium) Germline Transformation and Insertional Mutagenesis. *Cold Spring Harb. Protoc.* **4**, 1–6.

Biffar, L. and Stollewerk, A. (2014). Conservation and evolutionary modifications of neuroblast expression patterns in insects. *Dev. Biol.* **388**, 103–116.

Biggin, M. D. and Tijan, R. (1988). Transcription factors that activate the Ultrabithorax promoter in developmentally staged extracts. *Cell* **53**, 699–711.

Billin, A. N., Cockerill, K. A. and Poole, S. J. (1991). Isolation of a family of Drosophila POU domain genes expressed in early development. *Mech. Dev.* **34**, 75–84.

Boos, A., Distler, J., Rudolf, H., Klingler, M. and El-Sherif, E. (2018). A re-inducible gap gene cascade patterns the anterior–posterior axis of insects in a threshold-free fashion. *eLife* **7**, 1–27.

Bray, S. J. and Kafatos, F. C. (1991). Developmental function of Elf-1: an essential transcription factor during embryogenesis in Drosophila. *Genes Dev.* **5**, 1672–1683.

Bray, S. J., Burke, B., Brown, N. H. and Hirsh, J. (1989). Embryonic expression pattern of a family of Drosophila proteins that interact with a central nervous system regulatory element. *Genes Dev.* **3**, 1130–1145.

Brena, C. and Akam, M. (2013). An analysis of segmentation dynamics throughout embryogenesis in the centipede Strigamia maritima. *BMC Biol.* **11**, 1–18.

Brody, T. and Odenwald, W. F. (2000). Programmed transformations in neuroblast gene expression during Drosophila CNS lineage development. *Dev. Biol.* **226**, 34–44.

Brody, T. and Odenwald, W. F. (2002). Cellular diversity in the developing nervous system: a temporal view from Drosophila. *Dev. Camb. Engl.* **129**, 3763–3770.

Brody, T. and Odenwald, W. F. (2005). Regulation of temporal identities during Drosophila neuroblast lineage development. *Curr. Opin. Cell Biol.* **17**, 672–675.

Brown, S. J., Patel, N. H. and Denell, R. E. (1994). Embryonic expression of the single Tribolium engrailed homolog. *Dev. Genet.* **15**, 7–18.

Brown, S. J., Parrish, J. K., Beeman, R. W. and Denell, R. E. (1997). Molecular characterization and embryonic expression of the even-skipped ortholog of Tribolium castaneum. *Mech. Dev.* **61**, 165–173.

Brown, S. J., Shippy, T. D., Miller, S., Bolognesi, R., Beeman, R. W., Lorenzen, M. D., Bucher, G., Wimmer, E. A. and Klingler, M. (2009). The red flour beetle, Tribolium castaneum (Coleoptera): A model for studies of development and pest biology. *Cold Spring Harb. Protoc.* **4**, 1–10.

Bucher, G. (2009). The Beetle Book.

Bucher, G. and Klingler, M. (2004). Divergent segmentation mechanism in the short germ insect Tribolium revealed by giant expression and function. *Development* **131**, 1729–1740.

Capovilla, M., Eldon, E. D. and Pirrotta, V. (1992). The giant gene of Drosophila encodes a b-ZIP DNA-binding protein that regulates the expression of other segmentation gap genes. *Development* **114**, 99–112.

Casares, F. and Sánchez-Herrero, E. (1995). Regulation of the infraabdominal regions of the bithorax complex of Drosophila by gap genes. *Development* **1866**, 1855–1866.

Cenci, C. and Gould, A. P. (2005). Drosophila Grainyhead specifies late programmes of neural proliferation by regulating the mitotic activity and Hox-dependent apoptosis of neuroblasts. *Development* **132**, 3835–3845.

Cepeda, R. E., Pardo, R. V., Macaya, C. C. and Sarrazin, A. F. (2017). Contribution of cell proliferation to axial elongation in the red flour beetle Tribolium castaneum. *PLOS ONE* **12**, e0186159.

Cerny, A. C., Bucher, G., Schröder, R. and Klingler, M. (2005). Breakdown of abdominal patterning in the Tribolium Kruppel mutant jaws. *Development* **132**, 5353–5363.

Cerny, A. C., Grossmann, D., Bucher, G. and Klingler, M. (2008). The Tribolium ortholog of knirps and knirps-related is crucial for head segmentation but plays a minor role during abdominal patterning. *Dev. Biol.* **321**, 284–294.

Chang, Y.-C., Jang, A. C.-C., Lin, C.-H. and Montell, D. J. (2013). Castor is required for Hedgehog-dependent cell-fate specification and follicle stem cell maintenance in Drosophila oogenesis. *Proc. Natl. Acad. Sci.* **110**, E1734–E1742.

Charpentier, M. S., Christine, K. S., Amin, N. M., Dorr, K. M., Kushner, E. J., Bautch, V. L., Taylor, J. M. and Conlon, F. L. (2013). CASZ1 Promotes Vascular Assembly and Morphogenesis Through the Direct Regulation of an EGFL7/RhoA-mediated pathway. *Dev. Cell* **25**, 132–143.

Chipman, A. D. and Stollewerk, A. (2006). Specification of neural precursor identity in the geophilomorph centipede Strigamia maritima. *Dev. Biol.* **290**, 337–350.

Choe, C. P., Miller, S. C. and Brown, S. J. (2006). A pair-rule gene circuit defines segments sequentially in the short-germ insect Tribolium castaneum. *Proc. Natl. Acad. Sci.* **103**, 6560–6564.

Choi, H. M. T., Schwarzkopf, M., Fornace, M. E., Acharya, A., Artavanis, G. and Stegmaier, J. (2018). Third-generation in situ hybridization chain reaction: multiplexed, quantitative, sensitive, versatile, robust. *Development* **145**, 1–10.

Christine, K. S. and Conlon, F. L. (2008). Vertebrate CASTOR Is Required for Differentiation of Cardiac Precursor Cells at the Ventral Midline. *Dev. Cell* **14**, 616–623.

Cifuentes, F. J. and García-Bellido, A. (1997). Proximo-distal specification in the wing disc of Drosophila by the nubbin gene. *Proc. Natl. Acad. Sci. U. S. A.* **94**, 11405–11410.

Cinnamon, E., Gur-Wahnon, D., Helman, A., Johnston, D. S., Jiménez, G. and Paroush, Z. (2004). Capicua integrates input from two maternal systems in Drosophila terminal patterning. *EMBO J.* **23**, 4571–4582.

Clark, E. (2017). Dynamic patterning by the Drosophila pair-rule network reconciles long-germ and short-germ segmentation. *PLoS Biol.* **15**, 1–38.

Clark, E. and Peel, A. D. (2018). Evidence for the temporal regulation of insect segmentation by a conserved sequence of transcription factors. *Development* **145**, dev.155580.

Clark, E., Peel, A. D. and Akam, M. (2019). Arthropod segmentation. *Development* **146**, dev170480.

Cockerill, K. A., Billin, A. N. and Poole, S. J. (1993). Regulation of expression domains and effects of ectopic expression reveal gap gene-like properties of the linked pdm genes of Drosophila. *Mech. Dev.* **41**, 139–153.

Cooke, J. and Zeeman, E. C. (1976). A clock and wavefront model for control of the number of repeated structures during animal morphogenesis. *J. Theor. Biol.* **58**, 455–476.

Cui, X. and Doe, C. Q. (1992). ming is expressed in neuroblast sublineages and regulates gene expression in the Drosophila central nervous system. *Development* **116**, 943–952.

Dahmann, C. ed. (2008). *Drosophila Methods and Protocols*. Humana Press.

Damen, W. G. M., Saridaki, T. and Averof, M. (2002). Diverse Adaptations of an Ancestral Gill: A Common Evolutionary Origin for Wings, Breathing Organs, and Spinnerets. *Curr. Biol.* **12**, 1711–1716.

Dantoft, W., Davis, M. M., Lindvall, J. M., Tang, X., Uvell, H., Junell, A., Beskow, A. and Engström, Y. (2013). The Oct1 homolog Nubbin is a repressor of NF-κB-dependent immune gene expression that increases the tolerance to gut microbiota. *BMC Biol.* **11**, 99.

Dantoft, W., Lundin, D., Esfahani, S. S. and Engström, Y. (2016). The POU/Oct Transcription Factor Pdm1/nub Is Necessary for a Beneficial Gut Microbiota and Normal Lifespan of ***Drosophila***. *J. Innate Immun.* **8**, 412–426.

Davis, G. K. and Patel, N. H. (2002). Short, Long, and Beyond: Molecular and Embryological Approaches to Insect Segmentation. *Annu. Rev. Entomol.* **47**, 669–699.

Denans, N., Iimura, T. and Pourquié, O. (2015). Hox genes control vertebrate body elongation by collinear Wnt repression. *eLife* **4**, e04379.

Denell, R. (2008). Establishment of Tribolium as a Genetic Model System and Its Early Contributions to Evo-Devo. *Genetics* **180**, 1779–1786.

Dick, T., Yang, X. H., Yeo, S. L. and Chia, W. (1991). Two closely linked Drosophila POU domain genes are expressed in neuroblasts and sensory elements. *Proc. Natl. Acad. Sci. U. S. A.* **88**, 7645–7649.

Dönitz, J., Gerischer, L., Hahnke, S., Pfeiffer, S. and Bucher, G. (2018). Expanded and updated data and a query pipeline for iBeetle-Base. *Nucleic Acids Res.* **46**, D831–D835.

Dorr, K. M., Amin, N. M., Kuchenbrod, L. M., Labiner, H., Charpentier, M. S., Pevny, L. H., Wessels, A. and Conlon, F. L. (2015). Casz1 is required for cardiomyocyte G1-to-S phase progression during mammalian cardiac development. *Development* **142**, 2037–2047.

Duboule, D. (2007). The rise and fall of Hox gene clusters. *Development* **134**, 2549–2560.

Duboule, D. and Morata, G. (1994). Colinearity and functional hierarchy among genes of the homeotic complexes. *Trends Genet.* **10**, 358–364.

Dynlacht, B. D., Attardi, L. D., Admon, A., Freeman, M. and Tjian, R. (1989). Functional analysis of NTF-1, a developmentally regulated Drosophila transcription factor that binds neuronal cis elements. *Genes Dev.* **3**, 1677–1688.

Elliott, J., Jolicoeur, C., Ramamurthy, V. and Cayouette, M. (2008). Ikaros Confers Early Temporal Competence to Mouse Retinal Progenitor Cells. *Neuron* **60**, 26–39.

El-Sherif, E., Averof, M. and Brown, S. J. (2012). A segmentation clock operating in blastoderm and germband stages of Tribolium development. *Development* **139**, 4341–4346.

El-Sherif, E., Zhu, X., Fu, J. and Brown, S. J. (2014). Caudal Regulates the Spatiotemporal Dynamics of Pair-Rule Waves in Tribolium. *PLoS Genet.* **10**, e1004677.

Eriksson, B. J., Ungerer, P. and Stollewerk, A. (2013). The function of Notch signalling in segment formation in the crustacean Daphnia magna (Branchiopoda). *Dev. Biol.* **383**, 321–330.

Fisher, B., Weiszmann, R., Frise, E., Hammonds, A., Tomancak, P., Beaton, A., Berman, B., Quan, E., Shu, S., Lewis, S., et al. BDGP in situ homepage.

Frisch, S. M., Farris, J. C. and Pifer, P. M. (2017). Roles of Grainyhead-like transcription factors in cancer. *Oncogene* **36**, 6067–6073.

Furriols, M. and Casanova, J. (2003). In and out of Torso RTK signalling. *EMBO J.* **22**, 1947–1952.

Galindo, M. I., Pueyo, J. I., Fouix, S., Bishop, S. A. and Couso, J. P. (2007). Peptides Encoded by Short ORFs Control Development and Define a New Eukaryotic Gene Family. *PLoS Biol.* **5**, e106.

Gangishetti, U., Veerkamp, J., Bezdan, D., Schwarz, H., Lohmann, I. and Moussian, B. (2012). The transcription factor Grainy head and the steroid hormone ecdysone cooperate during differentiation of the skin of Drosophila melanogaster. *Insect Mol. Biol.* **21**, 283–295.

Gilbert, S. F. (2013). *Developmental Biology*. 10th edition. Sinauer Associates.

Graham, P. L., Anderson, W. R., Brandt, E. A., Xiang, J. and Pick, L. (2019). Dynamic expression of Drosophila segmental cell surface-encoding genes and their pair-rule regulators. *Dev. Biol.* **447**, 147–156.

Green, J. and Akam, M. (2013). Evolution of the pair rule gene network: Insights from a centipede. *Dev. Biol.* **382**, 235–245.

Grimaldi, D. and Engel, M. (2005). *Evolution of Insects*. Cambridge, UK: Cambridge University Press.

Grosskortenhaus, R., Robinson, K. J. and Doe, C. Q. (2006). Pdm and Castor specify late-born motor neuron identity in the NB7-1 lineage. *Genes Dev.* **20**, 2618–2627.

Hannibal, R. L., Price, A. L. and Patel, N. H. (2012). The functional relationship between ectodermal and mesodermal segmentation in the crustacean, Parhyale hawaiensis. *Dev. Biol.* **361**, 427–438.

Hemphälä, J. (2003). Grainy head controls apical membrane growth and tube elongation in response to Branchless/FGF signalling. *Development* **130**, 249–258.

Hrycaj, S., Mihajlovic, M., Mahfooz, N., Couso, J. P. and Popadić, A. (2008). RNAi analysis of nubbin embryonic functions in a hemimetabolous insect, Oncopeltus fasciatus. *Evol. Dev.* **10**, 705–716.

Huang, J. D., Dubnicoff, T., Liaw, G. J., Bai, Y., Valentine, S. A., Shirokawa, J. M., Lengyel, J. A. and Courey, A. J. (1995). Binding sites for transcription factor NTF-1/Elf-1 contribute to the ventral repression of decapentaplegic. *Genes Dev.* **9**, 3177–3189.

Hughes, C. L. and Kaufman, T. C. (2002). Hox genes and the evolution of the arthropod body plan. *Evol. Dev.* **4**, 459–499.

Hülskamp, M., Schröder, C., Pfeifle, C., Jäckle, H. and Tautz, D. (1989). Posterior segmentation of the Drosophila embryo in the absence of a maternal posterior organizer gene. *Nature* **338**, 629–32.

Ingham, P. W. (1988). The molecular genetics of embryonic pattern formation in Drosophila. *Nature* **335**, 25–34.

Irish, V. F., Martinez-Arias, A. and Akam, M. (1989a). Spatial regulation of the Antennapedia and Ultrabithorax homeotic genes during Drosophila early development. *EMBO J.* **8**, 1527–1537.

Irish, V. F., Lehmann, R. and Akam, M. (1989b). The Drosophila posterior-group gene nanos functions by repressing hunchback activity. *Nature* **338**, 646–648.

Isshiki, T., Pearson, B., Holbrook, S. and Doe, C. Q. (2001). Drosophila Neuroblasts Sequentially Express Transcription Factors which Specify the Temporal Identity of Their Neuronal Progeny. *Cell* **106**, 511–521.

Iwasa, J. H., Suver, D. W. and Savage, R. M. (2000). The leech hunchback protein is expressed in the epithelium and CNS but not in the segmental precursor lineages. *Dev. Genes Evol.* **210**, 277–288.

Jäckle, H., Tautz, D., Schuh, R., Seifert, E. and Lehmann, R. (1986). Cross-regulatory interactions among the gap genes of Drosophila. *Nature* **324**, 668–670.

Jacobs, C. G. C., Rezende, G. L., Lamers, G. E. M. and van der Zee, M. (2013). The extraembryonic serosa protects the insect egg against desiccation. *Proc. R. Soc. B Biol. Sci.* **280**, 20131082.

Jaeger, J. (2011). The gap gene network. *Cell. Mol. Life Sci.* **68**, 243–274.

Jaeger, J., Blagov, M., Kosman, D., Kozlov, K. N., Manu, Myasnikova, E., Surkova, S., Vanario-Alonso, C. E., Samsonova, M., Sharp, D. H., et al. (2004). Dynamical Analysis of Regulatory Interactions in the Gap Gene System of *Drosophila melanogaster*. *Genetics* **167**, 1721–1737.

Janssen, R., Budd, G. E. and Damen, W. G. M. (2011). Gene expression suggests conserved mechanisms patterning the heads of insects and myriapods. *Dev. Biol.* **357**, 64–72.

Jiménez-Guri, E., Wotton, K. R. and Jaeger, J. (2018). tarsal-less is expressed as a gap gene but has no gap gene phenotype in the moth midge Clogmia albipunctata. *R. Soc. Open Sci.* **5**,.

John, L. B. and Ward, A. C. (2011). The Ikaros gene family: Transcriptional regulators of hematopoiesis and immunity. *Mol. Immunol.* **48**, 1272–1278.

Jürgens, G., Wieschaus, E., Nüsslein-Volhard, C. and Kluding, H. (1984). Mutations affecting the pattern of the larval cuticle in Drosophila melanogaster. II. Zygotic loci on the third chromosome. *Rouxs Arch. Dev. Biol.* **193**, 283–295.

Kainz, F., Ewen-Campen, B., Akam, M. and Extavour, C. G. (2011). Notch/Delta signalling is not required for segment generation in the basally branching insect Gryllus bimaculatus. *Development* **138**, 5015–5026.

Kambadur, R., Koizumi, K., Stivers, C., Nagle, J., Poole, S. J. and Odenwald, W. F. (1998). Regulation of POU genes by *castor* and *hunchback* establishes layered compartments in the *Drosophila* CNS. *Genes Dev.* **12**, 246–260.

Kerner, P., Zelada González, F., Le Gouar, M., Ledent, V., Arendt, D. and Vervoort, M. (2006). The expression of a hunchback ortholog in the polychaete annelid Platynereis dumerilii suggests an ancestral role in mesoderm development and neurogenesis. *Dev. Genes Evol.* **216**, 821–828.

Khandelwal, R., Sipani, R., Govinda Rajan, S., Kumar, R. and Joshi, R. (2017). Combinatorial action of Grainyhead, Extradenticle and Notch in regulating Hox mediated apoptosis in Drosophila larval CNS. *PLOS Genet.* **13**, e1007043.

Kim, K. H. and Yoo, S. (2014). Sequence-specific interaction between ABD-B homeodomain and castor gene in Drosophila. *BMB Rep.* **47**, 92–97.

Knipple, D. C., Seifert, E., Rosenberg, U. B., Preiss, A. and Jackie, H. (1985). Spatial and temporal patterns of Krüppel gene expression in early Drosophila embryos. 5.

Kondo, T., Plaza, S., Zanet, J., Benrabah, E., Valenti, P., Hashimoto, Y., Kobayashi, S., Payre, F. and Kageyama, Y. (2010). Small Peptides Switch the Transcriptional Activity of Shavenbaby During Drosophila Embryogenesis. *Science* **329**, 336–339.

Kontarakis, Z., Copf, T. and Averof, M. (2006). Expression of hunchback during trunk segmentation in the branchiopod crustacean Artemia franciscana. *Dev. Genes Evol.* **216**, 89–93.

Kraut, R. and Levine, M. (1991). Mutually repressive interactions between the gap genes giant and Krüppel define middle body regions of the Drosophila embryo. **621**, 611–621.

Krumlauf, R. (1994). Hox genes in vertebrate development. *Cell* **78**, 191–201.

Lavore, A., Esponda-Behrens, N., Pagola, L. and Rivera-Pomar, R. (2014). The gap gene Krüppel of Rhodnius prolixus is required for segmentation and for repression of the homeotic gene sex comb-reduced. *Dev. Biol.* **387**, 121–129.

Lee, H. and Adler, P. N. (2004). The grainyhead transcription factor is essential for the function of the frizzled pathway in the Drosophila wing. *Mech. Dev.* **121**, 37–49.

Lehmann, R. and Nüsslein-Volhard, C. (1987). hunchback, a gene required for segmentation of an anterior and posterior region of the Drosophila embryo. *Dev. Biol.* **119**, 402–417.

Leulier, F. and Lemaitre, B. (2008). Toll-like receptors — taking an evolutionary approach. *Nat. Rev. Genet.* **9**, 165–178.

Lewis, D. L., DeCamillis, M. and Bennett, R. L. (2000). Distinct roles of the homeotic genes Ubx and abd-A in beetle embryonic abdominal appendage development. *Proc. Natl. Acad. Sci.* **97**, 4504–4509.

Li, X. and Noll, M. (1993). Role of the gooseberry gene in Drosophila embryos: maintenance of wingless expression by a wingless--gooseberry autoregulatory loop. *EMBO J.* **12**, 4499–4509.

Li, H. and Popadić, A. (2004). Analysis of nubbin expression patterns in insects. *Evol. Dev.* **6**, 310–324.

Liao, B.-K. and Oates, A. C. (2017). Delta-Notch signalling in segmentation. *Arthropod Struct. Dev.* **46**, 429–447.

Liaw, G.-J., Rudolph, K. M., Huang, J.-D., Dubnicoff, T., Courey, A. J. and Lengyel, J. A. (1995). The torso response element binds GAGA and NTF-1/Elf-l, and regulates tailless by relief of repression. *Genes Dev.* **9**, 3163–3176.

Lindberg, B. G., Tang, X., Dantoft, W., Gohel, P., Seyedoleslami Esfahani, S., Lindvall, J. M. and Engström, Y. (2018). Nubbin isoform antagonism governs Drosophila intestinal immune homeostasis. *PLOS Pathog.* **14**, e1006936.

Linne, V., Eriksson, B. J. and Stollewerk, A. (2012). Single-minded and the evolution of the ventral midline in arthropods. *Dev. Biol.* **364**, 66–76.

Liu, P. Z. (2005). even-skipped is not a pair-rule gene but has segmental and gap-like functions in Oncopeltus fasciatus, an intermediate germband insect. *Development* **132**, 2081–2092.

Liu, P. Z. and Kaufman, T. C. (2004a). hunchback is required for suppression of abdominal identity, and for proper germband growth and segmentation in the intermediate germband insect Oncopeltus fasciatus. *Development* **131**, 1515–1527.

Liu, P. Z. and Kaufman, T. C. (2004b). Krüppel is a gap gene in the intermediate germband insect Oncopeltus fasciatus and is required for development of both blastoderm and germband-derived segments. *Development* **131**, 4567–4579.

Liu, P. Z. and Patel, N. H. (2010). giant is a bona fide gap gene in the intermediate germband insect, Oncopeltus fasciatus. *Development* **137**, 835–844.

Liu, Z., Li, W., Ma, X., Ding, N., Spallotta, F., Southon, E., Tessarollo, L., Gaetano, C., Mukouyama, Y. and Thiele, C. J. (2014). Essential Role of the Zinc Finger Transcription Factor Casz1 for Mammalian Cardiac Morphogenesis and Development. *J. Biol. Chem.* **289**, 29801–29816.

Lloyd, A. and Sakonju, S. (1991). Characterization of two Drosophila POU domain genes, related to oct-1 and oct-2, and the regulation of their expression patterns. *Mech. Dev.* **36**, 87–102.

Lynch, J. A., Brent, A. E., Leaf, D. S., Anne Pultz, M. and Desplan, C. (2006). Localized maternal orthodenticle patterns anterior and posterior in the long germ wasp Nasonia. *Nature* **439**, 728–732.

Ma, Y., Niemitz, E. L., Nambu, P. A., Shan, X., Sackerson, C., Fujioka, M., Goto, T. and Nambu, J. R. (1998). Gene regulatory functions of Drosophila Fish-hook, a high mobility group domain Sox protein. *Mech. Dev.* **73**, 169–182.

Mace, K. A. (2005). An Epidermal Barrier Wound Repair Pathway in Drosophila Is Mediated by grainy head. *Science* **308**, 381–385.

Maeda, R. K. and Karch, F. (2006). The ABC of the BX-C: the bithorax complex explained. *Development* **133**, 1413–1422.

Mallo, M. and Alonso, C. R. (2013). The regulation of Hox gene expression during animal development. *Development* **140**, 3951–3963.

Margolis, J. S., Borowsky, M., Shim, C. W. and Posakony, J. W. (1994). A Small Region Surrounding the Distal Promoter of the hunchback Gene Directs Maternal Expression. *Dev. Biol.* **163**, 381–388.

Marques-Souza, H., Aranda, M. and Tautz, D. (2008). Delimiting the conserved features of hunchback function for the trunk organization of insects. *Development* **135**, 881–888.

Martinez-Arias, A. and Lawrence, P. A. (1985). Parasegments and compartments in the Drosophila embryo. *Nature* **313**, 639–642.

Mattar, P. and Cayouette, M. (2015). Mechanisms of temporal identity regulation in mouse retinal progenitor cells. *Neurogenesis* **2**, e1125409.

Mattar, P., Ericson, J., Blackshaw, S. and Cayouette, M. (2015). A Conserved Regulatory Logic Controls Temporal Identity in Mouse Neural Progenitors. *Neuron* **85**, 497–504.

Mattar, P., Stevanovic, M., Nad, I. and Cayouette, M. (2018). Casz1 controls higher-order nuclear organization in rod photoreceptors. *Proc. Natl. Acad. Sci.* **115**, E7987–E7996.

Maurange, C., Cheng, L. and Gould, A. P. (2008). Temporal Transcription Factors and Their Targets Schedule the End of Neural Proliferation in Drosophila. *Cell* **133**, 891–902.

McGregor, A. P., Pechmann, M., Schwager, E. E., Feitosa, N. M., Kruck, S., Aranda, M. and Damen, W. G. M. (2008). Wnt8 Is Required for Growth-Zone Establishment and Development of Opisthosomal Segments in a Spider. *Curr. Biol.* **18**, 1619–1623.

Mellerick, D. M., Kassis, J. A., Zhang, S.-D. and Odenwald, W. F. (1992). castor encodes a novel zinc finger protein required for the development of a subset of CNS neurons in drosophila. *Neuron* **9**, 789–803.

Mito, T., Sarashina, I., Zhang, H., Iwahashi, A., Okamoto, H., Miyawaki, K., Shinmyo, Y., Ohuchi, H. and Noji, S. (2005). Non-canonical functions of hunchback in segment patterning of the intermediate germ cricket Gryllus bimaculatus. *Development* **132**, 2069–2079.

Mito, T., Okamoto, H., Shinahara, W., Shinmyo, Y., Miyawaki, K., Ohuchi, H. and Noji, S. (2006). Krüppel acts as a gap gene regulating expression of hunchback and even-skipped in the intermediate germ cricket Gryllus bimaculatus. *Dev. Biol.* **294**, 471–481.

Morata, G. (1993). Homeotic genes of Drosophila. *Curr. Opin. Genet. Dev.* **3**, 606–614.

Naggan Perl, T., Schmid, B. G. M., Schwirz, J. and Chipman, A. D. (2013). The Evolution of the knirps Family of Transcription Factors in Arthropods. *Mol. Biol. Evol.* **30**, 1348–1357.

Nakamoto, A., Hester, S. D., Constantinou, S. J., Blaine, W. G., Tewksbury, A. B., Matei, M. T., Nagy, L. M. and Williams, T. A. (2015). Changing cell behaviours during beetle embryogenesis correlates with slowing of segmentation. *Nat. Commun.* **6**, 6635.

Nakao, H. (2015). Analyses of interactions among pair-rule genes and the gap gene Krüppel in Bombyx segmentation. *Dev. Biol.* **405**, 149–157.

Nakao, H. (2016). Hunchback knockdown induces supernumerary segment formation in Bombyx. *Dev. Biol.* **413**, 207–216.

Nasiadka, A., Dietrich, B. H. and Krause, H. M. (2002). Anterior-posterior patterning in the Drosophila embryo. In *Advances in Developmental Biology and Biochemistry*, pp. 155–204. Elsevier.

Ng, M., Diaz-Benjumea, F. J. and Cohen, S. M. (1995). Nubbin encodes a POU-domain protein required for proximal-distal patterning in the Drosophila wing. *Development* **121**, 589–99.

Nüsslein-Volhard, C. and Wieschaus, E. (1980). Mutations affecting segment number and polarity in Drosophila. *Nature* **287**, 795–801.

Nüsslein-Volhard, C., Wieschaus, E. and Kluding, H. (1984). Mutations affecting the pattern of the larval cuticle in Drosophila melanogaster. I. Zygotic loci on the second chromosome. *Rouxs Arch. Dev. Biol.* **193**, 267–282.

Olesnicky, E. C. (2006). A caudal mRNA gradient controls posterior development in the wasp Nasonia. *Development* **133**, 3973–3982.

Panfilio, K. A. (2008). Extraembryonic development in insects and the acrobatics of blastokinesis. *Dev. Biol.* **313**, 471–491.

Paré, A. C., Vichas, A., Fincher, C. T., Mirman, Z., Farrell, D. L., Mainieri, A. and Zallen, J. A. (2014). A positional Toll receptor code directs convergent extension in Drosophila. *Nature* **515**, 523–527.

Patel, N. H., Condron, B. G. and Zinn, K. (1994). Pair-rule expression patterns of even-skipped are found in both short- and long-germ beetles. *Nature* **367**, 429–434.

Peel, A. D., Chipman, A. D. and Akam, M. (2005). Arthropod Segmentation: beyond the Drosophila paradigm. *Nat. Rev. Genet.* **6**, 905–916.

Peel, A. D., Schanda, J., Grossmann, D., Ruge, F., Oberhofer, G., Gilles, A. F., Schinko, J. B., Klingler, M. and Bucher, G. (2013). Tc-knirps plays different roles in the specification of antennal and mandibular parasegment boundaries and is regulated by a pair-rule gene in the beetle Tribolium castaneum. *BMC Dev. Biol.* **13**,.

Pi, H., Huang, Y.-C., Chen, I.-C., Lin, C.-D., Yeh, H.-F. and Pai, L.-M. (2011). Identification of 11-amino acid peptides that disrupt Notch-mediated processes in Drosophila. *J. Biomed. Sci.* **18**, 42.

Pinnell, J., Lindeman, P. S., Colavito, S., Lowe, C. and Savage, R. M. (2006). The divergent roles of the segmentation gene hunchback. *Integr. Comp. Biol.* **46**, 519–532.

Posnien, N., Schinko, J., Grossmann, D., Shippy, T. D., Konopova, B. and Bucher, G. (2009). RNAi in the Red Flour Beetle (Tribolium). *Cold Spring Harb. Protoc.* **2009**, 10.1101/pdb.prot5256.

Prakash, K., Fang, X. D., Engelberg, D., Behal, A. and Parker, C. S. (1992). dOct2, a Drosophila Oct transcription factor that functions in yeast. *Proc. Natl. Acad. Sci.* **89**, 7080–7084.

Prpic, N.-M. and Damen, W. G. M. (2005). Diversification of nubbin expression patterns in arthropods: data from an additional spider species, Cupiennius salei. *Evol. Dev.* **7**, 276–279.

Prpic, N. M. and Damen, W. G. M. (2009). Notch-mediated segmentation of the appendages is a molecular phylotypic trait of the arthropods. *Dev. Biol.* **326**, 262–271.

Pueyo, J. I. and Couso, J. P. (2008). The 11-aminoacid long Tarsal-less peptides trigger a cell signal in Drosophila leg development. *Dev. Biol.* **324**, 192–201.

Pueyo, J. I. and Couso, J. P. (2011). Tarsal-less peptides control Notch signalling through the Shavenbaby transcription factor. *Dev. Biol.* **355**, 183–193.

Pueyo, J. I., Lanfear, R. and Couso, J. P. (2008). Ancestral Notch-mediated segmentation revealed in the cockroach Periplaneta americana. *Proc. Natl. Acad. Sci.* **105**, 16614–16619.

Pultz, M. A. (2005). A major role for zygotic hunchback in patterning the Nasonia embryo. *Development* **132**, 3705–3715.

Qian, S., Capovilla, M. and Pirrotta, V. (1991). The bx region enhancer, a distant cis-control element of the Drosophila Ubx gene and its regulation by hunchback and other segmentation genes. *EMBO J.* **10**, 1415–25.

Ray, S., Rosenberg, M. I., Chanut-Delalande, H., Decaras, A., Schwertner, B., Toubiana, W., Auman, T., Schnellhammer, I., Teuscher, M., Valenti, P., et al. (2019). The mlpt/Ubr3/Svb module comprises an ancient developmental switch for embryonic patterning. *eLife* **8**, e39748.

Rehm, P., Meusemann, K., Borner, J., Misof, B. and Burmester, T. (2014). Phylogenetic position of Myriapoda revealed by 454 transcriptome sequencing. *Mol. Phylogenet. Evol.* **77**, 25–33.

Riley, P. D., Carroll, S. B. and Scott, M. P. (1987). The expression and regulation of Sex combs reduced protein in Drosophila embryos. *Genes Dev.* **1**, 716–730.

Rothe, M., Pehl, M., Taubert, H. and Jäckle, H. (1992). Loss of gene function through rapid mitotic cycles in the Drosophila embryo. *Nature* **359**, 156–159.

Rudolf, H., Zellner, C. and El-Sherif, E. (2019). Speeding up anterior-posterior patterning of insects by differential initialization of the gap gene cascade. *Dev. Biol.* **460**, 20–31.

Sarrazin, A. F., Peel, A. D. and Averof, M. (2012). A Segmentation Clock with Two-Segment Periodicity in Insects. *Science* **336**, 338–341.

Savard, J., Marques-Souza, H., Aranda, M. and Tautz, D. (2006). A Segmentation Gene in Tribolium Produces a Polycistronic mRNA that Codes for Multiple Conserved Peptides. *Cell* **126**, 559–569.

Schindelin, J., Arganda-Carreras, I., Frise, E., Kaynig, V., Longair, M., Pietzsch, T., Preibisch, S., Rueden, C., Saalfeld, S., Schmid, B., et al. (2012). Fiji: an open-source platform for biological-image analysis. *Nat. Methods* **9**, 676–682.

Schmitt-Engel, C., Cerny, A. C. and Schoppmeier, M. (2012). A dual role for nanos and pumilio in anterior and posterior blastodermal patterning of the short-germ beetle Tribolium castaneum. *Dev. Biol.* **364**, 224–235.

Schröder, R. (2006). vasa mRNA accumulates at the posterior pole during blastoderm formation in the flour beetle Tribolium castaneum. *Dev. Genes Evol.* **216**, 277–283.

Schröder, R., Eckert, C., Wolff, C. and Tautz, D. (2000). Conserved and divergent aspects of terminal patterning in the beetle Tribolium castaneum. *Proc. Natl. Acad. Sci.* **97**, 6591–6596.

Schröder, R., Beermann, A., Wittkopp, N. and Lutz, R. (2008). From development to biodiversity—Tribolium castaneum, an insect model organism for short germband development. *Dev. Genes Evol.* **218**, 119–126.

Schroeder, M. D., Greer, C. and Gaul, U. (2011). How to make stripes: deciphering the transition from non-periodic to periodic patterns in Drosophila segmentation. *Development* **138**, 3067–3078.

Schwager, E. E., Pechmann, M., Feitosa, N. M., McGregor, A. P. and Damen, W. G. M. (2009). hunchback Functions as a Segmentation Gene in the Spider Achaearanea tepidariorum. *Curr. Biol.* **19**, 1333–1340.

Serano, J. M., Martin, A., Liubicich, D. M., Jarvis, E., Bruce, H. S., La, K., Browne, W. E., Grimwood, J. and Patel, N. H. (2016). Comprehensive analysis of Hox gene expression in the amphipod crustacean Parhyale hawaiensis. *Dev. Biol.* **409**, 297–309.

Shimell, M. J., Peterson, A. J., Burr, J., Simon, J. A. and O'Connor, M. B. (2000). Functional Analysis of Repressor Binding Sites in the iab-2 Regulatory Region of the abdominal-A Homeotic Gene. *Dev. Biol.* **218**, 38–52.

Sommer, R. J. and Tautz, D. (1993). Involvement of an orthologue of the Drosophila pair-rule gene hairy in segment formation of the short germ-band embryo of Tribolium (Coleoptera). *Nature* **361**, 448–450.

Sprecher, S. G. ed. (2020). A Protocol for Double Fluorescent In Situ Hybridization and Immunohistochemistry for the Study of Embryonic Brain Development in Tribolium castaneum. In *Brain Development: Methods and Protocols*, pp. 219–232. New York, NY: Springer New York.

Stollewerk, A., Schoppmeier, M. and Damen, W. G. M. (2003). Involvement of Notch and Delta genes in spider segmentation. *Nature* **423**, 863–865.

Stuart, J. J., Brown, S. J., Beeman, R. W. and Denell, R. E. (1993). The Tribolium homeotic gene Abdominal is homologous to abdominal-A of the Drosophila bithorax complex. *Development* 11233–243.

Surkova, S., Kosman, D., Kozlov, K., Manu, Myasnikova, E., Samsonova, A. A., Spirov, A., Vanario-Alonso, C. E., Samsonova, M. and Reinitz, J. (2008). Characterization of the Drosophila segment determination morphome. *Dev. Biol.* **313**, 844–862.

Tang, X., Zhao, Y., Buchon, N. and Engström, Y. (2018). The POU/Oct Transcription Factor Nubbin Controls the Balance of Intestinal Stem Cell Maintenance and Differentiation by Isoform-Specific Regulation. *Stem Cell Rep.* **10**, 1565–1578.

Thomas, J. B., Crews, S. T. and Goodman, C. S. (1988). Molecular genetics of the single-minded locus: a gene involved in the development of the Drosophila nervous system. *Cell* **52**, 133–141.

Tobias-Santos, V., Guerra-Almeida, D., Mury, F., Ribeiro, L., Berni, M., Araujo, H., Logullo, C., Feitosa, N. M., de Souza-Menezes, J., Pessoa Costa, E., et al. (2019). Multiple Roles of the Polycistronic Gene Tarsal-less/Mille-Pattes/Polished-Rice During Embryogenesis of the Kissing Bug Rhodnius prolixus. *Front. Ecol. Evol.* **7**, 379.

Tran, K. D. and Doe, C. Q. (2008). Pdm and Castor close successive temporal identity windows in the NB3-1 lineage. *Development* **135**, 3491–3499.

Trauner, J. and Büning, J. (2007). Germ-cell cluster formation in the telotrophic meroistic ovary of Tribolium castaneum (Coleoptera, Polyphaga, Tenebrionidae) and its implication on insect phylogeny. *Dev. Genes Evol.* **217**, 13–27.

Traylor-Knowles, N., Hansen, U., Dubuc, T. Q., Martindale, M. Q., Kaufman, L. and Finnerty, J. R. (2010). Evolutionary diversification of LSF and Grainyhead transcription factors preceded the radiation of basal animal lineages. *BMC Evol. Biol.* **10**,.

Tsuji, T., Hasegawa, E. and Isshiki, T. (2008). Neuroblast entry into quiescence is regulated intrinsically by the combined action of spatial Hox proteins and temporal identity factors. *Development* **135**, 3859–3869.

Turchyn, N., Chesebro, J., Hrycaj, S., Couso, J. P. and Popadić, A. (2011). Evolution of nubbin function in hemimetabolous and holometabolous insect appendages. *Dev. Biol.* **357**, 83–95.

Vacalla, C. M. H. and Theil, T. (2002). Cst, a novel mouse gene related to Drosophila Castor, exhibits dynamic expression patterns during neurogenesis and heart development. *Mech. Dev.* **118**, 265–268.

Vargas-Vila, M. A., Hannibal, R. L., Parchem, R. J., Liu, P. Z. and Patel, N. H. (2010). A prominent requirement for single-minded and the ventral midline in patterning the dorsoventral axis of the crustacean Parhyale hawaiensis. *Development* **137**, 3469–3476.

Verd, B., Clark, E., Wotton, K. R., Janssens, H. and Jim, E. (2018). A damped oscillator imposes temporal order on posterior gap gene expression in Drosophila. *PLoS Biol.* **16**, e2003174.

Wang, S. and Samakovlis, C. (2012). Grainy head and its target genes in epithelial morphogenesis and wound healing. *Curr. Top. Dev. Biol.* **98**, 35–63.

Wang, C., Dickinson, L. K. and Lehmann, R. (1994). Genetics of nanos localization in Drosophila. *Dev. Dyn.* **199**, 103–115.

Weigel, D., Jürgens, G., Klingler, M. and Jäckle, H. (1990). Two gap genes mediate maternal terminal pattern information in Drosophila. *Science* **248**, 495–498.

Wells, J., Lee, B., Cai, A. Q., Karapetyan, A., Lee, W.-J., Rugg, E., Sinha, S., Nie, Q. and Dai, X. (2009). Ovol2 Suppresses Cell Cycling and Terminal Differentiation of Keratinocytes by Directly Repressing c-Myc and Notch1. *J. Biol. Chem.* **284**, 29125–29135.

White, A. H. and Lehmann, R. (1986). A Gap Gene, hunchback, Regulates the Spatial Expression of Ultrabithorax. *Cell* **47**, 311–321.

Wieschaus, E. and Nüsslein-Volhard, C. (2016). The Heidelberg Screen for Pattern Mutants of Drosophila: A Personal Account. *Annu. Rev. Cell Dev. Biol.* **32**, 1–46.

Wieschaus, E., Nüsslein-Volhard, C. and Jürgens, G. (1984). Mutations affecting the pattern of the larval cuticle in Drosophila melanogaster. II. Zygotic loci on the X-chromosome and fourth chromosome. *Rouxs Arch. Dev. Biol.* **193**, 296–307.

Wilson, M. J., Havler, M. and Dearden, P. K. (2010). Giant, Krüppel, and caudal act as gap genes with extensive roles in patterning the honeybee embryo. *Dev. Biol.* **339**, 200–211.

Wolff, C., Sommer, R., Schröder, R., Glaser, G. and Tautz, D. (1995). Conserved and divergent expression aspects of the Drosophila segmentation gene hunchback in the short germ band embryo of the flour beetle Tribolium. *Development* **121**, 4227–4236.

Yeo, S. L., Lloyd, A., Kozak, K., Dinh, A., Dick, T., Yang, X., Sakonju, S. and Chia, W. (1995). On the functional overlap between two Drosophila POU homeo domain genes and the cell fate specification of a CNS neural precursor. *Genes Dev.* **9**, 1223–1236.

Young, T., Rowland, J. E., van de Ven, C., Bialecka, M., Novoa, A., Carapuco, M., van Nes, J., de Graaff, W., Duluc, I., Freund, J.-N., et al. (2009). Cdx and Hox Genes

Differentially Regulate Posterior Axial Growth in Mammalian Embryos. *Dev. Cell* **17**, 516–526.

Zhu, X., Rudolf, H., Healey, L., François, P., Brown, S. J., Klingler, M. and El-Sherif, E. (2017). Speed regulation of genetic cascades allows for evolvability in the body plan specification of insects. *Proc. Natl. Acad. Sci.* **114**, E8646–E8655.

Zinzen, R., Cande, J., Ronshaugen, M., Papatsenko, D. and Levine, M. (2006). Evolution of the ventral midline in insect embryos. *Dev. Cell* **11**, 895–902.

Zou, Z., Evans, J. D., Lu, Z., Zhao, P., Williams, M., Sumathipala, N., Hetru, C., Hultmark, D. and Jiang, H. (2007). Comparative genomic analysis of the Tribolium immune system. *Genome Biol.* **8**, R177.